INVESTIGATIONS INTO THE EFFECTIVENESS OF MEASURES TO REDUCE THE ENERGY REQUIREMENTS OF DOMESTIC DWELLINGS IN CYPRUS

A Thesis submitted for the degree of Doctor of Philosophy

by

Georgios A. Florides

Department of Mechanical Engineering
Brunel University

September 2001

BRUNEL UNIVERSITY

PUBLICATION OF THESES

Please complete in block capitals

NAME: GEORGIOS A. FLORIDES

DEPARTMENT: MECHANICAL ENGINEERING

TITLE OF THESIS: INVESTIGATIONS INTO THE EFFECTIVENESS OF MEASURES TO REDUCE THE ENERGY REQUIREMENTS OF DOMESTIC DWELLINGS IN CYPRUS

PLEASE COMPLETE EITHER PART A OR PART B

A. I agree that the abstract of my thesis may be published by the University without further reference to me.

In accordance with the University's Handbook of Procedures, the Head of Library Services may allow my thesis to be copied in whole or in part without further reference to me. Such Authority shall apply only to single copies made for study purposes and shall be subject to normal conditions of acknowledgement.

(See notes overleaf)

Signature: 

Date: 10/11/01

If you have completed Part A please return this form direct to the Library with evidence of your award.

B. I request that my thesis be held under confidential cover in the Library for a period of _____ years for the following reasons:

_____

_____

_____

_____

Once the period of confidentiality has expired, I agree that the conditions set down in Part A will apply without further reference to me.

Signature: _____

Date: _____

Please pass this form to your supervisor who should sign below indicating his/her agreement to the retention of the thesis under confidential cover.

Signature of Supervisor: _____

Additional comments: _____

_____

_____

Signature _____
(Senior Assistant Registrar)

Part B, when complete, should be returned to the Senior Assistant Registrar (Records & Systems) in the Registry.

For the attention of candidates who have completed Part A

i) Attention is drawn to the fact that the copyright of a thesis rests with its author.

ii) A copy of a candidate's thesis is supplied to the Library on condition that anyone who consults it is understood to recognise that its copyright rests with its author and that no quotation from the thesis and no information derived from it may be published without the prior written consent of the author or the University, as appropriate.

Requests for such permission should be addressed in the first instance to the Head of Library Services.

ABSTRACT

In recent years there has been an increasing trend in the provision of central heating and split vapour compression air conditioning systems to domestic dwellings in Cyprus. To minimise their economic and environmental impact, this study examines the feasibility and economic viability of energy conservation measures and the feasibility of the application of solar driven LiBr-water absorption system for space conditioning.

Initially, the study compares through simulation, the heating and cooling requirements of domestic dwellings constructed in Cyprus during the last century. The simulations required values for the thermal conductivity of local building materials, like the hollow brick and mud and straw block. These were not available, and measurements were performed on a machine specifically purchased for the project to establish these values for the first time. These material properties will be of value to building services engineers in Cyprus and the Middle East for the more precise determination of building heating and cooling loads.

Evaluation of the internal conditions resulting from the various types of constructions indicated that the traditional and insulated modern houses, could maintain indoor temperature in winter between 16°C and 20°C, but in the summer temperatures exceeded 36°C. The use of natural and mechanical ventilation could reduce slightly the maximum indoor summertime temperatures, but not to a level that could provide thermal comfort.

Window gains are an important factor in domestic building energy requirements, and significant savings can result when extra measures are taken. The savings in cooling energy demand for a well-insulated house may be as high as 24% when low-emissivity double glazed windows are used compared to clear double glazed windows giving a pay-back period of 3.8 years. Other factors investigated are the effect of overhangs, shape and orientation of buildings and thermal mass. The results show that the roof is the most important structural element of domestic dwellings in the Cypriot environment. For good thermal performance, the roof must offer a discharge time of 6 hours or more and have a thermal conductivity of less than 0.48 W/m-K. Life cycle cost analysis has shown that measures that increase the roof insulation pay back in a short period of time, between 3.5 to 5 years. However, measures taken to increase wall insulation pay back in a longer period of time, approximately 10 years.

The only natural energy resource abundantly available in Cyprus is solar energy, which could be used to power a low energy active cooling system based on the absorption cycle. To facilitate investigation of the feasibility of the application of solar driven absorption systems for domestic cooling, a 1 kW LiBr-water absorption-cooling unit was designed and constructed. The unit was used to determine experimentally the heat and mass transfer coefficients in the heat exchangers of absorption systems. In certain cases these were found to differ considerably from values obtained from heat and mass transfer correlations published by other investigators. The experimentally determined heat and mass transfer coefficients were employed in the design and costing of an 11 kW cooling capacity solar driven absorption cooling machine which, from simulations, was found to have sufficient capacity to satisfy the cooling needs of a well insulated domestic dwelling. Economic analysis has shown that for such a system to be economically competitive compared to conventional cooling systems its capital cost should be below C£ 2000. This drawback can be balanced by a lower total equivalent warming impact being 2.7 times smaller compared to conventional cooling systems.

Dedicated to

my wife, son and daughter

CONTENTS

CHAPTER 3

CHAPTER 4

CHAPTER 5

CHAPTER 6

CHAPTER 7

LIST OF FIGURES

LIST OF TABLES

ACKNOWLEDGEMENTS

I would like to express my sincere and honest appreciation to my thesis supervisors Professor Savvas Tassou and Professor Luiz Wrobel for their continuous help and constructive criticism and comments, without whom this work would not have been possible.

I would also like to thank on an equal share, the external project supervisor Dr. Soteris Kalogirou, for his valuable suggestions and constructive criticism and help during all the stages of the project.

Special thanks are also due to the former Head of the Mechanical Engineering Department of Brunel University, Professor Nicos Ladommatos for his understanding, interest and support and the Higher Technical Institute Research Committee for its financial aid for the construction work of the project.

Finally, I would like to thank my wife Evanthia, my son Andreas and daughter Yianna, for their never-ending support and patience they have shown during the development of this project.

NOMENCLATURE

A	indoor surface area of wall or roof, area of element under analysis, area of opening, total heat transfer area (m^2)
A_i	area of surface i (m^2)
A_p	absorption percentage
a	absorptance of absorber plate
ach	room air changes per hour
a_o	intercept efficiency
a_1	negative of the first order coefficient of the efficiency (kJ/hr-m^2-K)
a_2	negative of the second order coefficient of the efficiency (kJ/hr-m^2-K^2)
b_n, c_n, d_n	conduction transfer function coefficients for current and previous values of the sol air temperature (b, W/m^2-K), equivalent zone temperature (c, W/m^2-K), and heat flux (d, dimensionless)
Cap	capacitance of room air and furnishings (kJ/°C)
C_{EQ}	solution equilibrium concentration (mass fraction)
C_{IN}	solution inlet concentration (mass fraction)
COP	coefficient of performance
C_{OUT}	solution outlet concentration (mass fraction)
CPC	compound parabolic concentrating collectors
C_{pc}	specific heat of collector fluid (kJ/kg-K)
c	purchase cost at the end of year N
c_p	specific heat of air (J/kg-K)
dT	temperature difference (°C)
D_i	inside diameter of the tube (m)
D_o	outside diameter of the tube (m)
d	market discount rate (%)
e	effectiveness of the collector loop heat exchanger
F	cash flow, future fuel cost, correction factor depending on the type of the heat exchanger
F'	collector fin efficiency factor
F_I	fouling factors at the inside surface of the tube (m^2-K/W)
FL	load factors
F_m	flux history coefficients

F_o	fouling factors at the outside surface of the tube (m^2-K/W)
FR	radiation factors
F_{sa}	special allowance factor (Ballast factor in the case of fluorescent and metal halide fixtures)
FU	usage factor
F_{ul}	lighting use factor, ratio of wattage in use to total installed wattage
F_2	heat loss coefficient per meter of perimeter (W/m-K)
f_k	fraction of incoming beam radiation that strikes surface k
G_{test}	flow rate per unit area at test conditions (kg/hr-m^2)
g	gravitational constant, 9.81 m/s^2
g_i	transfer function coefficients (ASHRAE, 1992)
g_{ij}	linearised radiation heat transfer factor between interior surface i and interior surface j (W/m^2-K)
H	opening height (m)
h	truncated height of CPC
h_i	heat transfer coefficients for inside flow (W/m^2-K)
h_{av}	full height of CPC
h_c	inside convection coefficient (W/m^2-K)
$h_{c,i}$	inside convection coefficient (W/m^2-K)
h_{ci}	convective heat transfer coefficient at interior surface i (W/m^2-K)
h_{fg}	latent heat of condensation (kJ/kg)
h_m	average heat transfer coefficient (W/m^2-K)
h_o	heat transfer coefficients for outside flow (W/m^2-K)
h_s	solution convective heat transfer coefficient (W/m^2-K)
h_0	heat transfer coefficient for convection over the building (W/m^2-K)
h_{av}/h	ratio of truncated to full height of CPC
I	rate of moisture gain (other than people) (kg/hr)
I	global solar radiation on a horizontal surface at the next hour (W/m^2)
I_{act}	activity level of people
I_{bT}	incident beam radiation (W/m^2)
I_{bT1}, I_{bTi}	beam radiation on surface number 1or i (W/m^2)
I_{dn}	direct normal solar radiation at the next hour (W/m^2)
I_T	total incident radiation (W/m^2)

I_{T1}, I_{Ti}	total radiation on surface number 1or i (W/m^2)
It	total incident solar load (W/m^2)
i	surface number (1 to 6), fuel annual inflation rate, inside surface subscript
i_{fg}	enthalpy of evaporation (J/kg-K)
K_L	product of extinction coefficient and the thickness of each cover plate
K_I	constant air change per hour
K2	proportionality constant for air change due to indoor-outdoor temperature difference (1/°C)
K3	proportionality constant for air change due to wind effects (s/m)
k	thermal conductivity of tube material, thermal conductivity (W/m-K), first surface number of which beam of radiation strikes
k	order of CTF
k_l	thermal conductivity of liquid (W/m-K)
k_s	solution thermal conductivity (W/m-K)
L	length of plate (m)
LCC	life cycle cost
LHGp	latent heat gain per person
M	number of non-zero CTF values
m	time index variable, mass flow rate (kg/s)
$\dot{m}$	mass flow rate (kg/s)
m_a	air mass flow rate (kg/s)
m_{infl}	mass flow rate of air infiltration (kg/h)
$\dot{m}_{11}$	liquid carryover from evaporator
N	number of people, number of years from now
N_G	number of cover plates
N_I	number of surfaces on which transmitted beam radiation strikes
N_{people}	number of people in every zone
$\overline{Nu_D}$	Nusselt number = $h_i D_i / K$
n	summation index (each summation has as many terms as there are non-negligible values of coefficients), efficiency
η_R	index of refraction of cover material
o	outside surface subscript
P	perimeter of exposed edge of floor (m), present value, pressure (Pa)

Pr	Prandtl number
Pr_s	solution Prandtl number
PW	present worth
p_i	transfer function coefficients (ASHRAE, 1992)
Q	ventilation rate (m^3/s)
$\dot{Q}$	energy flow (kW)
$\dot{Q}_a$	absorber heat, rejected to the environment (kW)
$\dot{Q}_c$	condenser heat, rejected to the environment (kW)
$\dot{Q}_e$	capacity (evaporator output power) (kW)
$\dot{Q}_g$	heat input to the generator (kW)
Q_{int}	sum of all other instantaneous heat gain to space (kJ/hr)
Q_{IR}	radiative energy input due to lights, equipment, etc. (kJ/hr)
$Q_{i,\theta}$	volume flow rate of outdoor air infiltrating into the room at time θ (m^3/s)
Q_{lat}	latent load (kJ/h)
Q_{sens}	sensible load (kJ/h)
Q_T	total load (kJ/h)
$Q_{v,\theta}$	volume rate of flow of ventilation air at time θ (m^3/s)
q	heat loss through perimeter (W)
q_c	cooling load at the various times (W)
$q_{el,\theta}$	rate of heat from equipment and occupants absorbed by surface i at time θ (W)
q_{el}	rate of heat gain from lights (W)
$q_{e,\theta}$	heat gain through wall or roof, at calculation hour θ (W), rate of heat from equipment and occupants convected into the room air at timeθ (W)
$q_{i,\theta}$	rate of heat conducted into surface i at the inside surface at time θ (W)
ql	latent cooling load due to people (W)
$q_{l,\theta}$	rate of heat from the lights convected into the room air at time θ (W)
$q_{li,\theta}$	rate of heat from the lights absorbed by surface i at time θ (W)
q_s	rate of sensible cooling load due to people (W)

$q_{s,\theta}$	rate of solar heat coming through the windows and convected into the room air at time θ (W)
$q_{si,\theta}$	rate of solar heat coming through the windows and absorbed by surface i at time θ (W)
q_x	heat extraction rate (W), heat flux in the positive x direction (W/m^2)
Re_D	Reynolds number $= V_m D_i / \nu = 4m / \pi D_i \mu$
Re_s	solution Reynolds number for vertical tube
r	reflectance of inner surface to solar radiation
r_s	number of surfaces in the room
SC	shading coefficient
SHG_p	sensible heat gain per person
SHGF	solar heat gain factor varying according to orientation, latitude, hour and month
T	dry-bulb temperature at the next time step (°C)
T_a	ambient temperature (°C)
T_{av}	average collector fluid temperature (°C)
T_i	temperature of fluid entering cold side of heat exchanger or collector inlet if no heat exchanger present (°C)
T_{max}	set point temperature for cooling (°C)
T_{min}	set point temperature for heating (°C)
TMY	typical meteorological year
T_o	initial room temperature; also used for calculation of inside radiation coefficients (°C)
T_v	temperature of ventilation flow stream, vapour saturation temperature (°C)
T_w	wall surface temperature (°C)
T_z	zone temperature (°C)
t	temperature (°C), overall transmittance for solar radiation
$t_{a,\theta}$	inside air temperature at time θ (°C)
t_d	transmittance for diffuse solar radiation
t_e	sol-air temperature (°C)
$t_{e,\theta-n\delta}$	sol-air temperature at time θ-nδ (°C)
t_I	indoor temperature (°C)
$t_{i,\theta}$	average temperature of interior surface i at time θ (°C)

$t_{j,\theta}$	average temperature of interior surface j at time θ (°C)
t_1	room temperature used for cooling load calculations (°C)
t_0	current hour dry-bulb temperature (°C)
t_o	outdoor temperature (°C)
$t_{o,\theta}$	outdoor air temperature at time θ (°C)
t_r	actual room temperature at the various times (°C)
t_{rc}	constant indoor room temperature (°C)
$t_{v,\theta}$	ventilation air temperature at time θ (°C)
$(t_b - t_i)$	adjacent space–indoor temperature difference (°C)
$(t_0 - t_i)$	outdoor–indoor temperature difference (°C)
$(t_0 - t_1)$	temperature difference between incoming and room air (°C)
U	overall heat transfer coefficient (W/m^2-K), mean wind speed measured at a weather station (m/s)
U_{eff}	effective velocity (m/s)
U_g	loss coefficient of window (plus night insulation) not including convection at the inside or outside surface (W/m^2-K)
U_L	overall loss coefficient of collector per unit aperture area (W/m^2-K)
V_a	volume of air in the zone (m^3)
V_m	mean velocity (m/s)
v	mass flow rate of ventilation flow stream (kg/hr)
W	wind speed (m/s), total installed light wattage, rate of energy input from appliances (W)
W_{vel}	wind velocity at the next time step (m/s)
w	pump minimum work input, minimum work input
w_a	ambient humidity ratio (kg water/kg dry air)
w_{max}	set point humidity ratio for dehumidification (kg water/kg dry air)
w_{min}	set point humidity ratio for humidification (kg water/kg dry air)
w_o	initial room humidity ratio (kg water/kg dry air)
w_v	humidity ratio of ventilation flow stream (kg water/kg dry air)
X	concentration of LiBr in solution (%)
Y	cross CTF values
Z	interior CTF values

Greek

α	absorptance of surface for solar radiation
α	absorptance of exterior surface to solar radiation
Γ	mass flow rate per wetted perimeter (kg/m-s)
ΔT	temperature difference (K)
ΔT_L	temperature difference between the hot and cold fluid at outlet (K)
$\Delta T_{\ln}$	logarithmic mean temperature difference (LMTD) (K)
ΔT_m	mean temperature difference (K)
ΔT_0	temperature difference between the hot and cold fluid at the inlet, (K)
δ	film thickness (m)
δ	time interval (s)
δR	difference between long-wave radiation incident on the surface from the sky and surroundings and the radiation emitted by a black body at outdoor air temperature (W/m^2)
$\varepsilon\ \delta R / h_0$	long-wave radiation factor = -3.9°C for horizontal surfaces, 0°C for vertical surfaces
θ	time (s)
θ_c	half-acceptance angle of CPC (degrees)
μ	absolute viscosity ($N\text{-}s/m^2$) = $\nu\ \rho$
μ_l	absolute viscosity of liquid ($N\text{-}s/m^2$)
ν	specific volume (m^3/kg)
ν	kinematic viscosity (m^2/s)
ρ	density kg/m^3
ρ	air density (kg/m^3)
ρ_a	density of zone air (kg/m^3)
ρ_l	liquid density (kg/m^3)
ρ_R	reflectivity of walls of CPC
ρ_v	vapour density (kg/m^3)
ω	humidity ratio at the next time step
$(\omega_0 - \omega_i)$	humidity ratio difference between incoming and room air (kg/kg)

CHAPTER 1

INTRODUCTION

The quest to accomplish a safe and comfortable environment has always been one of the main preoccupations of the human race. In ancient times people used experience gained over many years to make best use of available resources to achieve adequate living conditions. The Greek historian Xenophon in his "Memorabilia" records some of the teachings of the Greek philosopher Socrates (470-399 BC) regarding correct orientation of dwellings in order to have houses cool in summer and warm in winter (Anderson, 1977). Central heating was pioneered by the Romans using double floors through whose cavity the fumes of a fire were passed. Also in Roman times windows were covered for the first time with materials like mica or glass. Thus, light was admitted in the house without letting in wind and rain (Kreider and Rabl, 1994). Iraqis on the other hand utilised the prevailing wind to take advantage of the night cool air and provide a cooler environment during the day. Additionally, running water was employed to provide some evaporative cooling.

As late as the 1960's though, house comfort conditions were only for the few. From then onwards central air conditioning systems became common in developed countries due to the development of mechanical refrigeration and the rise of the standard of living. The oil crises of the 1970's stimulated intensive research aimed at reducing energy costs. Also, Global Warming and Ozone depletion and the escalating costs of fossil fuels over the last few years, have forced governments and engineering bodies to re-examine the whole approach to building design and control. Energy conservation in the sense of fuel saving is also of great importance. Considering that the overall energy consumption in commercial and residential buildings represents approximately 40% of Europe's energy budget (Santamouris *et al.*, 1994) sensible energy conservation measures, which do not affect the environmental standards and the quality of life, must be introduced.

During resent years research aimed at the development of technologies that can offer reductions in energy consumption, peak electrical demand and energy costs without lowering the desired level of comfort conditions has intensified. Alternative cooling technologies are being developed which can be applied to residential and commercial

buildings, in a wide range of weather conditions. These include night cooling with ventilation, evaporative cooling, desiccant cooling, slab cooling etc. The design of buildings employing low energy cooling technologies, however, presents difficulties and requires advanced modelling and control techniques to ensure efficient operation.

Another method that can be used is ground cooling. This is based on the heat-loss dissipation from a building to the ground, which during the summer has a lower temperature than the ambient. This dissipation can be achieved either by direct contact of an important part of the building envelope with the ground, or by blowing air into the building that has first been past through an earth-to-air heat exchanger.

The role of designers and architects is very important too, especially with respect to solar energy control, the utilisation of thermal mass and correct ventilation of a building. In effective solar energy control, summer heat gains must be reduced while winter solar heat gains must be maximised. This can be achieved by the proper orientation and shape of the building, the use of shading devices and the selection of proper construction materials. Thermal mass, especially in hot climates with diurnal variation of ambient temperatures exceeding 10°C, can be used to reduce the instantaneous high cooling loads, reduce energy consumption and attenuate indoor temperature swings. Correct ventilation can enhance the roles of both solar energy control and thermal mass.

Reconsideration of the building structure, the readjustment of capital cost allocations (i.e., investing in energy conservation measures that may have a significant influence on thermal loads) and improvements in equipment and maintenance, can minimise the energy expenditure and improve thermal comfort.

In Cyprus, due to the high summertime temperatures low energy cooling technologies cannot alone satisfy the total cooling demand of domestic dwellings. For this reason an active cooling system is required. Today, vapour compression cooling systems are used, powered by electricity, which is expensive, and its production depends entirely on fossil fuel imports. The only resource abundantly available in Cyprus is solar energy, which could be used to power an active solar cooling system based on the absorption cycle. The problem with solar absorption machines is that they are expensive compared to vapour compression machines and are not readily available in the small capacity range

applicable to domestic cooling applications. For this reason the feasibility of manufacturing solar absorption air-conditioning systems in small sizes for residential buildings in Cyprus is investigated. There are possibilities of wider application of solar driven absorption cooling technologies in the broader Middle East area. Reducing the use of conventional vapour compression air-conditioning systems will reduce their effect on both, Global Warming and Ozone layer.

The integration of the building envelope with an absorption system should offer better control of the internal environment. Two types of absorption units are available; ammonia-water and lithium bromide (LiBr)-water units. The latter are more suitable for solar applications since their operating (generator) temperature is lower and thus more readily obtainable with low-cost solar collectors. A search in the world market has shown that only one manufacturer produces commercially small residential-size lithium bromide-water absorption refrigerators (Yazaki of Japan). This manufacturer was not willing to provide such a unit for use in Cyprus because it was not able to provide maintenance services for this market. A search through published papers has also shown that no clear guidance exists on how to construct such a small unit, although the theoretical analysis of the cycle is clear and extensively studied.

This project considers the technical feasibility and economic viability of applying solar driven absorption cooling systems to satisfy the cooling and heating requirements of domestic dwellings in Cyprus. To improve the cost effectiveness of the system, ways of reducing the thermal load of modern dwellings using passive techniques are also considered.

Seasonal energy simulations were carried out based on hourly weather parameters included in a typical meteorological year (TMY) file, constructed from a seven-year record, for the climatic conditions of Nicosia-Cyprus. These conditions are typical for the East Mediterranean and Middle East areas. The same climate is also encountered in certain areas in Australia and in California, USA.

1.1 OBJECTIVES

The main objective of this work is to study through modelling, ways to minimise the thermal energy requirements of domestic dwellings in Cyprus and investigate the application of LiBr-water absorption units for domestic cooling.

Specific objectives of the project are to:

1. Analyse the evolution of buildings in Cyprus and investigate methods used to create acceptable indoor environment.

2. Model a typical modern house in Cyprus by considering the various construction methods applied and draw conclusions on a cost effective building envelope, which can also reduce thermal loads. This requires measurements to establish, for the first time, the thermophysical properties of local building materials, which are used in the computer simulations.

3. Evaluate measures like controlled or natural ventilation, overhangs, various types of glazing, orientation, shape of building, and thermal mass to reduce the thermal load of the modern domestic dwellings.

4. Design and construct a small cooling capacity LiBr-water absorption refrigerator to appreciate the manufacturing difficulties and estimate the cost of production of a residential-size unit.

5. Model a complete system, consisting of a solar collector, storage tank, a boiler and a LiBr-water absorption refrigerator, to satisfy a typical domestic cooling load during the whole year. Perform system optimisation and select appropriate equipment, i.e., the collector type, the storage tank volume, the collector slope angle and area and the optimum setting of the auxiliary boiler thermostat. Also, evaluate the long-term integrated system performance and the dynamic behaviour of the system.

6. Finally draw conclusions on the economics of an integrated low energy design of buildings with solar absorption cooling and solar heating.

1.2 STRUCTURE OF THESIS

Chapter 2 examines the Cyprus energy scene and presents an analysis of the number of houses employing heating and cooling equipment. From this analysis it is observed that the number of cooling systems installed has increased tremendously during the last decade. The evolution of domestic dwellings in Cyprus in respect to methods of construction employed and building materials is studied. Also a review of solar and low energy cooling approaches is presented.

Chapter 3 examines the theory related to building thermal load estimation. The Heat balance method, which provides a dynamic modelling of the building load is explained. An overview of the TRNSYS simulation program is presented since this is the basic tool used for the analysis of the building thermal load. The various parameters and thermal properties of structural elements used in the thesis are outlined.

Chapter 4 compares the heating and cooling requirements and the maximum and minimum resulting temperatures of buildings constructed in Cyprus during the last century. Conclusions are extracted based on the evaluation of the comfort conditions created from the various types of constructions and it is acknowledged how through experience Cypriots of the past created acceptable environment conditions in their houses.

Chapter 5 presents the modeling and simulation of the energy flows of modern houses in Cyprus, followed by an energy consumption analysis. For the calculations, a Typical Meteorological Year for the Nicosia area and a typical model house are used. The effect on internal space temperature and the heating and cooling energy demands arising from the various wall and roof constructions is determined.

Chapter 6 examines the effect of measures to lower building energy requirements. The effects of controlled or natural ventilation, overhangs, various types of glazing, orientation, shape of buildings, and thermal mass are presented. Life cycle cost analysis is used for the economic analysis of the various constructions. Conclusions are drawn on an appropriate structure that can be used in Cyprus and similar weather environments.

Chapter 7 presents the design of a small 1 kW, LiBr-water absorption machine. A theoretical analysis of the absorption cycle is presented and individual parts of the absorption unit are designed.

Chapter 8 presents construction details of the designed LiBr-water absorption machine. Useful conclusions regarding the manufacture, operation and cost of these machines is extracted. Based on the gained experience, the life cycle cost of a unit that could cover the needs of a typical domestic dwelling load is estimated.

Chapter 9 deals with the modelling and simulation of a complete absorption solar cooling system. The system consists of a solar collector and storage tank, a boiler and a LiBr-water absorption refrigerator. A typical house is used for this purpose, modelled for a whole year. The cooling and heating performance is presented and the long term integrated system performance and the dynamic behaviour of the system are evaluated. An economic analysis of the system is carried out.

Chapter 10 outlines the conclusions drawn from this research project and gives recommendations for further work.

CHAPTER 2

BACKGROUND

In this chapter the Cyprus energy scene and an analysis of the number of houses employing heating and cooling equipment is presented. The evolution of domestic dwellings in Cyprus during the twentieth century and the methods of construction employed and materials used are then examined. Finally, a review of solar cooling and low energy cooling technologies is presented.

2.1 THE CYPRUS ENERGY SCENE

Cyprus has no natural oil resources and relies entirely on imported fuel for its energy demands. The only natural energy resource available in Cyprus is solar energy, which is used extensively for water heating with the utilisation of flat-plate solar collectors. In the absence of any newer study, the annual consumption needs for 1994 are presented in Table 2.1 (Kalogirou, 1997). The value for electricity refers to the output from the power stations and not the primary fuel energy input, which was 729,400 tons of oil equivalent (TOE) of heavy fuel oil (HFO).

Because of the rapid economic development during the last decade, mainly due to the expansion in the tourist industry and the rise in the standard of living, there has been an increase in the total annual energy consumption. This is indicated in Figure 2.1, which shows the total energy consumption during the years 1986 to 1994. The slowdown in the increase of the total energy consumption in 1991, is due to the effect of the Gulf War on the tourist industry of Cyprus.

The energy consumption of various sectors of the economy in TOE, in terms of type of energy consumed in 1994, is shown in Table 2.2. This table shows that, in the domestic sector, there has been a fair balance of requirements from the three types of fuels presented. Also, Table 2.2 shows that solar energy is being used almost exclusively (93%) by the domestic sector for hot water production.

Table 2.1. Energy consumption for 1994

Energy type	Consumption (TOE)	% of total consumption
Crude	2101	0.17
LPG	48,594	3.67
Gasoline	179,997	13.59
Kerosene	252,366	19.05
Diesel	388,371	29.32
LFO	52,684	3.97
HFO	49,567	3.74
Coal	89,930	6.79
Electricity	174,718	13.19
Solar	86,480	6.53
Total	1,324,808	100.00
Note: TOE (tons of oil equivalent) = 41.8 GJ		

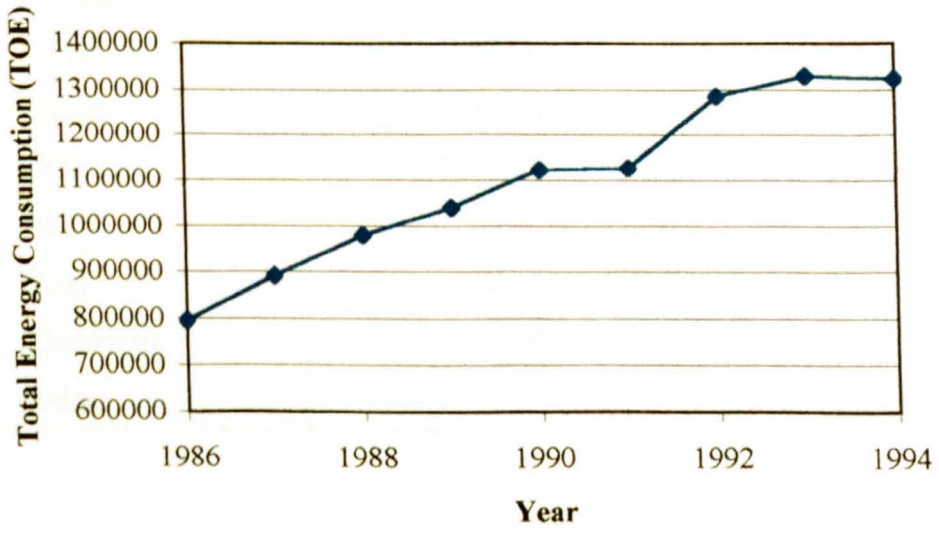

Figure 2.1. Total energy consumption for the years 1986 –1994.

Table 2.2. Energy consumption by different sectors of the economy for 1994

Sector	Fuel oil (TOE)	Electricity (TOE)	Solar (TOE)
Agricultural	64,104	5,289	--
Commercial	107,432	63,859	5,660
Domestic	63,612	58,055	80,820
Industrial	124,476	38,788	--
Transport	611,955	8,727	--
Total	971,579	174,718	86,480

Unpublished data of the Department of Statistics and Research of the Government of Cyprus for the year 2000 (Table 2.3), although not complete, show that the demand for energy is still increasing.

Table 2.3. Energy consumption for the year 2000

Energy type	Consumption (TOE)	% increase since 1994
Crude	-	-
LPG	52,771	8.5
Gasoline	206,449	14.7
Kerosene	308,350	22.2
Diesel	612,955	57.8
LFO	134,643	155.6
HFO	-	-
Coal	-	-
Electricity	212,900	21.9
Solar	-	-

The considerable rise in diesel consumption is due to the tremendous increase in the number of private cars especially those which use diesel as fuel.

An analysis of the available data, for the year 1993, shows that 34% of the total energy consumption was used for domestic purposes. The contribution of the various types of fuel used for domestic purposes, is shown in Figure 2.2.

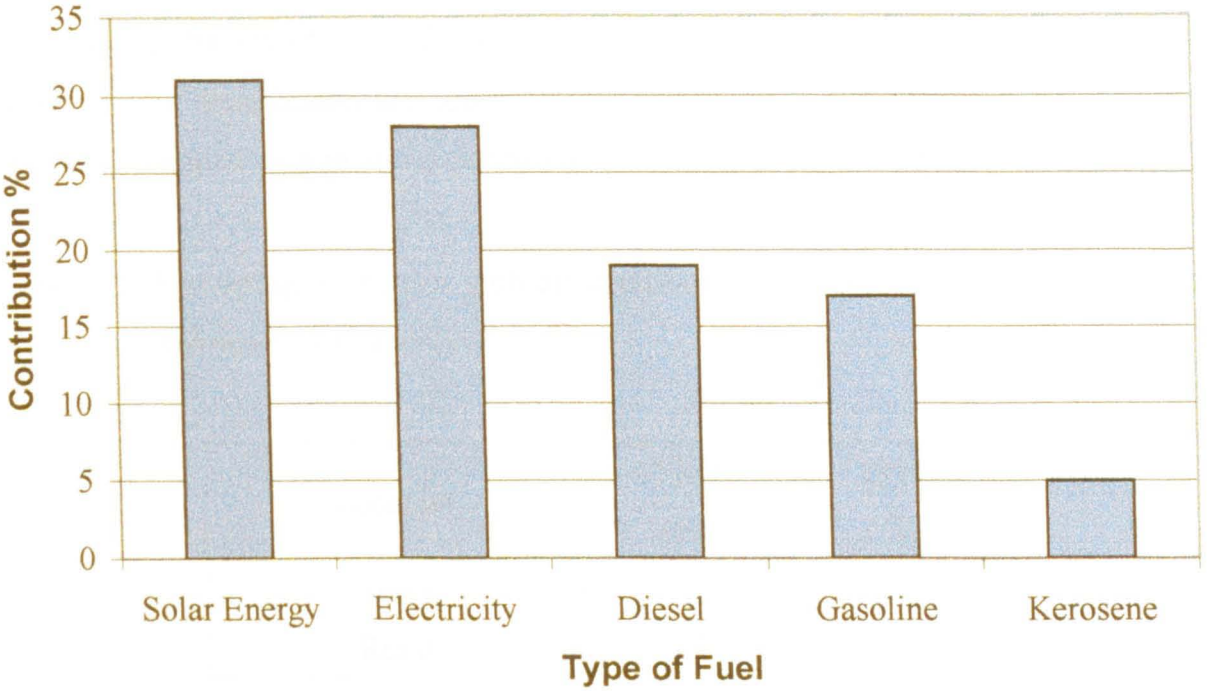

Figure 2.2. The contribution of various types of fuel, used for domestic purposes, for 1993.

Table 2.4 was constructed from data analysed by the Department of Statistics and Research of the Government of Cyprus (Research on family budgets 1996/97, 1999) and shows the percentage of houses in Nicosia district, with central heating, for the years 1992 and 1997. Unfortunately no newer data can be presented since the next study concerning the households for Nicosia will be conducted in 2003.

Table 2.4. Percentage of houses with central heating, in Nicosia district, for the years 1992 and 1997

Location	1992 (%)	1997 (%)
Town	31.6	46.5
Rural	11.6	29.3

Similarly, the corresponding percentage of houses for Nicosia district, with air conditioning, for the years 1992 and 1997 are shown in Table 2.5. It must be noted that about 10% of these houses are equipped with central air conditioning systems. The rest 90% are equipped with room air conditioning units (split and wall types).

Table 2.5. Percentage of houses with air conditioning devices, in Nicosia district, for the years 1992 and 1997

Location	1992 (%)	1997 (%)
Town	18.2	30.2
Rural	3.2	8.6

The above available data, although not collected specifically for the determination of the heating and cooling needs, can lead to the following conclusions:

(a) From Figure 2.2, it is shown that the energy used for heating purposes is approximately equal to the consumption of diesel and kerosene, which is mainly used as fuel for heating. To these figures an 11% of the consumption of electricity for domestic needs must be added, since this amount is spent for off-peak heating (Centre of Applied Research of Cyprus College, 1994). Therefore the total amount used for heating purposes represents 27% of the domestic needs for energy. Since, as mentioned above, the domestic needs for energy for 1993 represents the 34% of the total energy consumption, it is concluded that 9.2% of the total energy needs for Cyprus for that year was spent for heating purposes. From the data of the Department of Statistics and Research of the Government of Cyprus for 1997, every household in Nicosia district, spends on average C£67 for heating purposes. Table 2.4 indicates that roughly 45% of the houses in that area are fitted with central heating. Therefore on average, every household fitted with central heating spends approximately C£167.5 for fuel.

(b) There is no indication about energy used for cooling purposes in the domestic sector. At present this energy should be quite small, since only 3% of the dwellings in the Nicosia town area are fitted with central air conditioning devices. Another 27.2% of the dwellings in Nicosia are fitted with room air conditioners, which are used for only a few hours every day in the summer.

(c) In recent years, however, there has been an increasing trend in providing central heating and split air conditioning systems to domestic dwellings. For the period 1992 to 1997 the rate of increase of central heating installations has been 47% and that for air conditioning 66%.

(d) All the above figures show the importance of careful design of domestic dwelling to reduce energy consumption. In this way the accurate prediction of heating and cooling loads and the correct sizing of equipment should facilitate this process.

2.2 EVOLUTION OF DOMESTIC DWELLINGS IN CYPRUS

Traditional Cypriot houses were developed through experience to meet the everyday needs of the occupants and provide comfort. Availability of materials, functionality, climate, topography and style were the major factors considered. The building materials were chosen according to their local availability and consequently the buildings were in harmony with the environment. In places like the mountain areas, stones that were the prevailing material were used for building the walls. Wood, bush branches, soil and clay tiles were used for the construction of the roof. In the valleys like Mesaoria, which is the area around the capital Nicosia, the stones were replaced with mud mixed with straw for the construction of the walls. The walls were also covered with gypsum plastering on both sides. Additionally, marble plates were placed on the top end of the walls, projecting to the outer sides, to protect the wall surfaces from the rain (Figure 2.3).

Figure 2.3. Roof and wall of a Mesaoria house.

The foundation of these buildings was very simple. A shallow trench, 0.50 m wide by 0.50 m deep was usually excavated along the length of the walls. The trench was filled with large blocks of stone and was raised about 0.50 m above the ground level. In this way a stable base for the wall was constructed and the wall was also protected from the rain-water and moisture (Figure 2.4).

Figure 2.4. Stone blocks were used for the wall foundation.

The mud and straw blocks used for wall construction had standard dimensions of 0.30 m (length) by 0.45 m (width) by 0.05 m (thickness). This wall thickness was necessary since no supporting columns were used for the roof and the walls took all the weight. The height of the house was also important. In the middle the roof reached 5 m to 6 m and at the corners about 4 m. In this way the ratio of volume to the external area exposed to solar radiation is increased. This increase is preferable for a building that it is desired to heat up slowly. During summer, in low latitudes, the surface most exposed to solar radiation is the roof. High ceilings, which are traditionally found in hot climates, have little effect on the airflow pattern but they allow thermal stratification and decrease the heat transfer through the roof (Dimoudi, 1997).

The doors were rather high and the window openings, narrow and tall. The tall openings were necessary in order to increase the night ventilation effect and keep the house as cool as possible during the summer. The good insulation of the house and its large volume kept the building cool in the summer and warm in winter. The orientation of the buildings was usually dictated by parameters not related to energy factors (e.g. location of roads, plot size and shape etc.). Whenever possible bedrooms were located in a northwest direction to take advantage of the western winds which usually prevail during summer afternoons and evenings.

The occupation of the dwellers was the next important factor considered in the design of the house. In the area of Nicosia, in the Mesaoria valley, where the present study will focus, the inhabitants were dealing mainly with the agriculture of wheat and barley and were raising goats and sheep until the early years of the 20th century. For this reason houses were constructed in such a way so as to provide shelter to humans and animals at the same time. Figure 2.5, shows the basic design of this house and Figure 2.6 shows photographs of the front and rear view of an actual building.

The design was very simple. The front part of the house consisted of a main entrance hall, through which two main rooms were accessed, one at each side. One room was usually used for sleeping and the other for sitting and dining. There was no wall enclosing the main entrance hall at the backside and the yard could be reached through that area. In the yard and adjacent to one wall, one or two additional rooms were built, in which all the every day jobs, like cooking and washing were carried out.

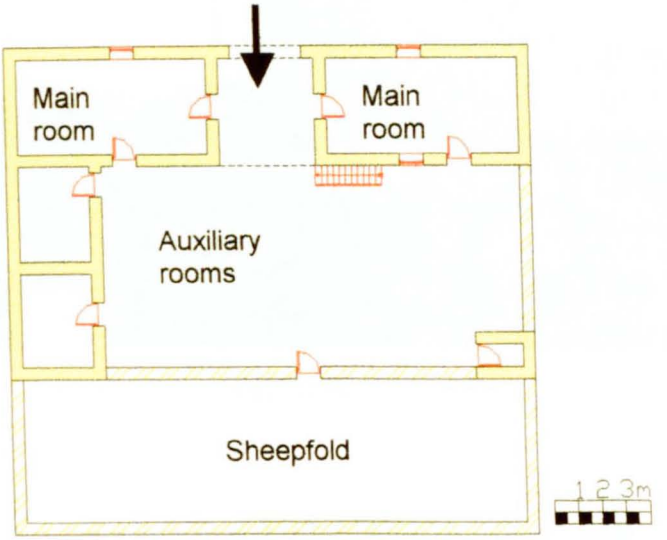

Figure 2.5. Basic design of Mesaoria house.

The flocks were passed from the main entrance and kept in the sheepfold at the backside of the house. The whole construction was enclosed in tall walls isolating the house area, for safety and protection.

In the period between 1920 and 1960 the occupation of the inhabitants of Mesaoria changed. Instead of growing crops and raising animals, they worked as builders and quarried soft stones from the near-by area, for the construction works. Since their needs changed, the form of their houses changed as well.

The design of the houses of this time is shown in Figure 2.7. As it is seen, the basic shape of the house of the older generation was kept unchanged, with two extra rooms added at the back of the house for a more comfortable life in the place of the sheepfolds.

(a) front view

(b) rear view

Figure 2.6. Front and rear view of a typical Mesaoria house before 1920.

The constructional materials remained basically the same since, they were cheap and by experience, they provided a comfortable house environment.

After the independence of Cyprus in 1960, the life of the inhabitants and their needs changed again. The sudden tourist development and the flow of foreign ideas, led to alteration of the inhabitants needs and character. New styles and morphological standards were used destroying the indigenous traditional values. Designers introduced plans from the west, which were used in industrialised societies. These designs have been applied to the Cypriot environment with no changes to fit the social or climatic conditions, loosing the comfort offered by the traditional house environment. Others, in an effort to keep the Cypriot character to the houses, imposed traditional patterns like arcades and facades on new buildings destroying the essence of Cypriot architecture.

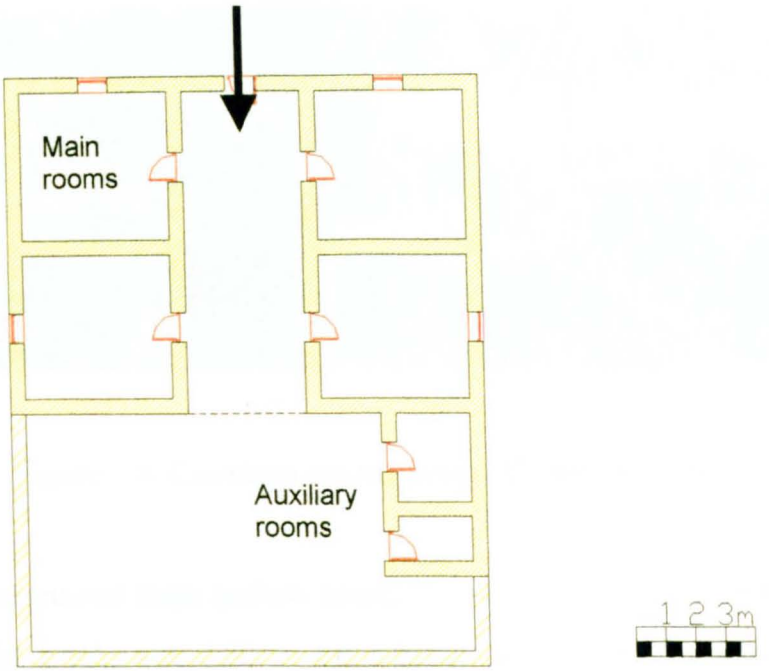

Figure 2.7. Basic design of the house of 1920 to 1960.

The residential buildings during this period were constructed from hollow bricks, resulting in a finished wall thickness of 0.25 m, and had a flat concrete roof of 0.15 m in thickness with no insulation. These constructions were cheap and offered low levels of comfort.

The sudden increase of the population in the towns and the desolation of the villages, especially after the Turkish invasion in 1974, was the next step that changed completely the character of the dwellings. Multi-storey buildings were built and the absence of town planning and regulations had a bad influence on the environment.

During the last two decades building codes and town planning have been introduced but are not yet as strict as in the rest of Europe. The present trend is to construct large houses that may be well in excess of the needs of the occupants with a lot of impressive elements for decoration (Figure 2.8).

The construction method is basically the same all over Cyprus. The structure consists of the foundations, the columns, the beams and slabs. The bearing structure is made of reinforced concrete (Figure 2.9) made of a mixture of Portland cement, fine aggregate (sand) and coarse aggregate.

Figure 2.8. Common contemporary Cypriot houses.

The walls are constructed from hollow bricks, covered with plaster on both sides. The dimensions of the bricks are 0.30 m by 0.20 m by 0.10 m. External walls have a thickness of about 0.25 m and internal walls a thickness of about 0.15 m. During the resent years, there is a trend to use cavity external walls, constructed of two brick walls with a layer of insulation of about 0.05 m in-between, as illustrated in Figure 2.10. The total thickness of the insulated external wall is about 0.30 m.

Figure 2.9. Private dwellings at the construction stage.

The floors are made of concrete slabs, covered with a layer of sand or screed of about 0.10 m in which all plumbing and other services are laid. The floor finishing consists of a layer of mortar usually covered with tiles, marble, or granite blocks.

Flat roofs consist of a concrete slab, usually 0.15 m in thickness, with an additional layer of plaster of 0.03 m at the underside, applied if the slab is not fair-faced i.e., smooth without irregularities at the underside. The roof is usually water proofed with a thin layer of bitumen and painted in white or aluminium colour.

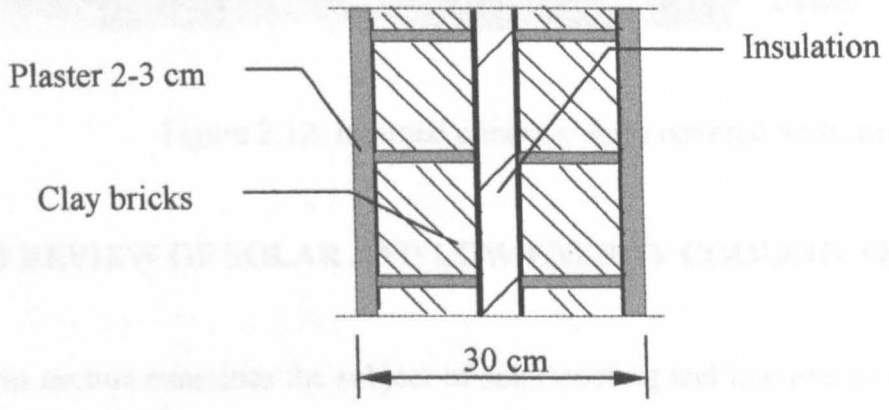

Figure 2.10. External wall detail.

More recently inclined roofs have become prominent. They are made of fair-faced slab, insulated very lightly and covered with a layer of mortar and roof tiles (Figures 2.11 and 2.12). This method is used because there is no need for any special skills and therefore results in a simpler and cheaper construction compared to the wooden sloping roof structure.

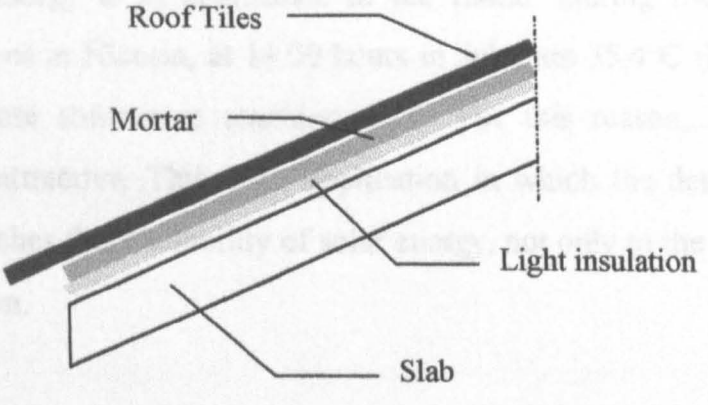

Figure 2.11. Roof construction detail.

Figure 2.12. Inclined concrete slabs covered with roof tiles.

2.3 REVIEW OF SOLAR AND LOW ENERGY COOLING TECHNOLOGIES

This section examines the subject of solar cooling and low energy cooling technologies. A brief review of various cooling systems is presented including solar sorption cooling, solar-mechanical systems, solar related air conditioning, and other low energy cooling technologies. The relative efficiencies and applications of the various technologies are presented. These technologies can be utilised to reduce both the energy consumption and environmental impact of mechanical cooling systems.

2.3.1 Solar Cooling Systems

Cyprus is called the "Sun Island" because sun shines for about 300 days per year. This means that solar energy is in abundance in the island. During the summer, mean monthly temperatures in Nicosia, at 14.00 hours in July, are 35.4°C (Kalogirou, 1991) with the temperature sometimes reaching 42°C. For this reason, solar cooling of buildings is quite attractive. This is an application in which the demand for cooling energy closely matches the availability of solar energy, not only to the seasonal but also to the daily variation.

Solar cooling systems can be classified into three categories: namely, solar sorption cooling, solar-mechanical systems and solar-related systems

(a) Solar Sorption Cooling

Sorbents are materials that have an ability to attract and hold other gases or liquids. This characteristic makes them very useful in chemical separation processes. Desiccants are sorbents that have a particular affinity for water. The process of attracting and holding moisture is described as either absorption or adsorption, depending on whether the desiccant undergoes a chemical change as it takes on moisture. Absorption changes the desiccant as for example the table salt, which changes from a solid to a liquid as it absorbs moisture. Adsorption, on the other hand, does not change the desiccant except by the addition of the weight of water vapour, similar in some ways to a sponge soaking up water (ASHRAE, 1989).

Absorption systems are similar to vapour-compression air conditioning systems but differ in the pressurisation stage. In general, an evaporating refrigerant is absorbed by an absorbent on the low-pressure side. Combinations include lithium bromide-water ($LiBr-H_2O$) where water vapour is the refrigerant and ammonia-water (NH_3-H_2O) systems where ammonia is the refrigerant.

The pressurisation is achieved by dissolving the refrigerant in the absorbent in the absorber section (Figure 2.13). Subsequently, the solution is pumped to a high pressure with an ordinary liquid pump.

The addition of heat in the generator is used to separate the low-boiling refrigerant from the solution. In this way, the refrigerant vapour is compressed without the need of large amount of mechanical energy that vapour-compression air conditioning systems demand.

The remainder of the system consists of a condenser, expansion valve and evaporator, which function in a similar way as in a vapour-compression air conditioning system.

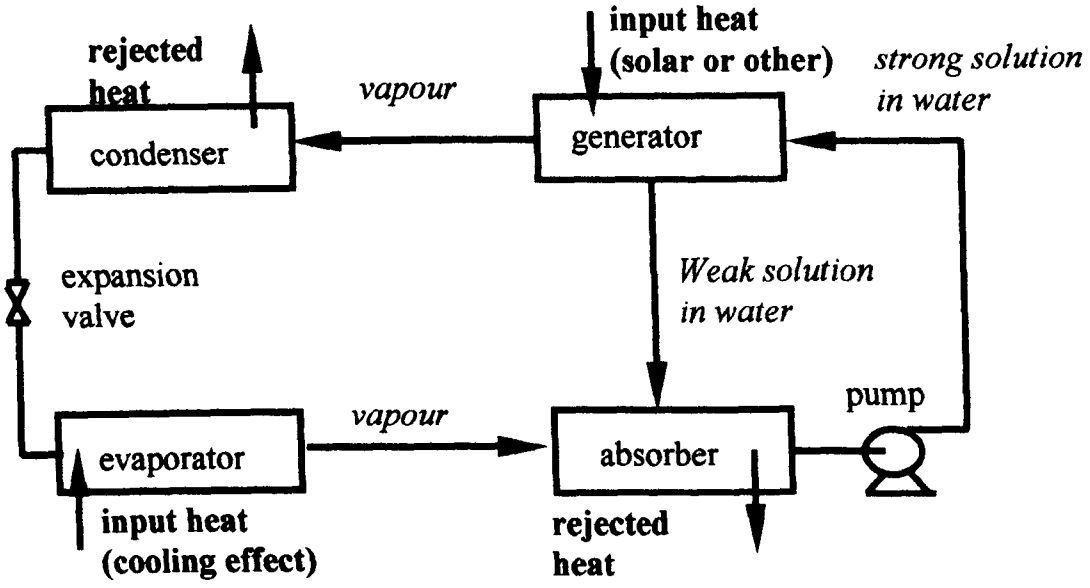

Figure 2.13. Basic principle of the Absorption Air Conditioning System.

The NH_3-H_2O system is more complicated than the LiBr-H_2O since it needs a rectifying column that assures that no water vapour enters the evaporator where it could freeze. The NH_3-H_2O system requires generator temperatures in the range of 125°C to 170°C with air-cooled absorber and condenser and 95°C to 120°C when water-cooling is used. These temperatures cannot be obtained with flat-plate collectors. The coefficient of performance (COP), which is defined as the ratio of the cooling effect to the heat input is between 0.6 to 0.7 for single effect (stage) systems. The LiBr-H_2O system operates at a generator temperature in the range of 70°C to 95°C with water used as a coolant in the absorber and condenser and has COP higher than the NH_3-H_2O systems, 0.6 to 0.8 for single effect systems (Duffie and Beckman, 1991). A disadvantage of LiBr-H_2O systems is that their evaporator cannot operate at temperatures much below 5°C since the refrigerant is water vapour.

Adsorption cooling is the other group of sorption air conditioners that utilises an agent (the adsorbent) to adsorb the moisture from the air (or dry any other gas or liquid) and then uses the evaporative cooling effect to produce cooling. Solar energy can be used to regenerate the drying agent. Solid adsorbents include silica gels, zeolites, synthetic zeolites, activated aluminas, carbons and synthetic polymers (ASHRAE, 1997). Liquid adsorbents can be triethylene glycol solutions of lithium chloride and lithium bromide solutions.

Many cycles have been proposed for adsorption cooling. The principle of operation of a typical system is indicated in Figure 2.14. The process followed at the points from 1 to 9 of Figure 2.14, is traced on the psychrometric chart of Figure 2.15. Ambient air is heated and dried by a dehumidifier from point 1 to 2, regeneratively cooled by exhaust air from 2 to 3, evaporatively cooled from 3 to 4 and introduced into the building. Exhaust air from the building is evaporatively cooled from 5 to 6, heated to 7 by the energy removed from the supply air in the regenerator, heated by solar or other source to 8 and then passed through the dehumidifier where it regenerates the desiccant.

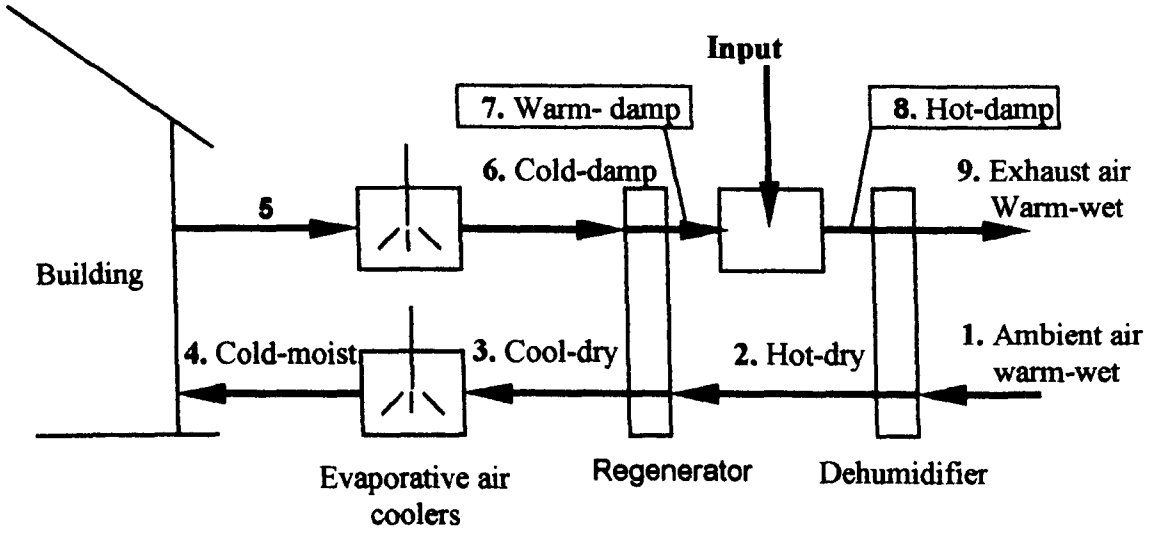

Figure 2.14. Schematic of a solar adsorption system.

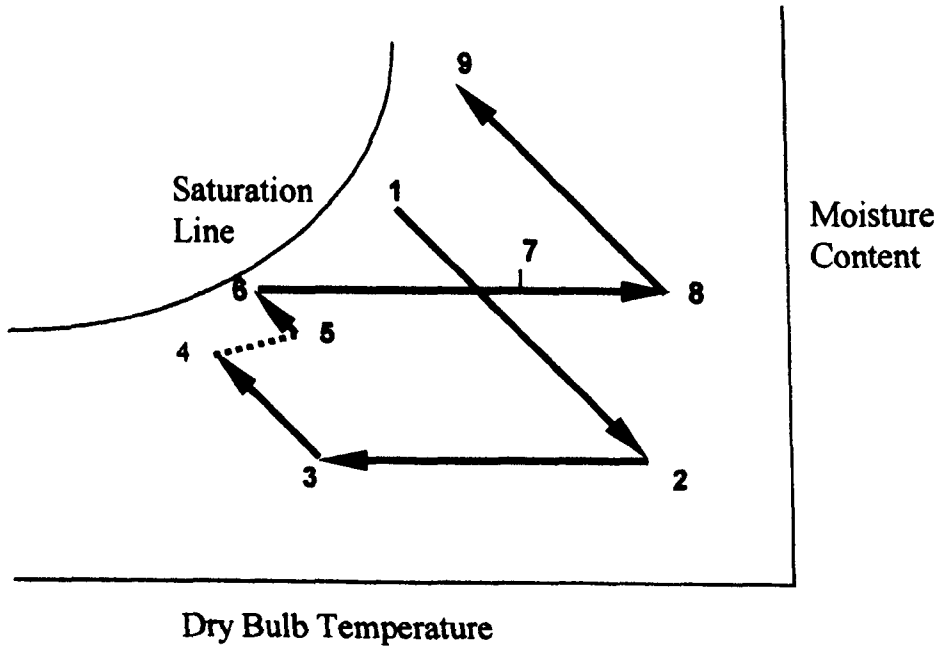

Figure 2.15. Psychrometric diagram of a solar adsorption process.

The selection of the adsorbing agent depends on the size of the moisture load and the application.

Rotary solid desiccant systems are the most common for continuous removal of moisture from the air. The desiccant wheel rotates through two separate air streams. In the first stream the process air is dehumidified by adsorption, which does not change the physical characteristics of the desiccant, while in the second stream the reactivation or regeneration air, which is first heated, dries the desiccant. A schematic of a possible solar-powered adsorption system is illustrated in Figure 2.16.

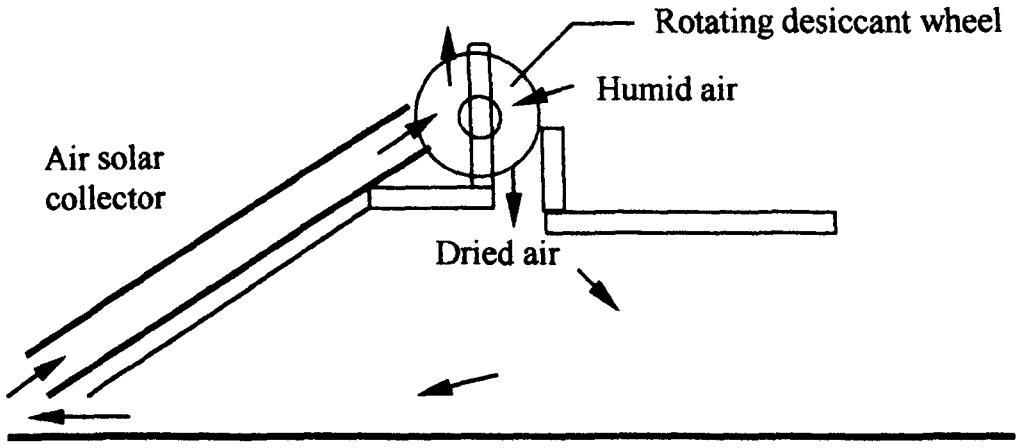

Figure 2.16. Solar adsorption cooling system.

When the drying agent is a liquid, such as triethylene glycol, the agent is sprayed into an absorber where it picks up moisture from the building air. Then it is pumped through a sensible heat exchanger to a separation column where it is sprayed into a stream of solar heated air. The high temperature air removes water from the glycol, which then returns to the heat exchanger and the absorber. Heat exchangers are provided to recover sensible heat, maximise the temperature in the separator and minimise the temperature in the absorber. This type of cycle is marketed commercially and used in hospitals and large installations (Duffie and Beckman, 1991).

The energy performance of these systems depends on the system configuration, geometries of dehumidifiers, properties of adsorbent agent, etc., but generally the COP of this technology is around 1.0.

(b) Solar-Mechanical Systems

These systems utilise a solar-powered prime mover to drive a conventional air-conditioning system. This can be done by converting solar energy into electricity by means of photovoltaic devices and then utilise an electric motor to drive a vapour compressor. The photovoltaic panels have a low efficiency (about 10%), which results in low overall efficiencies for the system.

The solar-powered prime mover can also be a Rankine engine. In a typical system, energy from the collector is stored, then transferred to a heat exchanger and finally energy is used to drive the heat engine. The heat engine drives a vapour compressor, which produces a cooling effect at the evaporator. As shown in Figure 2.17, the efficiency of the solar collector decreases as the operating temperature increases, whereas the efficiency of the heat engine of the system increases as the operating temperature increases. The two efficiencies meet at a point (A in Figure 2.17) giving an optimum operating temperature for steady state operation. The combined system has overall efficiencies between 17 and 23%.

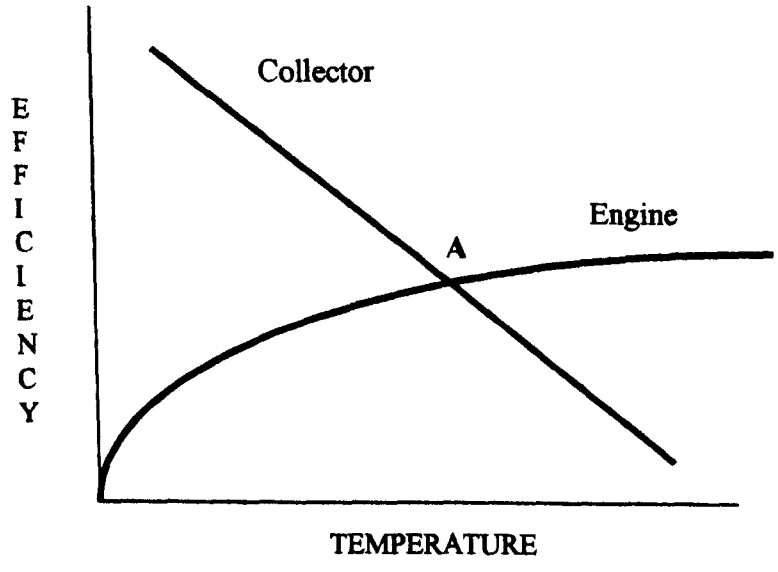

Figure 2.17. Collector and Power cycle efficiencies as a function of operating temperature.

Due to the diurnal cycle, the cooling load varies and also the storage tank temperature changes through the day. Therefore, designing such a system presents appreciable difficulties. When a Rankine heat engine is coupled with a constant speed air conditioner, the output of the engine seldom matches the input required by the air conditioner. Therefore, auxiliary energy must be supplied when the engine output is less than that required, or otherwise, excess energy may be used to produce electricity for other purposes.

(c) Solar Related Air Conditioning

Some components of systems installed for the purpose of heating a building can also be used to cool it but without the direct use of solar energy. Examples of these systems can be:

1. *Heat pumps.* A heat pump is a device that pumps heat from a low temperature source to a higher temperature sink. Heat pumps are usually vapour compression refrigeration machines where, the evaporator can take heat into the system at low temperature and the condenser can reject heat from the system at high temperature. In the heating mode a heat pump delivers thermal energy from the condenser for space heating and can be combined with solar heating. In the cooling mode the evaporator extracts heat from the air to be conditioned and rejects heat from the condenser to the atmosphere with solar energy not contributing to the energy for cooling.

2. *Rock bed regenerator.* Rock beds (or pebble beds) storage units of solar air heating systems can be night-cooled during summer to store "cold" for use the following day. This can be accomplished by passing outside air during the night when the temperatures and humidities are low, through an optional evaporative cooler, through the pebble bed and to the exhaust. During the day, the building can be cooled by passing room air through the pebble bed.

3. *Alternative cooling technologies or passive systems.* Passive cooling is based on the transfer of heat by natural means from a building to environmental sinks like clear skies, the atmosphere, the ground and water. The transfer of heat can be by

radiation, naturally occurring wind, airflow due to temperature differences, conduction to the ground or conduction and convection to bodies of water. The options depend on the climate type. Finally, other methods of cooling load reduction including hybrid methods, operated with mechanical energy and by passive means, can also be used.

2.3.2 Other Low Energy Cooling Technologies

(a) Night Cooling

In this system, night cool air is used to remove heat from the interior of a building. The outdoor air can enter into the building naturally, mechanically or with both methods. During natural ventilation (Figure 2.18), air enters into the building through intentional openings left to utilise either the indoor/outdoor temperature differences (stack effect) or the wind pressures.

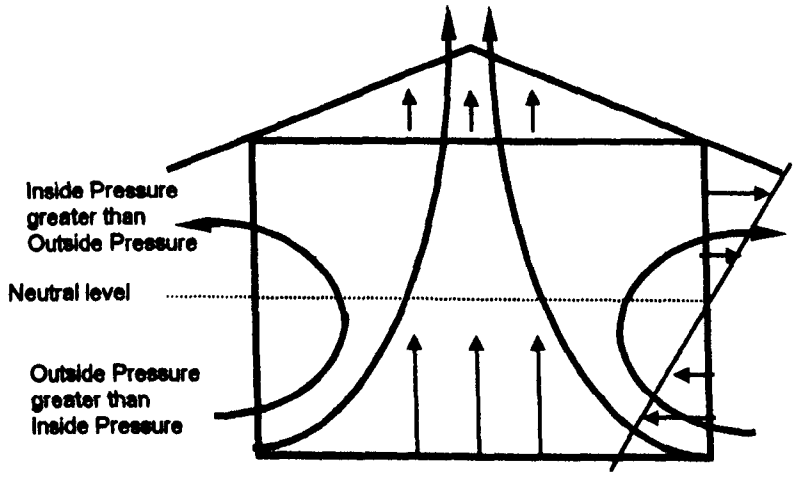

Figure 2.18. Air circulation due to stack effect. Arrows indicate pressure differences (ASHRAE, 1997).

Figure 2.19, indicates how the prevailing wind is utilised in a traditional Iraqi house, to take advantage of the night cool air and provide a cooler environment during the day. In mechanical ventilation a fan and a duct system can be used to force air into the building.

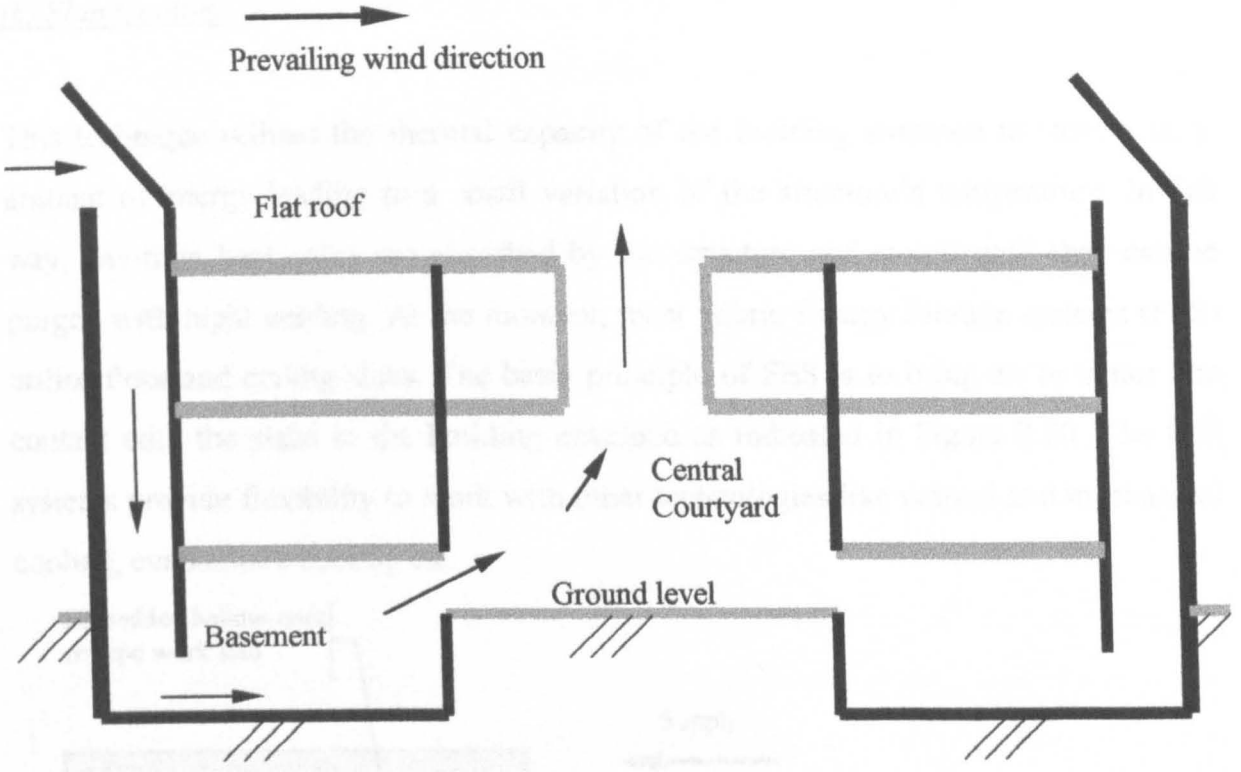

Figure 2.19. Schematic view of a traditional Iraqi dwelling, utilising the wind flow.

Natural night cooling is an unreliable method for air quality, quantity and controllability. Its effect depends largely on the magnitude of heat gains and ventilation rates.

Night cooling with mechanical ventilation is much more controllable and is especially suited for unoccupied buildings during the night (office buildings), where relatively high air flows can be used to maximise the cooling effect.

The building mass is of great importance when night cooling is used, since a large mass will absorb greater amounts of heat load during the day. Also, the interior surfaces of the building need to be exposed as much as possible to the airflow and lightweight materials such as carpets and false ceilings should be replaced by installing thermally-heavy dry coatings. In some cases, better results can be obtained when the airflow is directed through a false floor or through a cavity within the building.

(b) Slab Cooling

This technique utilises the thermal capacity of the building structure to store a large amount of energy leading to a small variation of the structure's temperature. In this way, day-time heat gains are absorbed by the structure and stored until they can be purged with night cooling. At the moment, most Fabric Energy Storage systems (FES) utilise floor and ceiling slabs. The basic principle of FES is to bring air or water into contact with the slabs in the building envelope as indicated in Figure 2.20. The FES systems provide flexibility to work with other technologies like natural and mechanical cooling, evaporative cooling etc.

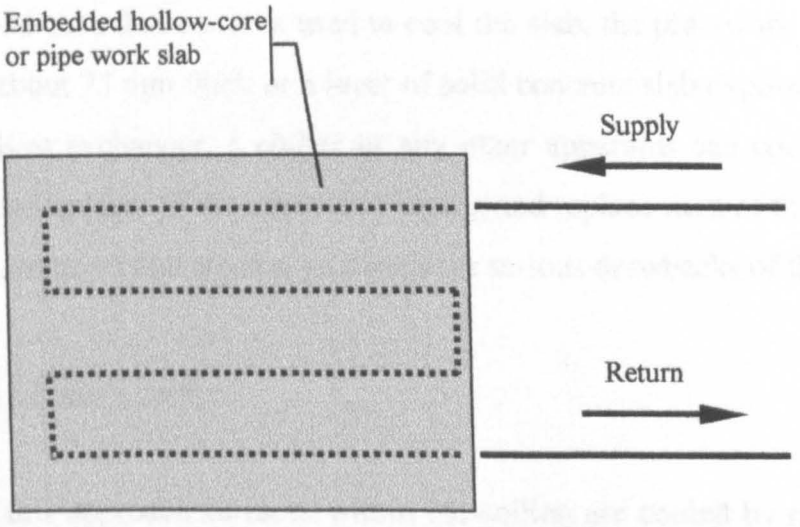

Figure 2.20. Basic principle of Fabric Energy Storage system (FES).

Air slab cooling techniques include (Winwood *et al.*, 1997):

1. The FES slab (Trade name Termodeck). This is a prefabricated rectangular concrete block with typical dimensions of 4 m length by 1.2 m width by 0.3 m depth. The interconnection of the hollow core slabs establishes the air paths, through which cooled or heated air is discharged via ceiling diffusers to the indoor spaces.

2. The plenum-and-slab system, which provides air through hollow core floor slabs, interconnected between a number of large air plenums. Operating experience indicated that this system is only suitable for floor slabs at the ground floor.

3. The hollow-core screed, which produces cross air paths between a layer of hollow-core screed and a solid concrete slab. The advantage of this system is that it can be retrofitted into an existing building and consists of square grids of semicircles, 37.5 mm in radius, covered with 75 mm thick screed. The narrow air channel design of this method may present difficulties in maintenance.

In general, the above methods provide low capital and operating cost but their potential depends on the level of overnight ambient air temperature and provide sensible cooling only.

In the case that water is used to cool the slab, the pipe-work can be in a layer of screed of about 75 mm thick or a layer of solid concrete slab exposed to the conditioned space. A heat exchanger, a chiller or any other apparatus can cool the circulating water but water leakage of the embedded piping and replacement of the embedded pipe-work due to corrosion and erosion problems are serious drawbacks of the method.

(c) Chilled Ceilings

In this approach surfaces within the ceiling are cooled by chilled water circulation for the removal of heat gains, leaving ventilation and humidity control to the air-distribution system.

An essential feature of these systems is that the entering chilled water temperature should be above the room dew-point by at least 1.5°C to allow for control tolerance, in order to avoid condensation from forming on the cooling surfaces. Typically, chilled ceiling systems have a flow water temperature of 14-15°C and a temperature increase across the exchange device of 2-3°C (Martin and Oughton, 1995).

The cooling surfaces may take any number of forms and are classified into radiant panels, convective panels and chilled beams.

In the case of radiant and convective panels, the cooling surface covers large areas of the ceiling. The radiant panels depend mainly on radiation heat transfer between their surface and the conditioned space, and can be of a metal or concrete slap type. The

radiant panels can be embedded within the false ceiling or be accommodated in shallow ceiling voids (Figure 2.21).

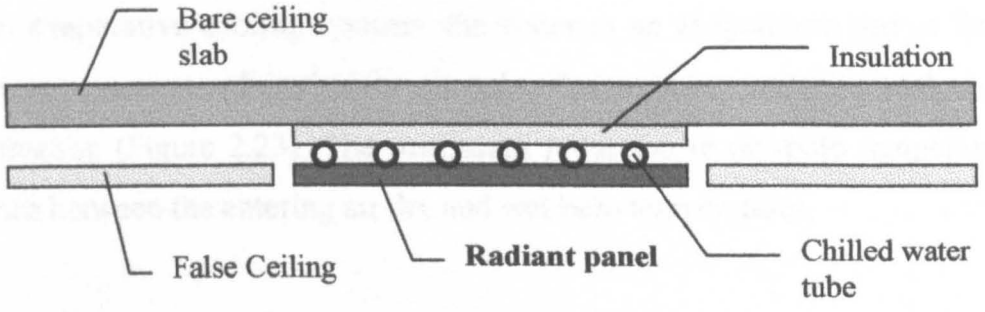

Figure 2.21. Radiant panel embedded within the false ceiling.

Convective panels can be finned pipe coils, which are located within the void above the false ceiling. In this case the false ceiling is perforated or slotted with at least 20% free area, to the room space. Warm air rising into the ceiling void is cooled by the coil and then falls down in the room due to its higher density.

Chilled beams work in a similar manner to convective panels. In this case, the finned coils are located into a unit, which can also supply ventilation air (Figure 2.22).

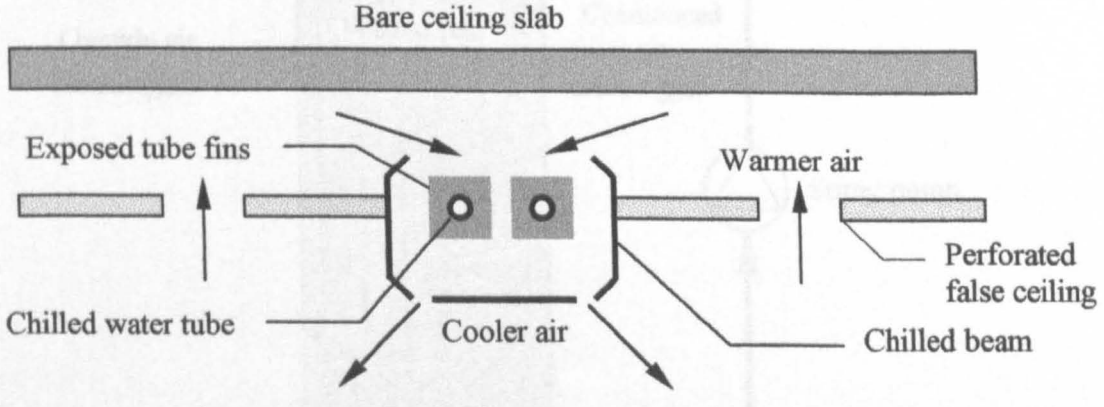

Figure 2.22. Chilled beam.

(d) Evaporative Air Coolers

Evaporative air-cooling is achieved by evaporating water at ambient temperature into the air stream. With this method the air dry-bulb temperature is reduced along a line of constant wet-bulb temperature, resulting in an increase of the latent heat and air moisture content. Evaporating cooling can be achieved through direct air-cooling,

indirect air-cooling, a combination of both and can also be combined with mechanical refrigeration systems and desiccant technologies.

In direct evaporative cooling systems, the water in an evaporative pad or from a fine water spray, evaporates directly into a supply of air stream, producing both cooling and humidification (Figure 2.23). The maximum reduction in dry-bulb temperature is the difference between the entering air dry and wet bulb temperatures.

When the air is saturated the air is cooled to the wet-bulb temperature and the process is 100% effective. System effectiveness is the depression of the dry-bulb temperature of the air leaving the apparatus divided by the difference between the dry and wet-bulb temperatures of the air. Evaporative cooling systems may be 85 to 90% effective. Direct evaporative cooling when used together with mechanical refrigeration can reduce cooling costs by between 25 and 40% (ASHRAE, 1995).

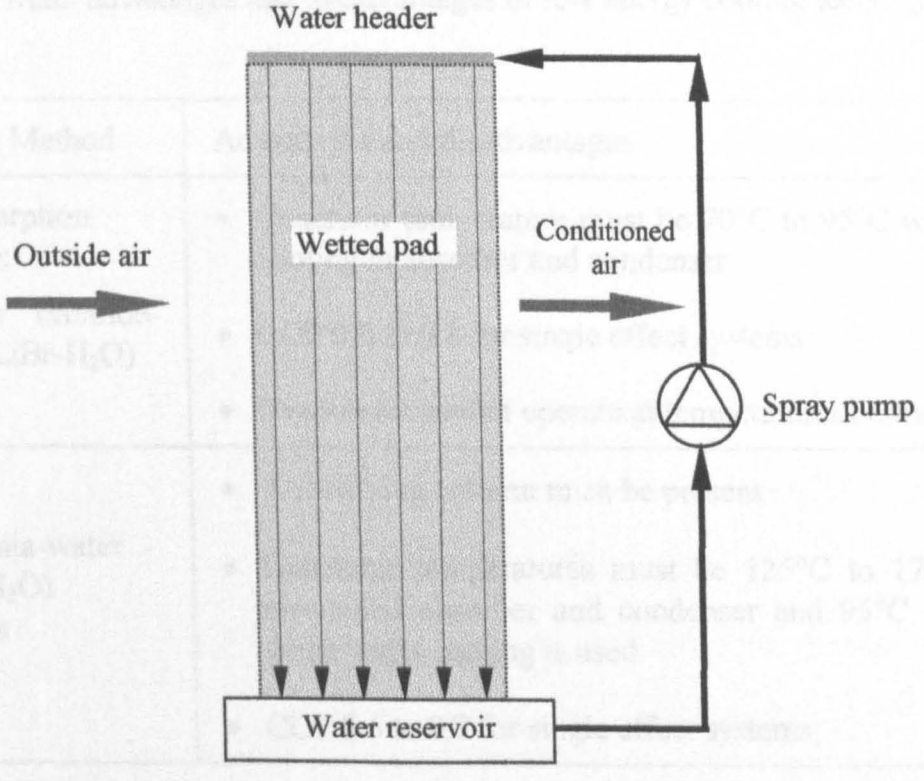

Figure 2.23. Direct evaporative cooling diagram.

Indirect evaporative air-cooling evaporates water into a secondary air stream through the channels of a heat exchanger. The heat exchanger cools air flowing in a primary stream. This results in sensible cooling only. Except in extreme dry climates, most indirect systems require several stages to further cool the primary air entering the conditioned spaces.

Indirect evaporative cooling can precede a direct evaporative stage and can reduce in this way the entering dry and wet bulb temperatures before the air enters the direct evaporative cooling unit (ASHRAE, 1995).

2.3.3 System Evaluation

Table 2.6, summarises the advantages and disadvantages of the cooling methods described above as well as their performance and main uses.

Table 2.6. Main advantages and disadvantages of low energy cooling techniques

Cooling Method	Advantages and disadvantages
Solar Sorption Cooling: Lithium bromide-water ($LiBr-H_2O$)	• Generator temperature must be 70°C to 95°C with water cooling in absorber and condenser • COP 0.6 to 0.8 for single effect systems • Evaporator cannot operate at temperatures below 5°C
Ammonia-water (NH_3-H_2O) systems	• A rectifying column must be present • Generator temperatures must be 125°C to 170°C with air-cooled absorber and condenser and 95°C to 120°C when water cooling is used • COP 0.6 to 0.7 for single effect systems

Table 2.6. Main advantages and disadvantages of low energy cooling techniques (cont.)

Cooling Method	Advantages and disadvantages
Desiccant cooling	• Independent control of humidity and temperature • Removal of certain airborne contaminants • Ability to use energy sources such as waste heat, solar power and natural gas • COP around 1.0
Solar-Mechanical Systems	• Efficiency of photovoltaic panels is very low about 10% • The solar-powered prime mover combined with a Rankine engine has low efficiency about 17 to 23%. Very expensive system viable for very large applications • Difficulty to ensure that only vapour enters the turbine since the boiler temperature changes during the day • Not steady output power
Heat pumps	• COP (useful effect/work done), between 2 and 5 • Heat pumps can be used in combination with solar energy for heating
Natural night cooling	• Unreliable air quality • Unreliable air quantity • Inefficient control of humidity and temperature • Effective for building mass in excess of 800 kg/m^2 • Provides sensible cooling only • Effective in cool, dry to semi-humid climates • Night air temperatures must be low (12-15°C)

Table 2.6. Main advantages and disadvantages of low energy cooling techniques (cont.)

Cooling Method	Advantages and disadvantages
Mechanical night cooling	• Good controllability of air flow and distribution • Extra fun energy consumption • Noise present, depending on air velocities • Additional space needed for extra flow to existing buildings (false floors or cavities in buildings) • Effective for building mass in excess of 800 kg/m^2 • Provides sensible cooling only • Used in commercial buildings
Slab Cooling	• Reduction of mechanical cooling • Utilisation of off-peak electricity • No need for suspended ceilings • High levels of human comfort • Slow thermal response to indoor load variations • Higher maintenance cost due to leakages • Provides sensible cooling only

Table 2.6. Main advantages and disadvantages of low energy cooling techniques (cont.)

Cooling Method	Advantages and disadvantages
Chilled ceilings	• Reduction of refrigeration capacity • Low energy consumption • Good acoustics and indoor air quality • Low maintenance costs • Reduction in the space required for pure air ductwork in the ceiling void • Risk of condensation • High capital cost, at least 50% higher compared to conventional air-conditioning systems • Possibility of water leakage in the ceiling installation • Active cooling surface needed is 30 to 70 % of the total ceiling area
Direct evaporative Air Coolers	• Provide relief or comfort cooling depending on weather conditions and types of building • Once-through airflow principle normally employed • Used in residential applications • Used in arid and semi-arid climates and relatively dry environments
Indirect evaporative Air Coolers	• Provides sensible cooling only • Provides relief or comfort cooling depending on weather conditions and types of building • Used in commercial buildings • Used in arid and semi-arid climates and relatively dry environments

2.3.4 Conclusions

The objective of the above work was to present various low energy cooling technologies that may be applied alone or in combination to meet the cooling needs of domestic dwellings. Due to the abundance of solar energy and the high ambient temperatures available in Cyprus a direct solar cooling system could meet a large portion of the daily cooling load. Low energy technologies such as slab cooling can be employed to minimise the daily cooling load requirements by utilising diurnal variations in temperature. Low energy cooling technologies can also be used in the intermediate seasons of autumn and spring to either absorb completely the cooling load or reduce it drastically, depending on the requirements. The adoption of these technologies however, presents a considerable challenge to both building services engineers and architects.

Further to the limitations/disadvantages of the low energy cooling technologies, presented in this section and summarised in Table 2.6, the success of low energy cooling technologies depends greatly on environmental conditions like ambient temperature and humidity. In the Cyprus environment, night time temperatures during summer are high and may exceed 24°C, therefore the effectiveness of night ventilation will be limited.

Low energy cooling technologies that require considerable amounts of water to operate, such as evaporative cooling systems are not suitable for use in Cyprus, because Cyprus suffers from water shortages and the supply is intermittent. Due to this fact water is also very expensive.

To ensure therefore, comfort conditions under the wide range of climatic conditions experience in Cyprus, an active cooling system would be required. A candidate system is absorption cooling which can make use of solar energy that is abundantly available in Cyprus in the summer months.

CHAPTER 3

THERMAL LOAD ESTIMATION

In this chapter the theory related to the building thermal load is examined. The method used in the present analysis is the heat balance, which is able to provide dynamic simulations of the building load. The basic nomenclature and the simultaneous equations used in the method are explained. An overview of the TRNSYS simulation program is presented since this is the basic tool used for the analysis of the building thermal load. Finally, the various parameters and thermal properties of structural elements used in the thesis are outlined.

3.1 THERMAL LOAD ESTIMATION

When estimating the design building thermal load, adequate results can be obtained by calculating heat losses and gains based on steady-state heat transfer analysis. For more accurate results and energy analysis, however, transient analysis must be employed since the heat gain into a conditioned space is quite variable with time, primarily because of the strong transient effects created by the hourly variation in solar radiation.

3.1.1 Basic Nomenclature

A description of the three basic terms, which are important in thermal load estimation follows:

(a) Heat Gain

Heat gain is the rate at which energy is transferred to or generated within a space and consists of sensible and latent gain. Heat gains usually occur in the following forms:

1. Solar radiation through glazing and other openings.
2. Heat conduction with convection and radiation from the inner surfaces into the space.

3. Sensible heat convection and radiation from internal objects.

4. Ventilation and infiltration.

5. Latent heat gains generated within the space.

(b) Thermal Load

The thermal load is the rate at which energy must be added or removed from a space to maintain the temperature and humidity at the design values.

The cooling load differs from the heat gain mainly because the radiant energy from the inside surfaces as well as the direct solar radiation passing into a space through openings, is mostly absorbed in the space. This energy becomes part of the cooling load only when the room air receives the energy by convection and occurs when the various surfaces in the room attain higher temperatures than the room air. This time lag depends on the storage characteristics of the structure and interior objects and is more significant when the thermal mass (product of mass and specific heat) is greater. Therefore, the peak-cooling load can be considerably smaller than the maximum heat gain and will occur much later than the maximum heat gain period. The heating load behaves in a similar manner as the cooling load.

(c) Heat Extraction Rate

The heat extraction rate is the rate at which energy is removed from the space by the cooling and dehumidifying equipment. This rate is equal to the cooling load when the space conditions are constant and the equipment is operating. Since the operation of the control systems induces some fluctuation in the room temperature the heat extraction rate will fluctuate and this will also cause fluctuations in the cooling load.

3.1.2 The Heat Balance Method

The heat balance method is the foundation for all calculation methods that can be used to estimate the cooling load. Since all energy flows in each zone must be balanced, a set of energy balance equations for the zone air and the interior and exterior surfaces of each wall, roof and floor must be solved simultaneously. The energy balance method combines various equations, such as equations for transient conduction heat transfer through walls and roofs, algorithms or data for weather conditions and internal heat gains.

To illustrate the method it can be considered that a zone consists of six surfaces, four walls a roof and a floor. The zone receives energy from solar radiation coming through windows, heat conducted through exterior walls and roof and internal heat gains due to lights, equipment and occupants. The heat balance on each of the six surfaces is generally represented by:

$$q_{i,\theta} = \left[h_{ci}\left(t_{a,\theta} - t_{i,\theta}\right) + \sum_{j=1, j\neq i}^{rs} g_{ij}\left(t_{j,\theta} - t_{i,\theta}\right) \right] A_i + q_{si,\theta} + q_{li,\theta} + q_{ei,\theta} \qquad (3.1)$$

where:

i = surface number (1 to 6)

rs = number of surfaces in the room

$q_{i,\theta}$ = rate of heat conducted into surface i at the inside surface at time θ (W)

A_i = area of surface i (m^2)

h_{ci} = convective heat transfer coefficient at interior surface i (W/m^2-K)

g_{ij} = linearised radiation heat transfer factor between interior surface i and interior surface j (W/m^2-K)

$t_{a,\theta}$ = inside air temperature at time θ (°C)

$t_{i,\theta}$ = average temperature of interior surface i at time θ (°C)

$t_{j,\theta}$ = average temperature of interior surface j at time θ (°C)

$q_{si,\theta}$ = rate of solar heat coming through the windows and absorbed by surface i at time θ (W)

$q_{li,\theta}$ = rate of heat from the lights absorbed by surface i at time θ (W)

$q_{ei,\theta}$ = rate of heat from equipment and occupants absorbed by surface i at time θ (W)

The equations governing conduction within the six surfaces cannot be solved independently of equation 3.1, since the energy exchanges occurring within the room affect the inside surface conditions, which in turn affect the internal conduction. Consequently, the above-mentioned six formulations of equation 3.1 must be solved simultaneously with the equations governing conduction within the six surfaces in order to calculate the space thermal load. Among the possible ways to model this process are numerical finite element and time series methods. Most commonly, due to the greater computational speed and little loss of generality, conduction within the structural elements is formulated using conduction transfer functions (CTFs) in the general form:

$$q_{i,\theta} = \sum_{m=1}^{M} Y_{k,m}\, t_{o,\theta-m+1} - \sum_{m=1}^{M} Z_{k,m}\, t_{i,\theta-m+1} + \sum_{m=1}^{k} F_m q_{i,\theta-m} \qquad (3.2)$$

where:

i = inside surface subscript

k = order of CTF

m = time index variable

M = the number of non-zero CTF values

o = outside surface subscript

t = temperature

θ = time

Y = cross CTF values

Z = interior CTF values

F_m = flux history coefficients

Conduction transfer function coefficients generally are referred to as response factors and depend on the physical properties of the wall or roof materials and on the scheme used for calculating them. These coefficients relate an output function at a given time to the value of one or more driving functions at a given time and at a set period immediately preceding (ASHRAE, 1997). The Y (cross CTF) values refer to the current and previous flow of energy through the wall due to the outside conditions, the Z (interior CTF) values refer to the internal space conditions and the F_m (flux history) coefficients refer to the current and previous heat flux to zone.

Equation 3.2, which utilises the transfer function concept, is a simplification to the strict heat balance calculation procedure, which could be used in this case for calculating conduction heat transfer.

It must be noted that the interior surface temperature $t_{i,\theta}$ is present in both equations 3.1 and 3.2 and therefore a simultaneous solution is required. In addition, the equation representing the energy balance on the zone air must also be solved simultaneously. This can be calculated from the cooling load equation:

$$q_\theta = \left[\sum_{i=1}^{m} h_{ci}\left(t_{i,\theta} - t_{a,\theta}\right)\right] A_i + \rho\ c_p Q_{i,\theta}\left(t_{0,\theta} - t_{a,\theta}\right) + \rho\ c_p Q_{v,\theta}\left(t_{v,\theta} - t_{a,\theta}\right) + q_{s,\theta} + q_{l,\theta} + q_{e,\theta} \tag{3.3}$$

where:

$t_{a,\theta}$ = inside air temperature at time θ (°C)

$t_{o,\theta}$ = outdoor air temperature at time θ (°C)

$t_{v,\theta}$ = ventilation air temperature at time θ (°C)

ρ = air density (kg/m^3)

c_p = specific heat of air (J/kg-K)

$Q_{i,\theta}$ = volume flow rate of outdoor air infiltrating into the room at time θ (m^3/s)

$Q_{v,\theta}$ = volume rate of flow of ventilation air at time θ (m^3/s)

$q_{s,\theta}$ = rate of solar heat coming through the windows and convected into the room air at time θ (W)

$q_{l,\theta}$ = rate of heat from the lights convected into the room air at time θ (W)

$q_{e,\theta}$ = rate of heat from equipment and occupants convected into the room air at time θ (W)

3.1.3 The Transfer Function Method

The ASHRAE Task Group on Energy Requirements developed the general procedure referred as the Transfer Function Method (TFM). This approach is a method that simplifies the calculations, can provide the loads originating from various parts of the building and can be used to determine the heating and cooling loads.

The method is based on a series of conduction transfer functions (CTFs) and a series of room transfer functions (RTFs). The CTFs are used for calculating wall or roof heat conductions while the RTFs are used for load elements that have radiant components such as lights and appliances. These functions are response time series, which relate a current variable to past values of itself and other variables in periods of one-hour.

(a) Wall and Roof Transfer Functions

Conduction transfer functions are used by the TFM to describe the heat flux at the inside of a wall, roof, partition, ceiling and floor. Combined convection and radiation coefficients on the inside (8.3 $W/m^2 K$) and outside surfaces (17.0 $W/m^2 K$) are utilised by the method. The approach uses sol-air temperatures to represent outdoor conditions and assumes constant indoor air temperature. Thus the heat gain though a wall or roof is given by:

$$q_{e,\theta} = A\left[\sum_{n=0} b_n\left(t_{e,\theta-n\delta}\right) - t_{rc}\sum_{n=0} c_n - \sum_{n=1} d_n\left(q_{e,\theta-n\delta}/A\right)\right] \qquad (3.4)$$

where:

$q_{e,\theta}$ = heat gain through wall or roof, at calculation hour θ (W)

A = indoor surface area of wall or roof (m^2)

θ = time (s)

δ = time interval (s)

n = summation index (each summation has as many terms as there are non-negligible values of coefficients)

$t_{e,\theta-n\delta}$ = sol-air temperature at time θ-nδ (°C)

t_{rc} = constant indoor room temperature (°C)

b_n, c_n, d_n = conduction transfer function coefficients

Conduction transfer function coefficients depend only on the physical properties of the wall or roof. These coefficients are given in tables (ASHRAE Fundamentals Handbook, 1997). The *b* and *c* coefficients must be adjusted for the actual heat transfer coefficient (U_{actual}) by multiplying them with the ratio $U_{actual}/U_{reference}$.

In equation 3.4, a value of the summation index n, equal to zero represents the current time interval, n equal to one is the previous hour and so on.

The sol-air temperature is defined as:

$$t_e = t_0 + \alpha\ I_t / h_0 - \varepsilon\ \delta R / h_0 \qquad (3.5)$$

where:

t_e = sol-air temperature (°C)

t_0 = current hour dry-bulb temperature (°C)

α = absorptance of surface for solar radiation

I_t = total incident solar load (W/m^2)

δR = difference between long-wave radiation incident on the surface from the sky and surroundings and the radiation emitted by a black body at outdoor air temperature (W/m^2)

h_0 = heat transfer coefficient for convection over the building (W/m^2-K)

$\varepsilon\ \delta R / h_0$ = long-wave radiation factor = -3.9°C for horizontal surfaces, 0°C for vertical surfaces

The term α/h_0 in equation 3.5 varies from about 0.026 m^2-K/W for a light-coloured surface to a maximum of about 0.053 m^2-K/W. The heat transfer coefficient for convection over the building can be estimated from:

$$h_0 = 5.7+3.8*W_{vel} \qquad (3.6)$$

where h_0 is in W/m^2-K and W_{vel} is the wind speed in m/s.

(b) Partitions, Ceilings and Floors

Whenever a conditioned space is adjacent to other spaces at different temperatures, the transfer of heat through the partition can be calculated from equation 3.4 by replacing the sol-air temperature with the temperature of the adjacent space.

When the air temperature of the adjacent space (t_b) is constant or when the variations of this temperature compared to the difference of the adjacent space and indoor temperature difference is small, the rate of heat gains (q_p) through partitions, ceilings and floors, can be calculated from the formula:

$$q_p = UA(t_b - t_i) \tag{3.7}$$

where:

A = area of element under analysis (m^2)

U = overall heat transfer coefficient (W/m^2-K)

$(t_b - t_i)$ = adjacent space–indoor temperature difference (°C)

(c) Glass

The total rate of heat admission through glass is the sum of the transmitted solar radiation, the portion of the absorbed radiation that flows inwards and the heat conducted through the glass whenever there is an outdoor–indoor temperature difference. The rate of heat gain (q_s) resulting from the transmitted solar radiation and the portion of the absorbed radiation that flows inwards is:

$$q_s = A\ (SC)\ (SHGF) \tag{3.8}$$

where:

A = area of element under analysis (m^2)

SC = shading coefficient

SHGF = solar heat gain factor varying according to orientation, latitude, hour and month

The rate of conduction heat gain (q) is:

$$q = UA(t_0 - t_i) \tag{3.9}$$

where:

A = area of element under analysis (m^2)

U = glass heat transfer coefficient (W/m^2-K)

$(t_0 - t_i)$ = outdoor–indoor temperature difference (°C)

(d) People

The heat gain from people is in the form of sensible and latent heat. The latent heat gains are considered as instantaneous loads. The total sensible heat gain from people is not converted directly to cooling load. The radiant portion is first absorbed by the surroundings and convected to the space at a later time, depending on the characteristics of the room. ASHRAE handbook gives tables for various circumstances and formulates the gains for the instantaneous sensible cooling load as:

$$q_s = N\,(SHG_p) \tag{3.10}$$

where:

q_s = rate of sensible cooling load due to people (W)

N = number of people

SHG_p = sensible heat gain per person

The rate of latent cooling load is:

$$q_l = N\,(LHG_p) \tag{3.11}$$

where:

q_l = latent cooling load due to people (W)

N = number of people

$LHGp$ = latent heat gain per person

(e) Lights

Generally, lighting is often a major internal load component. Some of the energy emitted by the lights is in the form of radiation that is absorbed in the space and transferred later to the air by convection. The manner in which the lights are installed the type of air distribution system and the mass of the structure affect the rate of heat gain at any given moment. Generally this gain can be calculated from:

$$q_{el} = W\,F_{ul}\,F_{sa} \tag{3.12}$$

where:

q_{el} = rate of heat gain from lights (W)

W = total installed light wattage

F_{ul} = lighting use factor, ratio of wattage in use to total installed wattage

F_{sa} = special allowance factor (Ballast factor in the case of fluorescent and metal halide fixtures)

(f) Appliances

Considerable data are available for this category of cooling load but careful evaluation of the operating schedule and the load factor for each piece of equipment is essential. Generally the sensible heat gains from the appliances (q_a) can be calculated from:

$$q_a = W\ F_U\ F_R \tag{3.13}$$

$$and \quad q_a = W\ F_L \tag{3.14}$$

where:

W = rate of energy input from appliances (W)

FU, FR, FL = usage factors, radiation factors and load factors

(g) Ventilation and Infiltration Air

Both a sensible (q_s) and latent (q_l) rate of heat gains will result from the incoming air, which may be estimated from:

$$q_s = m_a\, c_p\, (t_0 - t_i) \tag{3.15}$$

$$q_l = m_a\, (\omega_0 - \omega_i)\, i_{fg} \tag{3.16}$$

where:

m_a = air mass flow rate (kg/s)

c_p = specific heat of air (J/kg-K)

$(t_0 - ti)$ = temperature difference between incoming and room air (°C)

$(\omega_0 - \omega_i)$ = humidity ratio difference between incoming and room air (kg/kg)

i_{fg} = enthalpy of evaporation (J/kg-K)

An overview of the transfer function method as adopted by the ASHRAE Cooling and Heating Load Calculation Manual (ASHRAE, 1992), is presented in Figure 3.1.

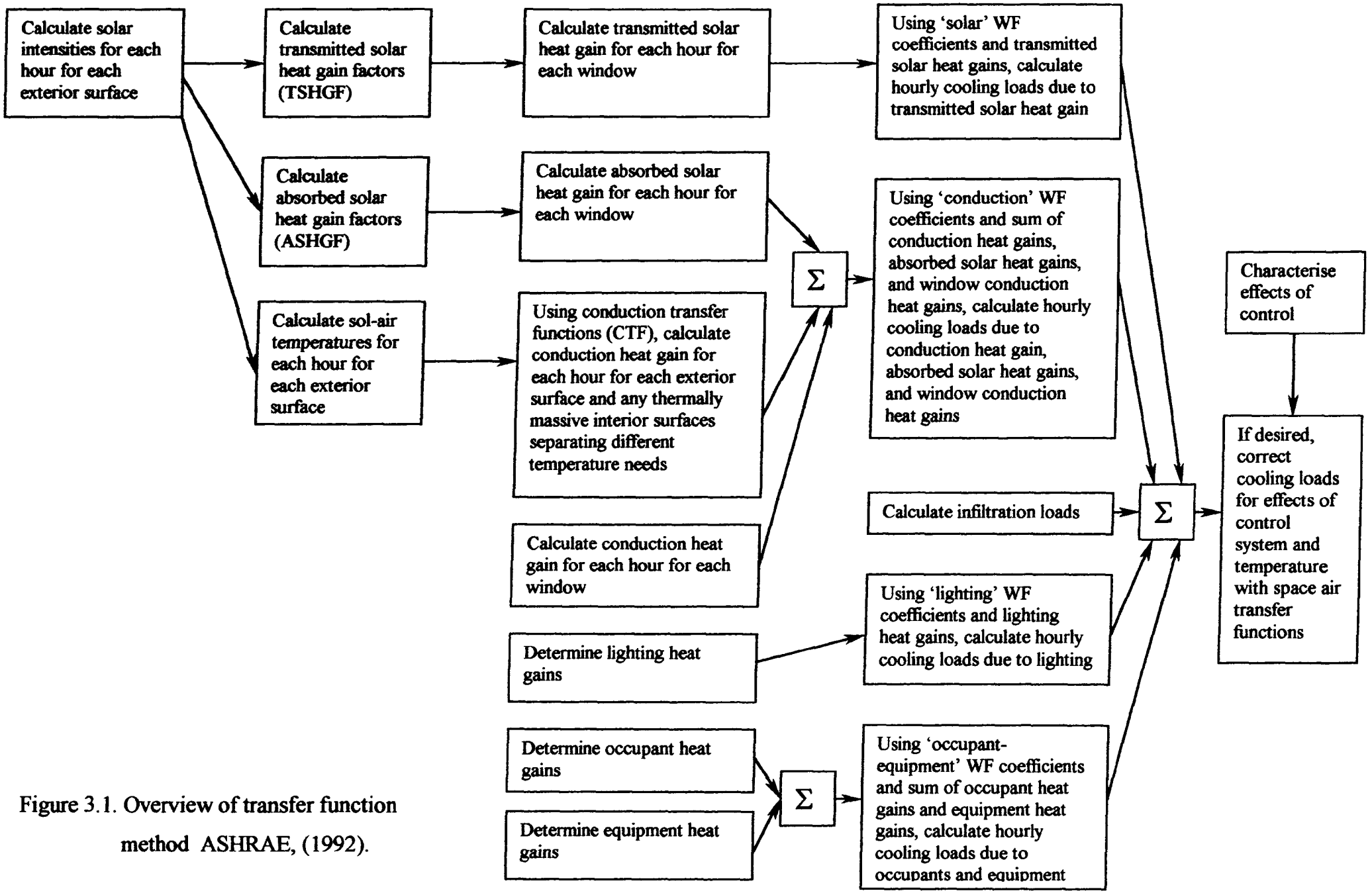

Figure 3.1. Overview of transfer function method ASHRAE, (1992).

3.1.4 Heat Extraction Rate and Room Temperature

The cooling equipment, in an ideal case, must remove heat energy from the space air at a rate equal to the cooling load. In this way the space air temperature will remain constant. However this is seldom true. Therefore a transfer function has been devised to describe the process. The room air transfer function is:

$$\sum_{i=0}^{1} p_i \, (q_{x,\theta-i\delta} - q_{c,\theta-i\delta}) = \sum_{i=0}^{2} g_i \, (t_i - t_{r,\theta-i\delta}) \qquad (3.17)$$

where :

p_i, g_i = transfer function coefficients (ASHRAE, 1992)

q_x = heat extraction rate (W)

q_c = cooling load at the various times (W)

t_i = room temperature used for cooling load calculations (°C)

t_r = actual room temperature at the various times (°C)

All g coefficients refer to unit floor area. The coefficients g_0 and g_i depend also on the average heat conductance to the surroundings (UA) and the infiltration and ventilation rate to the space. The p coefficients are dimensionless.

The characteristic of the terminal unit usually is of the form:

$$q_{x,\theta} = W + S \; t_{r,\theta} \qquad (3.18)$$

where W and S are parameters that characterise the equipment at time θ.

The equipment being modelled is actually the cooling coil and the associated control system (thermostat) that matches the coil load to the space load. The cooling coil can extract heat energy from the space air from some minimum to some maximum value. Equation 3.18 can be used in this range. Figure 3.2 indicates such a characteristic extraction curve.

Assuming that $t_{s,\theta}$ is the thermostat set point, then:

$$W = (q_{x,max} + q_{x,min}) / 2 - S \, t_{s,\theta} \qquad (3.19)$$

$$S = (q_{x,max} - q_{x,min}) / \Delta t_r \tag{3.20}$$

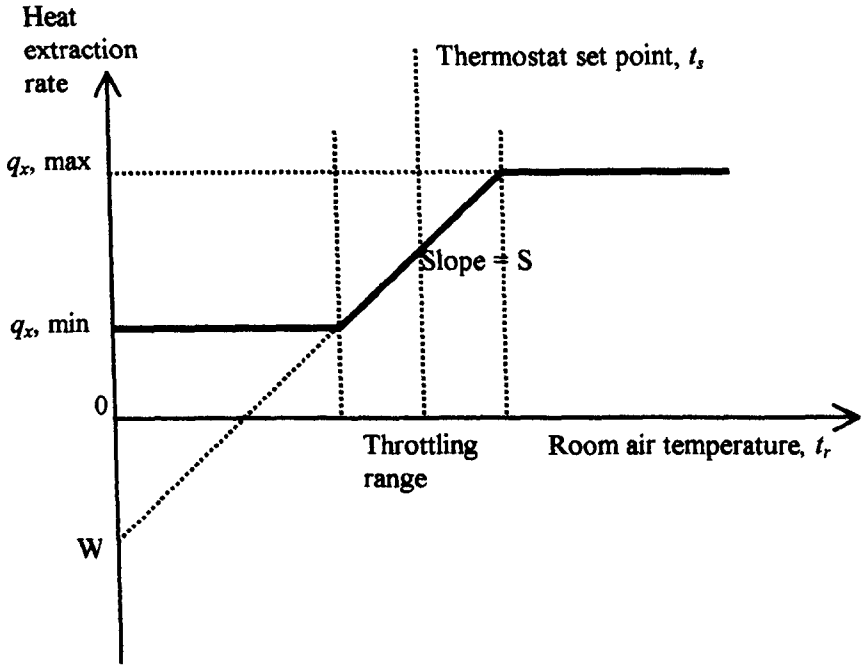

Figure 3.2. Characteristic extraction curve.

Equations 3.17 and 3.18 may be combined and solved for $q_{x,\theta}$

$$q_{x,\theta} = (W\ g_0 + S\ G_\theta) / (S + g_0) \tag{3.21}$$

where :

$$G_\theta = t_i \sum_{i=0}^{2} g_i - \sum_{i=1}^{2} g_i\ (t_{y,\theta-i\delta}) + \sum_{i=0}^{1} p_i\ (q_{c,\theta-i\delta}) - \sum_{i=1}^{1} p_i\ (q_{x,\theta-i\delta}) \tag{3.22}$$

When the value of $q_{x,\theta}$ computed by equation 3.21 is greater than $q_{x,max}$, it is taken to be equal to $q_{x,max}$, and when it is less than $q_{x,min}$ it is made equal to $q_{x,min}$. Finally equation 3.18 and 3.21 can be combined and solved for $t_{r,\theta}$

$$t_{r,\theta} = (G_\theta - q_{x,\theta}) / g_0 \tag{3.23}$$

3.2 TRNSYS PROGRAM OVERVIEW

TRNSYS (Klein *et al.*, 1996) is a transient systems simulation program with a modular structure and is used in the present study to derive the results. The modular nature of TRNSYS makes the program flexible, and facilitates the addition of extra mathematical models to the program. TRNSYS is suited to detailed analysis of systems whose behaviour is dependent on the passage of time and is designed to simulate the transient performance of thermal energy systems. The program can solve large systems of equations described by Fortran subroutines. Each Fortran subroutine contains a model for a system component. By creating an input file, called deck file, the user directs TRNSYS to connect the various subroutines to form a system. The TRNSYS engine calls the system components based on the input file and iterates at each time-step until the system of equations is solved. The flow diagram of the deck file, written as part of this study is shown in Figure 3.3. TRNSYS allows the users to completely describe and monitor all interactions between system components. The program library includes many components commonly found in thermal energy systems, as well as component routines to handle the input of weather data or other time-dependent forcing functions and the output of simulation results.

3.2.1 The TRNSYS Type 19 model

For the present study the TRNSYS Type 19 model is used to estimate the heating and cooling loads for a typical house. Type 19 was chosen for the simulations due to the simple design of the typical house. This type is useful for estimating thermal loads for single zones. Multi-zone buildings can be modelled through multiple uses of this component in a simulation. For complicated multi-zone buildings the TRNSYS Type 56 model can be used. This type can model up to 25 thermal zones in a simulation and the building characteristics are input through a separate computer program (Building Input Description program) to facilitate the process.

The Type 19 model has two basic modes of operation, i.e., the energy rate (mode 1) and the temperature level control (mode 2). In this study the energy rate control (mode 1) is selected, since with this mode the temperature of the building can be maintained between specified limits and the energy required to maintain the zone in the specified temperature is given as output along with the limit temperature. The zone humidity ratio

is also allowed to float between a maximum and a minimum limit specified by the user and the humidification or dehumidification energy is considered.

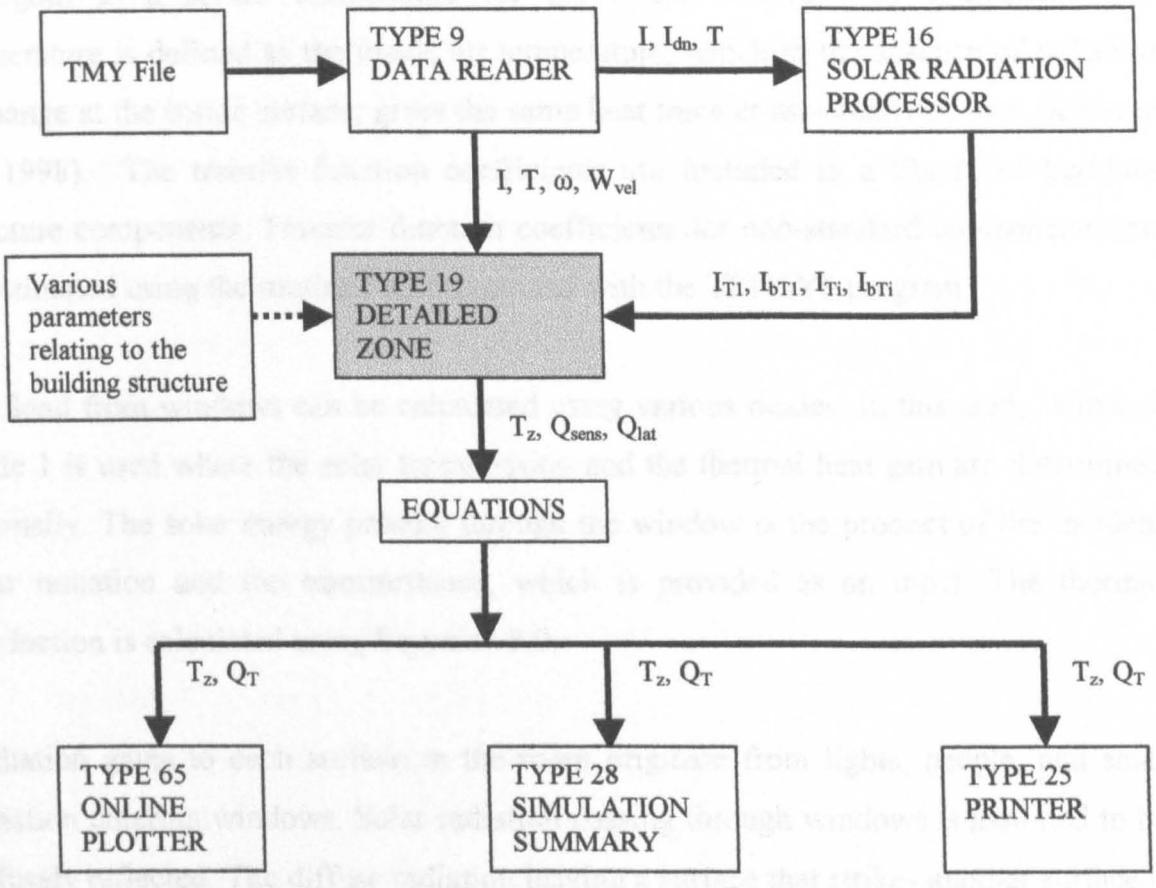

Note: the symbols represent:

I – global solar radiation on a horizontal surface at the next hour (W/m^2)
I_{dn} – direct normal solar radiation at the next hour (W/m^2)
T – dry-bulb temperature at the next time step (°C)
ω – humidity ratio at the next time step
W_{vel} – wind velocity at the next time step (m/s)
I_{T1}, I_{Ti} – total radiation on surface number 1or i (W/m^2)
I_{bT1}, I_{bTi} – beam radiation on surface number 1or i (W/m^2)
T_z – zone temperature (°C)
Q_{sens} – sensible load (kJ/h)
Q_{lat} – latent load (kJ/h)
Q_T – total load (kJ/h)

Figure 3.3. Flow diagram of the TRNSYS deck file.

Additionally, heat may be added or removed either by the use of a ventilation flow stream or by an instantaneous heat gain input. A controller is used in conjunction with this mode to control the heating or cooling equipment.

Type 19 model uses the transfer function coefficients of the ASHRAE load calculation method, as described in section 3.1.3 (a), for the estimation of the heating and cooling loads arising from external walls and roofs. Interior partitions and walls separating

zones are modelled in the same way as external walls with the modification that the sol-air temperature in Equation 3.4, is replaced by the equivalent zone temperature which is analogous to a sol-air temperature for the inside surface. The equivalent zone temperature is defined as the inside air temperature, which in the absence of radiative exchange at the inside surface, gives the same heat transfer as actually occurs. (Klein *et al.*, 1998). The transfer function coefficients are included in a library of building structure components. Transfer function coefficients for non-standard components can be estimated using the routine PREP provided with the TRNSYS program.

The load from windows can be calculated using various modes. In this study, window mode 1 is used where the solar transmission and the thermal heat gain are determined internally. The solar energy passing through the window is the product of the incident solar radiation and the transmittance, which is provided as an input. The thermal conduction is calculated using Equation 3.9.

Radiation gains to each surface in the room originate from lights, people, and solar radiation entering windows. Solar radiation passing through windows is assumed to be diffusely reflected. The diffuse radiation leaving a surface that strikes another surface is determined using the total exchange factor. All surfaces are assumed to be black for radiation from lights and people. Radiative gains from people are assumed to be 70% of their total sensible energy output.

The ventilation flow is an input, while the infiltration rate is determined from:

$$m_{infl} = \rho_a V_a (K_1 + K_2 \left|T_a - T_z\right| + K_3 W_{vel}) \tag{3.24}$$

where:

m_{infl} = mass flow rate of air infiltration (kg/h)

ρ_a = density of zone air (kg/m^3)

V_a = Volume of air in the zone (m^3)

T_a = ambient temperature (°C)

T_z = zone temperature (°C)

W_{vel} = wind speed (m/s)

K_1, K_2, K_3 = empirical constants

The empirical constants K_1, K_2 and K_3 depend on the construction qualities and the measures taken to prevent infiltration. For buildings constructed using conventional procedures these factors are: K_1=0.1, K_2 = 0.017 and K_3 =0.049 (Klein *et al.*, 1996)

The Type 19 model utilises a separate TRNSYS component to model a surface, which is a non-ASHRAE wall or roof, with conduction through this surface provided as an input to the zone. For calculating the losses of the floor area the floor perimeter method was used in the calculations since it can be shown that the total heat loss is more nearly proportional to the length of the perimeter than to the area of the floor. The equation used is (ASHRAE, 1997):

$$q = F_2 P (t_i - t_o) \tag{3.25}$$

where:

q = heat loss through perimeter (W)
F_2= heat loss coefficient per meter of perimeter (W/m-K)
P = perimeter of exposed edge of floor (m)
t_i = indoor temperature (°C)
t_o = outdoor temperature (°C)

3.2.2 TRNSYS Program Parameters

In order to describe a zone, it is necessary to specify characteristics of the internal space, external weather conditions, walls, windows etc. These characteristics were kept the same for all simulations that were used to examine the effect of the various constructional elements. To facilitate the description, the parameters and inputs for these characteristics are organised in separate lists according to type.

Zone parameters used in the calculations of this study are listed in Table 3.1. The parameter number shown in the table refers to the TRNSYS numbering system.

Table 3.1. Zone parameters used in the calculations with TRNSYS Type 19

PARAMETER		DESCRIPTION	SET VALUE
1	Mode	1-energy rate control, 2-temperature level control	1
2	V_a	Zone volume of air (m^3)	147
3	K_1	Constant air change per hour	0.1
4	K_2	Proportionality constant for air change due to indoor-outdoor temperature difference (1/°C)	0.017
5	K_3	Proportionality constant for air change due to wind effects (s/m)	0.049
6	Cap	Capacitance of room air and furnishings (kJ/°C)	500
7		Number of total surfaces comprising room description	7
8	T_o	Initial room temperature; also used for calculation of inside radiation coefficients (°C)	25
9	w_o	Initial room humidity ratio (kg water/kg dry air)	0.0075
Energy rate control-Mode 1 only:			
10	T_{min}	Set point temperature for heating (°C)	21
11	T_{max}	Set point temperature for cooling (°C)	25
12	w_{min}	Set point humidity ratio for humidification (kg water/kg dry air)	0.005
13	w_{max}	Set point humidity ratio for dehumidification (kg water/kg dry air)	0.008
INPUT NUMBER			
1	T_a	Ambient temperature (°C)	*
2	w_a	Ambient humidity ratio (kg water/kg dry air)	*
3	T_v	Temperature of ventilation flow stream (°C)	*
4	v	Mass flow rate of ventilation flow stream (kg/hr)	0
5	w_v	Humidity ratio of ventilation flow stream (kg water/kg dry air)	*
6	I	Rate of moisture gain (other than people) (kg/hr)	0
7	N_{people}	Number of people in every zone	1
8	I_{act}	Activity level of people	2
9	Q_{IR}	Radiative energy input due to lights, equipment, etc. (kJ/hr)	750
10	Q_{int}	Sum of all other instantaneous heat gain to space (kJ/hr)	0
11	W	Wind-speed (m/s)	*

* Parameter read from TMY file.

As it is seen, specified are the characteristics for infiltration according to Equation 3.24, the capacitance of room air and furnishings (in this case a nominal value of 500 kJ/°C, of which about 150 kJ/°C is for the zone air), as well as initial conditions and set limits of room temperature and humidity. The weather conditions, read from a typical

meteorological file, are also specified, as well as the radiative energy due to lights and equipment (in this case a nominal value of 750 kJ/hr) and the number of people and activity level (one person per room, seated and writing). The activity level assumed, results in 65 W sensible heat and in 55 W latent heat per person (Klein *et al.*, 1996).

The parameters required for the walls and windows are listed in Tables 3.2 and 3.3 respectively. The reflectance of the inner wall surfaces to solar radiation is taken as 0.7, which corresponds to light colour paints that are usually used in a room. The absorptance of the exterior surface to solar radiation is taken as 0.65, which corresponds to light to medium colour paints usually used for the exterior walls. The inside convection coefficient is taken as 2.66 W/m^2-K as indicated in the TRNSYS manual, since radiation is handled separately by Type 19.

Table 3.2. Wall parameters used in the calculations with TRNSYS Type19

PARAMETER		DESCRIPTION	SET VALUE
4	r	Reflectance of inner surface to solar radiation	0.7
5	α	Absorptance of exterior surface to solar radiation	0.65
7	h_c	Inside convection coefficient (W/m^2-K)	2.66

A double-glazed window with clear 3 mm glass is considered, with a transmittance of 0.8 and an inside convection coefficient of 8.33 W/m^2-K (Klein *et al.*, 1996). Since the transmitted solar energy is calculated internally, the number and surfaces on which the transmitted beam radiation strikes must be defined. In this case the floor is assumed to absorb the solar energy transmitted.

3.3 MODEL HOUSE CONSTRUCTION

For the estimations carried out in this project a model house was considered. This is illustrated in Figure 3.4. It has a floor area of 196 m^2 and consists of four identical external walls, 14 m in length and 3 m in height, with a total window opening of 5.2 m^2 on each wall.

The window area is approximately equal to the area that a typical house would have, but instead of considering a number of windows on each wall, only one window is considered. Since the same model will be used in evaluating the load for various

constructions this simplification is not important but will assist in drawing conclusions since similar features are present on every wall. The model house is further divided into four identical zones and the partition walls are considered as walls separating the four zones. For every zone a separate TRNSYS Type 19 unit is necessary.

Table 3.3. Window parameters used in the calculations with TRNSYS Type 19

PARAMETER		DESCRIPTION	SET VALUE
5	t_d	Transmittance for diffuse solar radiation	0.8
6	$h_{c,i}$	Inside convection coefficient (W/m^2-K)	8.33
7	N_I	Number of surfaces on which transmitted beam radiation strikes	1
8	k	First surface number of which beam of radiation strikes	5 (floor)
INPUT NUMBER - Window Mode 1			
1	I_T	Total incident radiation (W/m^2)	*
2	I_{bT}	Incident beam radiation (W/m^2)	*
3	t	Overall transmittance for solar radiation	0.8
4	U_g	Loss coefficient of window (plus night insulation) not including convection at the inside or outside surface (W/m^2-K)	3.41
5	f_k	fraction of incoming beam radiation that strikes surface k	1

* Parameter calculated by the solar radiation processor

In the simulations two types of roofs are examined, the flat and the inclined roof since, as explained in Section 2.2, these are the two most common constructions used. The relevant dimensions are indicated in Figure 3.4.

3.4 MEASUREMENTS OF THERMAL CONDUCTIVITY

The houses in Cyprus are usually built with hollow bricks made of fired clay. The thermal conductivity of these bricks was never measured with any accuracy before and values between 0.4 to 0.6 W/m-K were used in building load calculations. These values were obtained from data presented in handbooks but do not necessarily represent values applicable to local materials. To measure the thermal conductivity accurately a Heat Flow Meter Thermal Conductivity Instrument model FOX-314 was employed. With this

instrument the thermal conductivity of a specimen is determined by measuring the heat flux, specimen thickness, and temperature difference across the specimen.

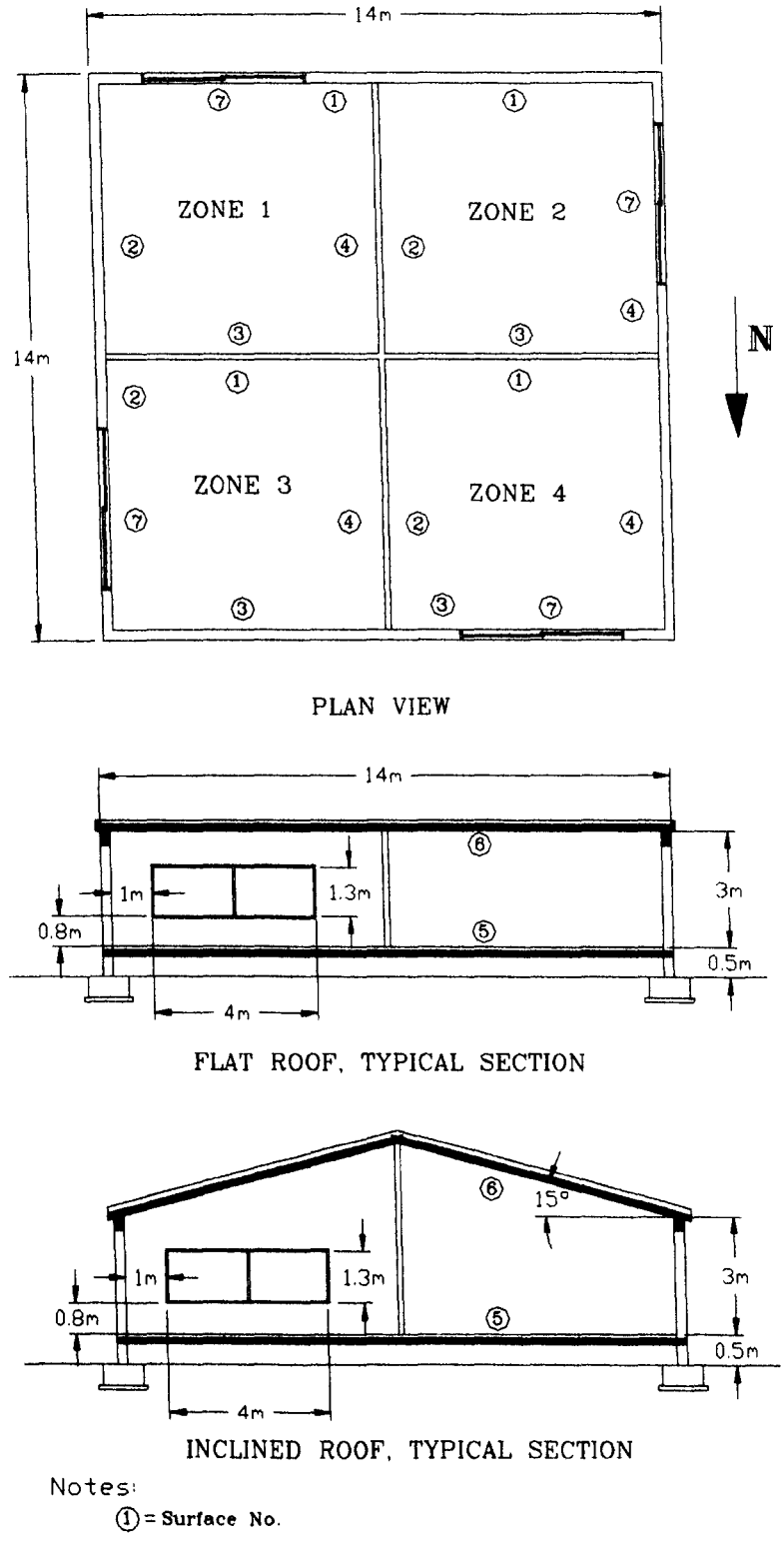

Figure 3.4. Model house.

The results are correlated with the Fourier equation:

$$q_x = -k\frac{dT}{dx} \tag{3.26}$$

where:

q_x = heat flux in the positive x direction (W/m^2)

k = thermal conductivity (W/m-K)

dT = temperature difference (°C)

The specimen tested was 305 mm square by 100 mm thick and was placed in the test chamber, in between the plates of the automatic feeder. The automatic feeder is a pneumatically actuated microprocessor controlled system, which automatically closes the plates on the sample and gives the thickness readout with an accuracy of 0.025 mm. The feeder plates utilise low thermal mass and solid-state heating/cooling and can operate between –20°C and 95°C. Thin film high output heat flux transducers are permanently bonded on every plate within 0.1 mm of the sample's surface. In this way the transducers provide accurate readings of the sample's surface heat flux and temperature to within 0.01°C.

A microprocessor controls all aspects of the instrument's operation, monitoring the temperatures of the plates and controlling the heating/cooling system in each plate. The instrument has a repeatability of 0.2%, a reproducibility of 0.5%, and an accuracy of about 1%. The obtained results are in accordance with ASTM C518 and ISO 8301.

Using the above method, the hollow brick thermal conductivity was found to be 0.310 W/m-K, for a temperature difference of 15°C (20-35°C). The normal density of the brick is 940 kg/m^3.

The same equipment was also used to determine the thermal conductivity of the mud and straw blocks used in the construction of the traditional house. The thermal conductivity of these blocks was found to be 0.257 W/m-K, for a temperature difference of 15°C (20-35°C). The density of the block is 1350 kg/m^3. Additional material properties used in the building construction are indicated in Table 3.4.

Table 3.4. Properties of construction materials

Material	Thickness (m)	Mean Temperature at which properties were measured (°C)	Thermal conductivity (W/m-K)	Density (Kg/m^3)	Specific heat (kJ/kg-K)
Hollow brick	0.1	27	0.310	940	0.84
Polystyrene	0.044	27	0.0344	32.6	1.21
Mud and straw block	0.45	27	0.257	1350	0.88
Screed	0.07	27	1.3	2000	0.84
Air *	0.05	27	0.0263	1.16	1.007
Asphalt *	0.004	27	0.062	2115	0.920

* Not measured, taken from Incropera and DeWitt, 1999.

3.5 STRUCTURAL ELEMENTS

In this study the effect that various structural elements, like walls and roofs, have on the thermal load is examined. These structural elements are assumed to be constructed from different materials and thickness, as actually occur in the Cyprus building industry. These elements together with their overall heat transfer coefficient are presented in Table 3.5.

3.6 THE TYPICAL METEOROLOGICAL YEAR (TMY)

TRNSYS runs through hourly values of various weather parameters included in a typical meteorological year (TMY) file. For this study the Typical Meteorological Year (TMY) for Nicosia-Cyprus, developed by Petrakis *et al.* (1998), is used. This has been generated from hourly measurements, of solar irradiance (global and diffuse on horizontal surface), ambient temperature, relative humidity, wind speed and direction, for a seven-year period, from 1986 to 1992.

The measurements were performed by the Meteorological Service of the Ministry of Agriculture and Natural Resources of Cyprus, at the Athalassa region, an area very close to the town of Nicosia. Athalassa is at a latitude of 35°09', longitude 33°24' and 162 m high, above the mean sea level.

Table 3.5. Overall heat transfer coefficient of structural elements

Type	Structural element	Overall heat transfer coefficient, U (W/m^2-K)
A	Traditional wall, 0.45m mud block and 0.025m gypsum plaster covering on each side	0.450
B	Traditional roof, semi-circular clay tiles 0.01m thick, 0.05m air gap below the tiles, 0.01m mud-block material and 0.01m wood	0.367
C	Traditional partition wall, 0.45m mud blocks and 0.025m gypsum plaster covering on each side	0.393
D	Single wall, hollow brick 0.2 m and 0.02m plaster on each side	0.886
E	Double-wall, 0.1m hollow brick and 0.02m plaster on each side and a layer of 0.025m polystyrene insulation in between	0.542
F	Double-wall, 0.1m hollow brick and 0.02m plaster on each side and a layer of 0.05m polystyrene insulation in between	0.389
G	Partition wall, constructed from 0.1m hollow brick and 0.02m plaster on each side	0.889
H	Flat non-insulated roof, constructed from fair-face 0.15m heavy-weight concrete	1.91
I	Flat insulated roof, fair-face 0.15m heavyweight concrete, 0.025m polystyrene insulation, 0.07m screed and 0.004m asphalt covered with aluminum paint of 0.55 solar absorptivity	0.736
J	Flat insulated roof, fair-face 0.15m heavy weight concrete, 0.05m polystyrene insulation, 0.07m screed and 0.004m asphalt covered with aluminum paint of 0.55 solar absorptivity	0.481
K	Inclined insulated roof, 0.15m heavyweight concrete, 0.004m asphalt for waterproofing, 0.05m plaster and clay tile on top	0.411

The weather data, contained in the TMY are analysed in respect to the radiation falling on every wall facing the four orientations. Such an analysis, although very useful for designers, is done for the first time. Examining the direct beam radiation day by day for most of the months, it is observed that in the morning hours it is usually much greater than it is during the afternoon hours. The pattern emerging shows that usually haze and clouds form in the afternoon blocking the sun. Collective results for the whole year shown in Table 3.6 indicate that the east wall receives 30% more total radiation than the south wall. The west wall receives only 20% of the beam radiation of the east wall. The diffuse radiation for the afternoon is about the same for all walls. In the morning hours

the east wall receives about 75% more diffuse radiation than the south wall. This of course depends on the model used for the contribution of diffuse radiation on a tilted surface. In the case of study the Reindl model was used which accounts for circumsolar diffuse (an increased intensity of diffuse radiation in the area around the sun) and also includes a horizon brightening diffuse term besides the isotropic radiation. All factors depend on the amount of beam radiation at the particular time.

Table 3.6. Collective results of the sun radiation for the morning and afternoon hours

Wall direction	Total radiation (kWh/m^2)			Beam radiation (kWh/m^2)			Diffuse radiation (kWh/m^2)		
	From sunrise to 12 noon	From 12 noon to Sunset	Total	From sunrise to 12 noon	From 12 noon to sunset	Total	From sunrise to 12 noon	From 12 noon to Sunset	Total
South	803	404	1208	408	207	615	395	198	593
East	1488	176	1664	793	0	793	695	176	871
North	338	176	515	43	1	43	295	176	471
West	261	358	619	0	162	162	261	196	457

Examining the sun radiation in the hot months (May to September-Table 3.7) it is seen that the east wall receives more than twice the total radiation received by the south wall and about 3 times the radiation received by the north and west walls. During this time the west wall receives approximately the same amount of total radiation as the north wall. This is partly due to the sun trajectory. During summertime the sun faces the north wall at sunrise and some time before sunset, therefore a small amount of beam radiation strikes the north wall.

According to the Meteorological Department of Cyprus, because of the heat of the morning hours and the position of Nicosia in the valley of Mesaoria, usually clouds form around 2 pm., which obstruct the west beam radiation. For the remaining months south and east walls receive approximately the same total radiation and west and north walls receive only 38% of the radiation of the south wall.

Table 3.7. Collective results of the sun radiation for the hot (May to September) and cold (October to April) months of the year

Wall direction	Total radiation (kWh/m^2)			Beam radiation (kWh/m^2)			Diffuse radiation (kWh/m^2)		
	Hot months	Cold months	Year total	Hot months	Cold months	Year total	Hot months	Cold months	Year total
South	420	787	1208	165	450	615	255	338	593
East	889	775	1664	442	351	793	447	423	871
North	299	216	515	41	3	43	258	213	471
West	320	298	619	81	81	162	240	217	457

An examination of the mean wind velocity is presented in Table 3.8. As can be seen, during the morning hours it is always smaller than the afternoon hours. The morning wind velocity during the whole year is about 60% of the afternoon velocity whereas during the hot months is reduced to about 50%. The mean direction of wind is generally SSW.

Table 3.8. Collective results for mean wind velocity and wind direction for the morning and afternoon hours

	Mean wind velocity (m/s)		Mean wind direction (degrees)	
	Morning 5 a.m. –12 noon	Afternoon 12 noon – 7 p.m.	Morning 5 a.m. –12 noon	Afternoon 12 noon – 7 p.m.
All year	2.7	4.7	205 (SSW)	204 (SSW)
Hot months	2.8	5.5	201 (SSW)	223 (SW)

These peculiarities of the Cypriot weather profile will facilitate understanding of the wall thermal load in the analysis presented in Chapters 4 and 5.

CHAPTER 4

COMPARISON OF THERMAL REQUIREMENTS OF TYPICAL DWELLINGS IN CYPRUS

The objective of this chapter is to determine and compare the thermal requirements and the maximum and minimum resulting temperatures of the buildings constructed in Cyprus during the last century. Cypriot houses changed radically in three phases during the last century, as described in Section 2.2. At the early years of the century, houses were constructed from easily obtainable local materials. Between 1960-1985 the construction changed to more readily available industrial materials like brick and concrete, resulting in a cheap construction and gradually from 1985 onwards to a more insulated and expensive construction.

To simulate the behaviour of the dwellings, the TRNSYS Type 19 model was used with the parameters as outlined in Section 3.2. The indoor design temperature is crucial for estimating the heating and cooling loads. Overall comfort is influenced by three general groups of parameters (Balaras, 1997). These are:

1. Physical parameters, which include dry bulb temperature, relative humidity, air velocity, barometric pressure, colour of surrounding environment etc.

2. Physiological parameters, which include age, sex and national characteristics, and

3. External parameters, which include human activity levels, type of clothing etc.

For this study, indoor design temperatures of 21°C for winter and 25°C for summer were considered, which are widely accepted levels of temperature for comfort conditions (ASHRAE, 1997). Indoor design temperatures refer to room air temperatures.

Conclusions are extracted based on the evaluation of the temperature resulting from the various construction types.

4.1 ANALYSIS OF THE ENERGY REQUIREMENTS OF BUILDINGS

The simulations were carried out for the model house plan described in Section 3.3. This plan is very similar to the basic plan of houses built between 1920 -1960, shown in Figure 2.7. Since the same plan will be used in evaluating the load for various constructions this simplification will assist in drawing conclusions.

Three building types are compared in this section, which correspond to the three construction periods. With reference to Table 3.5, which describes the various wall and roof construction types, the compared buildings are:

1. Traditional house, built from traditional materials i.e., traditional walls type A, traditional partition walls type C and traditional roof type B.

2. Flat roof house, built from single walls type D, partition walls type G and flat non-insulated roof type H, and

3. Insulated house, built from double walls type F, partition walls type G and inclined insulated roof type K.

It should be noted that the above building types employ the same plan shown in Figure 3.4. Additionally, as actually built, the traditional house model is assumed to have a height of 4 m at the corners, with a 15° inclined roof in the East-West direction with a ridge height of 5.9 m. For the flat roof house the wall height is 3 m. Finally for the insulated house, the wall height is 3 m and the roof is inclined at 15° in the East-West direction. Table 4.1 shows the resulting volumes and wall areas of the three constructions.

Due to the very large thickness of the traditional walls, TRNSYS cannot perform the calculations directly. This happens because TRNSYS can perform calculations for walls that have up to ten b, c, and d transfer function coefficients. The 0.50 m thickness of the traditional mud-block wall results in twelve. Since direct calculation of the annual

thermal load cannot be performed, this is extrapolated from the calculated load of walls of smaller thickness (up to 0.40 m), as shown in Figure 4.1.

Table 4.1. Corresponding volumes and external wall and roof areas for the three construction models

Parameter	Traditional house	Flat roof house	Insulated house
External wall area (m^2)	229.5	147.2	173.5
Volume (m^3)	242	147	193
Roof area (m^2)	203	196	203

The black lines in Figure 4.1, present the trend lines of the cooling and heating load calculated for 0.30 m, 0.35 m and 0.40 m mud-block wall thickness. Thus, a resulting annual load of the traditional house with 0.50 m wall thickness would be 26100 kWh for cooling and 6200 kWh for heating for a temperature range between 21°C and 25°C respectively.

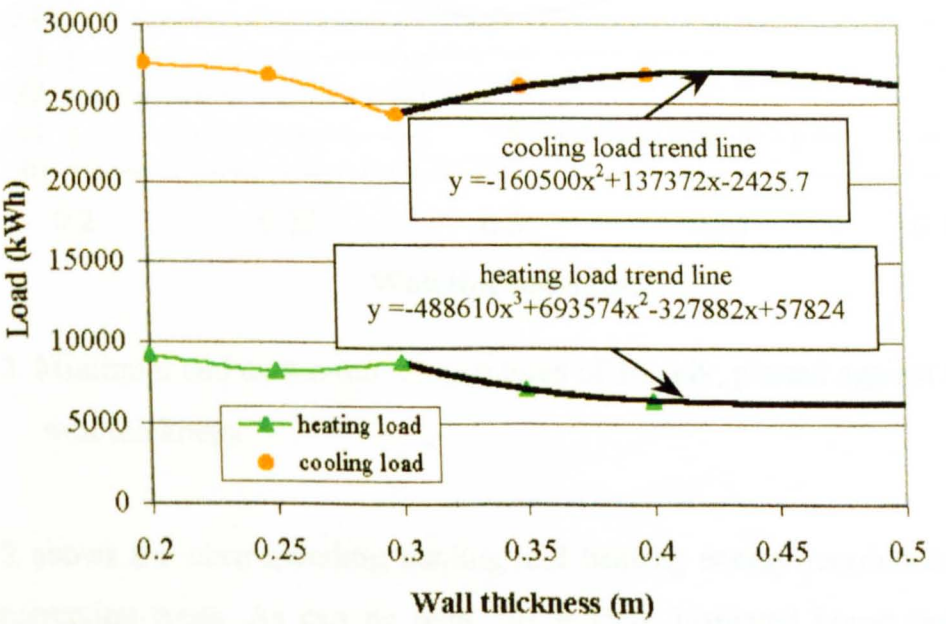

Figure 4.1. Annual cooling and heating loads plotted against mud-block wall total thickness.

Also, in Figure 4.1, it is observed that for a mud-block wall of 0.30 m total thickness, a minimum annual cooling load occurs.

This is due to the stored heat for a greater wall thickness, which is absorbed during the hot hours of the day and enters into the room at a later time. This effect can better be illustrated if the minimum and maximum temperatures of 16 July, which occur at 6 a.m. and 4 p.m. respectively, are plotted against the mud-block wall thickness. As can be seen in Figure 4.2, a thin 0.20 m mud-block wall has a bigger daily temperature fluctuation compared to a 0.30 m wall because it offers less resistance to the environmental gains. A 0.30 m wall offers high resistance to the gains therefore the house temperature is kept low during the day. At the same time the 0.30 m wall, has a time lag of eight hours since it requires eight sets of transfer function coefficients. This time lag seems to be the maximum that will allow a building to cool completely before the gains of the next day start. Increasing the wall thickness above this point causes some load to be carried to the next day thus keeping the temperature at a higher level.

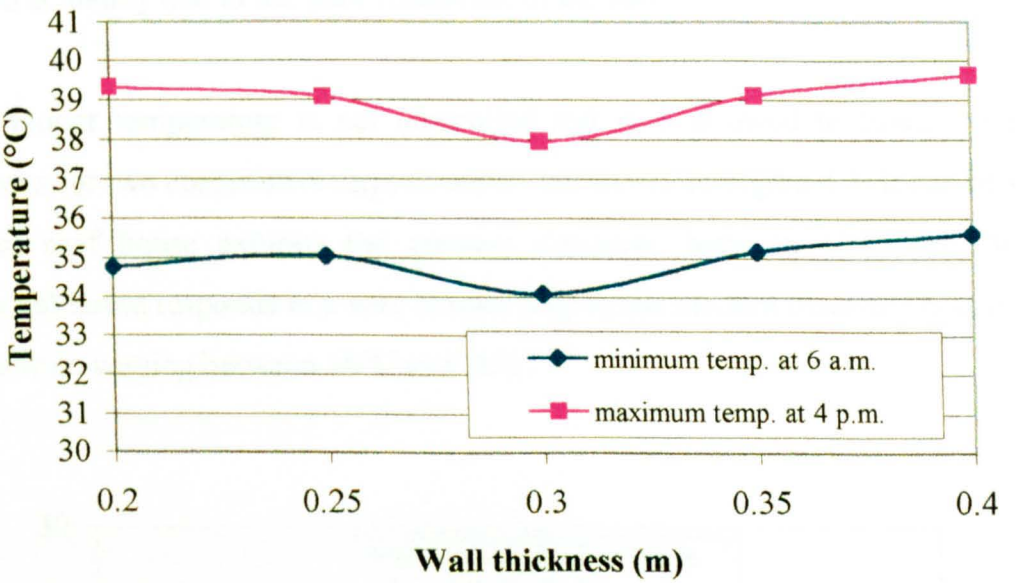

Figure 4.2. Minimum and maximum temperatures of 16 July, plotted against mud-block wall thickness.

Table 4.2 shows the corresponding cooling and heating energy requirements for the three construction types. As can be seen, the modern insulated house results in the lowest energy demand.

The traditional house which is greater in volume (by 12.5%) and in external wall area (by 13.2%) than the insulated house, has a 9.7% higher cooling energy demand and 33% higher heating demand compared to the modern insulated house.

Table 4.2. Cooling and heating loads of the model houses considered

Load	Insulated house	Traditional house		Flat roof house	
	(kWh)	(kWh)	% load increase	(kWh)	% load increase
Cooling at 25°C	23790	26130	9.7	42300	77.8
Heating at 21°C	4660	6200	33.0	16012	243.6

The flat roof house, although it has a smaller volume (by 7.6%) and a smaller external wall area (by 8.5%) than the modern insulated house, presents a cooling demand increase of 77.8% and a heating demand increase of 243.6%. The increase in the energy demand is mainly due to the poor insulation of the roof.

If the indoor temperature is not controlled but it is allowed to float, the resulting variations for two consecutive days in winter are shown in Figure 4.3. It can be seen that the flat roof house exhibits the greatest variation, between 11°C and 20°C. The traditional house responds in a very similar way to the modern insulated house, with the temperature varying between 16°C and 20°C.

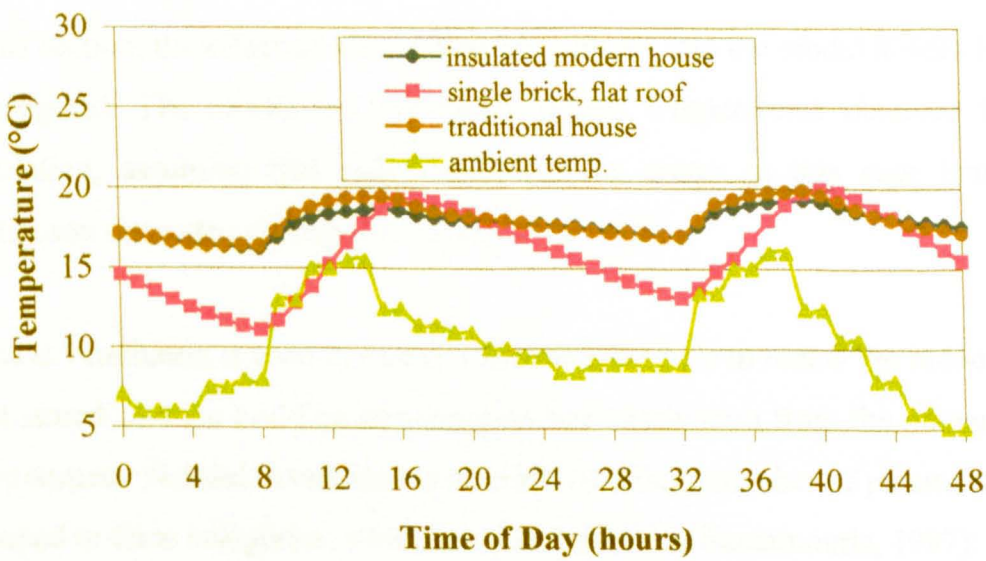

Figure 4.3. Predicted temperature variation in the model houses during 13 and 14 January.

During summer, similar effects are observed. As can be seen in Figure 4.4, the flat roof house, exhibits a wide temperature variation between 33°C and 46°C. The traditional and insulated houses respond in approximately the same manner, with the temperature varying between 36°C and 40°C.

It is also of interest to note that there is a three to four hours time lag between the time of maximum ambient temperature and maximum indoor space temperature.

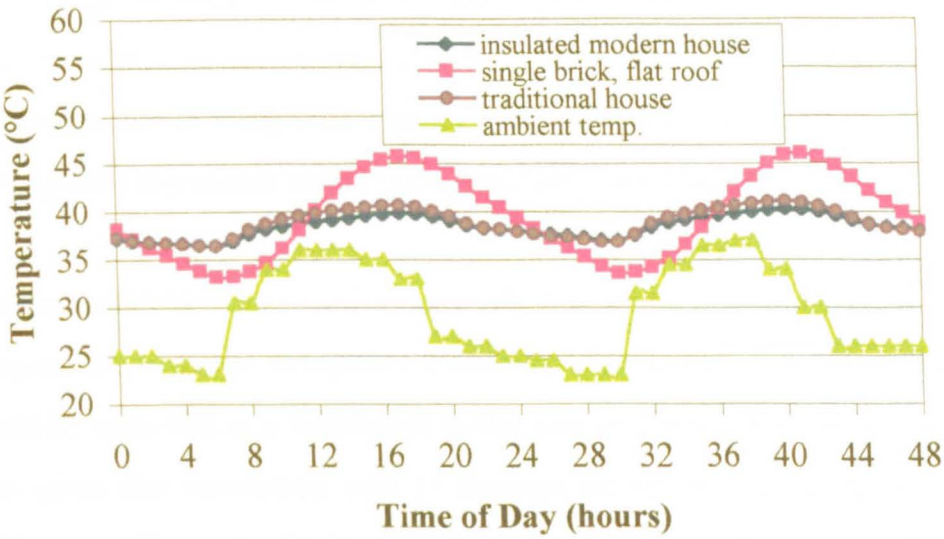

Figure 4.4. Temperature variation in the model houses, during 16 and 17 July.

4.2 EFFECT OF VENTILATION

In this section, the effect of introducing ambient air into the model houses for cooling is investigated. The results are compared against temperatures obtained for no extra ventilation, assuming that only infiltration air enters in this case into the house. Infiltration rates are calculated using equation 3.24.

Natural ventilation is used to create a flow in the house to renew the indoor air, remove heat stored into the building and enhance heat dissipation from the human body to the environment. Natural ventilation is affected by a large number of parameters. These are grouped in three categories, which are (Dascalaki and Santamouris, 1997):

a. Climate parameters, such as the wind velocity and direction, and the difference between the indoor and outdoor temperatures.

b. Environmental parameters, such as the plan area density and the relative building height compared to the surrounding buildings.

c. Building parameters, such as the airflow openings and their relative position.

New buildings allow 0.2 to 0.5 air changes per hour (ach) by infiltration, while with the windows wide open during summer it is possible to achieve 15-20 ach. Even greater ventilation rates, around 30 ach, can be achieved by natural means, but there is a need for a large number of window openings and careful placement within the space (Balaras, 1997). However, case studies have shown that air change rates up to about 10 ach reduce the cooling load significantly, whereas greater air change rates affect the cooling load to a minor extent (Dascalaki and Santamouris, 1997).

Natural ventilation was used extensively for the traditional house in order to keep the temperature between acceptable limits during summer. An indication of the ach that could be achieved in a traditional house can be obtained by using a general expression that gives the ventilation rate Q through an opening as a function of temperature difference ΔT, wind velocity U and wind turbulance. This empirical correlation, which can be applied for single sided ventilation through half an opening, is (De Gids and Phaff, 1995):

$$U_{eff} = \frac{Q}{A/2} = \sqrt{C_1 U^2 + C_2 H \Delta T + C_3} \qquad (4.1)$$

where:

U_{eff}= effective velocity (m/s)

Q = ventilation rate (m^3/s)

A= opening area (m^2)

U= mean wind speed measured at a weather station (m/s)

H= opening height (m)

ΔT= mean temperature difference between inside and outside temperature (°C)

C_1=dimensionless coefficient depending on the wind characteristics

C_2= dimensionless boundary constant

C_3= dimensionless turbulence constant

The values of the dimensionless constants of equation 4.1, obtained from measurements at various wind speeds and temperature differences were estimated as: C_1=0.001, C_2=0.0035 and C_3=0.01

Applying equation 4.1, a mean to high ventilation rate of 16.4 ach is calculated. This result is obtained by assuming a single door per zone of the traditional house, 2.5 m high and 2 m in width, wide open, an afternoon mean wind velocity for the hot months of 5.5 m/s (Table 3.8) and a mean temperature difference between the inside and outside temperature of 10°C.

Simulations were performed for different ventilation rates in the summer. The results for 16 and 17 July and ventilation rates of 3 ach, 6 ach and 9 ach are shown in Figures 4.5 to 4.8 respectively.

The controls employed assumed that ventilation would be effected only when the outdoor temperature was below the indoor temperature.

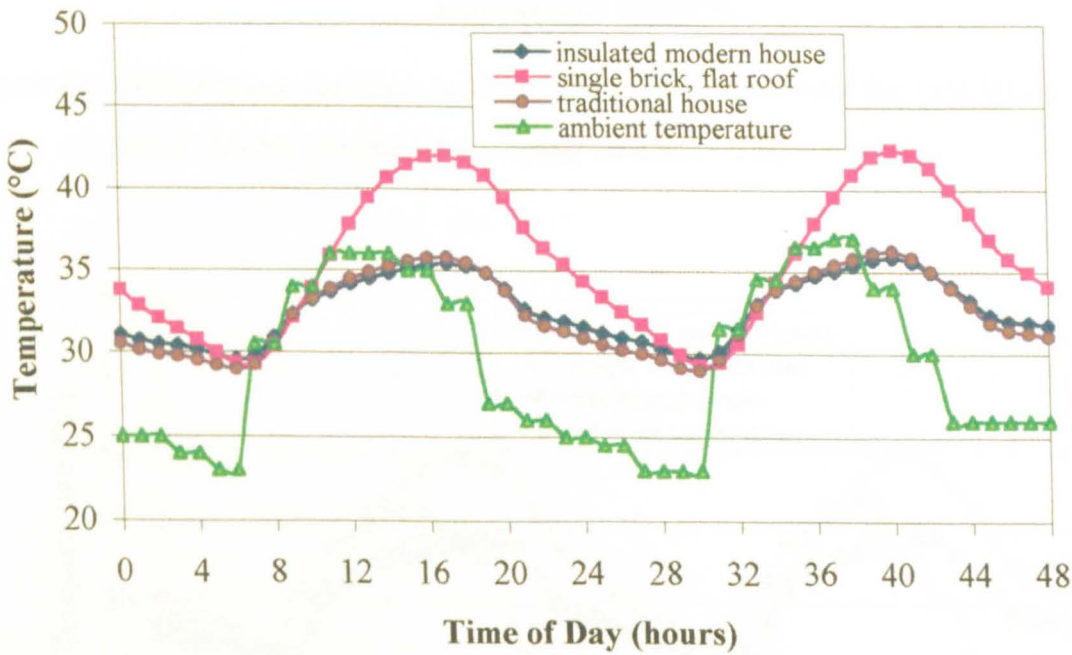

Figure 4.5. Temperature variation in the model houses indicating the ventilation effect for 3 air changes per hour, during 16 and 17 July.

Obviously the ventilation effect will depend on the airflow rate (ach) used. In July the maximum temperature in the flat roof house can reach 46°C (Figure 4.4). With ventilation, this temperature will reduce by about 4°C for three ach, 6°C for six ach and 7°C for nine ach. For the insulated house, which reacts in a similar way to the traditional house, in July the maximum temperature will be around 40°C. With ventilation this temperature will reduce by about 4°C for three ach, 5°C for six ach, and 6°C for nine ach.

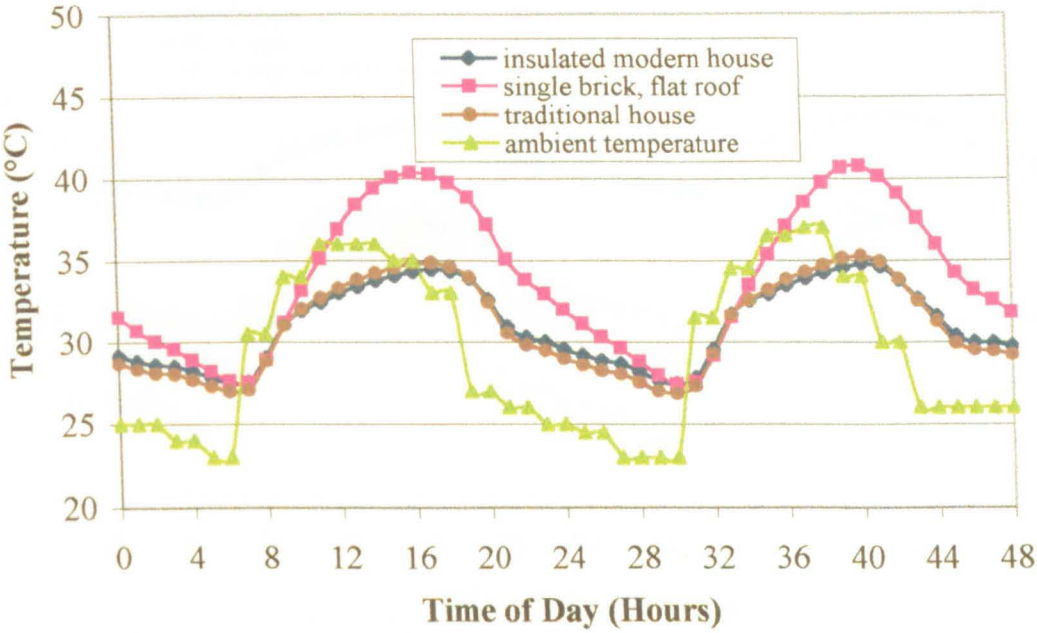

Figure 4.6. Temperature variation in the model houses indicating the ventilation effect for 6 air changes per hour, during 16 and 17 July.

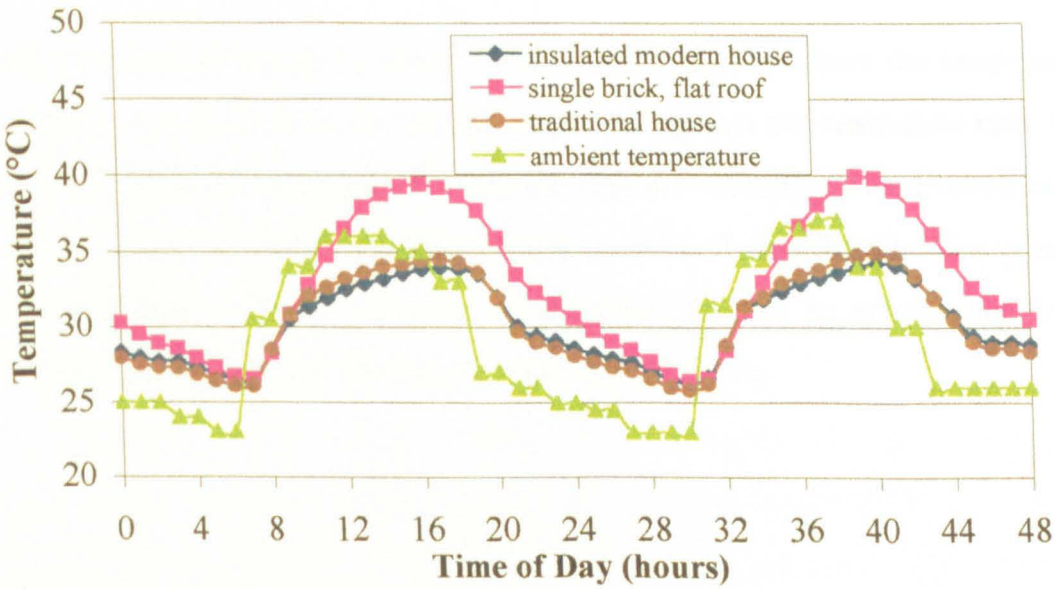

Figure 4.7. Temperature variation in the model houses indicating the ventilation effect for 9 air changes per hour, during 16 and 17 July.

The response of the traditional house to ventilation during the cooler hours of the day for various ventilation rates is indicated in Figure 4.8. As can be observed, the higher the ventilation rate the lower would be the maximum temperature in the house. This explains why large openings (like doors, reaching a height of 2.5 m) were constructed, preferably on walls directed on the side of the prevailing night time wind.

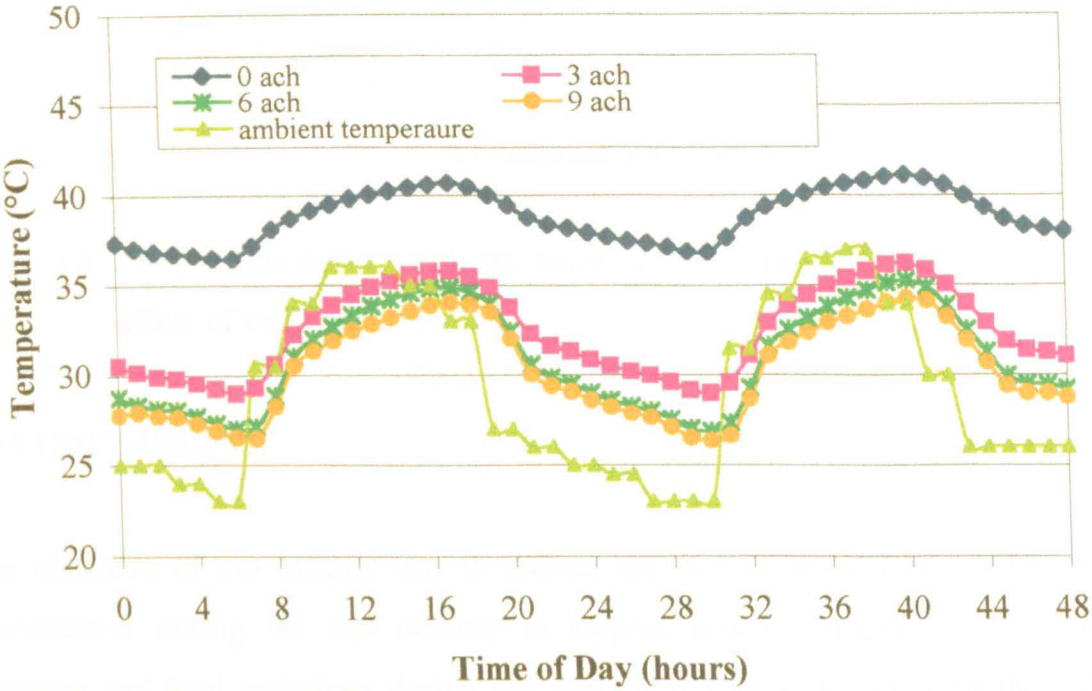

Figure 4.8. Temperature variation in the traditional house indicating the effect of ventilation for various ventilation rates, during 16 and 17 July.

The effect of ventilation can be better observed in Figure 4.9 where the temperature in the traditional house at 6 a.m. for 16 July is plotted against the ventilation rate. As it is observed the effect of ventilation is reduced with the increase of ventilation rate. For rates up to 9 ach the indoor air temperature is reduced significantly. For greater air change rates only a slight reduction is observed. This is in accordance with the observation of Dascalaki and Santamouris mentioned above.

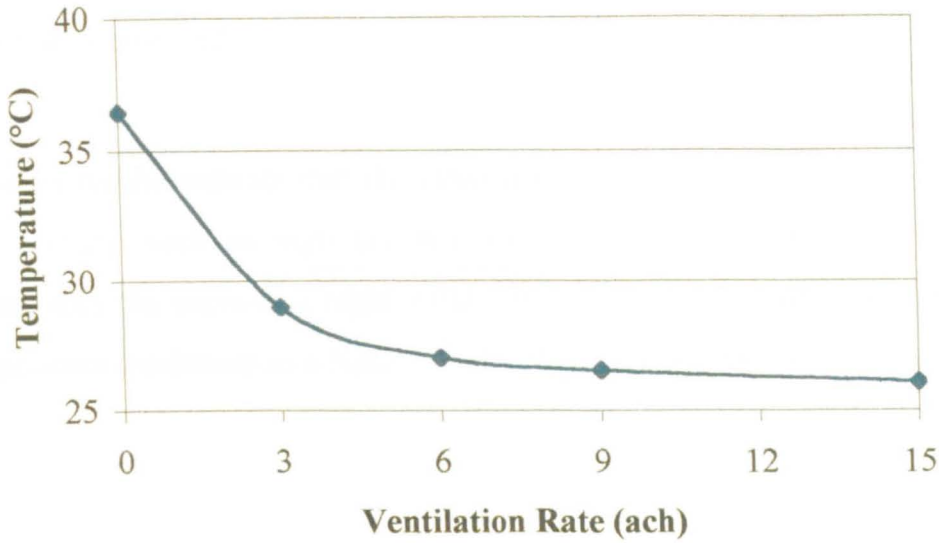

Figure 4.9. Temperature in the traditional house at 6 a.m. for 16 July, indicating the effect of ventilation rate.

4.3 CONCLUSIONS

The objective of this chapter was to present the various house construction methods encountered during the last century in Cyprus and investigate their temperature response and load variations during the year. This was achieved using the TRNSYS program, which performs the necessary calculations based on the transfer function method. For the simulations, a Typical Meteorological Year for the Nicosia area and a typical model house plan were used.

The cooling energy required to maintain the indoor temperature below 25°C was found to be 23,790 kWh for the insulated house, 26,130 kWh for the traditional house and 42,300 kWh for the flat roof house. The corresponding heating loads to maintain the indoor temperature above 21°C were found to be 4460 kWh, 6200 kWh and 16,012 kWh for the three construction types investigated.

For floating conditions, the indoor temperature for the traditional house and the modern insulated house varied between 16°C and 20°C for winter and between 25°C and 35°C for summer compared to 11°C and 20°C for winter and between 33°C and 46°C for summer for the flat roof house. With ventilation the peak summertime temperatures could be reduced by up to 6°C depending on the ventilation rate. For rates up to 9 ach

the indoor air temperature is reduced significantly. For greater air change rates only a slight reduction is observed.

The simulation results indicate that the materials and construction methods used in the early 20th century, such as high ceilings and doors and positioning of doors and windows towards the prevailing night winds resulted in a low cost house offering the same temperature conditions as a highly insulated and expensive modern house.

CHAPTER 5

MODELLING OF THE MODERN HOUSES OF CYPRUS AND ENERGY CONSUMPTION ANALYSIS

The reduction of the building energy requirements to a minimum is an important measure for economy. Therefore, the objective of this chapter is to model a typical modern house in Cyprus by considering the various construction methods applied today and draw conclusions on the suitable structure that should be used in the Cyprus environment for an energy-efficient building.

Abdul-Muhsen *et al.* (1992), investigated the effect on load and energy requirements of residential buildings in respect to their geographical location. For this analysis a detached two-floor house was used, with 464 m^2 total floor area. Four different cities, those of Dhahran, Riyadh, Jeddah and Khamis-Mushayt, representing four different climatic locations, were considered. The results showed the cooling energy demand to vary between 23185 kWh and 48952 kWh and the heating load between 0 kWh and 15590 kWh, depending on location. The analysis showed the most significant load determining parameters to be conduction through walls and roof, solar radiation through glazing and infiltration. The equivalent uniform annual cost (EUAC) method was used to compare the economic performance of the typical house in the four cities.

Santamouris *et al.* (1994), reported the findings of a monitoring campaign of 186 office buildings in Greece. The specific energy consumption of the buildings for heating, cooling and lighting purposes and the consumption of the office equipment was considered. It was found that 50% of the energy consumption was used for heating with only 12.6% for cooling. The remaining 37.4% was consumed by lighting and electrical office equipment. The investigators estimated that energy savings of between 22% and 37% could be achieved with different conservation measures. The applicability of natural ventilation techniques was also investigated but it was concluded that natural ventilation could cause indoor air quality problems due to polluted outdoor air in the cities.

Ghaddar and Bsat (1998), performed a detailed energy analysis of typical residential and office buildings. A number of insulation materials, double-glazed windows, shading, efficient air-conditioning systems, economical lighting and reduction of infiltration rates were considered. The simulations used weather and solar data for Beirut collected hourly for one year and assumed an indoor temperature of 18°C for winter and 23°C for summer. The study indicated that the factors contributing to the cooling load were: walls 12%, roofs 19%, glass 41% and infiltration 5%. The main factors contributing to the heating load were: walls 12%, roofs 14%, conduction through glass 17% and infiltration 19%. Principally it was shown that using better wall insulation could pay back in a short time (2-10 years) depending on the cost of the insulation used. Also multiple measures like better wall insulation, reflective window glass and fluorescent lighting could have a pay back of about 6 years.

This chapter presents results of simulations to determine the energy flows in modern houses in Cyprus using the TRNSYS computer programme. For the calculations, the typical model house is used with the typical meteorological year for the Nicosia area. The effect of different wall and roof constructions on the indoor temperature and resulting heating and cooling loads is presented.

5.1 LOAD ANALYSIS OF THE MODEL HOUSE

This section presents the predicted indoor temperatures and heating and cooling loads of a model house. The model house shown schematically in Figure 3.4, is considered as the reference basic construction, built from the following elements as described in Table 3.5:

1. Single walls, type D.
2. Partition walls, type G and
3. Flat non-insulated roof, type H.

The hourly temperature variation of the model house during a typical year is shown in Figure 5.1. The temperature varies approximately between 10°C and 20°C during winter and between 30°C and 50°C during summer.

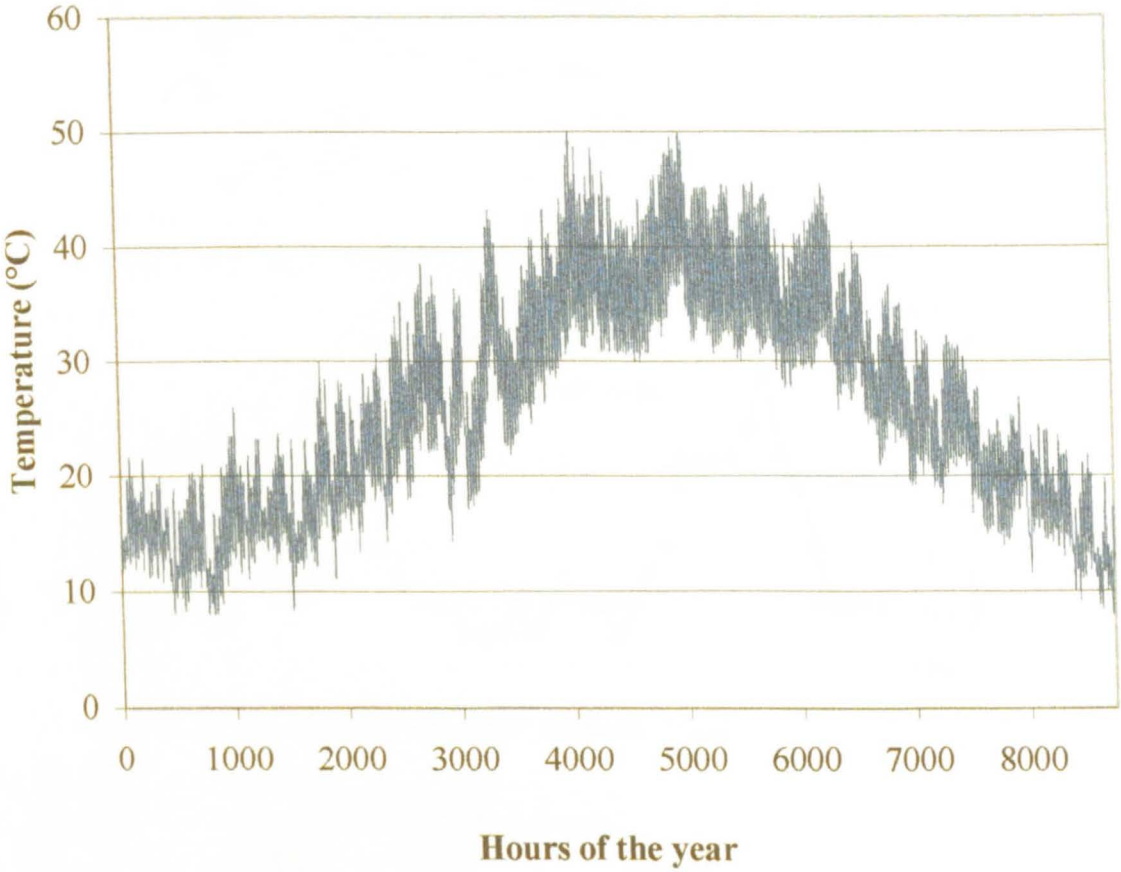

Figure 5.1. Temperature variation of a typical house for each hour of a typical year.

Since the model house is divided into four similar zones, the load resulting from each zone can be observed. In mid-January (Figure 5.2) the sun rises at 7.40 am with a solar azimuth angle of about 60° East. During this time, the direct solar radiation falling on the east window and wall causes the temperature of the N-E Zone (3) to increase sharply.

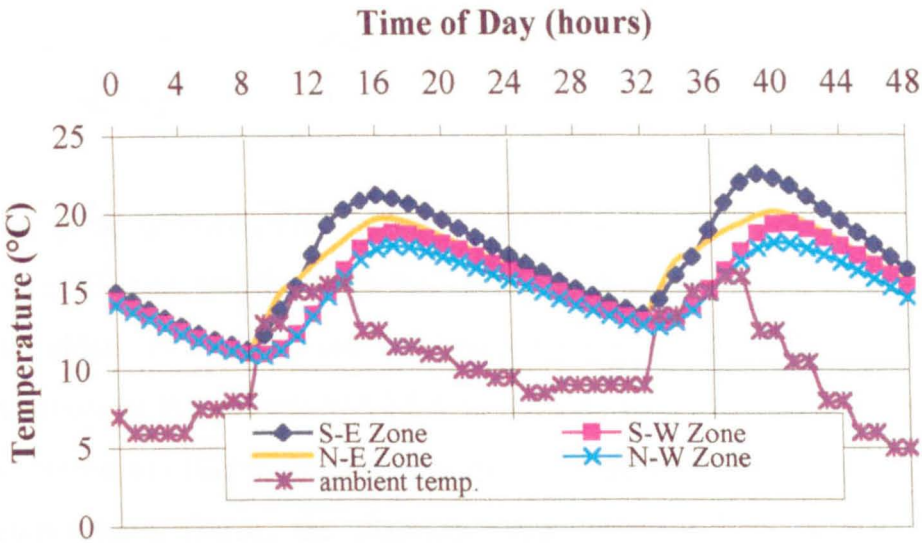

5.2 (a). Ambient and zone temperatures.

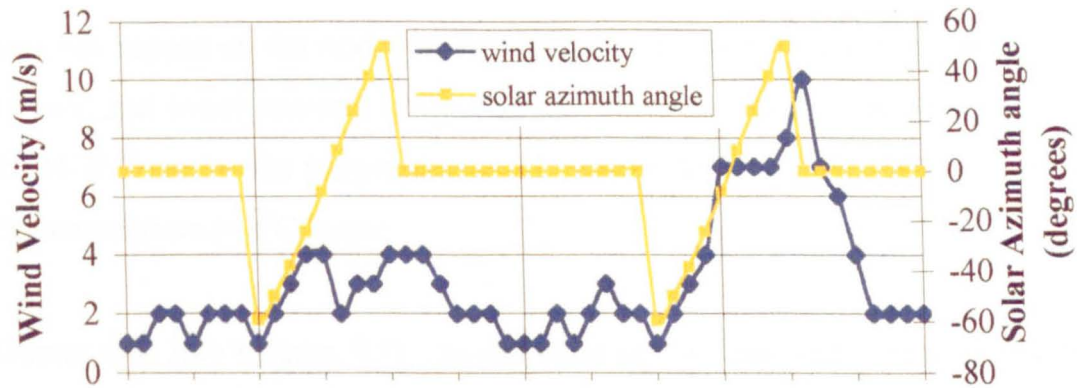

5.2 (b). Wind velocity and solar azimuth angle.

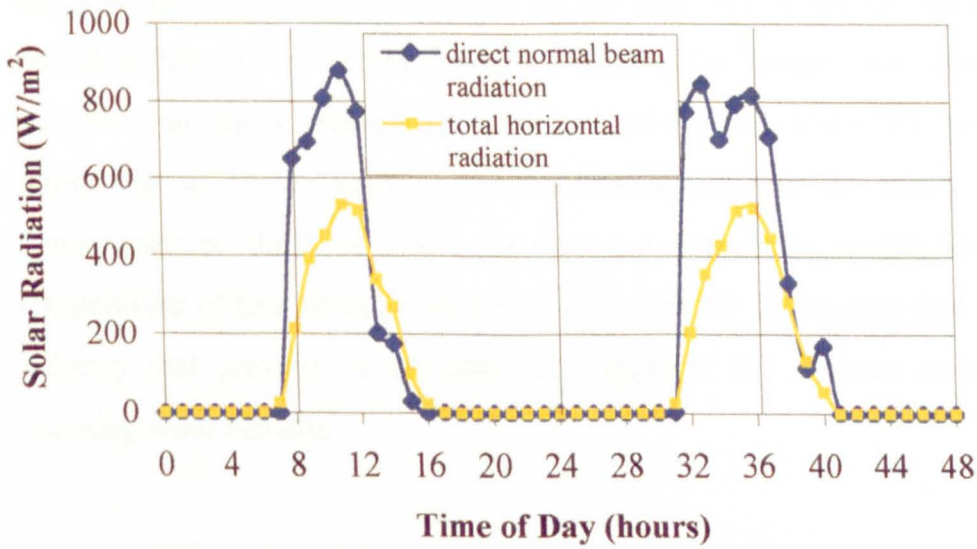

5.2 (c). Direct normal beam and total horizontal radiation.

Figure 5.2. Zone temperatures and relative weather data during 13 and 14 January.

The direct solar radiation then strikes the south window and wall increasing the temperature of the S-E Zone (1), which gives the highest temperature and thus the lowest heating load.

During the afternoon hours in these particular days, haze and clouds obstruct the direct beam radiation and therefore the change in the temperature of the S-W Zone (2) is not so sudden. The N-W Zone (4) gives the highest load. This zone receives no direct radiation, as the sun sets at 5:28 p.m., with an azimuth angle of about 60° west. It is also of interest to observe the effect of the wind speed and ambient temperature on the zone temperatures. During the afternoon hours of the 13th of January the wind velocity is between 1 m/s and 4 m/s and the ambient temperature does not drop below 8°C. This does not happen on the next day, 14th January, at which the greater wind velocity (up to 10 m/s) and lower ambient temperature cause lower zone temperatures. In the case of the N-W Zone (4) the temperature at 12 p.m. on 13 January is 16°C but on 14 January the temperature is 2°C lower.

During mid July (Figure 5.3), the sun rises at 5:15 am with a solar azimuth angle of about 120° East. The temperature of the N-E Zone (3) increases sharply because of the direct radiation striking the window on the east side of the building. The direct solar radiation then strikes the south window causing the temperature of the S-E Zone (1) to increase and nearly reach the temperature of the N-E Zone (3). Also, for these days, during the afternoon hours, haze and clouds obstruct the direct radiation thus the temperature of the S-W Zone (2) does not show any sudden increase. The lower temperature of this zone, as indicated in Figure 5.3 (a), is also due to the higher wind velocity that prevails in the afternoon hours of the summer as compared with the morning wind velocity.

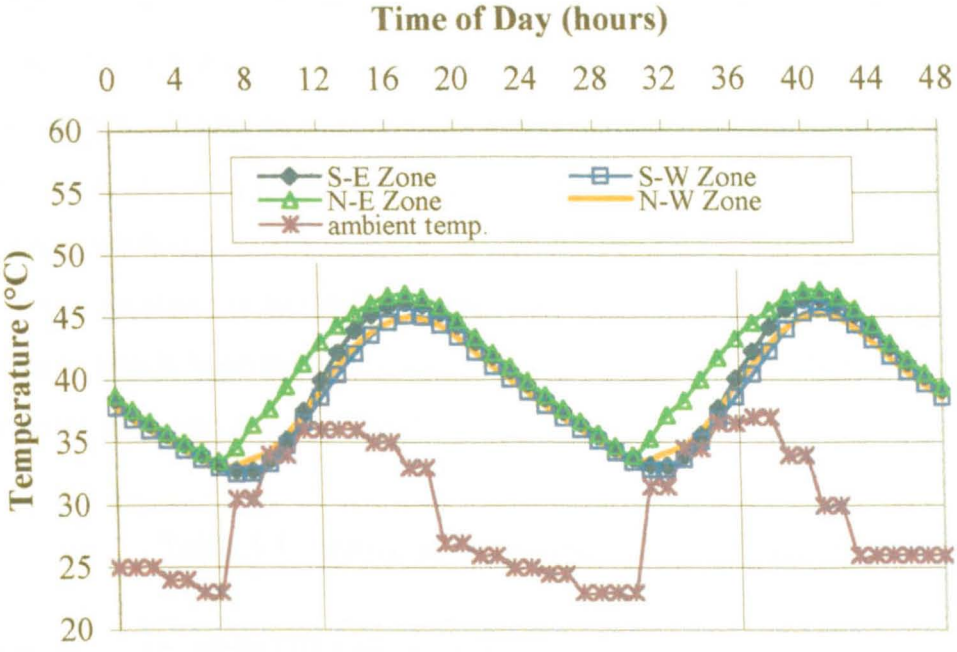

5.3 (a). Ambient and zone temperatures.

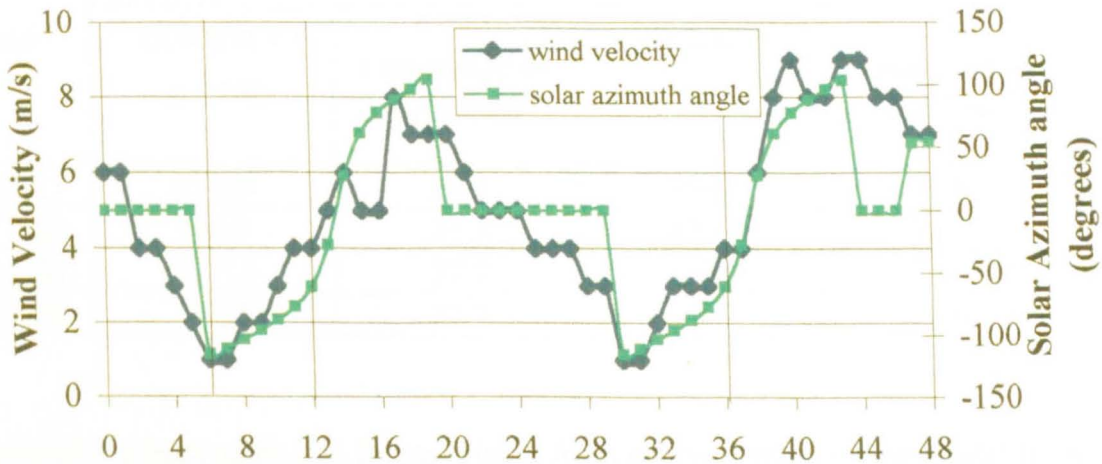

5.3 (b). Wind velocity and solar azimuth angle.

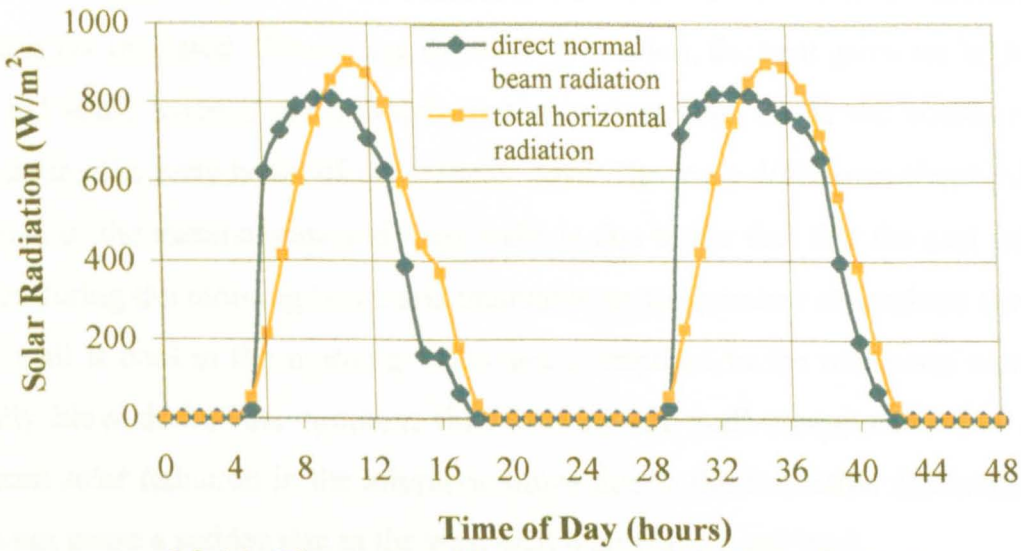

5.3 (c). Direct normal beam and total horizontal radiation.

Figure 5.3. Zone temperatures and relative weather data, during 16 and 17 July.

The annual cooling and heating loads arising from every zone, is indicated in Table 5.1. These loads are estimated by considering that the room temperature is maintained at 25°C during summer and 21°C during winter. As it is observed the cooling load is bigger for the N-E (3) and S-E (1) zones and the heating load is bigger for the N-W (4) and S-W (2) zones where the gains from the environment are smaller. This load distribution is attributed to the weather pattern as outlined in section 3.6, which shows that east walls receive the highest total radiation followed by the south walls, while in the afternoon, winds blowing at a mean velocity of about 5 m/s from the SSW to SW direction, cool the south and west walls.

Table 5.1. Annual zone cooling and heating loads

Zone	Cooling load		Heating load	
	(kWh/m^2) at 25°C	Percentage of total load	(kWh/m^2) at 21°C	Percentage of total load
S-E (Z1)	11125	26.3	3612	22.6
S-W (Z2)	9855	23.3	4227	26.3
N-E (Z3)	11715	27.7	3694	23.1
N-W (Z4)	9605	22.7	4479	28.0

An analysis of the heat gains and losses arising from every element of the model house is shown in Table 5.2. As can be observed, the main load is due to the horizontal roof, which is not insulated. Concerning the wall orientation, the heat gains are higher for the east and south external walls which receive and transfer inside the house more solar heat during the early hours of the summer days. The large difference observed between the load of the external east and west walls is due to the fact that the east wall warms earlier during the morning hours and maintains its temperature throughout the day. The west wall is cool in the morning hours and is exposed to the afternoon winds, which usually blow during the summer, thus keeping the wall temperature low. Also, the reduced solar radiation in the afternoon hours due to the formation of clouds and haze does not cause a sudden rise in the west wall temperature and load.

The heating load is higher for the north and west external walls since they receive and transfer less solar heat during the winter days.

Table 5.2. Heat gains and losses per year, arising from every constructional element of the model house

House Element	Heat Gains per year		Heat losses per year	
	(kWh) at 25°C	Percentage of total cooling load	(kWh) at 21°C	Percentage of total heating load
External East Wall	2254	5.3	468	2.9
External South Wall	1714	4.0	545	3.4
External West Wall	1590	3.8	679	4.2
External North Wall	1403	3.3	757	4.7
Floor	9540	22.6	2909	18.2
Roof	15712	37.1	6387	39.9
East Window	369	0.9	427	2.7
South Window	358	0.8	426	2.7
West Window	328	0.8	440	2.7
North Window	320	0.8	447	2.8
Walls between Zones	7450	17.6	1552	9.7
Other	1360	3.0	975	6.1
Total	42300	100 %	16012	100 %

The load from the windows, shown in Table 5.2, represents only the conduction heat gain and is about the same for all windows. The transmitted solar radiation is absorbed by the floor and other internal surfaces and released sometime later as a convection load. An analysis of the floor load is presented in Table 5.3. As can be seen, when no solar radiation passes through the windows, a reduction of 5940 kWh in the absorbed floor radiative gain occurs. This results in a reduction to the annual cooling load of 6400 kWh or 15.1% and an increase in the heating load of 2648 kWh or 16.5%. The annual floor loss by conduction affecting the cooling load is 400 kWh or 1% and that affecting the heating load is 2180 kWh or 13.6%.

Table 5.3. Effect of solar radiation passing through windows, on the load of the model house per year

Type	Cooling load (kWh)	Heating load (kWh)	Floor cooling load (kWh)	Floor heating load (kWh)	Total absorbed floor radiative gain (kWh)
Model house	42300	16012	9540	2909	8340
Model house, when no solar radiation enters through windows	35900	18660	7130	3780	2400
Model house when no solar radiation enters through windows and floor conduction load is zero	35500	16480	7210	2569	2400

5.2 LOAD ANALYSIS OF VARIOUS CONSTRUCTION METHODS

This section presents the effect that various wall construction methods have on the house indoor temperature. The analysis is performed for the following three wall types as described in Table 3.5:

(a) Single wall, type D.

(b) Double-wall, type E, and

(c) Double-wall, type F.

It must be noted that in all the above cases a flat non-insulated roof, type H is assumed.

The results, shown in Figure 5.4 for winter and Figure 5.5 for summer, indicate that the wall type would not affect considerably the indoor temperature of a non air conditioned building. The maximum difference in a mean air temperature for the different levels of wall insulation is only 0.5 °C.

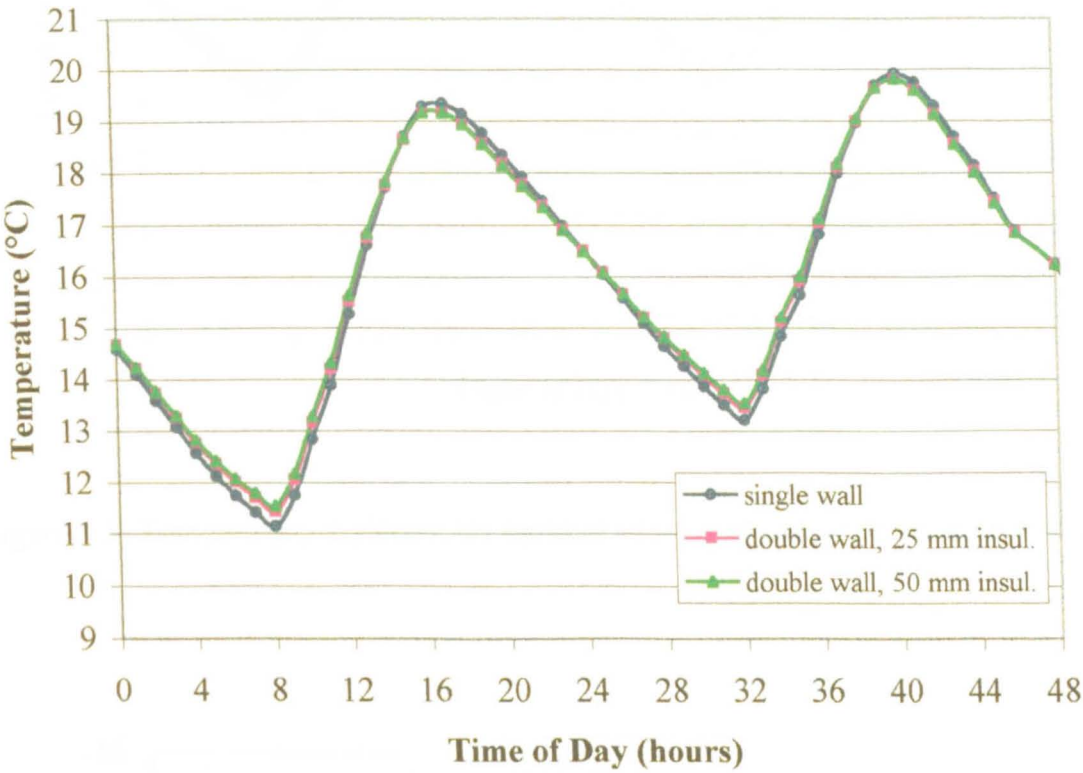

Figure 5.4. Temperature variation for various wall constructions during 13 and 14 January.

The variation in the heating load when the building is maintained at a temperature of 18 °C and 21°C in the two consecutive winter days is shown in Figure 5.6. It can be seen that a double wall with 50 mm of insulation will cause a reduction of 0.5 kW in the maximum heat demand of the house. Raising the indoor design temperature from 18 °C to 21°C will result in a 3 kW increase in the heat demand.

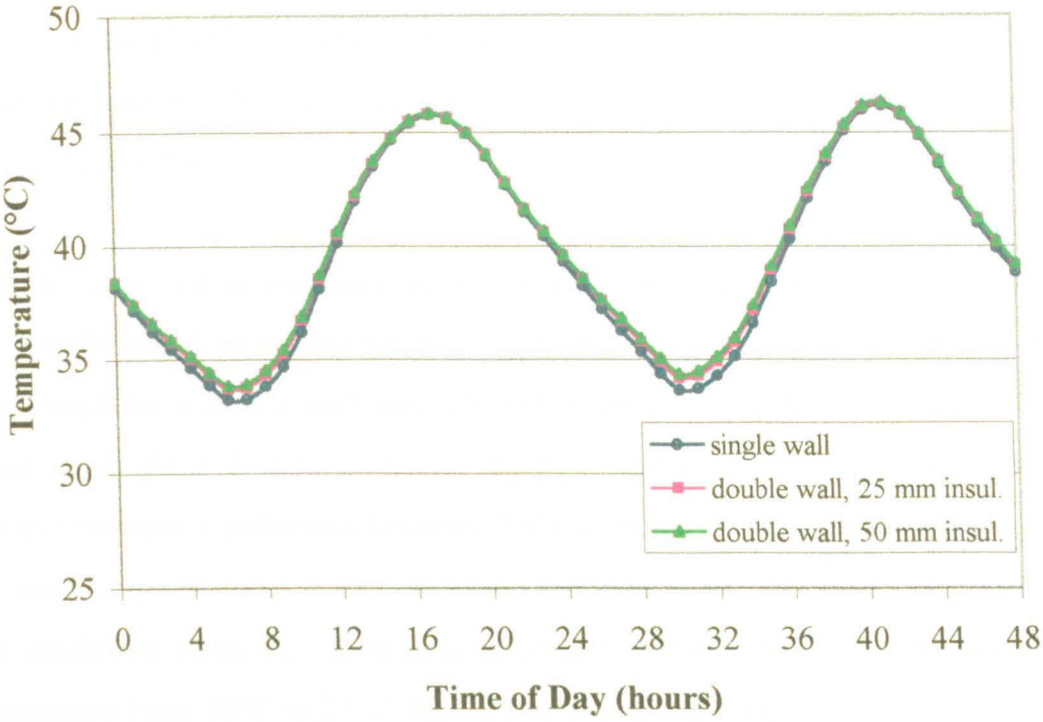

Figure 5.5. Temperature variation for various wall constructions during 16 and 17 July.

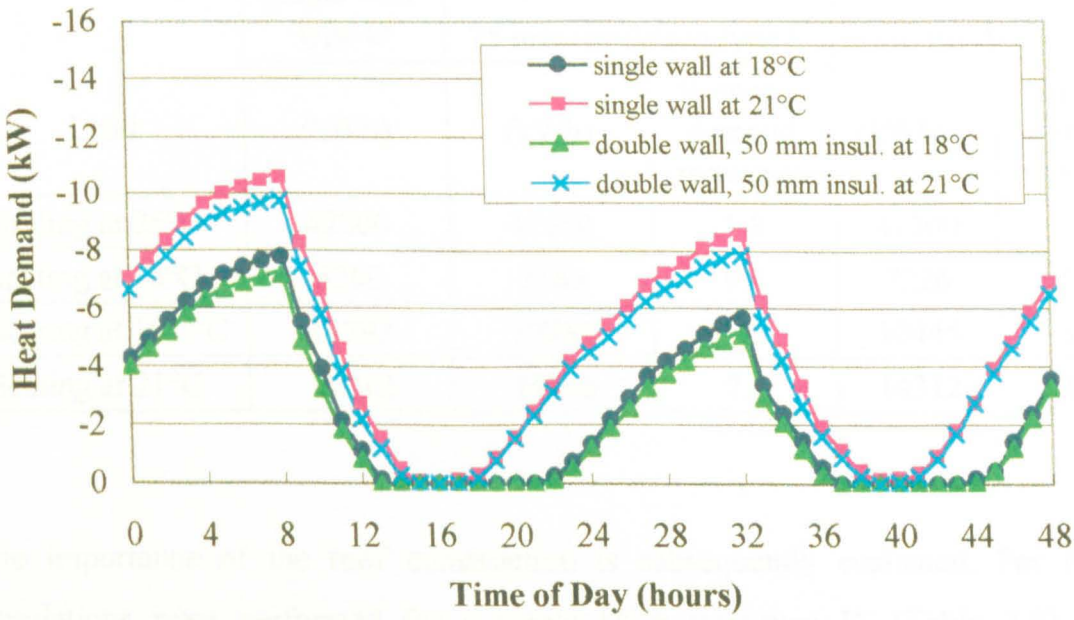

Figure 5.6. Heat demand (kW) against time of day (hours), during 13 and 14 January, to keep the indoor temperature at 18°C and 21°C.

The value of wall insulation can better be appreciated if the heating and cooling energy demand is calculated throughout the year in order to evaluate any savings. The results for design temperatures of 18°C, 19.5°C and 21°C in winter and 25°C in summer are shown in Table 5.4.

It can be seen that to maintain the temperature at 25°C, a cooling energy demand of 42300 kWh would be needed for the single wall construction. A load reduction of 1.8% could result for a double wall with 25 mm insulation (type E) and a reduction of 2.4% would result for a double wall with 50 mm insulation (type F). The heating energy demand presents a reduction between 7.9% and 9.4%, for a double wall with 25 mm insulation (type E) and a reduction between 10.6% and 12.5% for a double wall with 50 mm insulation (type F). It is also important to note that by increasing the design temperature from 18°C to 21°C, the heating energy demand would increase by 100%.

Table 5.4. Annual cooling and heating energy demand for different room design temperatures

Load	Single wall-type D	Double wall with 25 mm insulation-type E		Double wall with 5 cm insulation-type F	
	(kWh)	(kWh)	% energy demand reduction	(kWh)	% energy demand reduction
Cooling at 25°C	42300	41550	1.8	41300	2.4
Heating at 18°C	8260	7485	9.4	7226	12.5
Heating at 19.5°C	11792	10786	8.5	10445	11.4
Heating at 21°C	16012	14746	7.9	14312	10.6

The importance of the roof construction is subsequently evaluated. For this test, simulations were performed for a single brick wall-type D, (Table 3.5) and the following three variations in roof construction:

(a) A flat non-insulated roof, type H.

(b) A flat insulated roof, type I (25 mm insulation) and

(c) A flat insulated roof, type J (50 mm insulation).

The temperature variation inside the model house can be observed in Figures 5.7 and 5.8 for typical winter and summer days respectively. In winter (Figure 5.7), roof insulation will cause the minimum temperature to rise by about 4°C, from 11°C to 15°C. In summer (Figure 5.8), the insulated roof does not allow the room temperature during the day to exceed 40°C while with a non-insulated roof the temperature rises to 46°C, i.e., a significant reduction in the resulting room temperature is obtained. With the insulated roof, however, nightime room temperatures are higher than those for the uninsulated roof due to the lower heat transfer from the indoor to the outdoor air across the roof. An analysis of the annual cooling and heating loads for various roof constructions to keep the model house at various room temperatures is shown in Table 5.5.

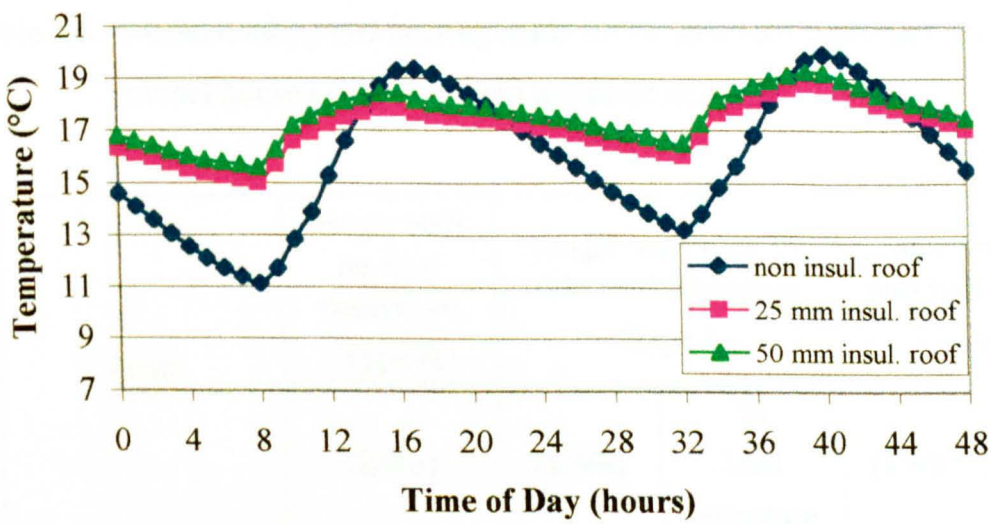

Figure 5.7. Temperature variation for various roof constructions during 13 and 14 January.

The Table shows that for a constant indoor temperature of 25°C, a cooling demand of 42300 kWh will be needed for the single wall construction. A load reduction of 41.7% will result from a roof insulation of 25 mm (type I) and a reduction of 45.5% will result from a roof with 50 mm insulation (type J).

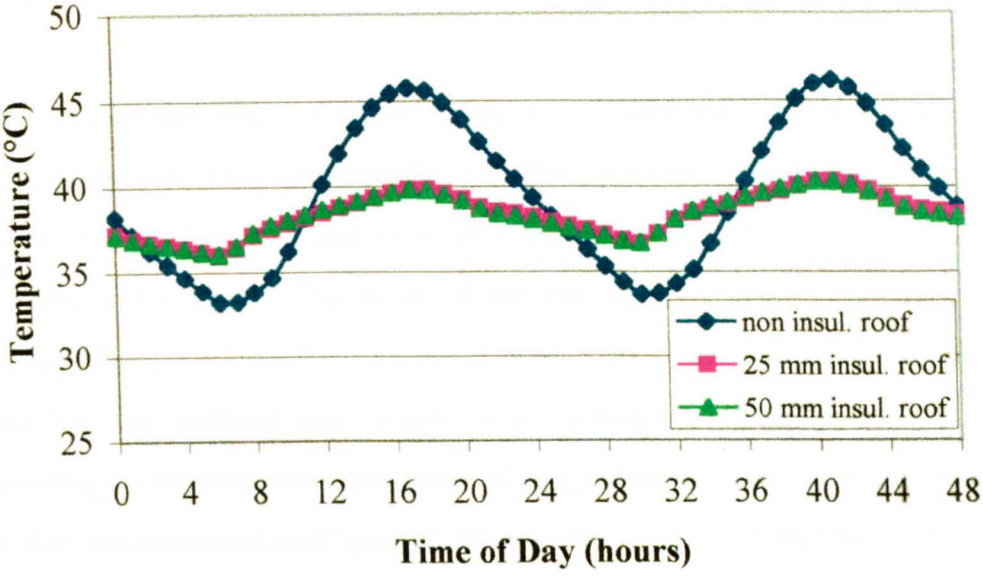

Figure 5.8. Temperature variation for various roof constructions during 16 and 17 July.

Table 5.5. Annual cooling and heating loads for various roof constructions, to keep the model house at various room temperatures

Load	Single wall no-roof insulation Type H	Single wall with 25 mm roof insulation Type I		Single wall with 50 mm roof insulation Type J	
	(kWh)	(kWh)	% load reduction	(kWh)	% load reduction
Cooling at 25°C	42300	24660	41.7	23050	45.5
Heating at 18°C	8260	2636	68.1	2055	75.1
Heating at 19.5°C	11792	4355	63.1	3500	70.3
Heating at 21°C	16012	6506	59.4	5348	66.6

In winter, a 25 mm roof insulation will cause a 68% reduction in the heat demand for a set-point temperature of 18°C. A 50 mm roof insulation will increase the reduction in the heat demand to 75%. Increasing the set-point temperature will lead to increased energy savings in kWh.

5.3 INCLINED ROOFS

In this section the effect of constructing an inclined roof instead of the traditional flat roof is examined. This construction is applied nowadays in Cyprus mainly for aesthetic reasons. A typical section and view of a model house with an east-west inclined roof is illustrated in Figure 3.4. The facets of the east-west inclined roof face east and west. A north-south inclined roof is rotated at 90° to the east-west direction. As it is seen in Table 5.6, the inclined roof results in an increase of load between 5.3% and 13.2% depending on its orientation and time of year, when constructed with the same materials as a flat non-insulated roof type H. This is due to the fact that by tilting the roof at 15° the roof surfaces are exposed to a greater amount of direct sun radiation compared to a flat surface.

Table 5.6. Annual cooling and heating demand for flat and inclined roofs

Load	Flat non-insulated roof Type H-Reference (kWh)	N-S, 15° Inclined roof				E-W, 15° Inclined roof			
		Concrete roof, no insulation	% Load Increase	Insulated roof, type K	% Load decrease	Concrete roof, no insulation	% Load Increase	Insulated roof, type K	% Load decrease
Cooling at 25°C	42300	44545	5.3	24750	41.5	45098	6.6	24960	41.0
Heating at 21°C	16012	18122	13.2	7280	54.5	17981	12.3	7257	54.7

It must be noted though, that for the inclined roof the typical construction is 150 mm heavyweight concrete, 4 mm asphalt for waterproofing and 50 mm plaster and clay tile on top. This construction, used as a decorative element, is an imitation of the traditional roof (type B, Table 3.5) and leads to a reduction in the air-conditioning load of between 41% and 55% compared to the flat non-insulated roof type H.

Also, as can be observed in Table 5.6, the direction of the roof inclination is of little importance since the load variation is very small. The cooling load is slightly reduced and the heating load slightly increased for the north-south inclined roof compared to the east-west ones, due to the fact that the north surface of the roof receives slightly less solar radiation during the year since it faces away from the sun.

5.4 CONCLUSIONS

In this section, the thermal load of a typical house was examined, for various building constructions encountered in Cyprus.

The results of the simulations indicate that the indoor temperature, when no air-conditioning is used, can vary between 10°C and 20°C for winter and between 30°C and 50°C for summer without ventilation. The evaluation of the heating and cooling loads for various wall and roof constructions indicates the importance of the roof insulation, which results in a reduction of up to 46% in the cooling load and up to 75% in the heating load.

Also, the effect of the inclined concrete roof structure is examined. The inclined concrete roof, used as a decorative element, is an imitation of the traditional roof. An insulated inclined roof will result in a reduction in the air-conditioning load of between 41% and 55% compared to the non-insulated flat roof.

CHAPTER 6

MEASURES TO LOWER BUILDING THERMAL LOAD AND THEIR COST EFFECTIVENESS

An important measure for economy is to lower building energy requirements to a minimum. The main concern of engineers however is to evaluate the cost effectiveness of the various measures, which may be applied. This chapter describes results and the cost effectiveness of measures that can be applied to minimise the thermal loads. The measures examined are natural and controlled ventilation, solar shading, various types of glazing, orientation, shape of buildings, and thermal mass.

With reference to Table 3.5, which describes the various wall and roof construction types, the compared buildings are labelled as:

1. No roof insulation, which refers to a house constructed from single walls type D and a flat non-insulated roof type H.

2. 25 mm roof insulation, which refers to a house constructed from single walls type D and a flat insulated roof type I.

3. 50 mm roof insulation, which refers to a house constructed from single walls type D and a flat insulated roof type J.

4. 50 mm roof and wall insulation, which refers to a house constructed from double walls type F and a flat insulated roof type J.

6.1 EFFECT OF VENTILATION

ASHRAE Standard 62.2 P, ventilation and acceptable indoor air quality in low-rise residential buildings, specifies the minimum requirements for mechanical and natural ventilation in spaces intended for human occupancy within single-family houses and low-rise multifamily structures. This new Standard is intended to replace ASHRAE Standard 62-1989 because it contains more detail and is clearer on how to apply the ventilation rates (Sherman, 1999). For a model house of floor area of 196 m^2, assuming

three bedrooms with four occupants, the required mechanical and or natural ventilation is about 0.31 air changes per hour (ach). This requirement, according to a study in the current stock of buildings in the USA, can be met through infiltration alone, since the buildings are quite leaky (Sherman, 1999). Also, according to Balaras (1997), new buildings allow for 0.2 ach to 0.5 ach by infiltration, while with the windows wide open during summer, it is possible to achieve 15 ach to 20 ach. Equation 3.24, used in the calculations for TRNSYS Type 19 predicts infiltration rates during all hours of the day, in excess of the minimum ventilation requirements, with a mean yearly infiltration rate of 0.38 ach.

In this section the effect of introducing naturally or mechanically ambient air into the space when the outdoor air is of a lower temperature than the indoor air during summer and visa-versa during winter, is investigated.

The simulations show that in winter, ventilation air will have negligible effect in increasing the indoor temperature during periods when the outdoor temperature exceeds the indoor design temperature. This is because these periods are quite short. In summer, the effect of ventilation air when the outdoor temperature is less than the indoor temperature is shown in Figure 6.1.

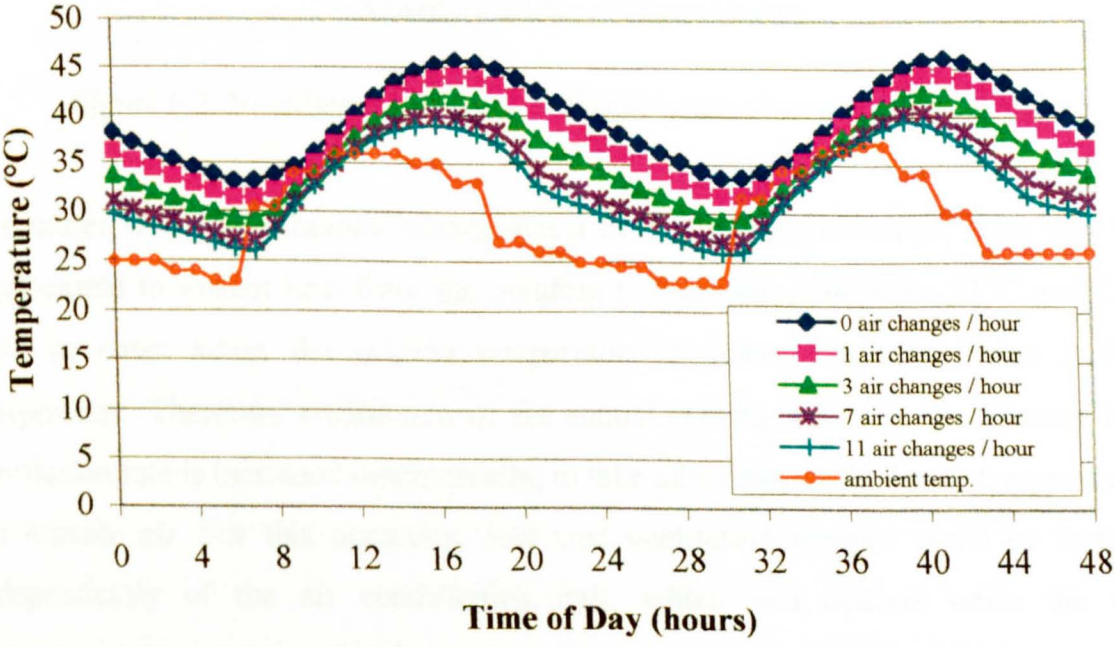

Figure 6.1. Temperature variation of a typical house indicating the effect of ventilation during 16 and 17 July.

It can be seen that the higher the ventilation rate, the lower will be the indoor temperature for a non-air conditioned building. The effect of ventilation rate on the reduction of the maximum indoor temperature for a building with no roof insulation is shown more clearly in Figure 6.2. It can be seen that without ventilation the indoor temperature will reach 46°C. With ventilation, this temperature will reduce by about 2°C for one air change per hour, 3°C for two air changes per hour and 7°C for eleven air changes per hour. Figure 6.2, also shows that ventilation will have a similar effect on a house with roof insulation. The level of roof insulation has no effect on ventilation effectiveness.

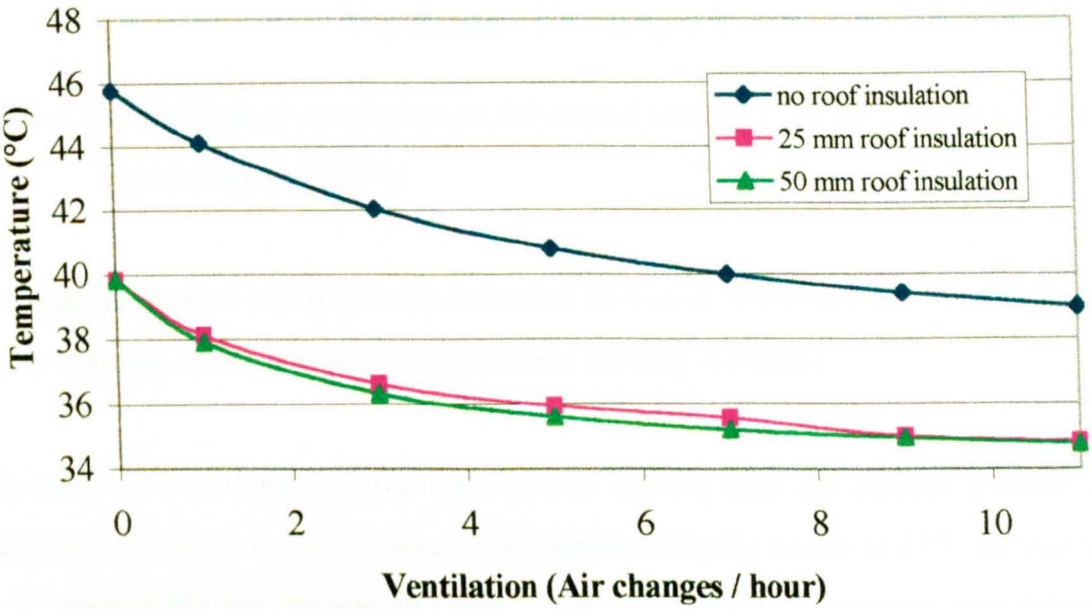

Figure 6.2. Ventilation effect for different types of construction in July.

In summer, due to the thermal storage effect of the building envelope, there may be a requirement to extract heat from the building to maintain it between 21°C and 25°C, even in cases when the outside temperature is lower than the inside building temperature. Therefore a reduction of the annual cooling load may be obtained if the ventilation rate is increased mechanically, to take advantage of the lower temperature of the outside air. For this operation, low cost ventilation systems could be installed, independently of the air conditioning unit, which will operate when the room temperature is above the outside temperature in summer, increasing the air changes per hour. The simulation results are presented in Figure 6.3 and show that a reduction of the annual cooling load is obtained, which increases when the air changes per hour increase.

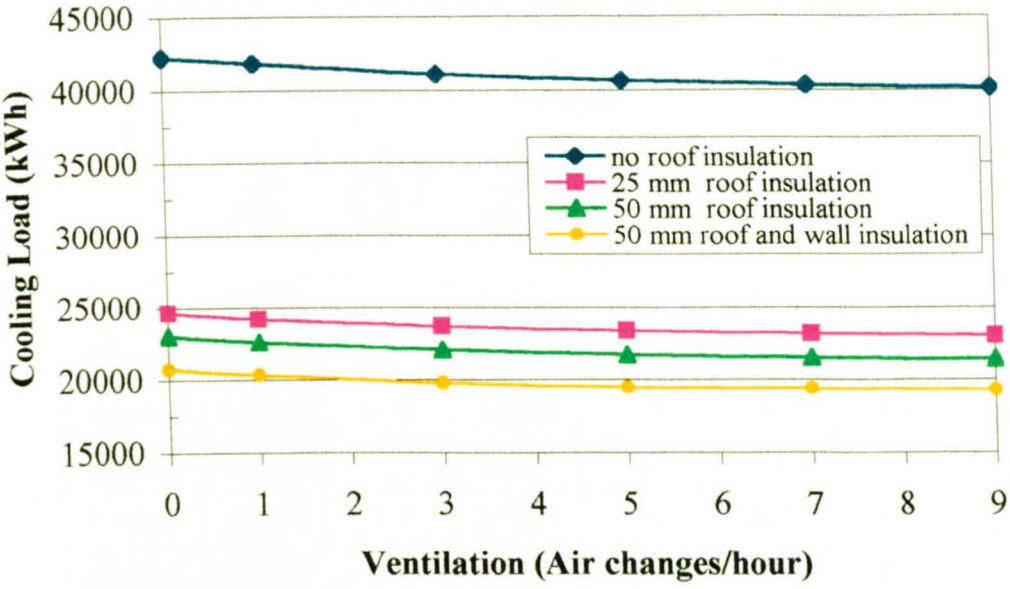

Figure 6.3. The effect of ventilation on the annual cooling load for maintaining the model house at 25°C.

The ventilation rate could also be increased in winter when the outside temperature is higher than the inside temperature and when heating is needed.

The effect of ventilation on the cooling and heating load for various constructions is analysed in Table 6.1. As it is seen, when maintaining the house at 21°C in winter, there is no appreciable load reduction arising from ventilation. In summer, ventilation leads to a maximum reduction of 7.7% for maintaining the house between 21°C and 25°C. The reduction in cooling load depends on the type of construction. Comparing the constructions presented in Table 6.1 it is observed that the ventilation effect increases with improved insulation levels.

6.2 EFFECT OF WINDOW GLAZING

In this section an analysis of the impact of window glazing on the cooling load is presented. A number of cases are investigated which can partly obstruct solar radiation and offer a wide range of conductance. These cases are presented in Table 6.2.

Table 6.1. Annual cooling and heating loads for various roof constructions indicating the effect of ventilation

Air changes per hour	Process	No-roof insulation		25 mm roof insulation		50 mm roof insulation		50 mm roof and wall insulation	
		Load (kWh)	Load reduction (%)	Load (kWh)	Load reduction (%)	Load (kWh)	Load reduction (%)	Load (kWh)	Load reduction (%)
0	Cooling	42300	-	24660	-	23050	-	20743	-
	Heating	16012	-	6506	-	5348	-	3740	-
1	Cooling	41902	0. 9	24239	1.7	22606	1.9	20346	1.9
	Heating	16012	-	6504	-	5347	-	3739	-
3	Cooling	41159	2.7	23707	3.9	22052	4.3	19785	4.6
	Heating	15999	0.1	6500	0.1	5345	0.1	3737	0.1
5	Cooling	40676	3.8	23393	5.1	21731	5.7	19465	6.2
	Heating	15979	0.2	6496	0.2	5335	0.2	3732	0.2
7	Cooling	40359	4.6	23192	6.0	21529	6.6	19270	7.1
	Heating	15967	0.3	6489	0.3	5331	0.3	3729	0.3
9	Cooling	40157	5.1	23062	6.5	21399	7.2	19150	7.7
	Heating	15948	0.4	6487	0.3	5329	0.4	3728	0.3

Table 6.2. Properties of window glazing

Case	Window type*	Unit conductance (U, W/m^2-K)	Unit conductance (U, kJ/hr-m^2-K)	Transmittance for visible radiation (τ_v)
W1	Clear double glazing	3.42	12.3	0.80
W2	Reflective double glazing, bronze	2.27	8.2	0.10
W3	Low-emissivity double glazing, bronze	1.89	6.8	0.41

*Sweitzer et al., 1987

The results of the simulations are presented in Table 6.3. As it is observed, a saving in the cooling load of between 3100 kWh and 7300 kWh can result, when compared to the corresponding construction with clear double glazing windows (case W1). The saving in cooling load for the house with 50 mm roof and wall insulation, can be as much as 35.3% in the case that no extra lighting is used for case W3. But since in this case (W3) the transmittance for visible radiation is only 0.41 extra lighting will be needed, depending on the occupant needs. Assuming an 150 W extra lighting consumption, the savings reduce to 24%. However, window glazing will also reduce solar radiation transmission into the house, which would have been beneficial in cold days. This will result in an increase of the heating load, which in the latter case would be 877 kWh or 23.5%.

Since the cooling load reduces but heat demand increases the appropriate glazing type can be decided only when an economic analysis is applied as indicated in Table 6.8.

Table 6.3. Effect of window shading on annual cooling loads

Wall and roof construction	Window type	Cooling load (kWh)	Cooling load decrease, compared to case W1 (kWh)	Cooling load decrease, compared to case W1 %	Heating load (kWh)	Heating load increase, compared to case W1 (kWh)	Heating load increase, compared to case W1 %
Single wall, no roof insulation	W1	42300	-	-	16012	-	-
	W2	39169	3131	7.4	16737	725	4.5
	W3	36725	5575	13.2	17934	1922	12
50 mm roof and wall insulation	W1	20743	-	-	3740	-	-
	W2	16520	4223	20.4	4655	915	24.5
	W3	13429	7314	35.3	6187	2447	65.4
50 mm roof and wall insulation plus extra lighting	W1	20743	-	-	3740	-	-
	W2 plus 100 W	17693	3050	14.7	3956	216	5.8
	W3 plus 150 W	15773	4970	24.0	4617	877	23.5

6.3 EFFECT OF OVERHANGS

Overhangs are devices that block direct solar radiation from entering a window during certain times of the day or the year. These are desirable for reducing the cooling loads and avoid uncomfortable lighting in perimeter rooms due to excessive contrast. To investigate the effect of the overhang length a number of simulations were performed. For these simulations the overhang was assumed to be located 0.5 m above the window and extend 1 m on both sides of the window. The cooling and heating load of the four zones of the model house, constructed from single walls with no roof insulation for various overhang projections is indicated in Figure 6.4. As can be seen, by increasing the overhang projection the yearly cooling load decreases but at the same time the yearly heating load increases as some useful solar radiation is blocked during wintertime. The effect on the cooling load, as expected, is greater for the east and south windows located in Zones 3 and 1, since these windows receive more solar radiation during the year. The rate of cooling load decrease in Figure 6.4 is higher than the rate of heating load increase for every zone.

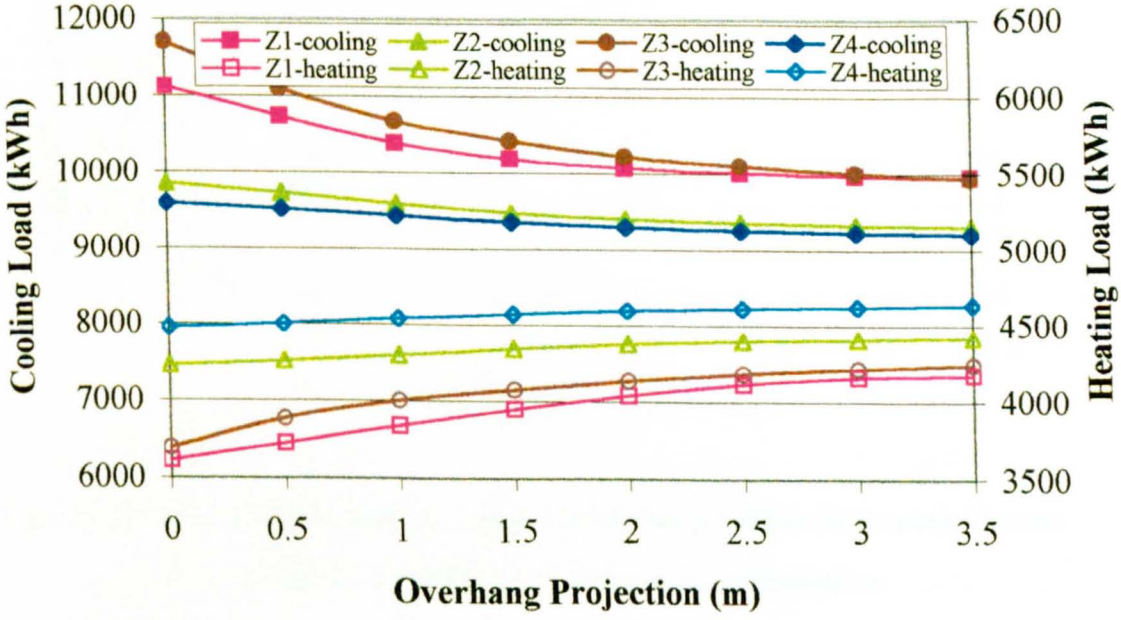

Figure 6.4. Annual cooling and heating load of the four zones against overhang length for a model house constructed from single walls with no roof insulation.

The total annual cooling and heating load difference of the model house is presented in Figure 6.5. As can be seen, the greater the overhang projection, the greater will be the cooling load decrease. The heating load will increase though, since some useful solar

radiation is also blocked during cold days. The difference between the cooling and heating load would increase with increasing overhang projection because greater amounts of direct and indirect radiation will be blocked both during summer and winter. Therefore, it would be advantageous to use long overhang projections in the summer that could be retracted in winter but in 'real' buildings the strategy will be based not only on economic but also on aesthetic grounds.

For the model house constructed from walls and roof with 50 mm insulation, the cooling and heating load of the four zones would change in a similar way. Figure 6.6 shows the annual load difference against overhang projection for this type of construction. As can be seen there would be about 25% greater savings resulting for the same overhang length, compared to the case above, because of the better insulation of the house.

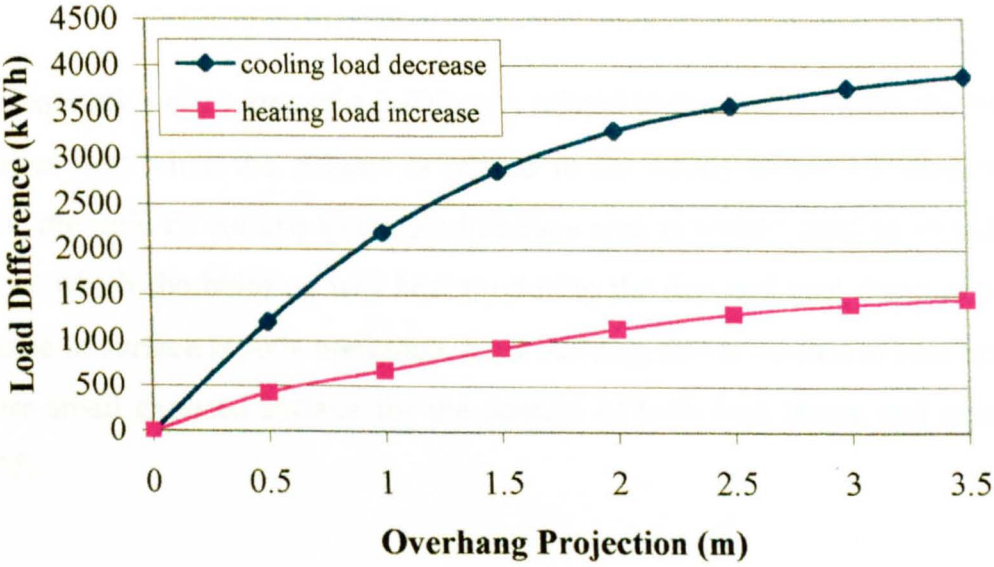

Figure 6.5. Annual load difference against overhang length for a model house constructed from single walls with no roof insulation.

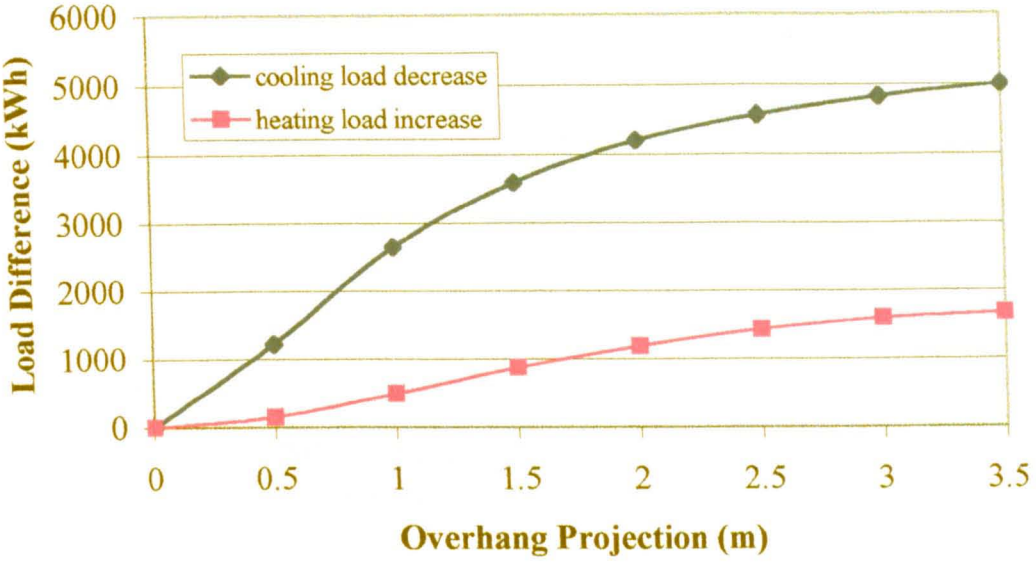

Figure 6.6. Annual load difference per year against overhang length for a model house constructed from walls and roof with 50 mm insulation.

6.4 EFFECT OF HOUSE SHAPE AND ORIENTATION

The exposed surface area of a building is related to the rate at which the building gains or loses heat while the volume is related to the ability of the building to store heat. Thus, the ratio of volume to exposed surface area is widely used as an indicator of the rate at which the building will heat up during the day and cool down at night. A high volume to surface ratio is preferable for a building that is desired to heat up slowly, as it offers small exposed surface for the control of both heat losses and gains (Dimoudi, 1997).

In order to examine the effect of the shape and orientation of the building a new model house plan is necessary that will increase the wall area but will keep the same volume. This model, named Shape 2 is illustrated in Figure 6.7. Shape 2, has half the width and double the length of the original model house resulting in a wall perimeter of 70 m instead of 56 m of the original model.

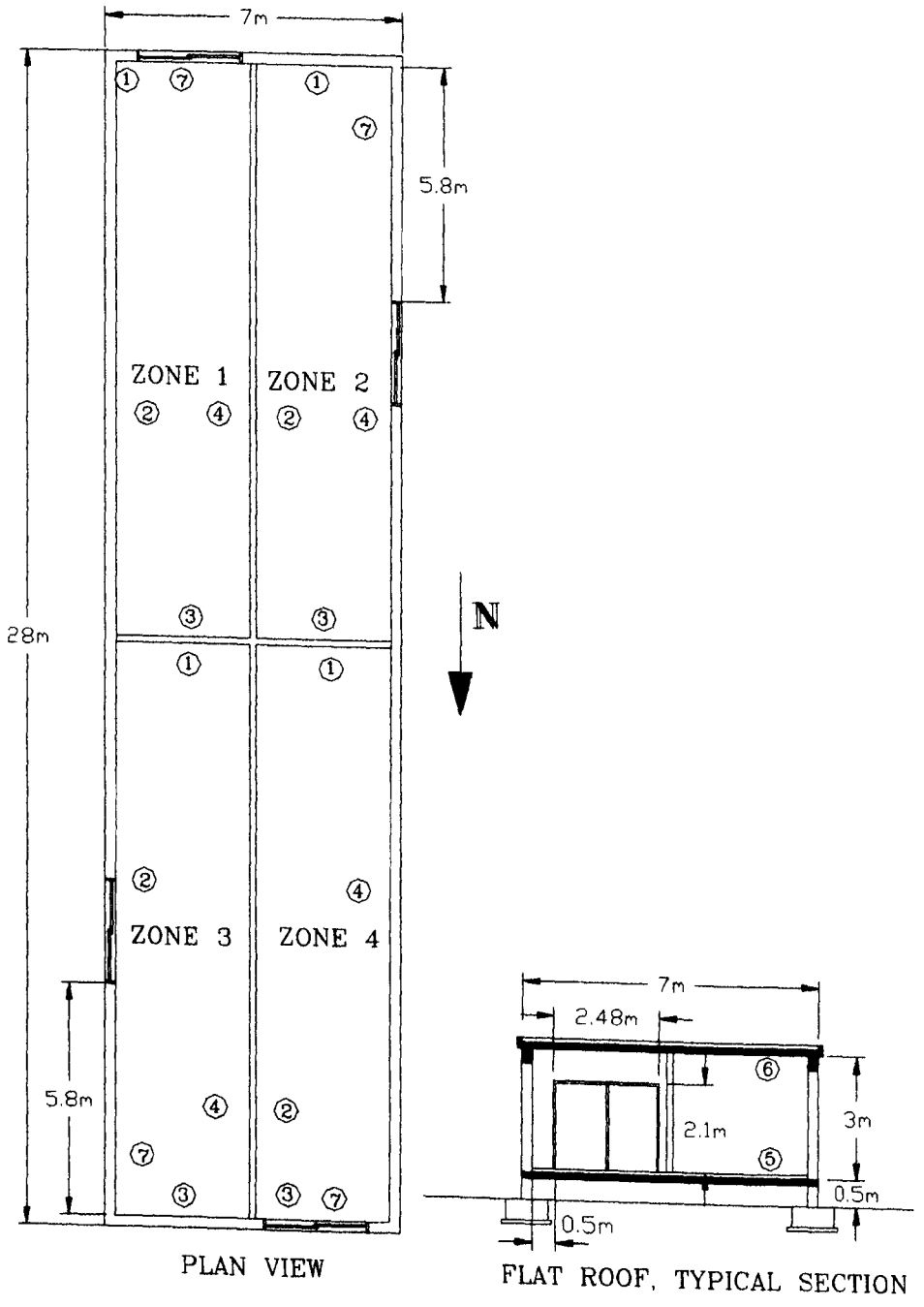

Figure 6.7. Model house Shape 2, with glass doors and changed dimension but with the same floor area and volume.

Table 6.4 presents the thermal load variation between the houses with different shapes. For this analysis two construction types were examined for every shape. These are the single wall (type D) model with no roof insulation (type H) and the 50 mm wall insulation (type F) model with roof insulation (type J). The results show that the elongated Shape 2 model has about the same cooling load but shows a significant increase in the heating load, between 8.2% and 26.7% in respect to the model house of Shape 1, depending on the construction type. Therefore the results show that a smaller wall area to volume ratio is preferable.

Table 6.4. Annual thermal load variation between houses of different shapes

Case	Model house type	Shape 1		Shape 2		Percentage difference in respect to Shape 1	
		Cooling load (kWh)	Heating load (kWh)	Cooling load (kWh)	Heating load (kWh)	Cooling load	Heating load
A	Single wall, no roof insulation (types D and H)*	42300	16012	43526	17323	2.9%	8.2%
B	50 mm wall and roof insulation (types F and J)*	21710	3485	21665	4417	-0.2%	26.7%

* Table 3.5

To examine the effect of orientation for the climate conditions encountered in Nicosia, Cyprus, the four models are rotated from their present orientation, in a clock-wise direction through 180°. Figure 6.8 shows the cooling load difference presented by the four models for different orientations.

Shape 1, presents the minimum cooling load at no rotation and at every 90 degrees because of the symmetry of its four sides. Depending on the construction type, an increase in load of between 400 kWh and 600 kWh occurs at a rotation of 45 degrees.

Shape 2, presents the minimum cooling load at 90 degrees because at this position the east wall area, which has the biggest load contribution, is minimised. Depending on the

construction type, an increase in the cooling load of 900 kWh can result, if the model is rotated by 45° from its minimum load position.

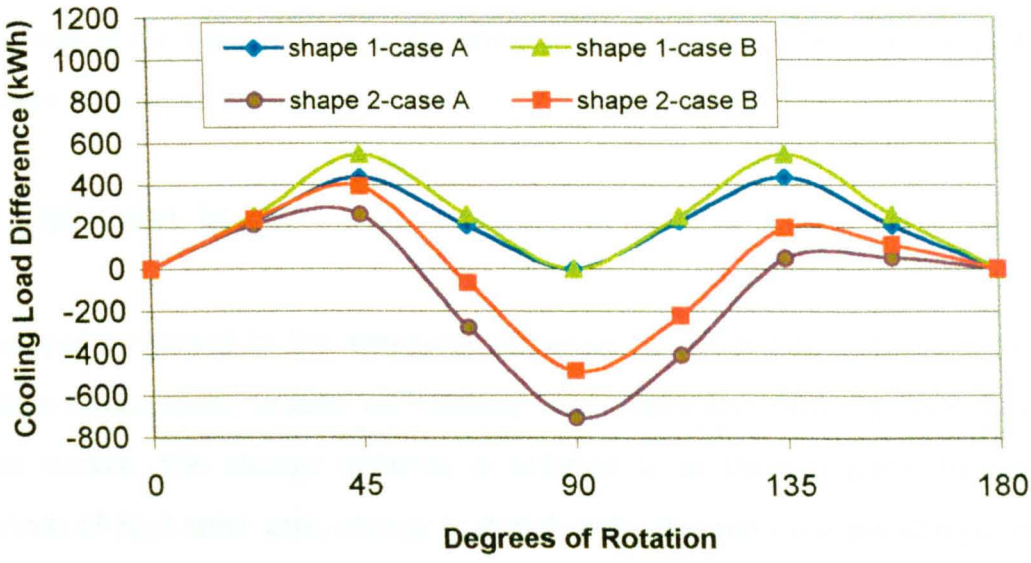

Figure 6.8. Annual cooling load difference against degrees of rotation of the models.

Figure 6.9 shows the heating load difference presented by the four models during rotation. Shape 1, presents minimum load at no rotation as happens with the cooling load. Depending on the construction type, an extra heating load of 125 kWh to 150 kWh results at a peak position of 45 degrees.

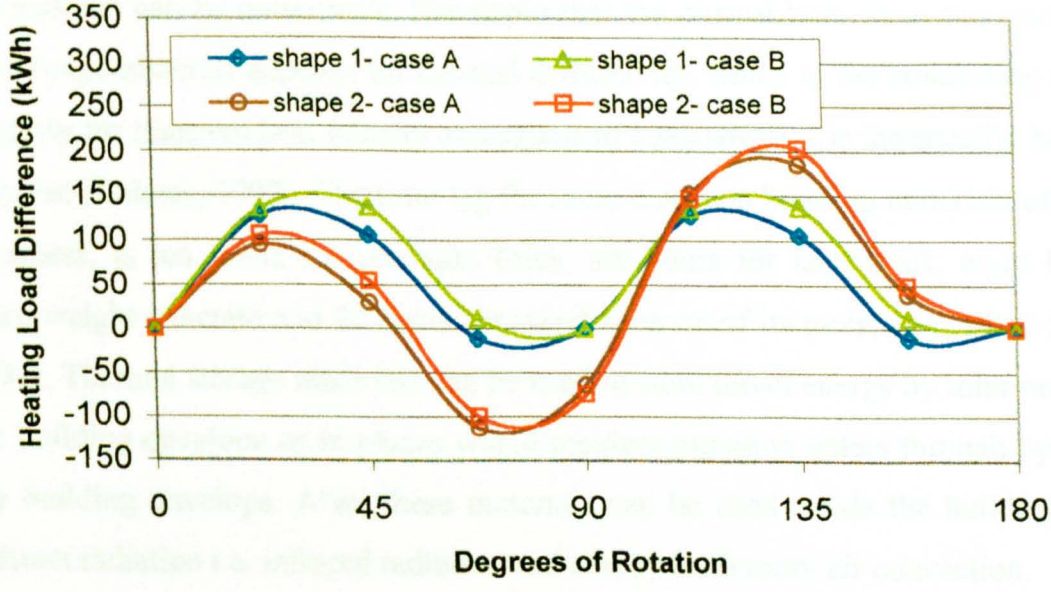

Figure 6.9. Annual heating load difference against degrees of rotation of the models.

Shape 2, presents the lowest heating load at about 75 degrees. Depending on the construction type, an extra heating load of 200 kWh can result, if the model is rotated from its minimum load position. Therefore, the best position for a rectangular house is to have its long side facing south. Of course architects cannot always orient the buildings at the best position since orientation is mainly dictated by the plot shape and location in respect to roads.

6.5 THERMAL MASS

Heat can be stored in the structural materials of the building in order to reduce the indoor temperature, reduce the cooling load peaks and shift the time that maximum load occurs. The storage material is referred to as thermal mass. In winter, during periods of high solar gain, energy is stored in the thermal mass avoiding overheating. In the late afternoon and evening hours, when energy is needed, heat is released into the building, satisfying part of the heating load. In summer thermal mass acts in a similar way as in winter reducing the cooling load peaks.

Thermal mass causes a time delay in the heat flow, which depends on the thermophysical properties of the materials used. To store heat effectively, structural materials must have high density (ρ), thermal capacity (C) and conductivity (k), so that heat may penetrate through all the material during the specific time of heat charging and discharging. A low value of ρCk indicates a low heat storage capacity even though the material can be quite thick. The depth that the diurnal heat wave can reach within the storage material depends on thermal diffussivity, which is the controlling transport property for transient heat transfer and equals to $k/\rho c_p$ where c_p is the specific heat of the material (Balaras, 1997). The time lag for some common building materials of 305 mm thickness, is ten hours for common brick, six hours for face brick, eight hours for heavyweight concrete and 20 hours for wood because of its moisture content (Lechner, 1991). Thermal storage materials can be used to store direct energy by solar radiation in the building envelope or in places where incident radiation enters through openings in the building envelope. Also, these materials can be used inside the building to store indirect radiation i.e. infrared radiation and energy from room air convection.

The distribution of thermal mass depends on the orientation of the given surface. According to Lechner (1991), a surface with north orientation has little need for time lag, since it only exhibits small heat gains. East orientation surfaces need either a very long time lag, greater than 14 hours so that heat transfer is delayed until the late evening hours, or a very short one, which is preferable because of the lower cost. South orientations can operate with eight-hour time lag, delaying the heat from midday until the evening hours. For west orientations, an eight-hour time lag is again sufficient since they receive radiation for only a few hours before sunset. Finally the roof requires a very long time lag since it is exposed to solar radiation during most hours of the day. However, because it is very expensive to construct heavy roofs, the use of additional insulation is usually recommended instead.

The performance of thermal mass is influenced by the use of insulation. Where heating of the building is the major concern, insulation is the predominant effective envelope factor. In climates where cooling is of primary importance, thermal mass can reduce energy consumption, provided the building is unused in the evening hours and the stored heat can be dissipated during the night. In this case either natural or mechanical ventilation can be used during the night, to introduce cool outdoor air into the space and remove heat from the massive walls and roof.

To check how the use of thermal mass can influence the performance of the model house a number of cases are investigated. Table 6.5 presents various wall and roof constructions of the model house of Figure 3.4 and their effect on the heating and cooling load. In order to examine the limits in which the effect is observed, two exaggerated cases are included, case MC with a very light construction and case MK with a very heavy construction.

The conduction transfer functions (CTF's) for the non-insulated roof (type H-Table 3.5) are:

b coefficients: 0.0646154, 0.5816295, 0.3101954, 0.0101877

c coefficients: 8.9761130, -9.3677430, 1.3641040, -0.0058420 and

d coefficients: 1.0, -0.9922078, 0.1328027, -0.0002878

In number, there are four conduction transfer functions for every coefficient.

As can be observed (Table 6.5), the number of CTF's of the various types of walls and roofs used in building the Cypriot houses (cases MA and MB) is high. This number varies from four, to seven. Since every conduction transfer function refers to the heat flux history of the structural element in time intervals of one hour, this number actually represents the discharge time in hours. Therefore, such materials when used in buildings need four to seven hours to be discharged. This effect is indicated in Figure 6.10 where for the days of 16 and 17 July the temperature of the model house is plotted for every hour.

Table 6.5. Thermal effect of various wall and roof types

Case	Wall type	Number of wall CTF's	Wall thermal conductivity (W/m-K)	Roof type	Number of roof CTF's	Roof thermal conductivity (W/m-K)	Heating load (kWh)	Cooling load (kWh)
MA	**Single wall**, hollow brick 0.2 m and 0.02 m plaster on each side (type D*)	6	0.886	**Flat non-insulated roof**, constructed from fair-faced 0.15 m heavy- weight concrete (type H*)	4	1.91	16012	42300
MB	**Double-wall**, 0.1 m hollow brick, 0.02 m plaster on each side and a layer of **0.05 m polystyrene insulation** in between (type F*)	7	0.389	**Flat insulated roof**, fair-faced 0.15 m heavy weight concrete, **0.05 m polystyrene insulation**, 0.07 m screed and 0.004 m asphalt covered with aluminum paint of 0.55 solar absorptivity (type J*)	6	0.481	3485	21710
MC	Steel siding $A3^+$, 0.025 m insulation $B2^+$, and Steel siding $A3^+$	2	0.978	Steel siding $A3^+$, 25 mm insulation $B2^+$, and Steel siding $A3^+$	2	0.978	13145	31978
MD	0.1 m face brick $A2^+$, 0.1 m insulation $B13^+$ and 0.025 m wood $B7^+$	6	0.325	0.012 m stone $E2^+$, 0.01 m felt and membrane $E3^+$, 0.15 m insulation $B15^+$ and 0.025 m wood $B7^+$	6	0.236	2793	21385
ME	**Single wall**, hollow brick 0.2 m and 0.02 m plaster on each side (type D*)	6	0.886	0.012 m stone $E2^+$, 0.01 m felt and membrane $E3^+$, 0.15 m insulation $B15^+$ and 0.025 m wood $B7^+$	6	0.236	4735	22550
MF	**Double-wall**, 0.1 m hollow brick, 0.02 m plaster on each side and a layer of **0.05 m polystyrene insulation** in between (type F*)	7	0.389	**Flat insulated roof**, fair-faced **0.25 m heavy weight concrete, 0.05 m polystyrene insulation**, 0.07 m screed and 0.004 m asphalt covered with aluminum paint of 0.55 solar absorptivity	7	0.468	3430	21625

Table 6.5. Thermal effect of various wall and roof types (cont.)

Case	Wall type	Number of wall CTF's	Wall thermal conductivity (W/m-K)	Roof type	Number of roof CTF's	Roof thermal conductivity (W/m-K)	Heating load (kWh)	Cooling load (kWh)
MG	**Double-wall**, 0.1 m hollow brick, 0.02 m plaster on each side and a layer of **0.05 m polystyrene insulation** in between (Double wall type F*)	7	0.389	**Flat insulated roof, 0.05 m wood (B10$^+$)** under-covering, fair-faced 0.15 m heavy weight concrete, **0.05 m polystyrene insulation**, 0.07 m screed and 0.004 m asphalt covered with aluminium paint of 0.55 solar absorptivity	7	0.397	3194	22035
MH	**For W and N walls: Double-wall**, 0.1 m hollow brick, 0.02 m plaster on each side and a layer of **0.05 m polystyrene insulation** in between (type F*) **For E and S walls: Double wall type F*, with additional 0.1 m heavy concrete inside**	7 8	W and N, 0.389 E and S 0.377	**Flat insulated roof**, fair-faced 0.15 m heavy weight concrete, **0.05 m polystyrene insulation**, 0.07 m screed and 0.004 m asphalt covered with aluminium paint of 0.55 solar absorptivity (type J*)	6	0.481	3438	21654
MI	**Double-wall**, 0.1 m hollow brick, 0.02 m plaster on each side and a layer of **0.05 m polystyrene insulation** in between (type F*), with additional **0.1 m heavy concrete inside**	8	0.377	**Flat insulated roof**, fair-faced 0.15 m heavy weight concrete, **0.05 m polystyrene insulation**, 0.07 m screed and 0.004 m asphalt covered with aluminium paint of 0.55 solar absorptivity (type J*)	6	0.481	3410	21619
MJ	**Double-wall**, 0.1 m hollow brick, 0.02 m plaster on each side and a layer of **0.05 m polystyrene insulation** in between (type F*), with additional **0.25 m heavy-weight concrete outside**	9	0.365	**Flat insulated roof**, fair-faced 0.15 m heavy weight concrete, **0.05 m polystyrene insulation**, 0.07 m screed and 0.004 m asphalt covered with aluminium paint of 0.55 solar absorptivity (type J*)	6	0.481	3399	21661
MK	0.6 m heavy-weight concrete	9	1.278	0.6 m heavy weight-concrete	9	1.278	11050	29884
ML	0.02 m plaster E1$^+$, 0.3 m clay brick, 0.1 m insulation B13$^+$ and 0.02 m plaster E1$^+$	9	0.261	0.2 m plaster E1$^+$, 0.3 m clay brick, 0.1 m insulation B13$^+$ and 0.2 m plaster E1$^+$	9	0.261	2772	20865

Table 6.5. Thermal effect of various wall and roof types (cont.)

Case	Wall type	Number of wall CTF's	Wall thermal conductivity (W/m-K)	Roof type	Number of roof CTF's	Roof thermal conductivity (W/m-K)	Heating load (kWh)	Cooling load (kWh)
MM	0.3 m heavy concrete C11+	6	1.638	**Flat non-insulated roof,** constructed from fair-faced 0.15 m heavy- weight concrete (type H*)	4	1.91	18704	43500
MN	0.3 m heavy concrete C11+	6	1.638	0.3 m heavy concrete C11+	6	1.638	14985	37739
MO	**Double-wall,** 0.1 m hollow brick and 0.02 m plaster on each side and a layer of **0.05 m polystyrene insulation** in between (type F*)	7	0.389	**Flat insulated roof,** fair-faced 0.15 m heavy weight concrete, **0.10 m polystyrene insulation,** 0.07 m screed and 0.004 m asphalt covered with aluminum paint of 0.55 solar absorptivity	6	1.022	2705	20669

+ASHRAE code numbers for wall and roof materials-Appendix 1,

*Table 3.5

As can be seen, the two construction cases MA and MB, used in Cyprus, attain their maximum temperature at 5 p.m. i.e., at the same time that an 600 mm heavy concrete wall and roof house (case MK) reaches its maximum temperature.

A much lighter construction made from metal panels and 25 mm insulation (case MC) attains its maximum temperature at 2 p.m. at which time the ambient temperature reaches a maximum value, therefore there is a time lag of three hours between the heavy and light constructions. Also as it is expected the lighter the building construction the closer it follows the ambient temperature variation throughout the day.

Figure 6.10 also shows that case MK has a daily variation of only two degrees attaining a very uncomfortable temperature of about 35°C to 37°C during day and night. The results for winter, during 13 and 14 January, are shown in Figure 6.11. During this period the temperature variation of case MK is again about two degrees, between 15°C and 17°C.

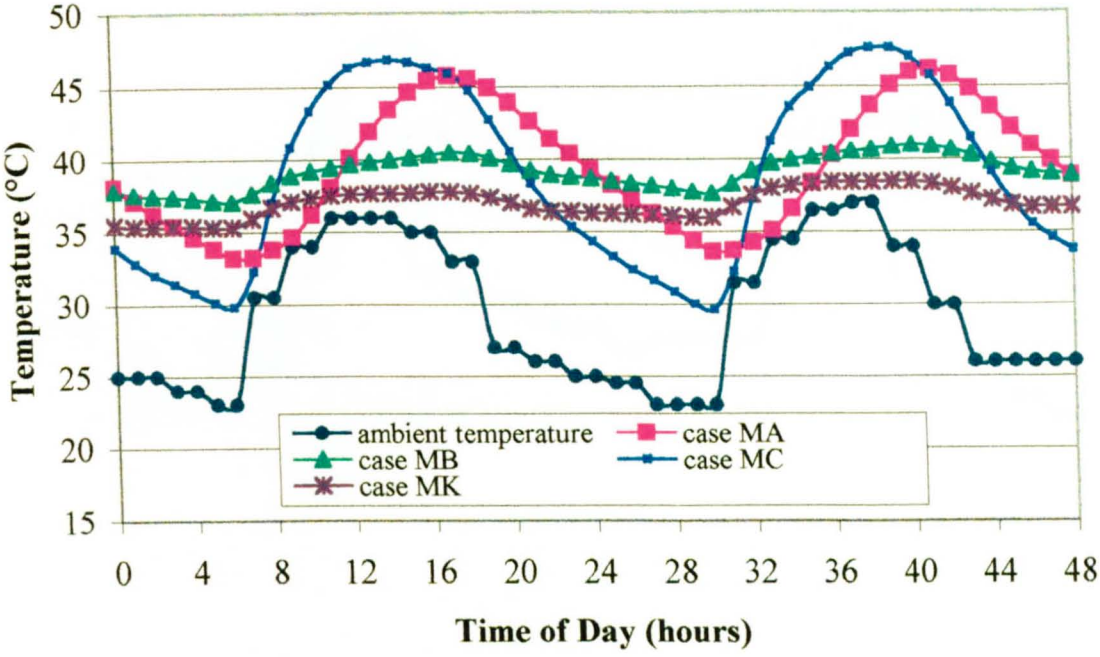

Figure 6.10. Temperature variation for various wall constructions during 16 and 17 July showing the effect of thermal mass.

The data presented in Table 6.5 clearly show that the thermal load is divided in three main categories. The first category presents cooling loads of about 32000 kWh and heating loads of 14000 kWh, the second 42000 kWh and 16000 kWh, and the third 21000 kWh and 3000 kWh respectively. The first category includes light constructions of roofs and walls with the number of CTF's being between 2 and 4. These materials absorb and release thermal energy, easily. The second category includes light constructions of roofs but heavier walls with 6 CTF's, which during summer, trap the energy passing through the roof inside the building. Finally the third category includes heavy constructions of roofs and walls with 6 to 9 CTF's, which present great resistance to the heat flow and high heat storage capacity. As it can also be seen, increasing the mass of roofs further than case MB, as for example in case MF, does not produce significant changes in the load. When though instead of the roof mass, the roof insulation is increased as in case MO, the cooling load decreases by about 1000 kWh and also the heating load decreases significantly by about 800 kWh. Increasing the mass of walls further than case MB, as for example in cases MH, MI and MJ does not result in significant changes in the load. Constructing both the walls and roof with 0.3 m heavy-weight concrete as in case MN, results in increasing the heating load by 4.2 times and the cooling load by 1.7 times compared to case MB.

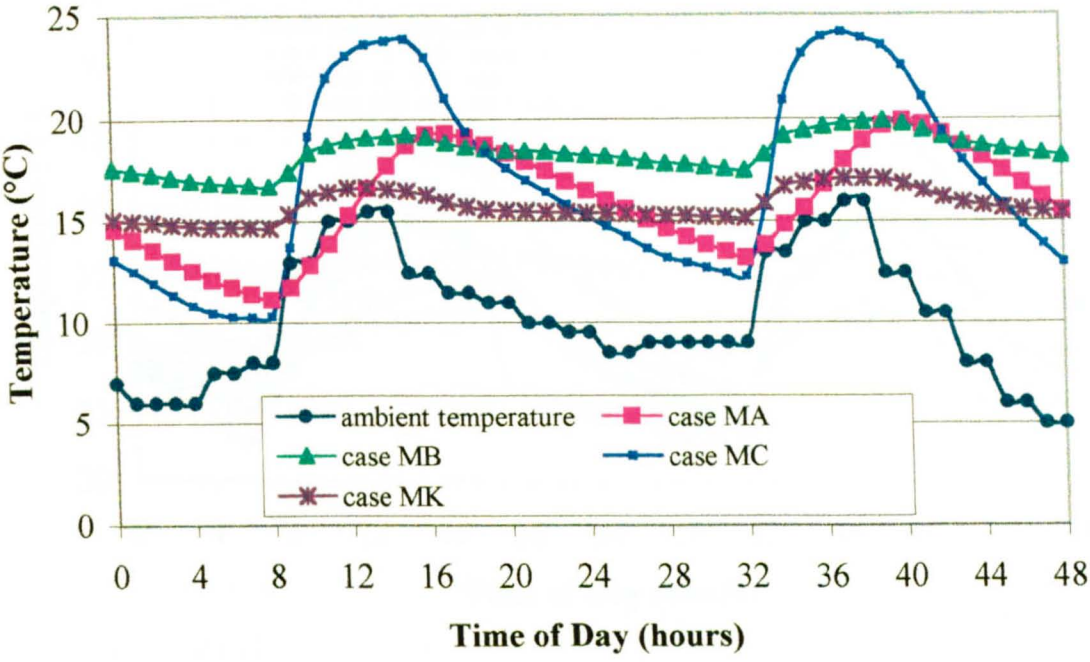

Figure 6.11. Temperature variation for various construction types during 13 and 14 January, showing the effect of thermal mass.

Thermal mass actually, is used to store heat during the day, for the purpose of dissipating it during the evening hours with ventilation. To check the effectiveness of this method in the Nicosia environment, the response of a model house constructed from various materials, with low-emissivity, double-glazed windows (Table 6.2) was simulated using a night ventilation rate of six air changes per hour. As can be seen in Figure 6.12, which presents the results, the model house of case MB is more sensitive than the more massive case MK, keeping the temperature between 27°C and 33°C. Case MK keeps the temperature about one to two degrees higher but in neither of the two cases the temperature reduces to acceptable levels. It must be noted that similar constructions to the above cases, give analogous results with very small variations in temperature that is less than half a degree. A very light-weight roof with thick insulation as in case MD, results in temperature variations of between 27°C and 35°C, again higher than case MB. Very light-weight constructions, like case MC, result in great temperature variations between 25°C and 40°C. Therefore, the above analysis shows that the roof is the most important structural element of the building in the Cypriot environment. The roof must offer a discharge time of 6 hours or more and be insulated, as in case MB or better.

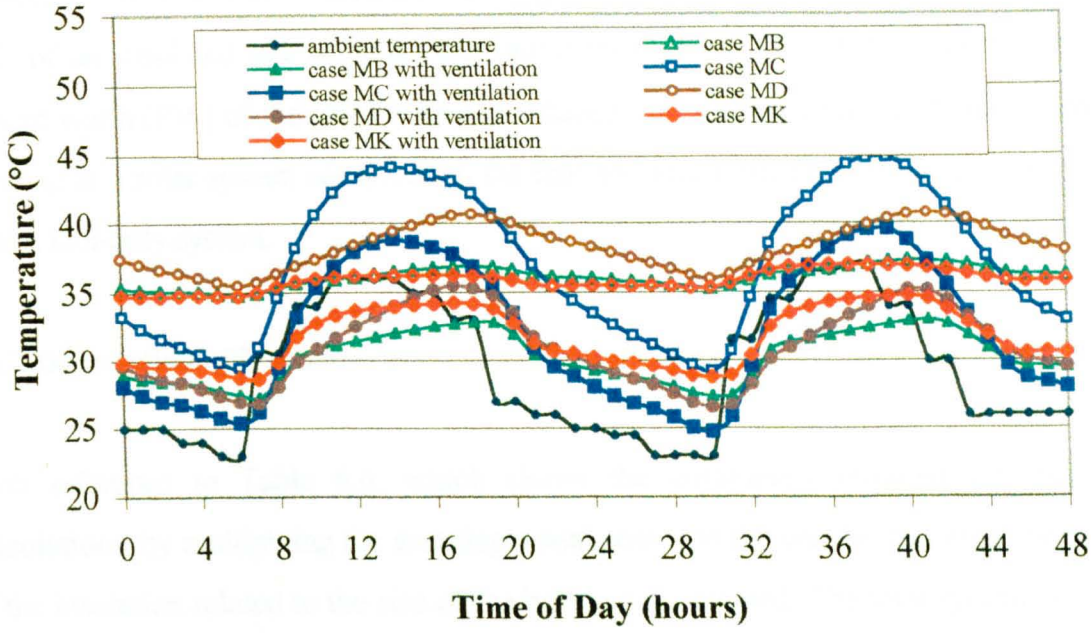

Figure 6.12. Effect of night ventilation for various wall constructions during 16 and 17 July in combination with thermal mass.

6.6 COST EFFECTIVENESS

This section presents a feasibility study of the various measures that can be taken to lower the building thermal load. For the economic study, the life savings analysis method was employed as describe below.

6.6.1 Life Savings Analysis Method

The life savings analysis method takes into account the time value of money and allows detailed consideration of the complete range of costs. Energy conservation measures such as use of insulation in buildings or use of solar energy systems are generally characterised by high initial cost and low operating costs, due to either the improved thermal resistance of the building envelope or reduction in conventional fuel use. Thus, the basic economic problem is that of comparing an initial known investment with the estimated future operating costs.

Life cycle cost (LCC) is the sum of all the costs associated with an energy delivery system over its lifetime in today's money, and takes into account the time value of money. The life cycle savings (LCS), for an insulated building or a solar system, is defined as the difference

between the LCC of a non-insulated building or of a conventional fuel-only system and the LCC of an insulated one or solar plus auxiliary system. This is equivalent to the total present worth (PW) of the gains from the reduced fuel and electricity costs for an insulated building or a solar system compared to the fuel and electricity costs for a non-insulated one or to a fuel-only system.

6.6.2 Description of Method

With reference to Table 6.6, which shows the parameters required for the various calculations, by multiplying the area dependent cost with the wall or roof area, the total cost of the insulation related to the size of the building is obtained. The total system cost can be obtained by adding to the above the area independent cost, which refers to labour.

Table 6.6. Economic analysis input parameters

Input parameters	Value	Units
Fuel inflation rate	6*	%
Wall area	147.2	m^2
Flat roof area	196	m^2
Inclined roof area	202.8	m^2
Boiler efficiency	85	%
Electric chiller efficiency	200	%
Area dependent extra cost:		
Double wall, 0.025 m polystyrene insulation (type E, Table 3.5)	3.5	C£/m^2
Double wall, 0.05 m polystyrene insulation (type F, Table 3.5)	5	C£/m^2
Insulated roof, 0.025 m polystyrene insulation (type I, Table 3.5)	11	C£/m^2
Insulated roof, 5 cm polystyrene insulation (type J, Table 3.5)	14	C£/m^2
Inclined roof, tile covered (type K, Table 3.5)	16	C£/m^2
Overhangs made of concrete and extending less than 2 m	27	C£/m^2
Overhangs made of concrete and extending more than 2 m	35	C£/m^2
Economic parameters:		
Annual market discount rate	6.5*	%
Price of electricity	0.0525	C£/kWh
Annual increase in electricity cost	4.9*	%
Current price of fuel	0.171	C£/lt

* Mean value for the years 1978-1998 (Statistical Abstracts, 1998)

The analysis is performed annually and the following amounts are evaluated (Kalogirou, 1996):

- Fuel savings
- Extra mortgage payment
- Electricity savings
- Extra tax savings
- Building energy savings

The word "extra" appearing in some of the above items assumes that the associated cost is also present for a non-insulated building and therefore only the extra part of the cost incurred by the installation of the insulation should be included. The inflation, over the period of economic analysis, of the fuel savings is estimated by using the equation (Duffie and Beckman, 1991):

$$F = c\,(1+i)^{N-1} \tag{6.1}$$

Where i is the fuel annual inflation rate, c the purchase cost at the end of the first time period, N the number of years, and F the future fuel cost.

The income tax law varies from country to country. In Cyprus, tax relief of 40% can be reclaimed against interest paid on loans made for building a house. Therefore, the equation used for the tax savings estimation is:

$$\text{Tax savings} = 0.4\ [\text{Interest paid}] \tag{6.2}$$

The building energy savings can be represented in the following equation form:

$$\text{Building energy savings} = \text{Electricity savings} + \text{Fuel savings} + \text{Extra tax savings} - \text{Extra mortgage payment} \tag{6.3}$$

Electricity will be assumed to be used for providing cooling and fuel oil (diesel) for heating.

Finally the present worth of each year's savings is determined by using equation (Duffie and Beckman, 1991):

$$P = F / (1+d)^N \quad (6.4)$$

Where F is the cash flow, occurring N years from now, reduced to its present value P, and d is the market discount rate (%). The values of P's are added for all years considered to give the total PW of the building energy consumption over its life.

6.6.3 Results of Analysis

The life cycle cost analysis method is applied for a 20-year period. As the building elements considered in this analysis are parts of the building structure, the economic scenario considers that the element cost (e.g. extra insulation) is included in the 20-year long-term loan required to build the house. The reference construction, built from single walls and flat non-insulated roof, is described in section 5.1. This construction presents a cooling load of 42300 kWh and a heating load of 16012 kWh per year, when the building is conditioned at all hours of the year. The extra cost refers to the added cost for applying the examined measure. The results are presented in Table 6.7.

As can be observed, measures that increase the roof insulation pay back in a short period of time, between 3.5 to 5 years. This is due to the fact that the main load in the building comes from the roof. However, measures taken to increase the wall insulation pay back in a longer period of time, of about 10 years.

The life cycle savings for a 20-year period that results for various window-glazing types is presented in Table 6.8. Although the window glazing reduces useful solar radiation during the cold days that results in an increase of the heating load, all types of glazing examined have a short pay back period of 3 to 4 years.

Finally, Table 6.9 presents the economic analysis for various types of overhangs for windows and doors. As it is observed concrete constructions hardly cover their cost over windows and result in loss when placed over doors because of their high initial cost. The appropriate construction that is economically sound should have a unit price of 10 C£/m^2 or less, which corresponds to cheap movable overhangs.

Table 6.7. Saving in C£ for cooling at 25°C and heating at 21°C for a 20-year period for various wall and roof constructions

Type of construction	Building cooling load (kWh)	Building heating load (kWh)	Additional expenditure required (C£)	Resulting life cycle savings (C£)	Payback period (years)
Reference construction: Single wall, hollow brick 0.2 m and 0.02 m plaster on each side and **flat non-insulated roof**, fair-faced 0.15 m heavy- weight concrete	42300	16012	-	-	-
Double-wall, 0.1 m hollow brick, 0.02 m plaster on each side and a layer of 0.025 **m polystyrene insulation** in between and **flat non-insulated roof**, fair-faced 0.15 m heavy-weight concrete	41550	14746	515	345	10
Double-wall, 0.1 m hollow brick, 0.02 m plaster on each side and a layer of 0.05 **m polystyrene insulation** in between and **flat non-insulated roof**, fair-faced 0.15 m heavy-weight concrete	41300	14312	735	423	10.5
Single wall, hollow brick 0.2 m and 0.02 m plaster on each side and **flat insulated roof**, fair-faced 0.15 m heavy weight concrete, **0.025 m polystyrene insulation**, 0.07 m screed and 0.004 m asphalt covered with aluminum paint of 0.55 solar absorptivity	24660	6506	2156	9143	3.5
Single wall, hollow brick 0.2 m and 0.02 m plaster on each side and **flat insulated roof**, fair-faced 0.15 m heavy weight concrete, **0.05 m polystyrene insulation**, 0.07 m screed and 0.004 m asphalt covered with aluminum paint of 0.55 solar absorptivity	23050	5348	2744	9762	3.8
Single wall, hollow brick 0.2 m and 0.02 m plaster on each side and **N-S Inclined roof**, 0.15 m heavy-weight concrete, 0.004 m asphalt for waterproofing, 0.05 m plaster and clay tile on top	24750	7280	3245	7931	4.9
Single wall, hollow brick 0.2 m and 0.02 m plaster on each side and **E-W Inclined roof**, 0.15 m heavy-weight concrete, 0.004 m asphalt for waterproofing, 0.05 m plaster and clay tile on top	24960	7257	3245	7848	4.9
Double-wall, 0.1 m hollow brick, 0.02 m plaster on each side and a layer of **0.05 m polystyrene insulation** in between and **flat insulated roof**, fair-faced 0.15 m heavy-weight concrete, **0.05 m polystyrene insulation**, 0.07 m screed and 0.004 m asphalt covered with aluminum paint of 0.55 solar absorptivity. (Case MB, table 6.5)	21710	3485	3479	10378	4.3
Double-wall, 0.1 m hollow brick, 0.02 m plaster on each side and a layer of **0.05 m polystyrene insulation** in between and **flat insulated roof, 0.05 m wood**, fair-faced 0.15 m heavy-weight concrete, **0.05 m polystyrene insulation**, 0.07 m screed and 0.004 m asphalt covered with aluminum paint of 0.55 solar absorptivity. (Case MG, table 6.5)	22035	3194	12495	2901	13.2
Double-wall, 0.1 m hollow brick and 0.02 m plaster on each side and a layer of **0.05 m polystyrene insulation** in between and **flat insulated roof**, fair-faced 0.15 m heavy weight concrete, **0.10 m polystyrene insulation**, 0.07 m screed and 0.004 m asphalt covered with aluminum paint of 0.55 solar absorptivity. (Case MO, table 6.5)	20669	2705	3871	10778	4.5

Table 6.8. Saving in C£ for cooling at 25°C and heating at 21°C for a 20-year period for various window glazing types

Type of construction	Window type	Additional expenditure required (C£), compared to clear double glazing (Case W1, Table 6.2)	Resulting life cycle savings (C£)	Payback period (years)
Single wall, no roof insulation	Reflective double glazing, bronze (Case W2, Table 6.2)	208	904	3
	Low-emissivity double glazing, bronze (Case W2, Table 6.2)	416	1368	3.8
50 mm roof and wall insulation plus 150W extra lighting	Reflective double glazing, bronze (Case W2, Table 6.2)	208	1060	2.8
	Low-emissivity double glazing, bronze (Case W2, Table 6.2)	416	1478	3.8

Table 6.9. Saving in C£ for cooling at 25°C and heating at 21°C for a 20-year period for various overhang types

Type of construction	Overhang length	Type of construction and cost	Additional expenditure required (C£)	Resulting life cycle savings (C£)	Payback period (years)
Single wall, no roof insulation	1.5 m over windows	Concrete, 30 C£/m^2	1080	17.2	16.5
	1.5 m over windows	Other 10 C£/m^2	360	610	6
50 mm roof and wall insulation	1.5 m over windows	Concrete, 30 C£/m^2	1080	317	12.2
	1.5 m over windows	Other 10 C£/m^2	360	910	4.4

6.7 CONCLUSIONS

This chapter describes results and cost effectiveness of measures for improving the thermal behaviour of the modern house. In summer, when ventilation air is entered into the house whenever the outside temperature is less than the house temperature and the room is not conditioned, may reduce the inside temperature by about 2°C for one air change per hour, 3°C for two air changes per hour and 7°C for eleven air changes per hour. When maintaining the house at 21°C in winter, there is no appreciable load reduction arising from ventilation. In summer, ventilation leads to a maximum reduction of 7.7% for maintaining the house at 25°C. The effect depends on the construction type, with the better-insulated house saving a higher percentage. The energy saved is between 400 kWh and 1500 kWh depending on the amount of air changes per hour.

Window gains are an important factor and significant savings can result when extra measures are taken. A saving in the cooling load of between 3050 kWh and 5000 kWh can result depending on the construction and glazing type. The saving in cooling load for a well-insulated house may be as much as 24% when low-emissivity double glazing windows are used, which are recommended since the payback period is short (3.8 years).

Overhangs can result in savings of 2000 kWh to 3000 kWh depending on the construction of the model house. Overhangs may have a length over windows of 1.5 m. In this way, about 7% of the load can be saved for a house constructed from single walls with no roof insulation. The savings are about 19% for a house constructed from walls and roof with 50 mm insulation.

The shape of the building affects the thermal load. The results show that the elongated Shape 2 model house shows an increase in the heating load, which is between 8.2% and 26.7% depending on the construction type, in respect to the model house of Shape 1. The heating load increase in this case is about 1000 kWh. Referring to orientation, the best position for a symmetrical house is to face the four cardinal points and for an elongated house to have its long side facing south in order to minimize the east wall area that has the biggest load contribution.

In respect to thermal mass, the analysis shows that increasing the wall and roof mass and utilising night ventilation is not enough to lower the house temperature to acceptable limits during summer. Also the analysis shows that the roof is the most important structural element of the buildings in the Cypriot environment. The roof must offer a discharge time of 6 hours or more and have a thermal conductivity of less than 0.48 W/m-K.

The life cycle cost analysis has shown that measures that increase the roof insulation pay back in a short period of time, between 3.5 to 5 years. However, measures taken to increase wall insulation pay back in a long period of time, of about 10 years. Low-emissivity double-glazing results in a short pay back period of 3 to 4 years, irrespective of the fact that useful solar radiation is also blocked during the cold days.

CHAPTER 7

DESIGN OF THE LIBR-WATER ABSORPTION MACHINE

The analysis presented in chapters 5 and 6 has shown that in Cyprus, the heating and cooling demand of domestic dwellings can be reduced to a large extent with various measures. However, due to the high summertime temperatures, the cooling demand cannot be reduced substantially with passive and low energy cooling techniques for thermal comfort and an active cooling system is therefore required. It is preferable that such a system is not powered by electricity whose production depends entirely on fuel imports, and results in atmospheric pollution.

The only resource abundantly available in Cyprus is solar energy, which can be used to power an active solar cooling system based on the absorption cycle. The investigation presented in section 2.3.1, shows that the lithium bromide (LiBr)-water absorption units are the most suitable for solar applications since low-cost solar collectors may be used in order to power the generator of the machine. Such units though, are not readily available in small residential-sizes. After a search in the world market, only one manufacturer was traced producing commercially lithium bromide-water absorption refrigerators (Yazaki of Japan). This manufacturer was not willing to provide such a unit for use in Cyprus, with the excuse that it was not able to provide maintenance services for this market. Therefore, the possibility of producing absorption air-conditioning systems in small sizes for residential buildings in Cyprus and the economics of using such a refrigerator, assisted by solar energy, needs to be investigated.

The objective of this chapter is to design the heat exchangers of a small LiBr-water absorption machine in order to construct and determine their performance characteristics and cost. The theoretical analysis of the thermodynamic cycle of these units has been extensively studied but the design and sizing of heat exchangers and other components is not well documented in the literature. This chapter presents theory and details of the designed absorption unit.

7.1 ABSORPTION COOLING

Absorption machines are thermally activated and for this reason, high input (shaft) power is not required. In this way, where power is expensive or unavailable, or where there is waste, gas, geothermal or solar heat available, absorption machines provide reliable and quiet cooling (ASHRAE, 1997). A number of refrigerant-absorbent pairs are used, for which the most common ones are water-lithium bromide and ammonia-water. These two pairs offer good thermodynamic performance and they are environmentally benign.

Absorption refrigeration system fluid pairs should meet a number of important requirements, which are (ASHRAE, 1997):

1. *Absence of solid phase* - The refrigerant-absorbent pair should not form a solid phase over the range of composition and temperature to which it will be subjected. The formation of solids may stop the flow and cause problems to the equipment.

2. *Volatility ratio* - The refrigerant should be more volatile than the absorbent so that it can be separated easily by heating.

3. *Affinity* - The absorbent should have a strong affinity with the refrigerant under the conditions in which absorption takes place. This affinity allows less absorbent to be circulated for the same refrigerating effect, therefore sensible heat losses are less. Also a smaller liquid heat exchanger is required to transfer heat from the absorbent to the pressurised refrigerant-absorbent solution. A disadvantage is that extra heat is required in the generator to separate the refrigerant from the absorbent.

4. *Pressure* - Moderate operating pressures, should be used in order to avoid the use of heavy-walled equipment and reduce the electrical power required to pump the fluids from the low-pressure side to the high-pressure side. Also, very low pressure (vacuum) will require the use of large volume equipment and special means of reducing pressure drop in refrigerant vapour flow.

5. *Stability* - High chemical stability is required to avoid the undesirable formation of gases, solids or corrosive substances.

6. *Corrosion* - The fluids should be non-corrosive. If the fluids are corrosive, corrosion inhibitors should be used which may influence the thermodynamic performance of the equipment.

7. *Safety* - Ideally fluids must be non-toxic and non-inflammable.

8. *Latent heat* - To keep the circulation rate of the refrigerant and absorbent at a minimum, the latent heat of the refrigerant should be as high as possible.

Considering the requirements of the present study, the ammonia-water pair is not suitable because of the high temperature needed in the generator (125°C to 170°C). This temperature can only be obtained with medium concentration ratio parabolic collectors, which are quite expensive.

The generator temperatures needed for the water-lithium bromide pair are lower (90°C to 120°C). These temperatures can be achieved with compound parabolic collectors (CPCs) and evacuated tube collectors that are of lower cost and easier to install and operate than medium ratio concentration parabolic collectors.

7.2 LITHIUM BROMIDE (LiBr) - WATER COOLING

This type of equipment is classified by the method of heat input to the primary generator (firing method) and whether the absorption cycle is single or multiple effect. The single effect absorption technology provides a peak-cooling coefficient of performance (COP) of approximately 0.7 and operates with heat input temperatures in the range of 90°C to 120°C. The multiple effect technology gives higher COPs but can only be utilised when higher temperature heat sources are available. Double effect systems can be achieved by adding an additional stage as a topping cycle on the single-effect cycle. In this way the heat rejection from the high temperature stage is used to power the lower temperature stage. It should be noted that the refrigerant in the water-lithium bromide system is water and the LiBr acts as the absorbent, which absorbs the water vapour thus making pumping from the absorber to the generator easier and economic. A single-effect, two shell, LiBr -water chiller is illustrated in Figure 7.1 and its schematic presentation on a pressure-temperature diagram is illustrated in Figure 7.2.

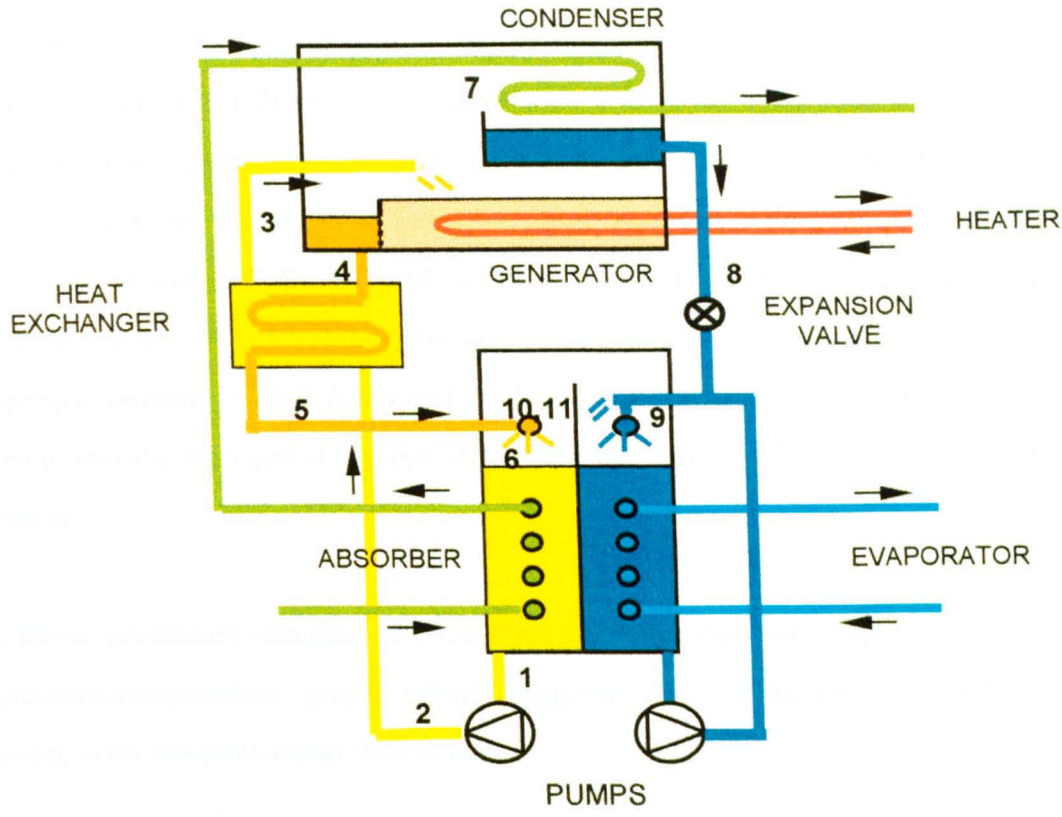

Figure 7.1. Two-shell, lithium bromide-water cycle cooling system.

With reference to the numbering system shown in Figure 7.1, at point (1) the solution is rich in refrigerant and a pump forces the liquid through a heat exchanger to the generator (3). The temperature of the solution in the heat exchanger is increased.

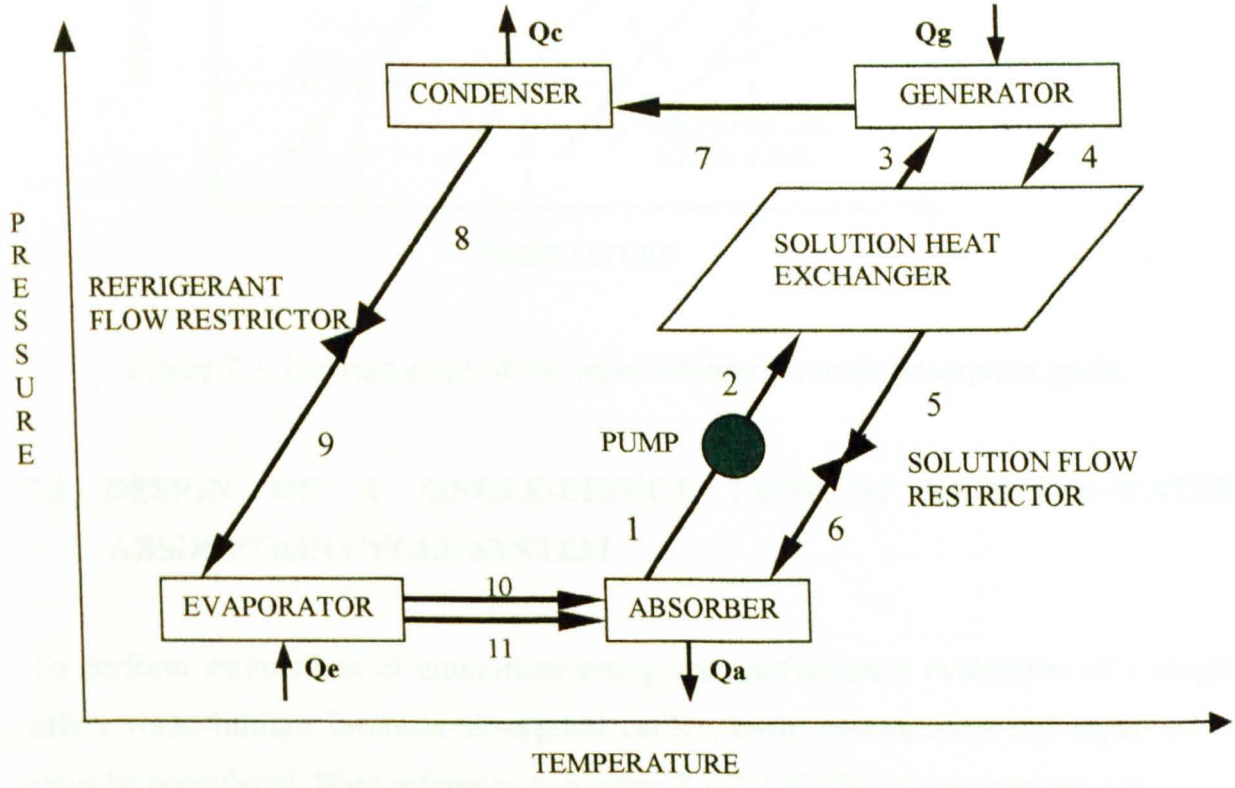

Figure 7.2. Single-effect, water-lithium bromide absorption cycle.

In the generator, thermal energy is added and refrigerant boils off the solution. The refrigerant vapour (7) flows to the condenser, where heat is rejected as the refrigerant condenses. The condensed liquid (8) flows through a flow restrictor to the evaporator (9). In the evaporator, the heat from the load evaporates the refrigerant, which flows back to the absorber (10). A small portion of the refrigerant leaves the evaporator as liquid spillover (11). At the generator exit (4), the steam consists of absorbent-refrigerant solution, which is cooled in the heat exchanger. From points (6) to (1), the solution absorbs refrigerant vapour from the evaporator and rejects heat through a heat exchanger.

The above procedure can also be presented in a Duhring chart (Figure 7.3). This chart is a pressure-temperature graph where diagonal lines represent constant LiBr mass fraction, with the pure water line at the left.

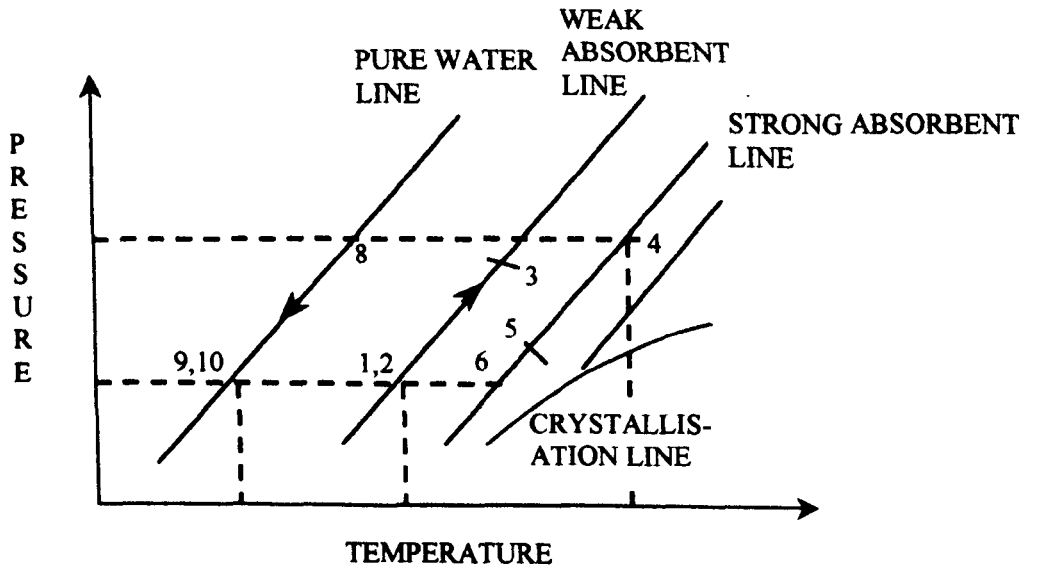

Figure 7.3. Duhring chart of the water-lithium bromide absorption cycle.

7.3 DESIGN OF A SINGLE-EFFECT LITHIUM BROMIDE–WATER ABSORPTION CYCLE SYSTEM

To perform estimations of equipment sizing and performance evaluation of a single-effect water-lithium bromide absorption cooler, basic assumptions and input values must be considered. With reference to Figures 7.1-7.3, the basic assumptions are:

1. The steady state refrigerant is pure water.

2. There are no pressure changes except through the flow restrictors and the pump.

3. At points 1, 4, 8 and 11 there is only saturated liquid.

4. At point 10 there is only saturated vapour.

5. Flow restrictors are adiabatic.

6. The pump is isentropic.

7. There are no jacket heat losses.

The objective is to design and construct a small pilot system of 1 kW of cooling power. The method of design is demonstrated below. The design parameters considered are listed in Table 7.1.

Table 7.1. Design parameters for the single-effect water-lithium bromide absorption cooler

Parameter	Symbol	Value
Capacity	$\dot{Q}_e$	1.0 kW
Evaporator temperature	T_{10}	6°C
Generator solution exit temperature	T_4	90°C
Weak solution mass fraction	X_1	55 % LiBr
Strong solution mass fraction	X_4	60 % LiBr
Solution heat exchanger exit temperature	T_3	65°C
Generator (desorber) vapour exit temperature	T_7	85°C
Liquid carryover from evaporator	$\dot{m}_{11}$	$0.025\,\dot{m}_{10}$

7.3.1 Evaporator Analysis

Since in the evaporator, the refrigerant is saturated water vapour and the temperature (T_{10}) is 6°C, the saturation pressure at (10) is 0.9346 kPa (Rogers and Mayhew, 1992) and the enthalpy is 2511.8 kJ/kg. Since at (11) the refrigerant is saturated liquid its enthalpy is 25.2 kJ/kg. The enthalpy at point (9) is determined from the throttling process applied to the refrigerant flow restrictor which yields that $h_9=h_8$. To determine h_8 the pressure at this point must be determined. Since at point (4) the solution mass fraction is 60% LiBr and the temperature at the saturated state was assumed to be 90°C, the LiBr –water charts (Appendix 2) give a saturation pressure of 9 kPa and h_4=212 kJ/kg (Appendix 3). Considering that the pressure at point (4) is the same as in (8) then $h_8= h_9$=183.4 kJ/kg (Rogers and Mayhew, 1992).

Once the enthalpy values at all ports connected to the evaporator are known, mass and energy balances can be applied to give the mass flow of the refrigerant and the evaporator heat transfer rate.

The mass balance on the evaporator is:

$$\dot{m}_9 = \dot{m}_{10} + \dot{m}_{11} \tag{7.1}$$

The energy balance on the evaporator is:

$$\dot{Q}_e = \dot{m}_{10} h_{10} + \dot{m}_{11} h_{11} - \dot{m}_9 h_9 \tag{7.2}$$

Since the evaporator output power $\dot{Q}_e$ is 1.0 kW and $\dot{m}_{11}$=2.5%$\dot{m}_{10}$ the mass flow rates can be calculated as shown in Table 7.2.

7.3.2 Absorber Analysis

Since the values of $\dot{m}_{10}$ and $\dot{m}_{11}$ are known, mass balances around the absorber give:

$$\dot{m}_1 = \dot{m}_{10} + \dot{m}_{11} + \dot{m}_6 \tag{7.3}$$

and

$$\dot{x}_1 \dot{m}_1 = \dot{x}_6 \dot{m}_6 \tag{7.4}$$

The mass fractions x_1 and x_6 in Equation (7.4) are inputs, therefore $\dot{m}_1$ and $\dot{m}_6$ can be calculated as shown in Table 7.2.

The heat transfer rate in the absorber can be determined from the enthalpy values at each of the connected state points. At point (1), the enthalpy is determined from the input mass fraction (55%) and the assumption that the state is saturated liquid at the same pressure as the evaporator (0.9346 kPa, see Appendix 2). This value is h_1=85 kJ/kg (Appendix 3). The enthalpy value at point (6) is determined from the throttling model which gives $h_6 = h_5$.

The enthalpy at point (5) is not known but can be determined from the energy balance on the solution heat exchanger, assuming an adiabatic shell as follows:

$$\dot{m}_2 h_2 + \dot{m}_4 h_4 = \dot{m}_3 h_3 + \dot{m}_5 h_5 \tag{7.5}$$

The temperature at point (3) is an input value (65°C) and since the mass fraction for points (1) to (3) is the same, the enthalpy at this point is determined as 145 kJ/kg (Appendix 3). Actually, the state at point (3) may be sub cooled liquid. However, at the conditions of interest, the pressure has an insignificant effect on the enthalpy of the subcooled liquid and the saturated value at the same temperature and mass fraction can be an adequate approximation. The enthalpy at state (2) is determined from an isentropic pump model. The minimum work input (w) can therefore be obtained from:

$$w = \dot{m}_1 v_1 (p_2 - p_1) \tag{7.6}$$

In Equation (7.6) it is assumed that the specific volume (v, m^3/kg) of the liquid solution does not change appreciably from point (1) to (2). The specific volume of the liquid solution can be obtained from a curve fit (Lee *et al.*, 1990).

For the present study, since all variables are known (Table 7.2), the pump power can be calculated as:

$w = 0.00529$ (Kg/s) * 0.00062 (m^3/kg) * [$9x10^3$ (Pa) - 0.9346 $x10^3$ (Pa)] = $0.026x10^{-3}$ kW

Equation (7.5) can now be solved for the unknown enthalpy value at point (5) giving h_5=146.6 kJ/kg. The temperature at point (5) can also be determined from the enthalpy value, and is 56°C (Appendix 3).

Finally, the energy balance on the absorber is:

$$\dot{Q}_a = \dot{m}_{10} h_{10} + \dot{m}_{11} h_{11} + \dot{m}_6 h_6 - \dot{m}_1 h_1 \qquad (7.7)$$

which gives $\dot{Q}_a$ = 1.34 kW

Table 7.2. Data for single-effect lithium bromide-water cooling system

Point #	h (kJ/kg)	$\dot{m}$ (kg/s)	p (kPa)	T (°C)	X (%LiBr)	Remarks
1	85	0.00529	0.9346	36	55	
2	85	0.00529	9	36	55	
3	145	0.00529	9	65	55	Sub-cooled liquid
4	212	0.00485	9	90	60	
5	146.6	0.00485	9	56	60	
6	146.6	0.00485	0.9346	46	60	
7	2659.2	0.000441	9	85	0	Superheated Steam
8	183.4	0.000441	9	43.8	0	Saturated liquid water
9	183.4	0.000441	0.9346	6	0	
10	2511.8	0.000430	0.9346	6	0	Saturated vapour
11	25.2	0.000011	0.9346	6	0	Saturated liquid water

7.3.3 Generator (desorber) Analysis

The heat input to the generator is determined from the energy balance, which is:

$$\dot{Q}_g = \dot{m}_4 h_4 + \dot{m}_7 h_7 - \dot{m}_3 h_3 \tag{7.8}$$

which results to: $\dot{Q}_g = 1.43$ kW

The enthalpy at point (7) can be determined since the temperature at this point is an input value. In general, the state at point (7) will be superheated water vapour and the enthalpy can be determined once the pressure and temperature are known.

7.3.4 Condenser Analysis

The condenser heat can be determined from an energy balance, which gives:

$$\dot{Q}_c = \dot{m}_7 (h_7 - h_8) \tag{7.9}$$

and therefore $\dot{Q}_c = 1.09$ kW

7.3.5 Coefficient of Performance

The coefficient of performance (COP) is defined as:

$$\text{COP} = \frac{\dot{Q}_e}{\dot{Q}_g} \tag{7.10}$$

which will give a value of 0.7.

A summary of the energy flows at the various components of the system is given in Table 7.3.

Table 7.3. Energy flows at the various components of the system

Description	Symbol	KW
Capacity (evaporator output power)	$\dot{Q}_e$	1.0
Pump minimum work input	w	0.000026
Absorber heat, rejected to the environment	$\dot{Q}_a$	1.3422
Heat input to the generator	$\dot{Q}_g$	1.434
Condenser heat, rejected to the environment	$\dot{Q}_c$	1.092
Coefficient of performance	COP	0.7

Utilising the same LiBr percentage ratios and the procedure described above, a sensitivity analysis was carried out using a computer program 'LITH' written in Quick Basic. A listing of the program is presented in Appendix 4. The program also incorporates mathematical correlations for obtaining the various fluid properties. The results are presented in Tables 7.4 to 7.8.

Table 7.4. Water - LiBr absorption refrigeration system calculations based on a generator temperature of 90°C and a solution heat exchanger exit temperature of 70°C

Point	H (kJ/kg)	$\dot{m}$ (Kg/s)	P (kPa)	T (°C)	%LiBr (X)	Remarks
1	85	0.005291	0.9346	36	55	
2	85	0.005291	9	36	55	
3	160	0.005291	9	**70**	55	Sub-cooled liquid
4	212	0.00485	9	**90**	60	
5	130.2	0.00485	9	50	60	
6	130.2	0.00485	0.9346	46	60	
7	2659.2	0.000441	9	**85**	0	Superheated Steam
8	183.4	0.000441	9	43.8	0	Saturated liquid
9	183.4	0.000441	0.9346	6	0	
10	2511.8	0.00043	0.9346	6	0	Saturated vapour
11	25.5	0.000011	0.9346	6	0	Saturated liquid

Description	Symbol	kW
Capacity (evaporator output power)	$\dot{Q}_e$	**1.0**
Absorber heat, rejected to the environment	$\dot{Q}_a$	1.26
Heat input to the generator	$\dot{Q}_g$	1.35
Condenser heat, rejected to the environment	$\dot{Q}_c$	1.09
Coefficient of performance	COP	0.74

Table 7.5. Water - LiBr absorption refrigeration system calculations based on a generator temperature of 90°C and a solution heat exchanger exit temperature of 75°C

Point	H (kJ/kg)	$\dot{m}$ (Kg/s)	P (kPa)	T (°C)	%LiBr (X)	Remarks
1	85	0.005291	0.9346	36	55	
2	85	0.005291	9	36	55	
3	168	0.005291	9	**75**	55	Sub-cooled liquid
4	212	0.00485	9	**90**	60	
5	121.5	0.00485	9	44	60	
6	121.5	0.00485	0.9346	46	60	
7	2659.2	0.000441	9	**85**	0	Superheated Steam
8	183.4	0.000441	9	43.8	0	Saturated liquid
9	183.4	0.000441	0.9346	6	0	
10	2511.8	0.00043	0.9346	6	0	Saturated vapour
11	25.2	0.000011	0.9346	6	0	Saturated liquid

Description	Symbol	kW
Capacity (evaporator output power)	$\dot{Q}_e$	**1.0**
Absorber heat, rejected to the environment	$\dot{Q}_a$	1.22
Heat input to the generator	$\dot{Q}_g$	1.31
Condenser heat, rejected to the environment	$\dot{Q}_c$	1.09
Coefficient of performance	COP	0.762

Table 7.6. Water - LiBr absorption refrigeration system calculations based on a generator temperature of 85°C and a solution heat exchanger exit temperature of 65°C

Point	H (kJ/kg)	$\dot{m}$ (Kg/s)	P (kPa)	T (°C)	%LiBr (X)	Remarks
1	85	0.005256	0.9346	36	55	
2	85	0.005256	7	36	55	
3	145	0.005256	7	**65**	55	Sub-cooled liquid
4	203	0.000482	7	**85**	60	
5	137.5	0.000482	7	54	60	
6	137.5	0.000482	0.9346	46	60	
7	2650	0.000438	7	**80**	0	Superheated Steam
8	168.8	0.000438	7	40.3	0	Saturated liquid
9	168.8	0.000438	0.9346	6	0	
10	2511.8	0.000427	0.9346	6	0	Saturated vapour
11	25.5	0.000011	0.9346	6	0	Saturated liquid

Description	Symbol	kW
Capacity (evaporator output power)	$\dot{Q}_e$	**1.0**
Absorber heat, rejected to the environment	$\dot{Q}_a$	1.29
Heat input to the generator	$\dot{Q}_g$	1.38
Condenser heat, rejected to the environment	$\dot{Q}_c$	1.09
Coefficient of performance	COP	0.726

Table 7.7. Water - LiBr absorption refrigeration system calculations based on a generator temperature of 80°C and a solution heat exchanger exit temperature of 60°C

Point	H (kJ/kg)	$\dot{m}$ (Kg/s)	P (kPa)	T (°C)	%LiBr (X)	Remarks
1	85	0.005215	0.9346	36	55	
2	85	0.005215	5.95	36	55	
3	133	0.005215	5.95	**60**	55	Sub-cooled liquid
4	190	0.004781	5.95	**80**	60	
5	137.6	0.004781	5.95	52	60	
6	137.6	0.004781	0.9346	46	60	
7	2640.5	0.000435	5.95	**75**	0	Superheated Steam
8	150.7	0.000435	5.95	36	0	Saturated liquid
9	150.7	0.000435	0.9346	6	0	
10	2511.8	0.000424	0.9346	6	0	Saturated vapour
11	25.2	0.000011	0.9346	6	0	Saturated liquid

Description	Symbol	kW
Capacity (evaporator output power)	$\dot{Q}_e$	**1.0**
Absorber heat, rejected to the environment	$\dot{Q}_a$	1.28
Heat input to the generator	$\dot{Q}_g$	1.36
Condenser heat, rejected to the environment	$\dot{Q}_c$	1.08
Coefficient of performance	COP	0.734

Table 7.8. Water - LiBr absorption refrigeration system calculations based on a generator temperature of 75°C and a solution heat exchanger exit temperature of 55°C

Point	H (kJ/kg)	$\dot{m}$ (Kg/s)	P (kPa)	T (°C)	%LiBr (X)	Remarks
1	83.0	0.00517	0.93	34.9	55	
2	83.0	0.00517	4.82	34.9	55	
3	124.7	0.00517	4.82	**55**	55	Sub-cooled liquid
4	183.2	0.00474	4.82	**75**	60	
5	137.8	0.00474	4.82	51.5	60	
6	137.8	0.00474	0.93	44.5	60	
7	2612.2	0.000431	4.82	**70**	0	Superheated Steam
8	131.0	0.000431	4.82	31.5	0	Saturated liquid
9	131.0	0.000431	0.93	6	0	
10	2511.8	0.000421	0.93	6	0	Saturated vapour
11	23.45	0.000011	0.93	6	0	Saturated liquid

Description	Symbol	kW
Capacity (evaporator output power)	$\dot{Q}_e$	**1.0**
Absorber heat, rejected to the environment	$\dot{Q}_a$	1.28
Heat input to the generator	$\dot{Q}_g$	1.35
Condenser heat, rejected to the environment	$\dot{Q}_c$	1.07
Coefficient of performance	COP	0.74

In Cyprus solar heat is in abundance and is usually collected with locally made, flat plate collectors, working at low temperatures. Therefore, a low generator temperature is preferable and the design of the absorption unit was based on a low generator temperature of 75 °C and the characteristics presented in Table 7.8.

A schematic representation of the system is shown in Figure 7.4. The design of the various parts of the system is detailed below.

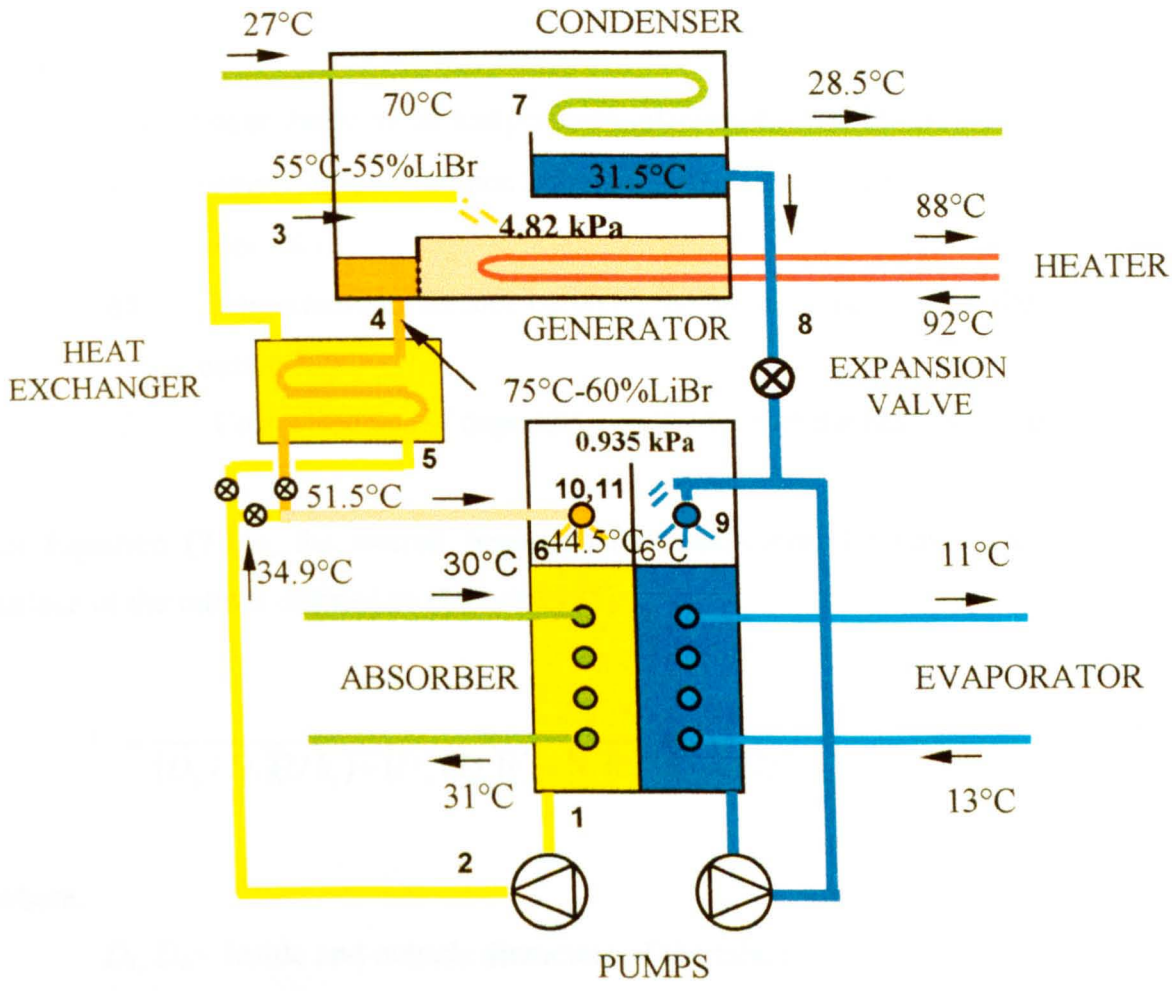

Figure 7.4. Schematic representation of the system to be constructed.

7.4 HEAT EXCHANGERS SIZING

In single-pass heat exchangers, the temperature difference ΔT between the hot and the cold fluids is not constant but it varies with distance along the heat exchanger. In the heat transfer analysis, it is convenient to establish a mean temperature difference (ΔT_m) between the hot and cold fluids such that the total heat transfer rate $\dot{Q}$ between the fluids can be determined from the following simple expression:

$$\dot{Q} = AU\Delta T_m \tag{7.11}$$

where A (m^2) is the total heat transfer area and U (W/m^2-K) is the average overall heat transfer coefficient, based on that area. For Equation (7.11),

$$\Delta T_m = F^* \Delta T_{ln} = F\left(\frac{\Delta T_0 - \Delta T_L}{\ln(\Delta T_0 / \Delta T_L)}\right) \quad (7.12)$$

where :

ΔT_{ln} = Logarithmic mean temperature difference (LMTD), (K)

ΔT_0 = Temperature difference between the hot and cold fluid at the inlet, (K)

ΔT_L = Temperature difference between the hot and cold fluid at the outlet, (K)

F = Correction factor depending on the type of the heat exchanger

For Equation (7.11), the overall heat transfer coefficient (U) based on the outside surface of the tube is defined as (Ozisik 1985):

$$U = \frac{1}{(D_o / D_i)(1/h_i) + (D_o / D_i)F_i + [1/(2k)]D_o \ln(D_o / D_i) + F_0 + 1/h_o} \quad (7.13)$$

where:

D_i, D_o = Inside and outside diameters of the tube (m), respectively

h_i, h_o = Heat transfer coefficients for inside and outside flow (W/m^2-K), respectively

k = Thermal conductivity of tube material (W/m-K)

F_I, F_o = Fouling factors at the inside and outside surfaces of the tube (m^2-K/W), respectively

Program 'LITH' (Appendix 4), used for the design of the unit, also includes all necessary formulae for the design procedure of the heat exchangers. Mathematical correlations are also added which yield the properties of materials and fluids used.

7.4.1 Condenser Heat Exchanger Design

For the condenser heat exchanger design the data shown in Table 7.9 are used. These data are extracted from Table 7.8 and Figure 7.4.

Table 7.9. Condenser heat exchanger characteristics

Parameter	Type / Value
Heat Exchanger Type	Single pass horizontal tubes (with outside diameter (D_o) = 9.5 mm and inside diameter (D_i) = 8.1 mm)
Cooling water inlet temperature	27°C
Cooling water outlet temperature	28.5°C
Mass flow rate $(\dot{m})$	0.171 kg/s
Condenser load $(\dot{Q}_c)$	1070 W
Condensing water vapour temperature	From 70°C to 31.5°C
Condensing water vapour pressure	4.82 kPa
Condensing water vapour mass flow rate	0.000431 kg/s

The overall heat transfer coefficient is given by Equation (7.13). For this equation, the value of the fouling factors (F_I, F_o) at the inside and outside surfaces of the tube can be taken as 0.09 m^2-K/kW (Howell *et al.*, 1998) and k for copper = 383.2 (W/m-K). The heat transfer coefficients, h_i, h_o, for the inside and outside flow need to be calculated.

The Petukhov-Popov equation (in Kreith and Bohn, 1997) for turbulent flow inside a smooth tube gives:

$$\overline{Nu_D} = \frac{(f/8)\mathrm{Re}_D \,\mathrm{Pr}}{K_1 + K_2(f/8)^{1/2}(\mathrm{Pr}^{2/3}-1)} \tag{7.14}$$

where:

$\overline{Nu_D}$ = Nusselt number = $h_i D_i / K$

Pr = Prandtl number

Re_D = Reynolds number = $V_m D_i / \nu = 4m / \pi D_i \mu$

$f = (1.82 \log_{10} \mathrm{Re}_D - 1.64)^{-2}$

$K_1 = 1 + 3.4f$

$K_2 = 11.7 + \frac{1.8}{\mathrm{Pr}^{1/3}}$

V_m = mean velocity (m/s)

m = mass flow rate (kg/s)

ν = kinematic viscosity (m^2/s)

μ = absolute viscosity ($N\text{-}s/m^2$) = $\nu \rho$

ρ = density kg/m^3

Equation (7.14) applies for Reynolds numbers $10^4 < Re_D < 5x10^6$ and Prandtl numbers, $0.5<Pr<2000$. The Petukhov-Popov equation agrees with the experimental results for the specified range within ± 5%.

The water properties at the mean temperature of (27+28.5)/2 = 27.75°C are:

ρ = 997.5 kg/m^3

ν = $0.8365x10^{-6}$ m^2/s

k = 0.610 W/m K

Pr = 5.72

c_p = 4178 J/kg K

$\dot{Q}_c$ equals to 1070 W (Table 7.9), therefore:

$$\dot{m} = \dot{Q}_c / (c_p * \Delta t) = 1070 / (4178*(28.5-27)) = 0.171 \text{ kg/s}$$

$$Re = (4*0.171) / (3.14*0.0081*997.5*0.8365*10^{-6}) = 32115$$

Substituting the above values into Equation (7.14) and replacing Nu by $h_i D_i / K$ gives:

h_I = 16255 W/m^2-K

Nusselt's analysis of heat transfer for condensation on the outside surface of a horizontal tube, gives the average heat transfer coefficient as (Nusselt in Ozisik, 1985):

$$h_m = 0.725\left[\frac{g\rho_l(\rho_l - \rho_v)h_{fg}k_l^{\ 3}}{\mu_l(T_v - T_w)D_o}\right]^{0.25} \qquad (7.15)$$

where:

h_m = average heat transfer coefficient (W/m^2-K)

g = gravitational constant, 9.81 m/s^2

ρ_l = liquid density (kg/m^3)

ρ_v = vapour density (kg/m^3)

h_{fg} = latent heat of condensation (kJ/kg)

k_l = thermal conductivity of liquid (W/m-K)

μ_l = absolute viscosity of liquid (N-s/m^2)

T_v = vapour saturation temperature (°C)

T_w = wall surface temperature (°C)

D_o = outside tube diameter (m)

The physical properties in Equation (7.15) should be evaluated at the mean wall surface and vapour saturation temperature.

The above equation is recommended in the case of condensation on a single horizontal tube, although a comparison of the average heat transfer coefficient for vertical surfaces with that found by experiments has shown that the measured heat transfer coefficient is about 20% higher than the values suggested by theory (Ozisik 1985).

In the case of this study, the average temperature of the condensate film is (31.5+27.75)/2=29.6°C and its physical properties are:

ρ_l = 996.97 kg/m^3

ρ_v = 0.03285 kg/m^3

h_{fg} = 2431.2x10^3 J/kg

k_l = 0.613 W/m-K

μ_l = 801.4x10^{-6} kg/m-s

T_v = 31.5°C

T_w = 27.0°C

D_o = 0.0095 m

Therefore h_m = 15202 W/m^2-K.

By substituting the above values in Equation (7.13) a resulting overall heat transfer coefficient of U=2980 W/m^2-K is determined.

From the temperature values shown in Table 7.9 the required temperature differences can be calculated as: ΔT_L = 3°C and ΔT_o = 4.5°C, Therefore the logarithmic mean temperature difference is:

$$\Delta T_{ln} = \frac{\Delta T_0 - \Delta T_L}{\ln(\Delta T_0 / \Delta T_L)} = 3.66°C.$$

and Equation (7.11) gives:

$A = 1080/(3.7*2980)\ m^2 = 0.098\ m^2$

The heat exchanger tubes that are used have a length of 1.0 m and an outside diameter of 0.0095 m, resulting in an area of 0.0298 m^2. The calculated length of pipe is therefore 3.3 m. Assuming the average heat transfer coefficient (h_m) for condensation on the outside surface of a horizontal tube to be 20% higher, 3.19 m of pipe is calculated. If h_m is considered to be 20% lower, then 3.46 m of pipe would be necessary. Therefore 4 horizontal pipes are used in the construction.

7.4.2 Generator Heat Exchanger Design

For the generator heat exchanger design the data shown in Table 7.10 are used. These data are extracted from Table 7.8 and Figure 7.4.

The generator provides sensible heat and latent heat of vaporisation. The sensible heat raises the inlet stream temperature up to the saturation temperature. This amount of heat, is normally 13% of the total heat required (Herold *et al.*, 1996). The heat of vaporisation consists of the heat of vaporisation of pure water and the latent heat of mixing of the liquid solution. Typically, the heat of mixing is about 11% of the heat of vaporisation for water/ lithium bromide.

The above analysis indicates that the heat to be provided by the generator can be based on the heat of vaporisation of pure water, increased by about 23% in a typical design.

Table 7.10. Generator heat exchanger characteristics

Parameter	Type/ Value
Heat Exchanger Type	Single pass horizontal tubes (with outside diameter (D_o) = 9.5 mm and inside diameter (D_i) = 8.1 mm)
Generator load ($\dot{Q}_g$)	1350 W
Generator pressure	4.82 kPa
Generator solution	Entering: 55% LiBr at 55°C Leaving: 60% LiBr at 75°C
Generator water vapour mass flow rate ($\dot{m}$)	0.000431 kg/s

Although considerable research work has been done in the past on pool boiling of liquids, data on water/ lithium bromide solutions are not extensive (Varma *et al.*, 1994). Experimental results indicate that boiling is not significantly affected by the tube diameter but is affected significantly by the solution concentration. As the solution concentration increases the heat transfer coefficient decreases. Also the heat transfer coefficient increases as the heat flux increases. Average heat transfer coefficients were found to vary between 1600 W/m^2-K and 7500 W/m^2-K (Varma *et al.*, 1994). For the above work, stainless steel tubes were used. The tube material also affects the heat transfer coefficient as shown by an empirical relation developed by Rohsenow (in Kreith and Bohn, 1997) for nucleate boiling. Since no formula is available for calculating the exact heat transfer coefficient, the generator was constructed with a number of tubes that could be isolated, as detailed in section 8.1.2. In this way, the exact heat transfer coefficient was determined experimentally.

7.4.3 Solution Heat Exchanger Design

For the solution heat exchanger design the data shown in Table 7.11 were considered. These data are extracted from Table 7.8 and Figure 7.4. Equation (7.13) was used to calculate the overall heat transfer coefficient. As before, the value of the fouling factors (F_I , F_o) at the inside and outside surfaces of the tube were taken as 0.09 m^2-K/kW (Howell *et al.*, 1998) and k for copper at a mean temperature of 54.7°C as 381.5 W/m-K.

The Heat transfer coefficients, h_i, h_o, for the inside and outside flow were determined as detailed below.

Table 7.11. Solution heat exchanger characteristics

Parameter	Type / Value
Heat Exchanger Type	Single pass annulus, with 15.0 mm outside pipe diameter – 1.0 mm wall thickness and 9.5 mm inside pipe diameter with 0.7 mm wall thickness
Cooled solution (60% LiBr) inlet temperature	75°C
Cooled solution (60% LiBr) outlet temperature	51.5°C
Cooled solution Mass flow rate ($\dot{m}$)	0.00474 kg/s
Heated solution (55% LiBr) inlet temperature	34.9°C
Heated solution (55% LiBr) outlet temperature	55°C
Heated solution Mass flow rate ($\dot{m}$)	0.00517 kg/s

The 60% LiBr solution properties at (75+51.5)/2 = 63.2°C are:

$\mu = 3.52 \times 10^{-3}$ N-s/m^2

$k = 0.465$ W/m-K

$Pr = c_p * \mu / k = 14.6$

$c_p = 1926$ J/kg-K

Since:

$$Re = 4\dot{m} / \pi D \mu = (4*0.00474) / (3.14*0.0081*3.52*10^{-3}) = 212$$

the flow is laminar, and in this case the Nusselt number (Nu) is (Nusselt in Ozisik, 1985):

$$Nu = h_i D_i / K = 3.66 \qquad (7.16)$$

Therefore $h_i = 3.66*0.465/0.0081 = 210.2$ W/m^2-K

The 55% LiBr solution properties at (55+34.9)/2 = 44.9°C are:

μ = 3.2x10^{-3} kg/m-s

k = 0.465 W/m-K

Pr = c_p* μ/ k = 14.2

c_p = 2057 J/kg-K

The hydraulic diameter D_H for the annulus is the difference between the inside diameter of the external tube (D_2) and the outside diameter of the internal tube (D_1) (Kreith and Bohn, 1997). In the case of the present study this is:

$D_H = D_2 - D_1 = 0.013\text{-}0.0095 = 0.0035\text{m}$

The Reynolds number based on the hydraulic diameter and the bulk temperature properties is:

$$\mathrm{Re}_{D_H} = \frac{\rho \bar{U} D_H}{\mu} = \frac{\dot{m} D_H}{A\mu} = (0.00517*0.0035) / (3.2*10^{-3}*61.8*10^{-6}) = 91.5$$

and:

$Nu = h_o D / K = 3.66$

Therefore:

h_o = 3.66*0.465/0.0035 = 486 W/m^2-K

By substituting the above values in Equation (7.13) the resulting overall heat transfer coefficient (U) based on the outside surface of the tube is:

$$U = \frac{1}{1.173/210.2 + (1.173)*0.00009 + [0.0095/(2*381.5)]*\ln(1.173) + 0.00009 + 1/486}$$

and U = 127.6 W/(m^2-K)

From the temperature values shown in Table (7.11) the required temperature differences can be calculated as: ΔT_o=75-55=20°C and ΔT_L=51.5-36=15.5°C. Therefore the logarithmic mean temperature difference is:

$$\Delta T_{ln} = \frac{\Delta T_0 - \Delta T_L}{\ln(\Delta T_0 / \Delta T_L)} = 18.24$$

Finally, from Equation 7.11, the area of the heat exchanger needed is:

$A = 0.00474*1926*(75-51.5) / (127.6*18.24) = 0.0923\ m^2$

The heat exchanger tube will have an outside diameter of 0.0095 m, resulting in an area of $(1.0*\pi*0.0095) = 0.0298\ m^2$.

Therefore a length of 0.0923/0.0298 = 3.1 m tube is needed.

7.4.4 Horizontal Tube Absorber

For this design, the solution film can flow downward either on horizontal or on vertical tubes. The first attempt was to construct the absorber using a steel frame. A frame 1x1 m, made of steel, 100 mm x 50 mm x 5 mm thick channel section was constructed. Inside this structure a number of 15 mm tubes, 1 m in length, were placed as shown in Figure 7.5. A falling film created from a horizontal pipe with small holes 1 mm in diameter and 10 mm apart wetted the tubes. A plastic mesh, with 3 mm x 3 mm openings, was inserted in between the horizontal pipes in an attempt to improve the uniformly of the water film distribution over the tubes.

The construction of the horizontal tube absorber, presented a problem of not being able to maintain vacuum because of the large length of welds. For this reason an alternative design with vertical tubes housed in a cylindrical shell was employed, as shown in Figure 7.6. The theoretical analysis of the vertical tube absorber is presented in section 7.4.5.

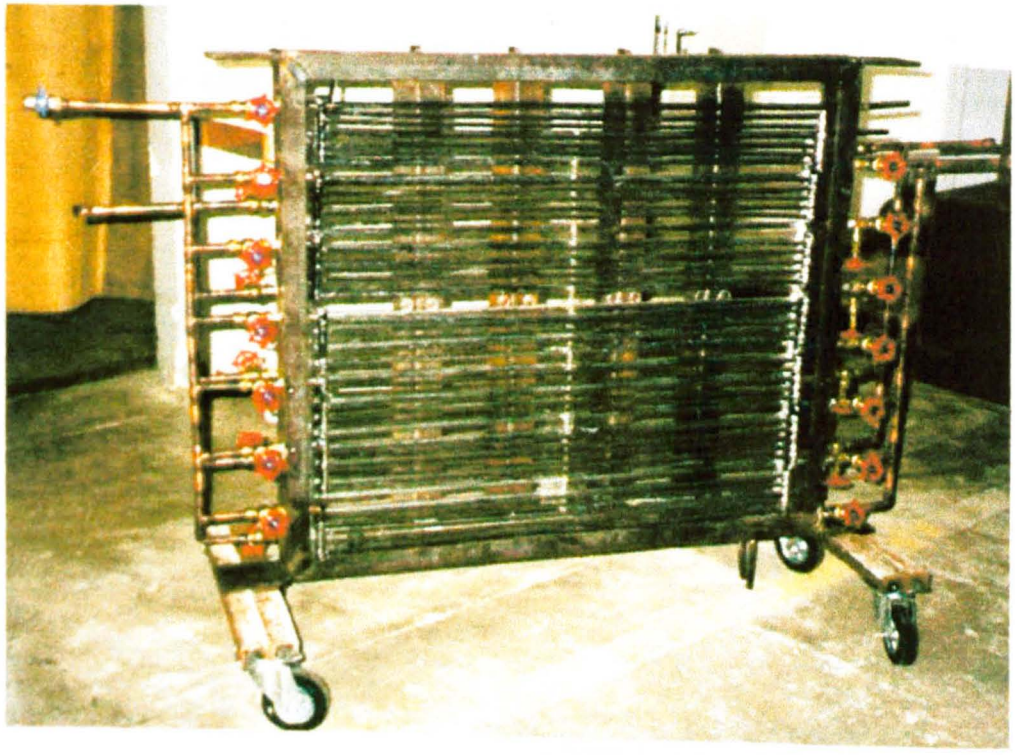

Figure 7.5. Horizontal tube absorber.

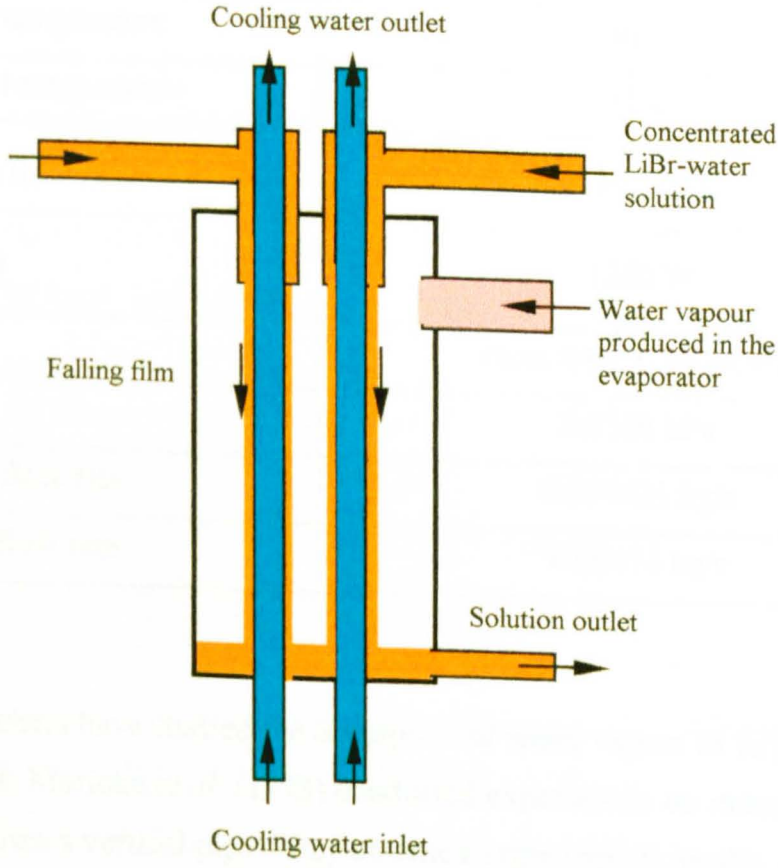

Figure 7.6. Schematic representation of the vertical tube absorber.

7.4.5 Absorber Heat Exchanger Design

For the absorber heat exchanger design the data shown in Table 7.12 are considered. These data are extracted from Table 7.8 and Figure 7.4.

In the case of this study the water vapour produced in the evaporator (Figure 7.6) is absorbed in the flow of the LiBr-water solution and is not condensing directly on the heat exchanger tubes. The design of the heat exchanger therefore requires values for heat and mass transfer coefficients.

Table 7.12. Absorber heat exchanger characteristics

Parameters	Type / Value
Heat Exchanger Type	Single pass vertical tubes, with outside diameter (D_o) = 9.5 mm, inside diameter (D_i) = 8.1 mm and 0.02983 m^2 external area per meter length.
Cooling water inlet temperature	30°C
Cooling water outlet temperature	31°C
Cooling water mass flow rate $(\dot{m})$	0.307 kg/s
Absorber load $(\dot{Q}_a)$	1280 W
Solution cooling	From 44.5°C to 34.9°C
Absorber pressure	0.9346 kPa
Water vapour mass flow rate	0.000421 kg/s
Inlet solution mass flow rate	0.00474 kg/s

A number of researchers have studied the absorption of water vapour in falling films of LiBr-water solutions. Morioka *et al.* (1993) conducted experiments on steam absorption for films flowing down a vertical pipe. They obtained experimental results, which show that for film Reynolds numbers in the range of 40-400 the heat transfer coefficients of the film are between 1500 W/m^2-K and 3000 W/m^2-K. The average absorption of mass flux (kg/m^2-s) is compared with the numerical results derived from a laminar flow

theoretical model proposed by the authors. The agreement of the results is good for film Reynolds numbers up to 100, but the experimental values are far higher above film Reynolds numbers of 200.

Grossman (1983), described a theoretical analysis of the combined heat and mass transfer process in the absorption of gas or vapour into a laminar liquid film. Simultaneous equations are described which give the temperature and concentration variations at the liquid-gas interface and at the wall. A constant temperature and an adiabatic wall case were considered. The Nusselt and Sherwood numbers were found to depend on the Peclet and Lewis numbers as well as on the equilibrium characteristics of the working fluids.

Conlisk (1992), developed a design procedure for predicting the absorption capacity of a given tube based on the governing geometrical and physical parameters. The theoretical approach developed can predict the amount of mass absorbed in a given length of tube.

Patnaik *et al.* (1993) presented a model, based on the solution of differential equations to calculate axial solution concentration and temperature distributions along a vertical tube absorber. The absorption of water vapour into the falling film of the solution of lithium-bromide was modelled employing equations extracted from the literature, incorporating information on wavy-laminar flows. The usefulness of the model was demonstrated by generating absorber performance charts.

A practical model for absorption of vapours into a laminar film of water and LiBr falling down along a constant temperature vertical plate was described in Andberg and Vliet (1983). The model developed considers non-isothermal absorption and the equations showed good agreement to experimental results. The objective of the study was to develop an effective model of the absorption process, in order to facilitate the study of absorber design from a theoretical viewpoint. For this reason some simplifications were made, like assuming that the bank of tubes of an actual absorption unit are replaced with a constant temperature vertical flat plate. Also, because of the complexity of the problem involving the solution of momentum, energy and diffusion equations with their boundary conditions, a simplified method was developed for determining the various quantities involved. Because of the simplicity and the good

agreement to experimental results this method was chosen for determining the number of the absorber tubes required.

The independent variables, which affect the absorption of vapours, are solution mass flow rate, solution inlet concentration, absorber pressure and wall temperature.

The length of plate (L) is correlated to the solution mass flow rate by the expression:

$$L = a\dot{m}^{b} \tag{7.17}$$

where:

$$a = -132 * \ln\frac{100 - A_P}{86.0}$$

$b = 1.33$

$\dot{m}$ = mass flow rate per unit width of plate (kg/m-s) and

A_p = the "absorption percentage"

The "absorption percentage" (A_p), is defined as:

$$A_p = \frac{C_{IN} - C_{OUT}}{C_{IN} - C_{EQ}} * 100 \tag{7.18}$$

where: C_{IN} = solution inlet concentration (mass fraction)

C_{OUT} = solution outlet concentration (mass fraction)

C_{EQ} = solution equilibrium concentration (mass fraction)

Determination of the equilibrium concentration, C_{EQ}, requires the solution of the following set of expressions:

$A = -2.00755 + .16976 * X - 3.133362 * .001 * X^2 + 1.97668 * .00001 * X^3$

$B = 321.128 - 19.322 * X + .374382 * X^2 - 2.0637 * .001 * X^3$

$C = 6.21147$

$D = -2886.373$

$E = -337269.46$

$T' = (-2\,E / [D + (D^2 - 4\,E\,(C - LOG(P / 6894.8))]^{.5}) - 459.72$

$T_W = (5 / 9) * (A * T' + B - 32)$

where:

X=concentration of LiBr in solution (%)

$C_{EQ} = X_{EQ}/100$

P= pressure (Pa)

T_W= wall temperature (°C)

The above set of expressions requires an iterative type of solution to find C_{EQ}, given T_W and P. In the case of this study T_W=30.5 °C and P=935 Pa therefore C_{EQ}=0.52 and from equation (7.18) A_P=62.5.

Assuming the length of every tube of the absorber to be 1 m, Equation (7.17) gives $\dot{m}$=0.0292 kg/m-s. Since the tube external area per meter length is 0.02983 m^2 and the required solution mass flow rate is 0.00474 kg/s (Table 7.12), 5.4 tubes are required. Therefore 6 pipes are used.

The next step is to check the area of tubes needed to cool the solution to the required level. Patnaik *et al.* (1993), suggest that Wilke's correlation, valid for constant heat flux wall with progressively decreasing difference from isothermal wall outside the entrance region, can be used for the falling film. It is assumed that the flow is fully developed in a wavy, laminar regime and that the bulk solution temperature profile is linear with respect to the transverse coordinate. Wilke's correlation is:

$$h_s = \frac{k_s}{\delta}\left(0.029 * (Re_s)^{0.53}\, Pr_s^{\,0.344}\right) \qquad (7.19)$$

where:

h_s= solution convective heat transfer coefficient (W/m^2-K)

k_s= solution thermal conductivity (W/m-K)

Re_s= solution Reynolds number for vertical tube

Pr_s= solution Prandtl number

δ = film thickness (m)

The film thickness δ, (m) is given by:

$$\delta = \left(\frac{3\mu\Gamma}{\rho^2 g}\right)^{1/3} \tag{7.20}$$

where:

μ = dynamic viscosity (N-s/m^2)

Γ= mass flow rate per wetted perimeter (kg/m-s)

ρ= density (kg/m^3)

g= gravitational acceleration (m/s^2)

and the solution Reynolds number (Re_s) for the vertical tube is:

$$Re_s = 4\Gamma/\mu \tag{7.21}$$

where:

μ = dynamic viscosity (N-s/m^2)

Γ= mass flow rate per wetted perimeter (kg/m-s)

In the case of this study the mean properties of the solution at 39.7°C and 57.5% LiBr are:

ρ = 1663 kg/m^3

μ = 4.29x10^{-3} N-s/m^2

k = 0.429 W/m-K

c_p = 1991 J/kg-K

with a resulting Pr= 18.9

Assuming 6 pipes and substituting the above values into Equations (7.19) to (7.21), a solution convective heat transfer coefficient h_s *of* 855 W/m^2-K results.

The cooling water properties at the mean temperature of (30+31)/2 = 30.5°C are:

ρ = 996.7 kg/m^3

ν = 0.7876x10^{-6} m^2/s

k = 0.615 W/m-K

$Pr = 5.34$

$c_p = 4177.5$ J/kg-K

Therefore, substituting the above values into Equation (7.14) and replacing $Nu = h_i D_i / K$:

$$h_I = 6175 \text{ W/m}^2\text{-K}$$

By substituting the above values into Equation (7.13) the resulting overall heat transfer coefficient (U) based on the outside surface of the tube is:

$$U = 642 \text{ W/m}^2\text{-K}$$

In this case $\Delta T_{ln} = 9.3°C$. Therefore from Equation (7.11), the resulting length of each pipe is 1.38 m instead of 1m assumed. This means that the area of 6 pipes is not enough to cool the solution to the required level. Checking for 9 pipes by repeating the above procedure, a length of 1.0 m results in h_s= 790 W/m^2-K, h_I = 4450 W/m^2-K and U= 580 W/m^2-K, which indicates that 9 pipes are adequate to cool the solution.

7.4.6 Evaporator Heat Exchanger Design

For the evaporator heat exchanger design the data shown in Table 7.13 are considered. These data are extracted from Table 7.8 and Figure 7.4.

To facilitate construction, it was decided to construct the evaporator heat exchanger in a similar way to the absorber heat exchanger. Figure 7.7 shows a schematic representation of the vertical tube evaporator. Water passing through the evaporator tubes supplies the required heat to vaporise the falling film of water around every tube. A search in the literature has shown that the preferred construction method is to allow the liquid to enter inside a tube. The fluid inside the tube is heated by the run of fluid at the outer surface of the tube, so that progressive vaporisation occurs. The heat transfer coefficient increases with distance from the entrance since heat is added continuously to the fluid. It is also not yet possible to predict all of the characteristics of this process quantitatively because of the great number of variables upon which the process depends and the complexity of the various two-phase flow patterns that occur as the quality of the vapour-liquid mixture increases during vaporisation (Kreith and Bohn, 1997).

Therefore, in the case of this study, the mean heat transfer coefficient was determined experimentally as detailed in section 8.1.5.

Table 7.13. Evaporator heat exchanger characteristics

Parameter	Type / Value
Heat Exchanger Type	Single pass horizontal tubes (outside diameter (D_o) = 9.5 mm and inside diameter (D_i) = 8.1 mm)
Water inlet temperature	27°C
Water outlet temperature	17°C
Mass flow rate ($\dot{m}$)	0.0239 kg/s
Evaporator load ($\dot{Q}_e$)	1000 W
Evaporator pressure	0.9346 kPa
Evaporator water vapour mass flow rate	0.000431 kg/s

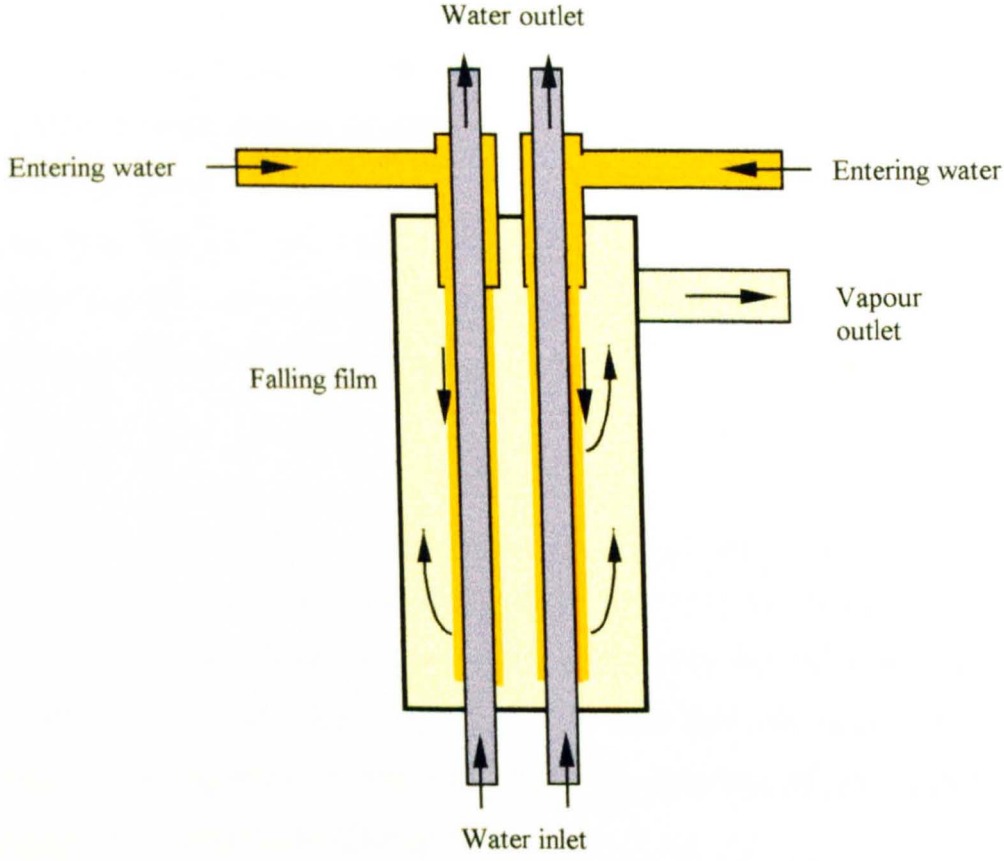

Figure 7.7. Schematic representation of the vertical tube evaporator.

7.5 CONCLUSIONS

The objective of this chapter was to present the design of a small 1 kW, LiBr-water absorption machine. A theoretical analysis of the absorption cycle is presented and a sensitivity analysis is carried out using the computer program 'LITH', written in Quick Basic for this purpose.

Based on a low generator temperature of 75°C, the characteristics of the unit were determined and the heat exchangers of the system were designed. Details of the construction and performance of the designed unit components are presented in chapter 8.

CHAPTER 8

CONSTRUCTION OF THE LiBr-WATER ABSORPTION UNIT, EXPERIMENTAL RESULTS AND COST ANALYSIS

All heat exchangers described in Chapter 7, were constructed in a way that permitted the use of varying number of tubes. The objective was to modify the number of heat exchanger tubes and thus the heat exchange area, until the required operating conditions, depicted in Tables 7.9 to 7.13, were obtained. This would ensure a design with a good COP as shown in Table 7.8. For this purpose thermometer pockets and flow meters were installed at various points in the unit for measurements and adjustments.

8.1 CONSTRUCTION DETAILS AND EXPERIMENTAL RESULTS

8.1.1 Condenser Heat Exchanger

The shell of the condenser was constructed from a copper tube 1 m in length, 67 mm external diameter and 1.2 mm thick. The shell was insulated with 13 mm thick armaflex insulation. Inside the shell, 8 copper tubes with 9.5 mm outside diameter and 8.1 mm inside diameter were housed as shown in Figure 8.1. These tubes were connected externally with hoses. In this way the required length of pipe could be utilized. The condenser tube was inclined, with its right side at a slightly lower level than the left side. In this way the condensate was collected in a measuring tube. The vapour reached the condenser tubes through a vertical copper tube 0.3 m length and 35 mm external diameter.

The experimental results showed that 3 pipes were adequate for the condensation of the produced vapour indicating that the overall heat transfer coefficient is slightly higher that the calculated one. The experimental overall heat transfer coefficient is 3265 W/m^2-K, i.e. 10% greater than the theoretical. In the case that the vapour produced in the generator is not liquefied in the condenser, the pressure of the system gradually increases and the system becomes unbalanced.

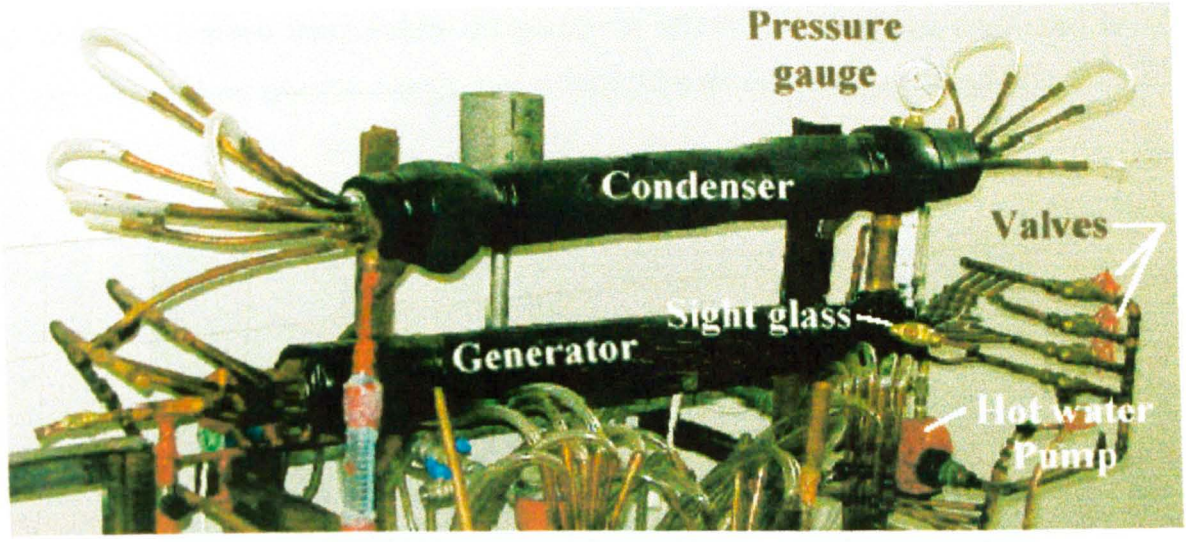

Figure 8.1. Generator and condenser.

8.1.2 Generator Heat Exchanger

Since no formula is available for calculating the exact heat transfer coefficient, the generator was constructed in such a way so that variable lengths of tube could be used in order to heat the solution. The shell of the generator was constructed from a copper tube 1 m in length, 67 mm external diameter and 1.2 mm thick. The shell was insulated with 13 mm thick armaflex insulation. Ten copper tubes with 9.5 mm outside diameter and 8.1 mm inside diameter were housed inside the shell as shown in Figure 8.1. Every tube could be isolated with a valve; therefore the required number of tubes could heat the water/lithium bromide solution. A sight glass was also fitted on the generator to observe the solution level. Hot water was circulated in the pipes with a pump.

The water was heated to the required temperature with two electrical heaters, 3 kW each. The electrical heaters were fitted on a water cylinder consisting of a galvanised pipe 150 mm in diameter and 1 m in length (Figure 8.2). The temperature was controlled by two thermostats, which permitted accurate setting.

The energy flow, $\dot{Q}$ supplied to the generator, is calculated from the formula, $\dot{Q} = \dot{m}\ c_p\ \Delta t$. The experimental results indicate that for 92°C heating water inlet temperature and 88°C outlet temperature, 1.4 kW were delivered to the solution of the generator per meter tube. Since the solution temperature of the generator is about 70°C,

the logarithmic mean temperature difference is 19.9°C and the tube area used is 0.03 m^2, the average heat transfer coefficient is 1400/(19.9*0.03) = 2345 W/m^2-K.

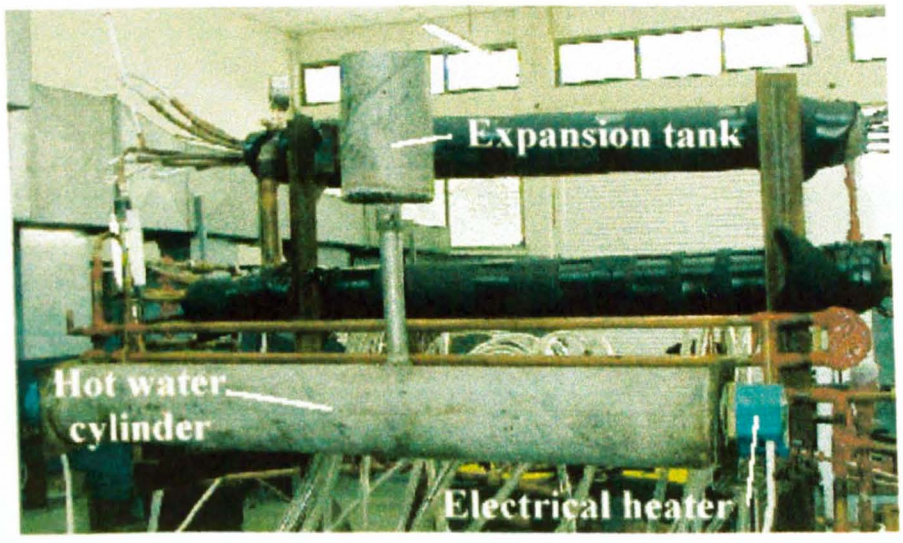

Figure 8.2. Hot water cylinder.

For 88°C heating water inlet temperature and 85°C outlet temperature, 1.14 kW was delivered to the generator solution per meter tube. The logarithmic mean temperature in this case is 16.5°C and the average heat transfer coefficient is 1140/(16.5*0.03) = 2300 W/m^2-K.

Lowering the heating water inlet temperature to 80°C the outlet temperature became 78°C and the input heat to the generator was 0.61 kW per meter tube. The average heat transfer coefficient in this case becomes 2270 W/m^2-K.

Therefore for delivering the required amount of heat to the generator solution (1.36 kW), 1 pipe can be used with 92°C heating water inlet temperature, 2 pipes with 88°C and just over 2 pipes with 80°C. In every case the flow in the tubes is intermittent in order not to overheat the generator solution.

8.1.3 Solution Heat Exchanger

The solution heat exchanger was of the single pass annulus type. It was constructed using copper pipes with 15.0 mm outside pipe diameter, 1.0 mm wall thickness and 9.5 mm inside pipe diameter, 0.7 mm wall thickness. The heat exchanger was positioned

slightly below the generator as indicated in Figure 8.3. During operation the flow of the solution from the generator was adjusted with a valve. The solution rich in refrigerant was pumped from the absorber to the generator through the solution heat exchanger. The operation of the heat exchanger showed that the theoretical estimations specified in Table 7.11 were met within an accuracy of $\pm 0.5°C$, therefore the predicted length of pipes was correct.

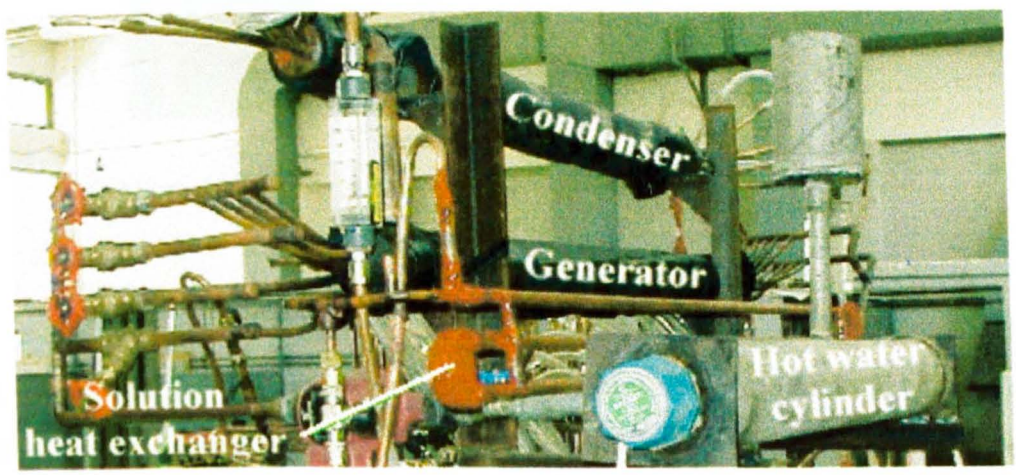

Figure 8.3. Solution heat exchanger

8.1.4 Absorber Heat Exchanger

The absorber was constructed from a number of vertical tubes with 9.5 mm outside diameter. On the top part of every tube, another tube 12 mm inside diameter and 100 mm in length was fitted in such a way that the absorber solution could pass inside the 2 mm gap between the two tubes as shown in Figure 8.4. The top part of the 100 mm tube was soldered onto the vertical tube so that the thin film of fluid could escape only downwards. The film of the absorber solution could thus be cooled by water flowing inside the vertical tube.

In the case of this study, two absorber shells were constructed from a copper tube each being 1 m in length, 67 mm external diameter and 1.2 mm thick. The two-absorber shells were joint to the evaporator shell with copper tubes 0.2 m in length and 35 mm external diameter insulated with 13 mm thick armaflex insulation (Figure 8.5). Eight vertical tubes, constructed as explained above were housed inside each shell, as shown in Figure 8.6. The required number of tubes was connected externally with hoses. The solution tubes were also grouped for easy feeding of the solution.

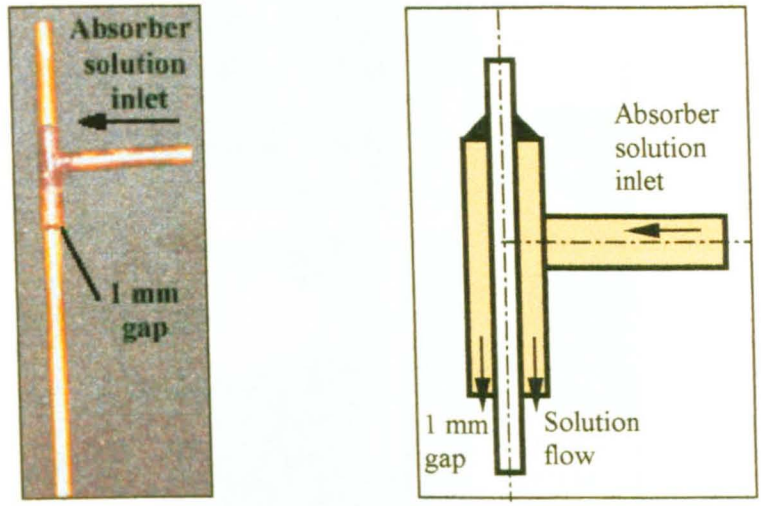

(a) Constructed tube (b) Schematic representation

Figure 8.4. Absorber tubes.

During the operation of the unit it was observed that the overall heat transfer coefficient (U) based on the outside surface of the tube was 400 W/m^2-K. Therefore for removing the heat load of the absorber approximately 12 tubes (six on every side) were needed instead of the 9 calculated. This is due to a lower value of the overall heat transfer coefficient attributed to the fact that in practice the wetting of the tubes is not uniform.

Also, during operation no increase of the absorber pressure was observed indicating that the water vapour produced in the evaporator was absorbed completely.

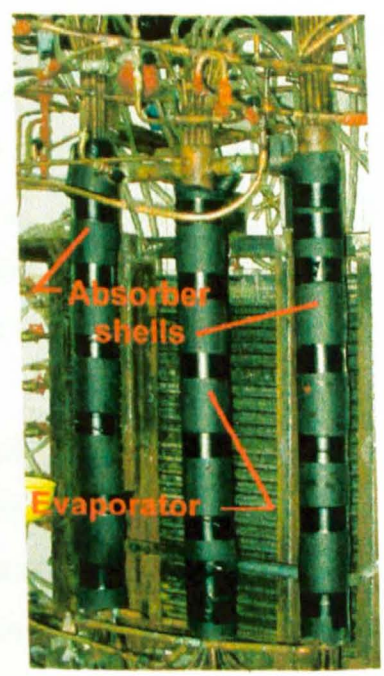

Figure 8.5. Absorber and evaporator shells.

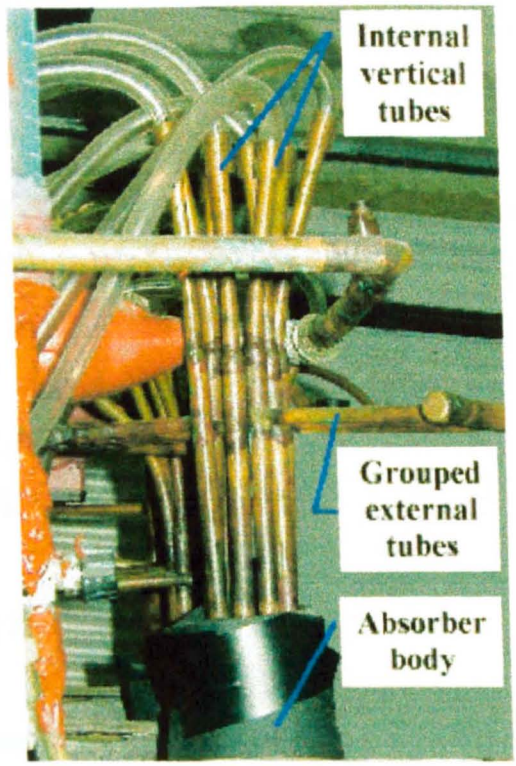

Figure 8.6. Absorber detail.

8.1.5 Evaporator Heat Exchanger

The evaporator heat exchanger (Figure 8.5) was constructed in the same way as the absorber heat exchanger. The shell was made from a copper tube 1m in length, 67 mm external diameter and 1.2 mm thick. The shell was insulated with 13 mm thick armaflex insulation. Inside the shell eleven vertical tubes, similar to the absorber tubes, were fitted. Supplied water run on the external surface of every tube where it evaporated. In the case of falling films, evaporating on the outer side of a tube, it is difficult to predict the heat transfer coefficient. The advantage of high coefficient in falling-film exchangers is partially offset by the difficulties involved in distribution of the film and maintaining complete wettability of the tube (Perry and Green, 1984). For this reason the heat transfer coefficient of the specific construction was determined experimentally.

In the case of the present study in order to avoid the secondary heat exchanger, water from a storage tank was directly used in a single pass. Also to improve wettability, a mass flow rate of 0.3 g/s per tube was applied. The resulting overall heat transfer coefficient determined experimentally was U= 195 W/m^2-K at a ΔT_{ln} = 15.5°C.

The heat transfer coefficients, h_i *and* h_b, for the inside and outside flow could therefore be determined as follows:

During the experiment the entering water temperature was 27°C and the leaving temperature was 17°C. The water properties at (27+17)/2 = 22°C are:

ρ = 999.2 kg/m^3

ν = 0.9581x10^{-6} m^2/s

k = 0.600 W/m-K

Pr = 6.67

c_p = 4180.7 J/kg K

Since 11 vertical tubes were used, the mass flow rate per tube is:

$$\dot{m} = \dot{Q}e / 11*(c_p * \Delta t) = 1000 / (11*4180.7*(27-17) = 0.00217 \text{ kg/s}$$

and

$$Re = (4*0.00217) / (3.14*0.0081*999.2*0.9581*10^{-6}) = 356.5$$

Therefore the flow is laminar, and Equation (7.16) gives:

$h_i = 3.66*K / D_i = 271.1$ W/m^2-K

Substituting the known values into Equation (7.13), gives h_o = 695 W/m^2-K. Based on this value and a cooling load of 1 kW but with cooling water entering at 13°C and leaving at 11°C, which would represent a practical application, the resulting heat transfer area would be 0.86 m^2, which corresponds to 29 tubes.

8.2 GENERAL OBSERVATIONS

The absorption refrigeration unit constructed as explained above operates under the design conditions, specified in Tables 7.9 to 7.13. For the operation of the unit two pumps were used, one for the evaporator and one for the absorber. The flow of the two

pumps needed to be adjusted in such a way so as to provide the required flow to the two heat exchangers. The evaporator pump simply re-circulated water from a reservoir (Figure 8.7) to the tubes of the evaporator. Care was needed to maintain the level of the water in the reservoir steady, thus allowing only the extra water fed from the condenser to evaporate.

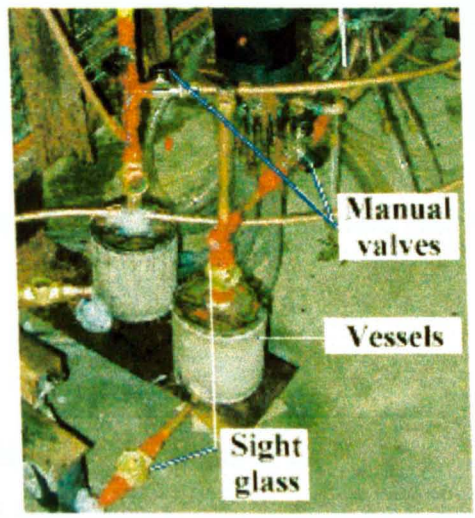

Figure 8.7. Absorber and evaporator liquid vessels.

The absorber pump circulated the required amount of solution back to the generator. The solution level in the generator should be maintained constant.

In the experimental unit the generator solution passes to the solution heat exchanger and to the absorber by the pressure difference and by gravity. Also the condenser water runs down to the evaporator due to the same reasons. A manual throttle valve was used in both cases to adjust the flow. During operation fine adjustment of the operation of the pumps and the setting of the valves was necessary to maintain the operation of the unit at the design level. This operation was not easy and continuous observation was necessary. In commercial units automatic control devices are employed.

Another point of interest is the introduction of the LiBr solution into the unit. For this task a vessel can be connected with a valve to the appropriate point of the unit (i.e., generator) as shown in Figure 8.8. When the air in the unit is removed, the atmospheric pressure will drive the solution into the unit. In the experimental unit 5 kg of LiBr salt were used.

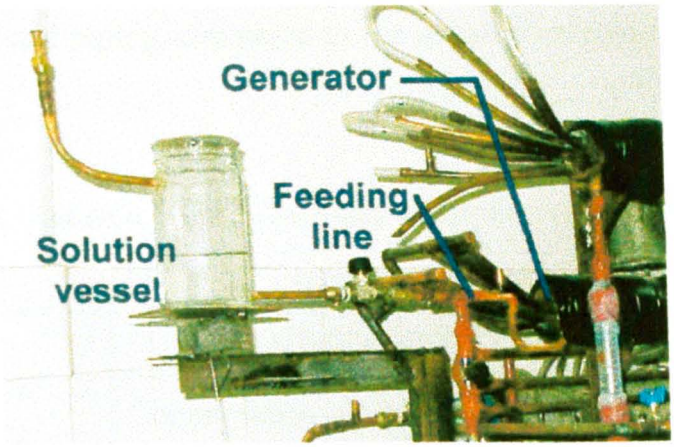

Figure 8.8. Introduction of LiBr solution into the generator.

8.3 COST ANALYSIS

The unit manufactured for this project is a prototype unit and the total cost of its construction is about C£ 3,000. A large part of this amount was spent for the purchasing of flow meters (C£ 500), auxiliary equipment like vacuum pumps, glass tubes etc (C£ 500) and experimentation with different types of valves and materials. The actual cost of a working unit of 1 kW capacity can be as low as C£ 1,550. A breakdown of this cost is shown in Table 8.1. Based on the 1 kW unit, the cost of an 11 kW unit, which can cover the needs of a typical insulated house, can be estimated as C£ 4,300 (Table 8.2).

It must also be stated that the above unit cannot be produced in a basic workshop. Automatic or semi automatic welding machines and personnel specialised on welding components for vacuum are necessary. Also special equipment for weld testing and soundness is necessary. The cost of such infrastructure is not included in the unit costing. On the other hand the produced unit is only a prototype and a lot of research can be done in order to improve the efficiency of the heat exchangers by using a surfactant additive, called octyl alcohol. Such an additive can increase the heat transfer performance in the absorber. Also other types of heat exchanging surfaces, like rough or finned surfaces may increase the efficiency and reduce the size of the unit.

It must also be noted that in order to complete the requirements of an 11 kW unit, a cooling tower or water from a well is necessary to provide adequate cool water for the condenser and absorber heat exchangers. The cost of such a tower is about C£ 400.

Also the installation of the absorption unit and cooling tower will demand about C£ 100 extra cost for pumps and piping, compared to the installation cost of a conventional 11 kW electric chiller.

Table 8.1. Cost of a 1 kW LiBr-water absorption refrigeration unit

Item	Observations	Cost in C£
Generator and Condenser Unit	Copper tubes welded or soldered	50
Evaporator	Copper tubes welded or soldered	150
Absorber	Copper tubes welded or soldered	150
Piping		30
Pumps	2 hermetic pumps	370
Automatic controls, censors and valves		600
LiBr salt	5 kg	200
	Total Cost:	**C£ 1,550**

Table 8.2. Comparative cost of a 1 kW and an 11 kW LiBr-water absorption refrigeration unit

Item	Cost of the 1 kW unit (C£)	Cost of the 11 kW unit (C£)
Generator and Condenser Unit	50	400
Evaporator	150	1000
Absorber	150	1000
Piping	30	100
Pumps	370	500
Automatic controls, censors and valves	600	700
LiBr salt	200	600
Total Cost	**1550**	**4300**

8.4 CONCLUSIONS

The 1 kW unit, which was designed in Chapter 7, was constructed and the heat transfer area of each heat exchanger was varied to provide the required output. In this way the designed COP was ensured. The construction of the small unit facilitated the determination of the heat transfer coefficients in the heat exchangers and the sizing of the major components of a full-scale unit with a cooling output of 11 kW.

The cost for an 11 kW unit, that can cover the needs of a typical insulated house, was estimated to be C£ 4300. The total cost of an absorption unit together with all necessary secondary devices and installation cost is estimated as C£ 4800. The price therefore of a LiBr-water absorption refrigeration unit is high compared to a similar capacity electric chiller that is only C£ 1500. It should be noted however, that the absorption units offer possibilities of use of renewable energy sources and waste heat, whereas the electric chiller uses electricity that is produced from fossil fuel.

CHAPTER 9

MODELLING AND SIMULATION OF AN ABSORPTION SOLAR COOLING SYSTEM FOR CYPRUS

Solar energy is in abundance in Cyprus. In summer, mean monthly temperatures for Nicosia at 14.00 hours in July, are 35.4°C (Kalogirou, 1991) with the temperature sometimes reaching 43°C. Therefore, there is a need to lower the indoor temperature considerably in order to be able to provide comfort. Solar cooling of buildings seems to be one of the most attractive solutions. This is an application in which the demand for cooling energy closely matches the availability of solar energy, not only to the seasonal but also to the daily variation.

Many researchers have developed solar assisted absorption refrigeration systems. Most of them have been produced as experimental units and computer codes were written to simulate the systems. Some of these designs are presented here.

Hammad and Audi (1992), described the performance of a non-storage, continuous, solar operated absorption refrigeration cycle. The maximum ideal coefficient of performance of the system was determined to be equal to 1.6, while the peak actual coefficient of performance was determined to be equal to 0.55.

Haim *et al.* (1992), performed a simulation and analysis of two open-cycle absorption systems. Both systems comprise a closed absorber and evaporator as in conventional single stage chillers. The open part of the cycle is the regenerator, used to reconcentrate the absorber solution by means of solar energy. The analysis was performed with a computer code developed for modular simulation of absorption systems under varying cycle configurations (open and closed-cycle systems) and with different working fluids. Based on the specified design features, the code determined the operating parameters in each system. Results indicated a definite performance advantage of the direct-regeneration system over the indirect one.

Hawlader *et al.* (1993), developed a lithium bromide absorption cooling system employing an 11x11 m collector/regenerator unit. They also developed a computer model, which they validated against real experimental values with good agreement. The

experimental results showed a regeneration efficiency varying between 38% and 67% and the corresponding cooling capacities ranged from 31 kW to 72 kW.

Ameel *et al.* (1995), give performance predictions of alternative low-cost absorbents for open cycle absorption using a number of absorbents. The most promising of the absorbents considered, was a mixture of two elements, lithium chloride and zinc chloride. The estimated capacities per unit absorber area were 50% to 70% less than those of lithium bromide systems.

Ghaddar *et al.* (1997), presented modelling and simulation of a solar absorption system for Beirut. The results showed that, for each ton of refrigeration, it is required to have a minimum collector area of 23.3 m^2 with an optimum water storage capacity ranging from 1000 to 1500 liters, for the system to operate solely on solar energy for about 7 hours per day. The monthly solar fraction of total energy use in cooling is determined as a function of solar collector area and storage tank capacity. The economic analysis performed showed that the solar cooling system is marginally competitive only when it is combined with domestic water heating.

Erhard and Hahne (1997), simulated and tested a solar-powered absorption cooling machine. The main part of the device is an absorber/desorber unit, which is mounted inside a concentrating solar collector. Results obtained from field tests are discussed and compared with the results obtained from a simulation program developed for this purpose.

Hammad and Zurigat (1998), described the performance of a 5.3 kW solar cooling unit. The unit comprises a 14 m^2 flat-plate solar collector system and five shell and tube heat exchangers. The unit was tested in April and May in Jordan. The maximum value obtained for actual coefficient of performance was 0.85.

Computer modelling of thermal systems presents many advantages the most important of which are the elimination of the expense of building prototypes, the optimisation of the system components, estimation of the amount of energy delivered from the system, prediction of temperature variations of the system and many other less important ones.

The objective of this chapter is to model a complete system, composing of a solar collector, storage tank, a boiler and a LiBr-water absorption refrigerator (designed according to the data collected for the 1 kW unit in chapters 7 and 8, which will cover a typical house load during the whole year.

For this analysis the typical Cypriot house indicated in Figure 3.4 is considered. The house load is minimised by considering an insulated roof, insulated walls, double glazed windows, internal shading and night ventilation (3 ach) in summer. The above factors were found to be economically viable in the analysis presented in chapter 6. The double-walls are made of 0.10 m hollow brick and 0.02m plaster on each side and a layer of 0.05 m insulation in between. The roof is constructed from fair-faced 0.15 m heavy concrete, 0.05 m polystyrene insulation, 0.07 m screed and 0.004 m asphalt, covered with aluminum paint of 0.55 solar absorptivity.

The above construction requires an annual cooling load at 25°C of 17,600 kWh with a peak load of 10.3 kW and an annual heating load at 21°C of 3,530 kWh with a peak load of 5.5 kW.

The TRNSYS program is used to model the complete system (house load estimation with solar powered heating and absorption cooling), together with the weather values of a typical meteorological year (TMY) file for Nicosia, Cyprus.

The solar powered system consists of an array of solar collectors, boiler, storage tank, 11 kW absorption cooling unit, pumps and thermostats.

Using this approach a system optimisation is performed in order to select the right equipment, i.e., the collector type, the storage tank volume and the collector slope angle and area. The collector area is decided by performing an economic analysis of the system. Also the long-term integrated system performance and the dynamic system behaviour is evaluated.

9.1 CHARACTERISTICS OF AN 11 KW WATER-LIBR ABSORPTION CHILLER

Nowadays the majority of the city-houses in Cyprus are provided with boilers for heating, and solar collectors (mainly flat plate) for domestic water heating production. Therefore, in the present study, the absorption chiller is powered by both a conventional boiler and solar energy collectors. The prospects of using a coupling system powered with diesel oil are favourable as the relative cost of electricity in Cyprus at present is about 4 times that of diesel oil.

The characteristics needed in TRNSYS deck file are the generator load, the mass flow of the heating water to the generator heat exchanger and its input and output temperatures. Program 'LITH' which was used for the design of the small 1kW unit can also be used to evaluate the characteristics of an 11 kW unit. A unit with this capacity, operating at the conditions set for the 1 kW unit, can cover the cooling load of the typical model house constructed as outlined above. The 11 kW unit characteristics, as calculated with program 'LITH', are shown in Table 9.1.

An operational unit needs to be equipped with a number of controls to:

1. Keep the levels of the solution and water in the various vessels constant, thus keep the LiBr-water percentages within the designed limits.

2. Prevent the preset pressure in the generator to exceed the designed limit by adjusting the heat input not to exceed the designed maximum capacity.

3. Prevent the preset pressure in the absorber to increase by adjusting the flow of cooling water in the absorber heat exchanger.

Table 9.1. Water-LiBr absorption refrigeration system calculations based on a generator temperature of 75°C and a solution heat exchanger exit temperature of 55°C

Point	H (kJ/kg)	$\dot{m}$ (Kg/s)	P (kPa)	T (°C)	%LiBr (X)	Remarks
1	83	0.05691	0.93	34.9	**55**	
2	83	0.05691	4.82	34.9	55	
3	124.7	0.05691	4.82	**55**	55	Sub-cooled liquid
4	183.2	0.05217	4.82	**75**	**60**	
5	137.8	0.05217	4.82	51.5	60	
6	137.8	0.05217	0.93	44.5	60	
7	2612	0.00474	4.82	**70**	0	Superheated Steam
8	131.0	0.00474	4.82	31.5	0	Saturated liquid
9	131.0	0.00474	0.93	6	0	
10	2511.8	0.00463	0.93	6	0	Saturated vapour
11	23.45	0.00011	0.93	6	0	Saturated liquid

Description	Symbol	kW
Capacity (evaporator output power)	$\dot{Q}_e$	**11.0**
Absorber heat, rejected to the environment	$\dot{Q}_a$	14.1
Heat input to the generator	$\dot{Q}_g$	14.9
Condenser heat, rejected to the environment	$\dot{Q}_c$	11.8
Coefficient of performance	COP	0.74

An actual 11 kW unit has the heat exchangers sized for the appropriate capacity. Therefore, the unit has oversized heat exchangers when it delivers a smaller capacity. This of course does not present a problem since the generator, condenser, evaporator and absorber heat exchangers can be controlled externally by adjusting the valves of the cooling or heating source water in such a way as to keep the cycle temperatures at their preset values. The solution heat exchanger though, will affect the efficiency of the cycle since for less capacity, the mass flows will be smaller but the heat exchanger area will be the same. To check this effect computer program 'LITH' was modified so that the temperature at the output of the solution heat exchanger of the fluid returning to the generator (T_3, Table 9.1) is not an input. This temperature, resulting from the new mass flows in the solution heat exchanger, can be calculated assuming that the area of the solution heat exchanger is the one needed for the 11 kW unit (i.e., 0.3426 m^2, calculated with 'LITH'). The modifications needed to program 'LITH' are indicated in Appendix 5.

Figure 9.1 shows the effect of the unit capacity on T_3 and the coefficient of performance of the unit. Figure 9.2 shows the variation of the generator input heat with reduced unit capacity.

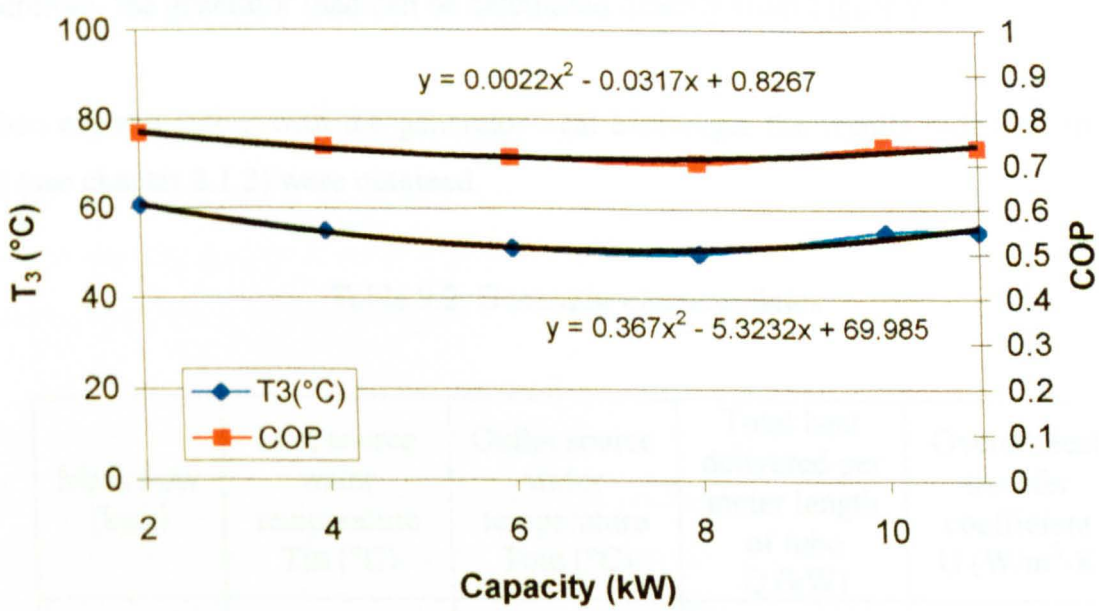

Figure 9.1. Variation of temperature at the output of the solution heat exchanger of the fluid returning to the generator (T_3, °C) and coefficient of performance (COP) with unit capacity (kW).

The temperature of the generator inlet heating water affects the amount of heat delivered to the generator. Since the pressure in the generator is set to 4.82 kPa and the % LiBr/water solution to 60% (this is done by checking the solution levels in the generator and absorber) the generator water evaporates from the solution always at the same temperature (T_4, 75°C), which depends on the working fluid properties.

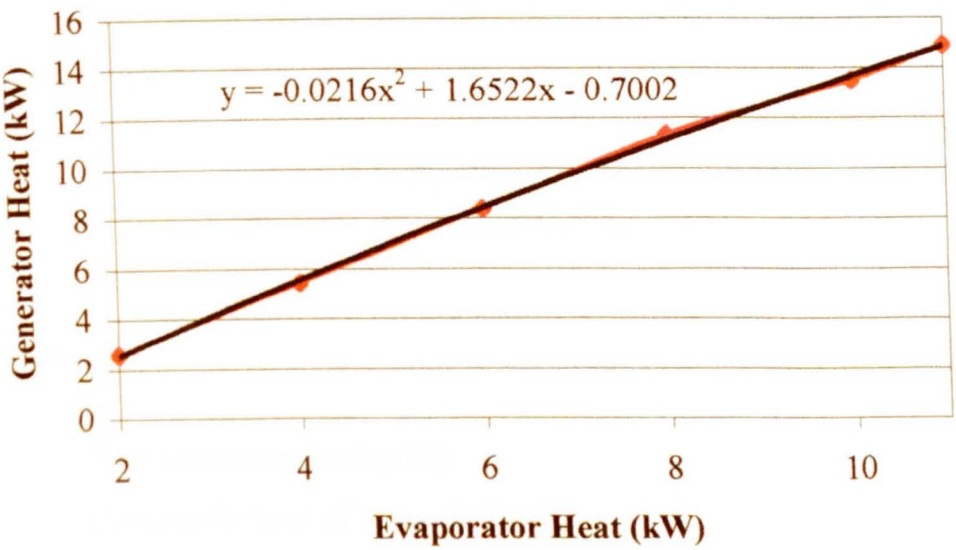

Figure 9.2. Variation of generator input heat with unit capacity.

Therefore, the generator load can be calculated directly from Figure 9.2

When experimenting with the generator heat exchanger the results indicated in Table 9.2 (see chapter 8.1.2) were obtained.

Table 9.2. Generator characteristics

Mass flow (kg/s)	Inlet source water temperature Tin (°C)	Outlet source water temperature Tout (°C)	Total heat delivered per meter length of tube Q (kW)	Overall heat transfer coefficient U (W/m^2-K)
0.0833	92	88	1.4	2345
0.090	88	85	1.14	2300
0.073	80	78	0.61	2270

As can be seen the overall heat transfer coefficient changes slightly with temperature, i.e., the temperatures used for the input water can be 85°C to 92°C without any significant variation in the operation of the heat exchanger.

Since the maximum heat needed in the generator is 15 kW, 14 one-meter tubes could be used in the generator with total mass flow of 14*0.09=1.26 kg/s. The output temperature can then be calculated according to the delivered load from equation:

$$\dot{Q}_g = 1.26 * C_p * (T_{in} - T_{out}) \quad (9.1)$$

where:

$\dot{Q}_g$ = Generator load (kW)

C_p=specific heat of water (kJ/kg-K)

T_{in}=inlet source water temperature (°C)

T_{out}=outlet source water temperature (°C)

9.2 THE COMPLETE SYSTEM CHARACTERISTICS

The complete system besides the absorption refrigerator consists of a number of solar collectors, a thermally insulated vertical storage tank, a conventional boiler and interconnecting piping. A schematic of the system showing also the simulation program information flow is shown in Figure 9.3.

The system was modelled with the TRNSYS simulation program. The program consists of many subroutines that model subsystem components. The type number of every TRNSYS subroutine used to model each component is also shown in Figure 9.3. The complete TRNSYS deck file is shown in Appendix 6.

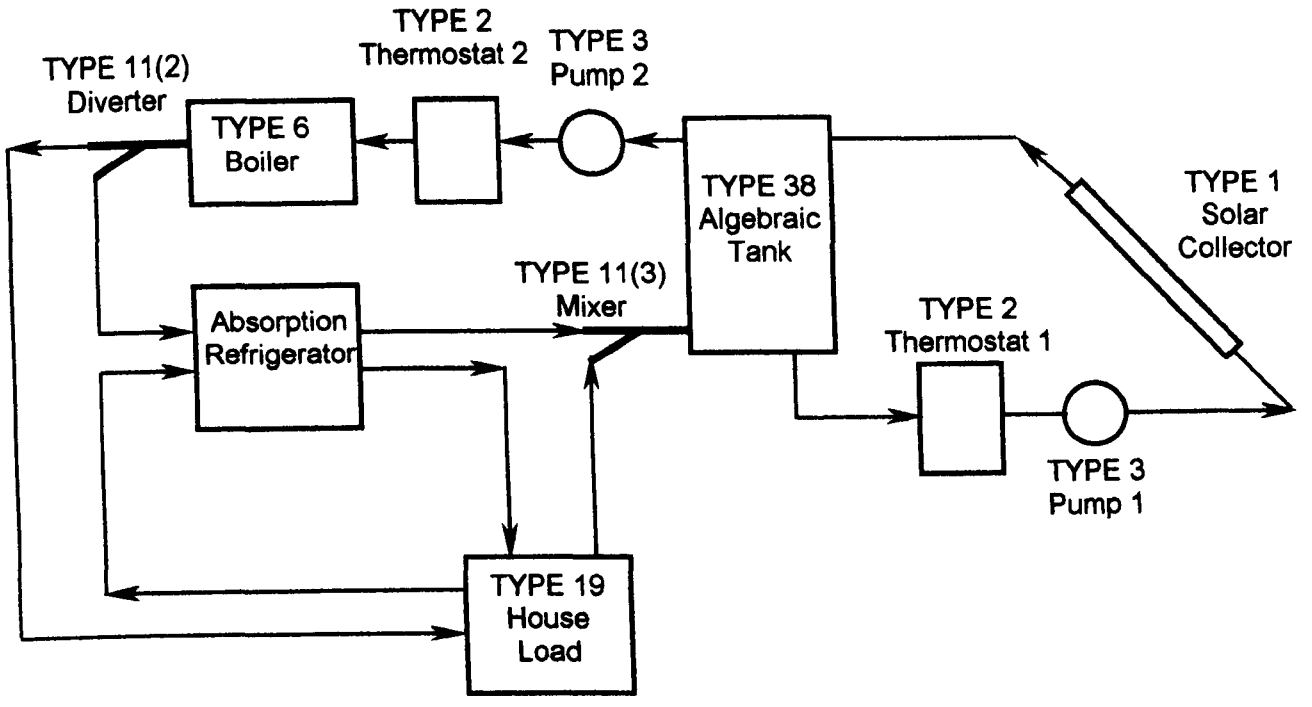

Figure 9.3. Circuit diagram and TRNSYS types used for modelling the system.

The construction and type of the solar collectors is important and relevant to the operation and efficiency of the whole system. Three types of solar collectors, modelled with TRNSYS Type 1, are evaluated in this study as follows:

a. *Flat Plate Collectors*. These are predominantly used for domestic hot water production. The external casing of the collectors considered in this study, which are manufactured locally, is made of high corrosion resistant galvanised steel sheet, sprayed with aluzinc paint. The casing is covered with a 4 mm thick single glass and sealed with a rubber gasket. The absorber plate is made of copper. High radiation absorption is achieved by the use of black fine matt finish on the copper surface, which has a high absorption coefficient. The underside of the absorber plate and the side casing are well insulated to reduce conduction losses with 50 mm and 30 mm fibreglass insulation respectively. Each flat plate collector consist of 12 evenly spaced parallel copper pipes, 15 mm in diameter, embossed by semi-circular grooves formed in the flat plate absorber.

The efficiency (n) of a flat plate collector is defined as the quotient of the actual useful energy collected, to the total solar energy incident on or intercepted by the collector. In a quadratic approach the collector efficiency is formulated as:

$$n = a_0 - a_1 \frac{(T_i - T_a)}{I_T} - a_2 \frac{(T_i - T_a)^2}{I_T} \quad (9.2)$$

where:

n = collector efficiency

a_0 = intercept efficiency

a_1 = negative of the first order coefficient of the efficiency (kJ/hr-m^2-K)

a_2 = negative of the second order coefficient of the efficiency (kJ/hr-m^2-K^2)

T_i = inlet temperature of fluid to collector (°C)

T_a = ambient temperature (°C)

I_T = total incident radiation on a flat surface (kJ/hr-m^2)

The important characteristics of this type of flat plate collector are shown in Table 9.3.

Table 9.3. Flat plate collector characteristics used in the TRNSYS simulations

Parameter No.	Value
C_{pc} – Specific heat of collector fluid (kJ/kg-K)	4.19
Efficiency mode	n v_s (Ti - Ta)/I_T
G_{test} – flow rate per unit area at test conditions (kg/hr-m^2)	54
a_o – intercept efficiency	0.792
a_1 – negative of the first-order coefficient of the efficiency (kJ/hr-m^2-K)	23.994
a_2 – negative of the second-order coefficient of the efficiency (kJ/hr-m^2-K^2)	0
e – effectiveness of the collector loop heat exchanger	no heat exchanger used
Symbols: 1. n - efficiency 2. Ti - temperature of fluid entering cold side of heat exchanger or collector inlet if no heat exchanger present (°C) 3. Ta - ambient temperature (°C) 4. I_T - incident radiation (kJ/m^2-hr)	

Conventional flat plate collectors are developed for use in sunny and warm climates. During cold, cloudy and windy days their performance is greatly reduced. Furthermore, condensation and moisture can cause early deterioration of internal materials resulting in reduced performance and system failure.

b. *Compound Parabolic Concentrating Collectors (CPC).* These collectors use curved reflecting surfaces to concentrate sunlight onto a small absorber area. CPC's are used for higher water temperature applications than the flat plate collectors. Such a focusing collector performs very well in direct sunlight but, depending on the concentration ratio, does not perform well under cloudy or hazy skies because only a few rays are captured and reflected onto the absorber. A compound parabolic collector system can work either as a stationary system, or it can track the sun. In stationary systems, much of the sunlight that hits the concentrator's reflector often misses the absorber. Tracking devices allow the collector to follow the sun's movement across the sky. This ensures that the concentrator always faces toward the sun. Such systems are usually employed for higher temperature applications. Since residential applications only require medium temperatures, stationary systems are usually employed. Stationary systems are also less expensive and are easier to install and maintain. Concentrating collectors work best in climates with a high amount of direct solar radiation as in Cyprus. The geometry of this type of collector is shown in Figure 9.4 and its characteristics in Table 9.4.

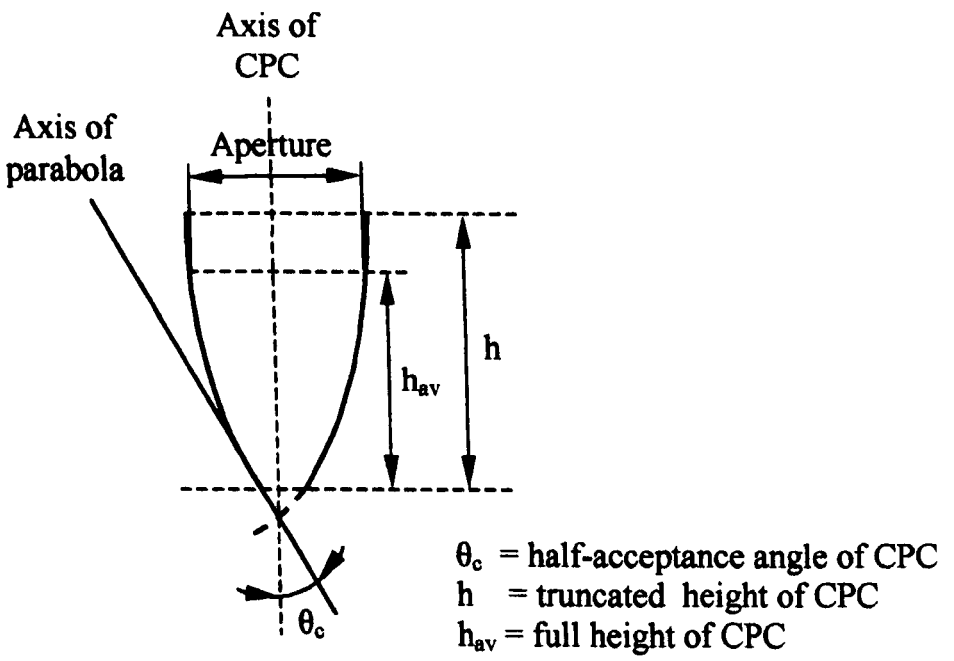

Figure 9.4. Geometry for compound parabolic collectors.

Table 9.4. Compound parabolic collector (CPC) characteristics used in the TRNSYS simulations

Parameter No.	Value
C_{pc} – Specific heat of collector fluid (kJ/kg-K)	4.19
F'- collector fin efficiency factor	0.9
U_L – overall loss coefficient of collector per unit aperture area (kJ/hr-m^2-K)	5.4
ρ_R – reflectivity of walls of CPC	0.85
θ_c - half-acceptance angle of CPC (degrees)	45
h_{av}/h – ratio of truncated to full height of CPC	0.67
Axis orientation	receiver axis is horizontal and in a plane with a slope of β (transverse)
a – absorbtance of absorber plate	0.95
N_G – number of cover plates	1
η_R – index of refraction of cover material	1.526
K_L – product of extinction coefficient and the thickness of each cover plate	0.0375

c. *Evacuated Tube Collectors*: These collectors are highly efficient, made of an absorber pipe enclosed within a larger glass tube. The absorber pipe may also be attached to a black copper fin that fills the tube (absorber plate). The space between the glass and the absorber is evacuated. Only radiant heat is transmitted from the absorber pipe to the outside of the collector and in this way the efficiency of the collector is substantially increased.

The tubes are usually mounted into a manifold and the heated liquid is either used directly or circulates through a heat exchanger and gives off its heat to water. The coated surface of the absorber pipe has high absorption (> 92 %) of solar radiation and low emittance (< 6 %) for the infrared heat radiation.

The absorber coating also has high resistance to long-term vapour condensation, high corrosive sulphur dioxide and high operating temperature. The characteristics of this type of collector are shown in Table 9.5

Table 9.5. Evacuated solar tube collector characteristics used in the TRNSYS simulations

Parameter No.	Value
C_{pc} – Specific heat of collector fluid (kJ/kg-K)	4.19
Efficiency mode	$n\ v_s\ (Tav - Ta)/I_T$
G_{test} – flow rate per unit area at test conditions (kg/hr-m^2)	50
a_o – intercept efficiency	0.82
a_1 - negative of the first-order coefficient of the efficiency (kJ/hr-m^2-K)	7.884
e – effectiveness of the collector loop heat exchanger	no heat exchanger used
Symbols: 1. n – efficiency 2. Tav – average collector fluid temperature (°C) 3. Ta - ambient temperature (°C) 4. I_T- incident radiation (kJ/m^2-hr)	

The performance of the system employing these three types of collectors is investigated in order to select the most suitable for the present application. The final selection is made by considering the financial viability of the system.

Hot water is stored in a TRNSYS Type 38 tank. The vertical cylinder construction is made of copper and is thermally insulated with polyurethane. Also the tank is protected by a galvanised outer shell 0.6 mm thick.

The backup boiler (TRNSYS Type 6) is assumed to have a maximum heating rate of 18 kW and a set upper temperature of 93°C.

A number of thermostats (TRNSYS Type 2) are also used in order to control:

a. The flow to the solar panels, allowing the fluid to circulate only when the temperature of the fluid returning from the collectors to the storage tank is higher than that of the fluid delivered to the load; and

b. The operation of the boiler, allowing the boiler to operate only when the temperature of the fluid delivered to the load is below an optimum value. In this case the boiler will keep the water temperature delivered to the absorption cooler always above 85°C.

9.3 SYSTEM OPTIMISATION

A number of simulations were carried out in order to optimise the various factors affecting the performance of the system. The parameters considered are as follows:

a) *The collector slope angle.* The solar heat gain from the system for various collector slope angles is shown in Figure 9.5. As can be seen, the optimum angle in the Cyprus environment is:

   i. 25°-30° for the flat plate collector

   ii. 30° for the compound parabolic collector, and

   iii. 30° for the evacuated tube solar collector

This is due to the solar altitude angle, which for the latitude of Cyprus (35°) can reach to 78° during noon in June. Also, because of the load characteristics, with the total cooling loads being about 6 times bigger than the heating loads, the optimum angle should be such that the collectors are absorbing greater heat during summer.

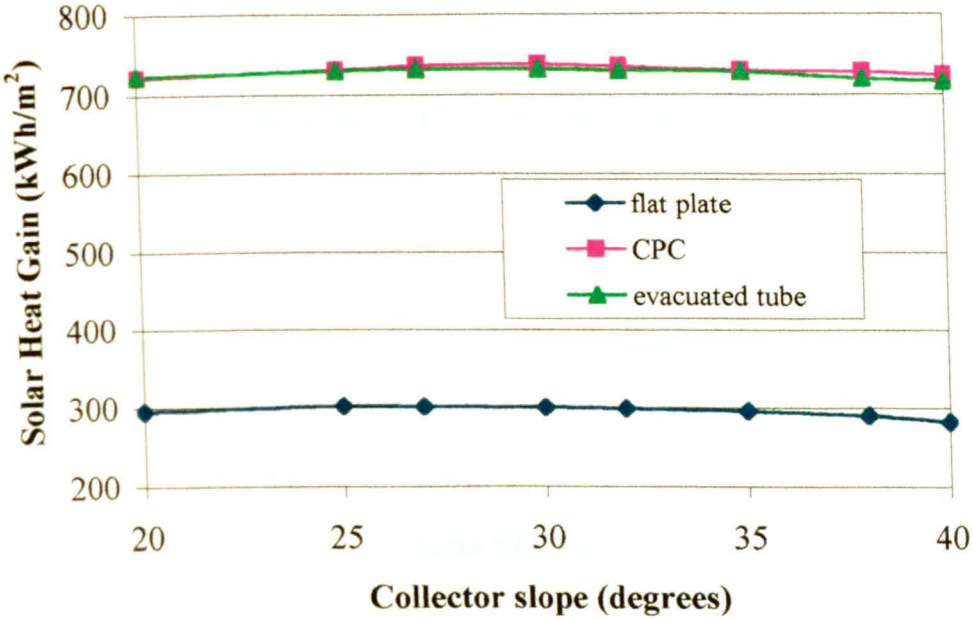

Figure 9.5. Effect of collector slope angle on solar energy gain.

b) *Storage tank size.* This factor also plays a role in the optimisation of the system. The boiler heat required by the system for different storage volumes is shown in Figures 9.6 to 9.8 for the three collector types. As can be seen, in all cases, a smaller tank size results in slightly less energy consumption by the boiler and slightly less energy collected by the solar collectors.

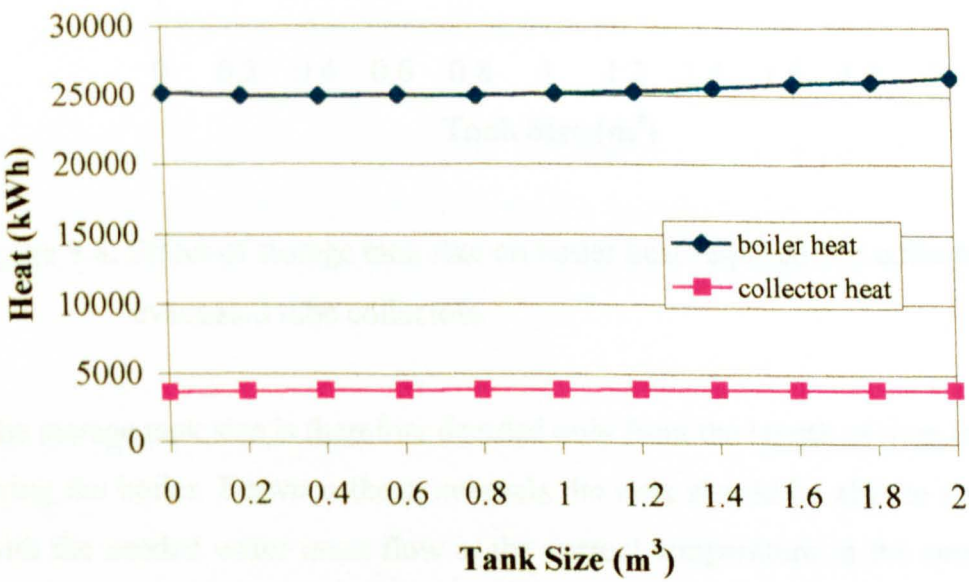

Figure 9.6. Effect of storage tank size on boiler heat required and collected heat for flat plate collectors.

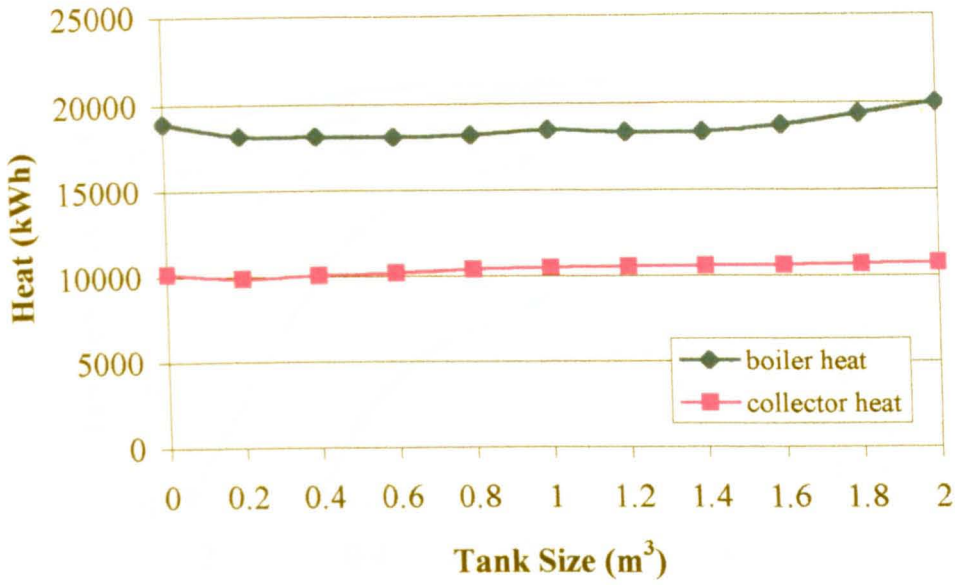

Figure 9.7. Effect of storage tank size on boiler heat required and collected heat for compound parabolic concentrating collectors.

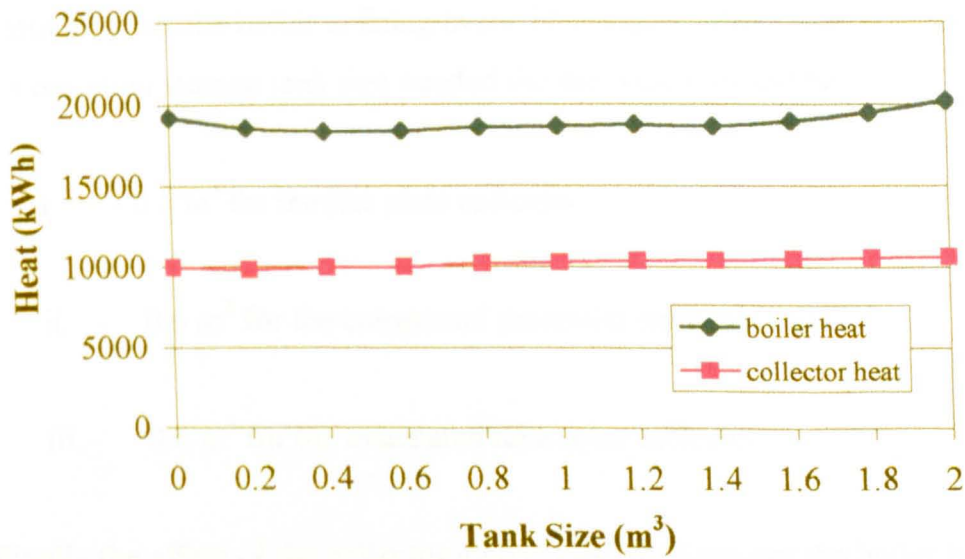

Figure 9.8. Effect of storage tank size on boiler heat required and collected heat for evacuated tube collectors.

The storage tank size is therefore decided only from the length of time intervals between firing the boiler. Between these intervals the tank should be able to supply the system with the needed water mass flow at the correct temperature in the summer. As can be seen in Figure 9.9, when the storage tank size is small the temperature in the cylinder cannot be kept above 85°C for long periods of time.

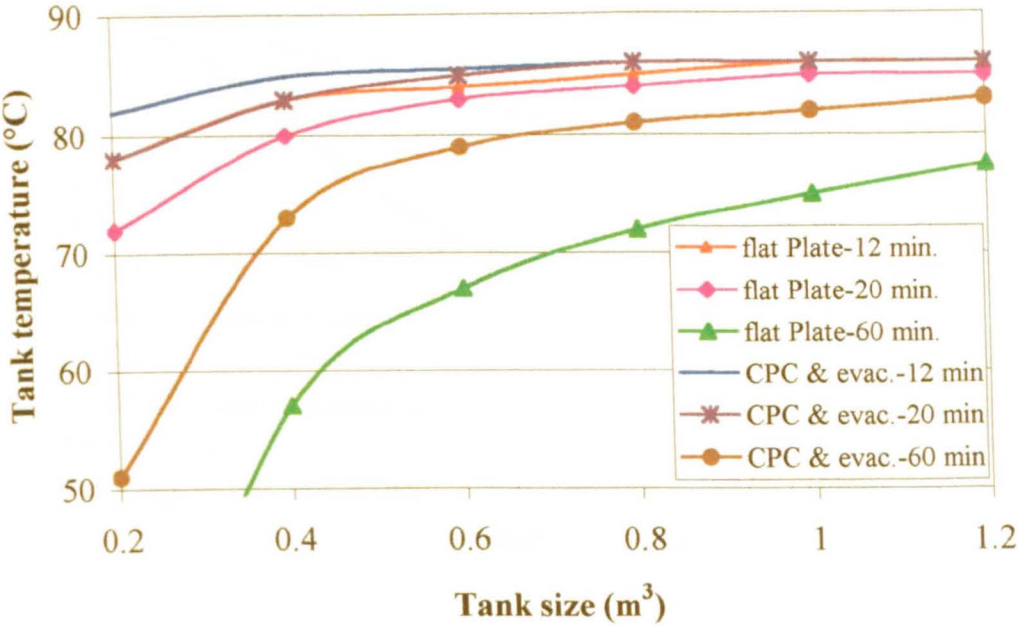

Figure 9.9. Effect of storage tank size on the boiler heat.

Assuming that the boiler is firing every 12 minutes, which may be a reasonable interval, the optimum storage tank size needed for the system would be:

i. 0.8 m^3 for the flat plate collector

ii. 0.6 m^3 for the compound parabolic collector and

iii. 0.6 m^3 for the evacuated tube solar collector

Finally the effect of the collector area is evaluated against the boiler heat required. As it is expected the greater the collector area the less the boiler heat needed as indicated in Figure 9.10 and the more the collected heat as indicated in Figure 9.11.

To determine the optimum collector area the cost of the solar system must be compared against the fuel saved due to its use. The cost of the various types of collectors is shown in Table 9.6.

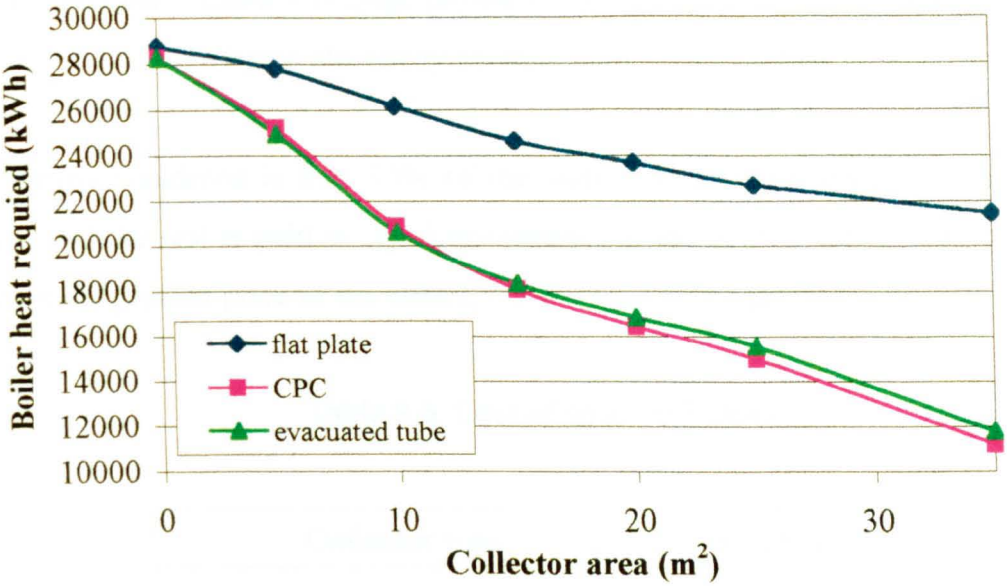

Figure 9.10. Effect of the collector area on the boiler heat required by the system.

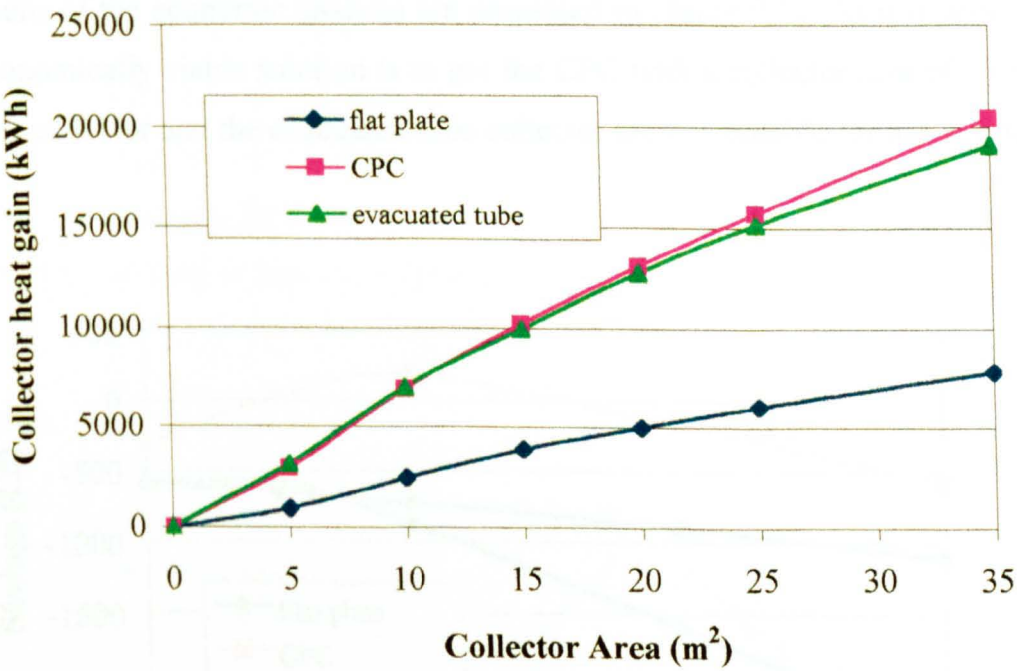

Figure 9.11. Effect of the collector area on the collector heat gain.

The economic method used, is the life cycle analysis as outline in section 6.6. For solar systems Equation 6.3 can be modified as:

System annual cost = Extra mortgage payment + Maintenance cost – Extra fuel savings – Extra electricity savings – Extra tax savings (9.3)

The scenario considered is that 30% of the initial cost of the system is paid at the beginning and the rest is paid in equal instalments in the next 10 years. The evaluation is based on the present price of the diesel, which is C£ 0.171 per lt.

Table 9.6. Cost of solar collectors

Collector type	Cost (C£/ m^2)
Flat plate collector	110
Compound parabolic collector	180
Evacuated tube collector	250

The results of the economic analysis are presented in Figure 9.12. As it is observed the only economically viable solution is to use the CPC with a collector area of 15 m^2. The flat plate collector and the evacuated tube collector are not suitable for this application.

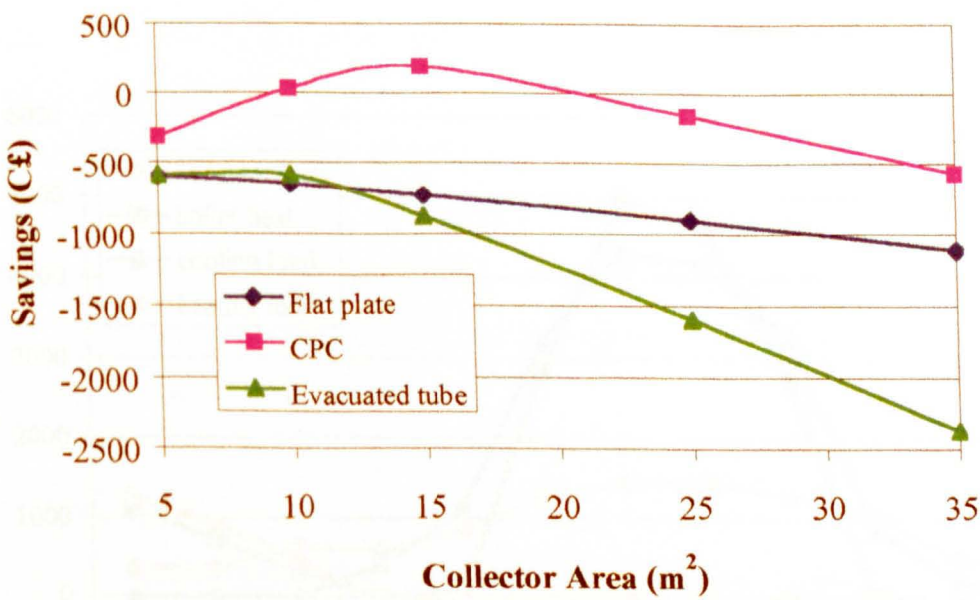

Figure 9.12. Collector area against life cycle savings in C£ for a fuel price of C£ 0.171 per lt and a 20-year period.

9.4 SYSTEM LONG-TERM PERFORMANCE AND ECONOMIC ANALYSIS

The specifications of the final system obtained from the optimisation study are shown in Table 9.7.

Table 9.7. The final system

Item	Value/Type
Collector type	CPC
Collector area	15 m^2
Collector slope	30°
Storage tank size	600 lt

The energy flows of the system are shown in Figure 9.13. The cooling load of the building reaches a maximum monthly value of 4200 kWh (in July), whereas the maximum monthly heating load occurs during January and is equal to 1250 kWh. The heat required from the conventional boiler is also shown in Figure 9.13. The maximum monthly load supplied by the solar system is 1500 kWh and as can be seen from the difference of the curves for the cooling load and boiler heat, nearly all collector heat can be utilised for cooling or heating purposes.

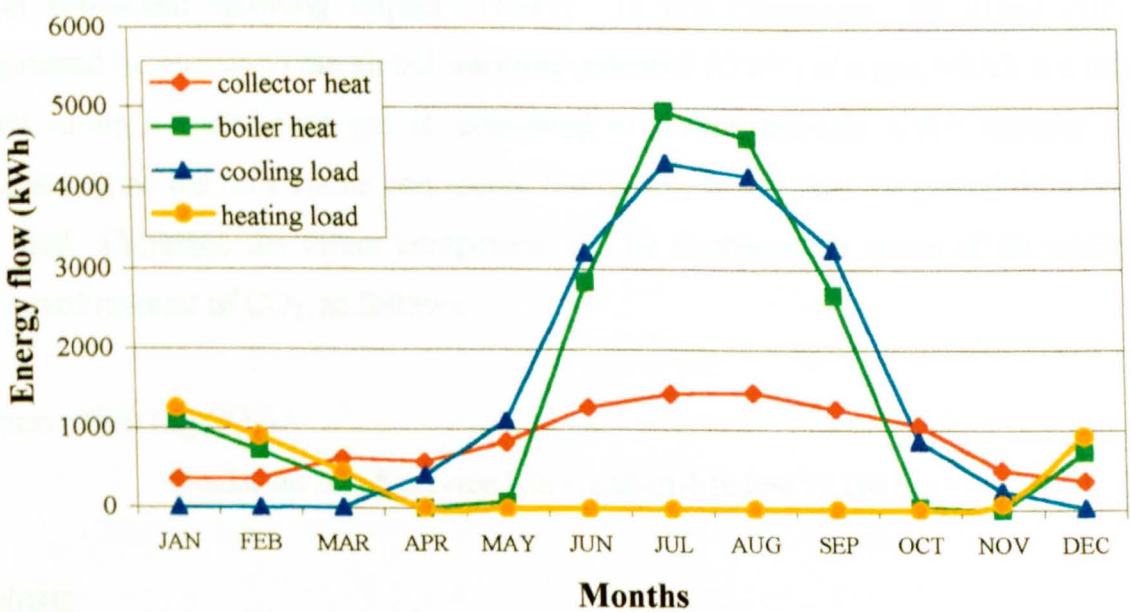

Figure 9.13. System energy flows.

The annual cooling load of 17,600 kWh is covered with a total supply of 15,220 kWh of boiler heat, supplemented by 8500 kWh of solar heat, offered by the solar system. The annual heating load of 3530 kWh is covered with a total supply of 2880 kWh of boiler heat and 1500 kWh of solar heat.

The total life cycle cost of the complete system described above, for a 20-year period, is C£ 13,380. The corresponding total life cycle cost of a system using an electric chiller (with a purchase price of C£ 1500) is only C£ 10,630. In order to have the same total life cycle cost, the price of the absorption unit together with its accessories must not be higher than C£ 2000. It should be noted however, that the costing of the 11 kW unit was based on the production of the prototype 1 kW unit. It is believed that a mass-produced unit will be cheaper.

9.5 GLOBAL WARMING IMPACT

The depletion of the stratospheric ozone layer leads to global warming and was identified as a major environmental problem during the last 20 years. Air conditioners, heat pumps and refrigerating machines are thought to be major contributors to the ozone depletion. Examination of the global warming impact of these machines requires consideration of both direct and indirect effects. The direct component relates to release of refrigerants that are greenhouse gases, and the indirect one to carbon dioxide production in powering the equipment. One expression of the combined effects is the total equivalent warming impact (TEWI). In this expression, the direct effect is expressed in relation to the global warming potential (GWP) of a gas, which is a ratio of how strong a greenhouse gas is, compared to carbon dioxide. GWP actually varies depending on the time frame considered but usually a 100 year integrated time horizon is used. Therefore the direct component can be expressed in terms of an equivalent released amount of CO_2, as follows:

direct effect (kg CO_2) =

(make-up rate * service life + end-of-life loss) * charge * GWP (9.4)

where:

charge = initial charge of refrigerant in the system (kg)

make-up rate = percent refrigerant charge lost per year (averaged over the entire equipment life)

service life = service life (yrs)

GWP = global warming potential of gas

The indirect effect is caused by the emission of CO_2 from power plants used to generate the electrical power needed to run the system and is:

$$\text{indirect effect (kg } CO_2) = \text{operation power} * \text{service life} * \text{emitted } CO_2 \qquad (9.5)$$

where:

operation power = the power required by the system per year (kWh/yr)

service life = service life (yrs)

emitted CO_2 = amount of CO_2 (kg) emitted from the power plan per kWh received by the system

In the case of this study where the annual cooling load is 17,600 kWh, it is of interest to compare the total equivalent warming impact of the absorption solar cooling system to a conventional vapour compression cooler.

For the case of the absorption solar cooling system, since no hydro fluorocarbon (HFC) refrigerants are used, only the indirect effect needs to be estimated by Equation 9.5. In this case, for a service life of 20 years, the amount of CO_2 emitted from the boiler is 75,000 kg. This figure is calculated considering the following:

1. Required boiler heat = 15,220 kWh.

2. Boiler efficiency (Table 6.6) = 85% resulting in 17,900 kWh to be supplied by fuel.

3. Calorific value of fuel = 42,900 kJ/kg, resulting in 1500 kg of fuel consumption.

4. Every kg of fuel produces about 2.5 kg of CO_2.

In the case that a conventional R-22 air conditioner is used with an 11 kW capacity, the direct effect for a service life of 20 years, as calculated from Equation 9.4, is 63,175 kg CO_2. This result is estimated with the following data:

1. Charge of R-22 = 3.5 kg (average figure from manufacturers catalogs).

2. Assumed make-up rate = 4% ; and an end-of-life loss = 15%.

3. GWP for R-22 for a 100 year period = 1900 (Cavallini *et al.*, 2001).

The indirect effect for covering the annual cooling load (Equation 9.5) for a 20-year period would be 105,000 kg of CO_2, assuming a world average value of CO_2 release for electric energy production of 0.6 kg/kWh (Cavallini *et al.*, 2001).

Therefore the TEWI when using a conventional R-22 air conditioner would be 63,175+105,000 = 168,175 kg of CO_2 or 2.7 times greater than when using the absorption solar cooling system.

9.6 CONCLUSIONS

The final optimum system as obtained from the complete system simulations, consists of 15 m^2 compound parabolic collector tilted at 30° from horizontal and 600 liters hot water storage tank. The typical insulated house considered, requires an annual cooling load at 25°C of 17,600 kWh with a peak load of 10.3 kW and an annual heating load at 21°C of 3,530 kWh with a peak load of 5.5 kW. This annual load can be met by using about 28,100 kWh of boiler heat. The present price of diesel, which is C£ 0.171 per lt indicates that it is economical to replace about 10,000 kWh with solar energy collected with 15 m^2 of CPC and the life cycle savings of such a system are C£ 187. It must also be stated that the total life cycle cost of a complete system comprising the collector and the absorption unit, for a 20-year period is C£ 13,380 with an estimated price for the absorption unit together with its accessories equal to C£ 4800. In order to have the same total life cycle cost the price of the absorption unit together with its accessories must not be higher than C£ 2000. This may be possible only when absorption units are mass-produced.

Referring to the global warming issue, conventional air conditioning machines contribute both by the release of HFC refrigerants and by the emission of carbon dioxide for their energy requirements, to the destruction of the ozone layer. The TEWI of a conventional R-22 air conditioner is about 168,000 kg of CO_2 or 2.7 times greater than that of the absorption solar cooling system. This factor is in favour of the absorption solar cooling system and should not be underestimated in the analysis and selection of appropriate equipment since the environmental impact has become a major aspect during the last years.

CHAPTER 10

CONCLUSIONS, RECOMMENDATIONS FOR FURTHER WORK AND PUBLICATIONS

10.1 CONCLUSIONS

The main objective of this work was to study through modelling, ways to minimise the thermal energy requirements of domestic dwellings in Cyprus and investigate the application of LiBr-water absorption units for domestic cooling. In particular, the evolution of buildings in Cyprus and the various construction methods applied today were examined. Measures like controlled or natural ventilation, overhangs, various types of glazing, orientation, shape of buildings, and thermal mass and insulation for reducing the thermal load of the modern house were evaluated. A 1 kW unit was designed and constructed and the heat transfer area of each heat exchanger was varied to provide the required output. The construction of the small unit facilitated the determination of the heat transfer coefficients in the heat exchangers and the sizing of the major components of a full-scale unit which was used to predict the performance of an overall solar assisted system.

Specific conclusions are presented at the end of each chapter. The major conclusions are summarised below:

1. The most important structural element in respect to thermal mass and control of indoor conditions of 'free running' domestic dwellings in the Cypriot environment is the roof. For maximum effectiveness, the roof must offer a discharge time of 6 hours or more and have a thermal conductivity of less than 0.48 W/m-K. If possible, the walls should also have a similar discharge time and thermal conductivity. A house constructed with the above structural element characteristics, will be able to maintain summertime temperatures between 27°C and 32°C with night ventilation rates of six air changes per hour.

2. Life cycle cost analysis has shown that measures which increase the roof insulation would pay back in a shorter period of time, between 3.5 to 5 years

compared to measures to increase wall insulation which would pay back over a longer period of time of about 10 years.

3. Window gains are an important factor with respect to overall solar gains and significant savings can result when low conductance and low transmittance window glazing is used. For the model house investigated, energy savings of up to 24% could be achieved if low-emissivity double glazed windows are used compared to clear double glazed windows. Life cycle cost analysis has shown the low-emissivity double-glazed windows to have a short pay back period of 3 to 4 years, irrespective of the fact that solar gains through glazing will also be reduced in the winter months which will result in a slight increase in the energy demand for heating.

4. External shading of windows is important in reducing solar gains. Overhangs over windows with extension of 1.5 m can provide energy savings of the order of between 7% and 19% depending on the level of insulation provided by the structural elements. The better insulated the house the higher will be the energy savings arising from the reduction of the direct solar radiation entering the house.

5. For `free running' domestic dwellings, night time ventilation in the summer months can provide reductions in the peak indoor temperature of around 2°C for one air change per hour, 3°C for two air changes per hour and 7°C for eleven air changes per hour. For a well insulated air conditioned dwelling controlled to maintain the indoor temperature at 25°C, a ventilation rate of 9 air changes per hour during the night will lead to a 7.7% reduction in the cooling energy demand. The effect of night time ventilation will depend on the construction type, with greater savings for the better-insulated house.

6. Due to the high summertime temperatures, the above passive measures such as high thermal mass, natural ventilation and reduction of solar gains through low emissivity glazing, are not sufficient to reduce the indoor temperature of `free running buildings' to acceptable levels to provide thermal comfort without the use of active cooling systems.

7. An active cooling system which can utilise solar energy as the heat input source, that is abundantly available in Cyprus, is the LiBr-water absorption system. The design, construction and testing of a 1 kW LiBr-water absorption refrigerator enabled the determination of the heat transfer coefficients in the heat exchangers, which in turn facilitated the sizing of components for a full scale system of 11 kW cooling output. Integrated system simulations have shown that an 11 kW unit will be sufficient in maintaining indoor temperatures to or below 25°C at peak load conditions. The cost of such a system, including all necessary secondary devices and installation, has been estimated to be C£ 4800.

8. A typical domestic dwelling in Cyprus will require approximately 28,100 kWh of heat input to maintain comfortable conditions in winter. This heat is normally provided by oil fired boilers. If an integrated solar absorption cooling system is employed, the solar collectors will be able to replace directly approximately one third of this energy, saving on the heating cost of the house. The total life cycle cost of a complete system, comprising the collector and the absorption unit, for a lifetime of 20-years will be of the order of C£13,380. For this system to be able to provide the same life-cycle cost as a conventional vapour compression cooling system its price should reduce to below C£2000. This may become possible in the future with the more widespread application and mass production of low capacity absorption units.

9. TEWI calculations have shown that over a system lifetime of 20 years, a vapour compression air conditioner using R22 as a refrigerant will lead to CO_2 emissions of the order of 168,000 kg. The emissions from a solar driven absorption cooling system will be 2.7 times lower than that of the vapour compression system, providing considerable reductions in the environmental impact of active cooling systems. Concerns over the environmental impact of active heating and cooling systems may accelerate the introduction of legislation with respect to the use of HFCs and this will give added impetus to the further development and mass production of low capacity solar driven absorption cooling systems.

10.2 RECOMMENDATIONS FOR FURTHER WORK

Although the transfer function method employed by the TRNSYS simulation environment has been extensively validated by other investigators, the results presented in the thesis concerning the thermal load analysis, need to be experimentally verified against the environmental conditions encountered in Cyprus. This can be achieved by carrying out measurements in an actual domestic dwelling or a test house.

There is also a need to generalise the results in terms of different house design styles, volume and surface areas and present them in a form that can be easily interpreted by architects and building designers. This will enable them to make informed decisions on the impact that alterations in the design will have on the overall energy consumption without the need to model the house in detail.

With respect to the construction and operation of the lithium-bromide absorption refrigerator, only basic operations were tested. The design and construction of the heat exchangers of the unit can be improved considerably not only in effectiveness but also in cost. This of course demands experimentation with various construction methods and additives, which can improve performance.

To fully evaluate the performance and cost effectiveness of such a system, a full-scale prototype should be constructed and tested over a period of time.

10.3 PUBLICATIONS

A number of papers related to this study have been published. A list of these is shown in Appendix 7. Reprints of papers published in peer review journals are presented in Appendix 8 and 9.

REFERENCES

Abdullagatov I.M. and Magomedov U.B. (1997). Measurements of Thermal Conductivity of Aqueous LiCl and LiBr Solutions, *Physics and Chemistry*, Vol. 101, No. 4, pp. 708-711.

Abdul-Muhsen, Al-Hammad and Said S. A. M. (1992). Load and Energy Requirements in Residential Buildings in Saudi Arabia: A Comparative Study, *International Journal of Energy Research*, Vol. 16, pp. 533-543.

Ameel T. A., Gee K. G. and Wood B. D. (1995). Performance Predictions of Alternative, Low Cost Absorbents For Open-Cycle Absorption Solar Cooling, *Solar Energy*, Vol. 54, No. 2, pp. 65-73.

Andberg J. W. and Vliet G. C. (1983). Design Guidelines for Water-Lithium Bromide Absorbers, *ASHRAE Transantions*, Vol. 89, Part 1B, pp 220-232.

Anderson B. (1977). Solar Energy: Fundamentals in building design, McGrawhill Book Co.

ASHRAE (1989). Handbook of fundamentals.

ASHRAE (1992). Cooling and Heating Load Calculation Manual.

ASHRAE (1997). Handbook of fundamentals.

ASHRAE (1995). HVAC Applications Handbook.

Balaras C. (1997). In: *Passive Cooling of Buildings*, Santamouris M. and Asimakopoulos D., Editors, ISBN 1 873936 47 8.

Cavallini A., Censi G., Del Col D., Doretti L., Rossetto L., Longo G. (2001). Reduction of Global Warming Impact in the HP/AC Industry by Employing New HFC Refrigerants. *Proceedings of CLIMA 2000 Conference on CD-ROM,* 7th Rehva World Congress, Naples, Italy, 2001.

Conlisk A. T. (1992). Falling Film Absorption on a Cylindrical Tube, *AICHE Journal,* Vol.38, No. 11, pp. 1716-1728.

Centre of Applied Research of Cyprus College (1994). *Research for the collection of data in relation to the fuel expenditure for various groups of consumers (in Greek).* A research for the Ministry of Commerce, Industry and Tourism.

Dascalaki E. and Santamouris M. (1997). In: *Natural ventilation, Passive Cooling of Buildings,* Santamouris M. and Asimakopoulos D., Editors, ISBN 1 873936 47 8, pp. 220-306.

De Gids W. and Phaff H. (1995). In: *Ventilation of Buildings,* Awbi H., E & FN Spon, London, ISBN 0 442 31257 1, pp. 89-90.

Dimoudi A. (1997). In *'Urban Design'. Passive Cooling of Building,* Santamouris M. and Asimakopoulos D., Editors, ISBN 1 873936 47 8, pp. 95-128.

Duffie J.A. and Beckman W.A. (1991). *Solar Engineering of Thermal Processes,* Second Edition, John Wiley & Sons, New York.

Erhard A. and Hahne E. (1997). Test and Simulation of a Solar-Powered Absorption Cooling Machine, *Solar Energy,* Vol. 59, Nos. 4-6, pp. 155-162.

Ghaddar N. and Bsat A. (1998). Energy Conservation of Residential Buildings in Beirut, *International Journal of Energy Research,* Vol. 22, pp. 523-546.

Ghaddar, N.K., Shihab M. and Bdeir F. (1997). Modelling and Simulation of Solar Absorption System Performance in Beirut, *Renewable Energy,* Vol. 10, No. 4, pp. 539-558.

Grossman G. (1983). Simultaneous Heat and Mass Transfer in Film Absorption Under Laminar Flow, *International Journal of Heat and Mass Transfer*, Vol. 26, No. 3, pp. 357-371.

Incropera and DeWitt (1999). *Fundamentals of Heat and Mass Transfer*, Jonh Wiley & Sons, New York, ISBN 0-471-30460-3.

Haim I., Grossman G. and Shavit A. (1992). Simulation and Analysis of Open Cycle Absorption Systems for Solar Cooling, *Solar Energy*, Vol. 49, No. 6, pp. 515-534.

Hammad M. A. and Audi M. S. (1992). Performance of a Solar LiBr-Water Absorption Refrigeration System, *Renewable Energy*, Vol. 2, No. 3, pp. 275-282.

Hammad M. and Zurigat Y. (1998). Performance of a Second Generation Solar Cooling Unit, *Solar Energy*, Vol. 62, No. 2, pp. 79-84.

Hawlader M. N. A., Noval K. S. and wood B. D. (1993). Unglazed Collector / Regenerator Performance for a Solar Assisted Open Cycle Absorption Cooling System, *Solar Energy*, Vol. 50, No. 1, pp. 59-73.

Herold K. E. and Klein S. A. (1996). *Absorption Chillers and Heat Pumps*, CRC Press, Inc. USA, ISBN 0-8493-9427-9.

Howell R. H., Sauer J. H. and Coad J. W. (1998). *Principles of HVAC*, ASHRAE, Refrigeration Equipment, Section 18.21.

Kalogirou S. (1991). *Solar Energy Utilisation Using Parabolic Trough Collectors*, Masters Thesis, The Polytechnic of Wales, UK.

Kalogirou S. (1996). Economic Analysis of Solar Energy Systems Using Spreadsheets, *Proceedings of the Forth World Renewable Energy Congress*, Denver, Colorado, USA, Vol. 2, pp. 1303-1307.

Kalogirou S. (1997). Solar Water Heating in Cyprus. Current Status of Technology and Problems, *Renewable Energy Journal*, Vol. 10, No. 1, pp. 107-112.

Keith E. H., Radermacher R. and Klein S. A. (1996). *Absorption Chillers and Heat Pumps*, CRS Press, ISBN 0-8493-9427-9.

Klein *et al.*, (1998). *TRNSYS manual*, University of Wisconsin.

Kreider J. F. and Rabl A. (1994). *Heating and cooling of buildings- Design for efficiency*. McGraw-Hill, Book Co. Singapore, ISBN 0-07-113438-7.

Kreith F. and Bohn M. S. (1997). *Principles of Heat Transfer (Fifth Edition)*, PWS Publishing Company, ISBN 0-534-95420-0.

Lechner, N. (1991). *Heating, Cooling, Lighting*, John Wiley & Sons, New York, ISBN 0471241431.

Lee R. J., DiGuilio R. M., Jeter S. M., and Teja A. S. (1990). Properties of Lithium Bromide–Water Solutions at High Temperatures and Concentration. II. Density and Viscocity. *ASHRAE Trans.*, Vol. 96, Pt. 1, pp 709-728.

Martin P. L. and Oughton D. R. (1995). *Faber and Kell's, Heating and Air Conditioning of Buildings*, Eight Edition, Butterworth-Heinemann Ltd.

Morioka I., Kiyota M. and Nakao R. (1993).Absorption of Water Vapor into a Film of Aqueous Solution of LiBr Falling Along a Vertical Pipe. *JSME International Journal*, Series B, Vol. 36, No.2, pp. 351-356.

Ozisik M. (1985). *Heat Transfer-A Basic Approach*, McGraw-Hill Book Company, ISBN 0-07-Y66460-9.

Perry R. H. and Green D. (1984). *Perry's Chemical Engineers' Handbook*, (Six Edition), McGraw-Hill Book Company, ISBN 0-07-049479-7.

Patnaik V., Perez-Blanco H., and Ryan W. A. (1993). A Simple Analytical Model for the Design of Vertical Tube Absorbers. *ASHRAE Transactions: Research*, pp.69-80.

Petrakis M, Kambezides H. D., Lykoudis S., Adamopoullos A. D., Kassomenos P., Michaelides I. M., Kalogirou S.A., Roditis G., Chrysis I. and Hadjigianni A. (1998). Generation of a Typical Meteorological Year for Nicosia Cyprus. *Renewable Energy*, Vol. 13, No. 3, pp. 381-388.

Research on Family Budgets 1996/97 (1999). Department of Statistics and Research, Ministry of Finance, Government of Cyprus, ISBN 9963-34-397-X.

Rogers G. F. C. and Mayhew Y. R. (1992). *Thermodynamic and Transport Properties of Fluids: SI Units*, Fourth Edition, Blackwell Publishers UK, ISBN 0-631-90265-1.

Santamouris M., Argiriou A., Daskalaki E., Balaras C., and Gaglia A. (1994). Energy Characteristics and Savings Potential in Office Buildings, *Solar Energy*, Vol. 52, No. 1, pp. 56-59.

Sherman M. (1999). Indoor Air Quality for Residential Buildings, *ASHRAE Journal*, May 1999, pp. 26-30.

Statistical Abstracts (1998). Government of Cyprus, Department of Statistics and Research, *General Statistics Series I*, Report No. 44.

Swartman R.K. (1979). In *Solar Energy Application in Buildings*, A. M. Sayigh, Academic Press Inc.

Sweitzer G., Arasteh D. and Selkowitz S. (1987). In *Heating and Cooling of Buildings-Design for Efficiency*, Kreider J. F. and Rabl A. (1994). McGraw-Hill, Book Co. Singapore, ISBN 0-07-113438-7.

Varma H. K., Mehrotra R. K. and Agrawal K. N. (1994). Heat Transfer During Pool Boiling of LiBr-Water Solutions at Subatmospheric Pressures, *International Communications in Heat and Mass Transfer*, Vol. 21, No. 4, pp. 539-548.

Winwood R., Benstead R. and Edwards R. (1997). Advanced Fabric Energy Storage, *Building Services Engineering Research and Technology*, Vol.18, No.1.

APPENDIX 1

ASHRAE Code Numbers and Thermal Properties of Layers Used in Wall and Roof Descriptions.

Code Number	Description	Thickness and Thermal Properties					
		L	k	ρ	c_p	R	Mass
A0	Outside surface resistance	0	0.000	0	0.00	0.059	0.00
A1	25 mm Stucco	25	0.692	1858	0.84	0.037	47.34
A2	100 mm Face brick	100	1.333	2002	0.92	0.076	203.50
A3	Steel siding	2	44.998	7689	0.42	0.000	11.71
A4	12 mm Slag	13	0.190	1121	1.67	0.067	10.74
A5	Outside surface resistance	0	0.000	0	0.00	0.059	0.00
A6	Finish	13	0.415	1249	1.09	0.031	16.10
A7	100 mm Face brick	100	1.333	2002	0.92	0.076	203.50
B1	Air space resistance	0	0.000	0	0.00	0.160	0.00
B2	25 mm Insulation	25	0.043	32	0.84	0.587	0.98
B3	50 mm Insulation	51	0.043	32	0.84	1.173	1.46
B4	75 mm Insulation	76	0.043	32	0.84	0.207	2.44
B5	25 mm Insulation	25	0.043	91	0.84	0.587	2.44
B6	50 mm Insulation	51	0.043	91	0.84	1.173	4.88
B7	25 mm Wood	25	0.121	593	2.51	1.760	15.13
B8	65 mm Wood	63	0.121	593	2.51	0.524	37.58
B9	100 mm Wood	100	0.121	593	2.51	0.837	60.02
B10	50 mm Wood	51	0.121	593	2.51	0.420	30.26
B11	75 mm Wood	76	0.121	593	2.51	0.628	45.38
B12	75 mm Insulation	76	0.043	91	0.84	1.760	6.83
B13	100 mm Insulation	100	0.043	91	0.84	2.347	9.27
B14	125 mm Insulation	125	0.043	91	0.84	2.933	11.71
B15	150 mm Insulation	150	0.043	91	0.84	3.520	14.15
B16	4 mm Insulation	4	0.043	91	0.84	0.088	0.49
B17	8 mm Insulation	8	0.043	91	0.84	0.176	0.49
B18	12 mm Insulation	12	0.043	91	0.84	0.264	0.98
B19	15 mm Insulation	15	0.043	91	0.84	0.352	1.46
B20	20 mm Insulation	20	0.043	91	0.84	0.440	1.95
B21	35 mm Insulation	35	0.043	91	0.84	0.792	2.93
B22	42 mm Insulation	42	0.043	91	0.84	0.968	3.90
B23	60 mm Insulation	62	0.043	91	0.84	1.408	5.86
B24	70 mm Insulation	70	0.043	91	0.84	1.584	6.34
B25	85 mm Insulation	85	0.043	91	0.84	1.936	7.81
B26	92 mm Insulation	92	0.043	91	0.84	2.112	8.30
B27	115 mm Insulation	115	0.043	91	0.84	2.640	10.74
C1	100 mm Clay tile	100	0.571	1121	0.84	0.178	113.70
C2	100 mm low density concrete block	100	0.381	609	0.84	0.266	61.98
C3	100 mm high density concrete block	100	0.813	977	0.84	0.125	99.06
C4	100 mm Common brick	100	0.727	1922	0.84	0.140	195.20
C5	100 mm high density concrete	100	1.731	2243	0.84	0.059	227.90
C6	200 mm Clay tile	200	0.571	1121	0.84	0.352	227.90
C7	200 mm low density concrete block	200	0.571	609	0.84	0.352	123.46
C8	200 mm high density concrete block	200	1.038	977	0.84	0.196	198.62
C9	200 mm Common brick	200	0.727	1922	0.84	0.279	390.40
C10	200 mm high density concrete	200	1.731	2243	0.84	0.117	455.79
C11	300 mm high density concrete	300	1.731	2243	0.84	0.176	683.20
C12	50 mm high density concrete	50	1.731	2243	0.84	0.029	113.70
C13	150 mm high density concrete	150	1.731	2243	0.84	0.088	341.60
C14	100 mm low density concrete	100	0.173	641	0.84	0.587	64.90
C15	150 mm low density concrete	150	0.173	641	0.84	0.880	97.60
C16	200 mm low density concrete	200	0.173	641	0.84	1.173	130.30
C17	200 mm low density concrete block (filled)	200	0.138	288	0.84	1.467	58.56
C18	200 mm high density concrete block (filled)	200	0.588	849	0.84	0.345	172.75
C19	300 mm low density concrete block (filled)	300	0.138	304	0.84	2.200	92.72
C20	300 mm high density concrete block (filled)	300	0.675	897	0.84	0.451	273.28
E0	Inside surface resistance	0	0.000	0	0.00	0.121	0.00
E1	20 mm Plaster or gypsum	20	0.727	1602	0.84	0.026	30.74
E2	12 mm Slag or stone	12	1.436	881	1.67	0.009	11.22
E3	10 mm Felt and membrane	10	0.190	1121	1.67	0.050	10.74
E4	Ceiling air space	0	0.000	0	0.00	0.176	0.00
E5	Acoustic tile	19	0.061	481	0.84	0.314	9.27

L = thickness, mm
k = thermal conductivity, W/(m·K)
ρ = density, kg/m^3
c_p = specific heat, kJ/(kg·K)
R = thermal resistance, (m^2·K)/W
Mass = mass per unit area, kg/m^2

APPENDIX 2

Equilibrium Chart for Aqueous Lithium Bromide Solutions (ASHRAE 1997)

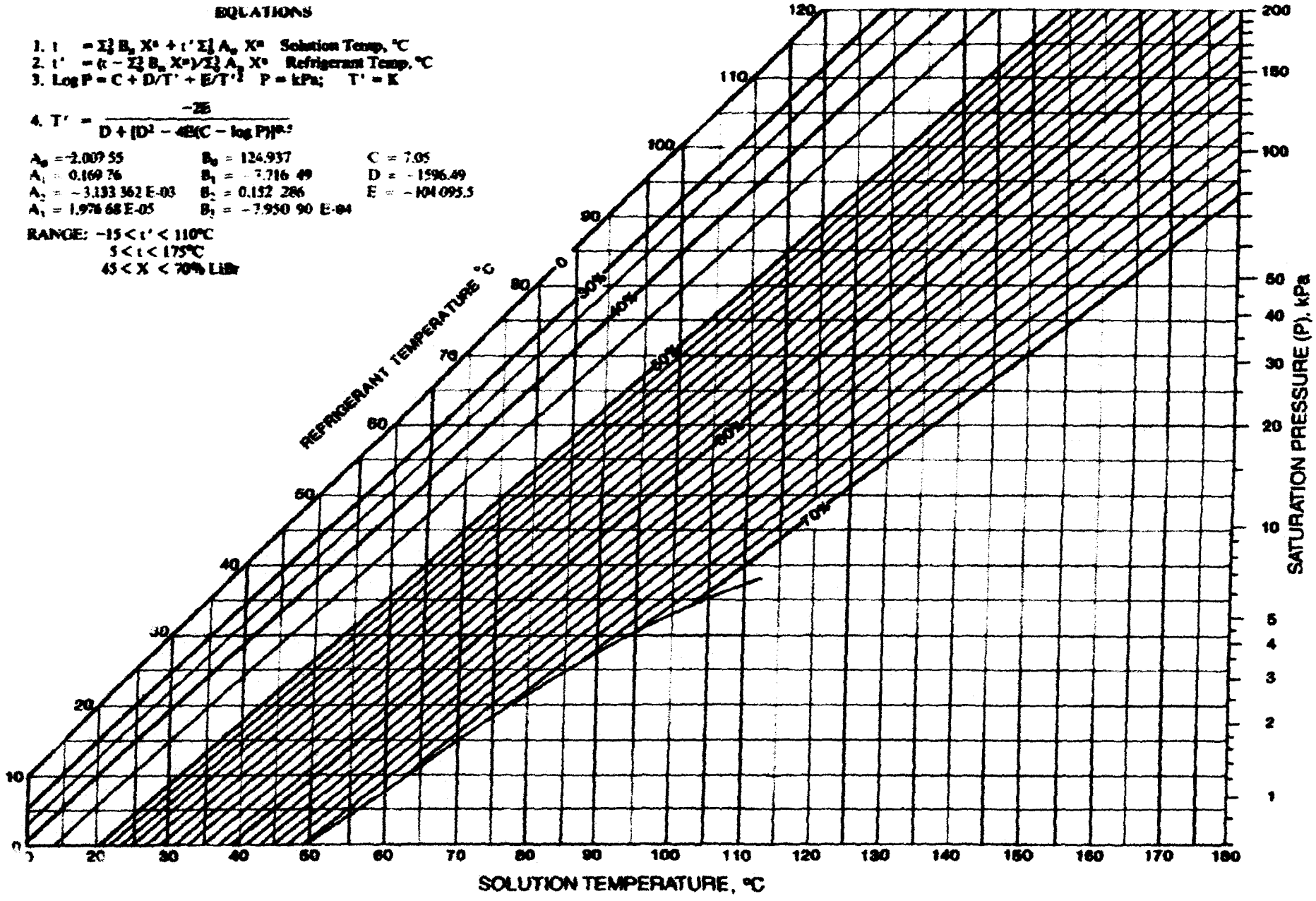

APPENDIX 3

Enthalpy-Concentration Diagram for Water-Lithium Bromide Solutions (ASHRAE 1997)

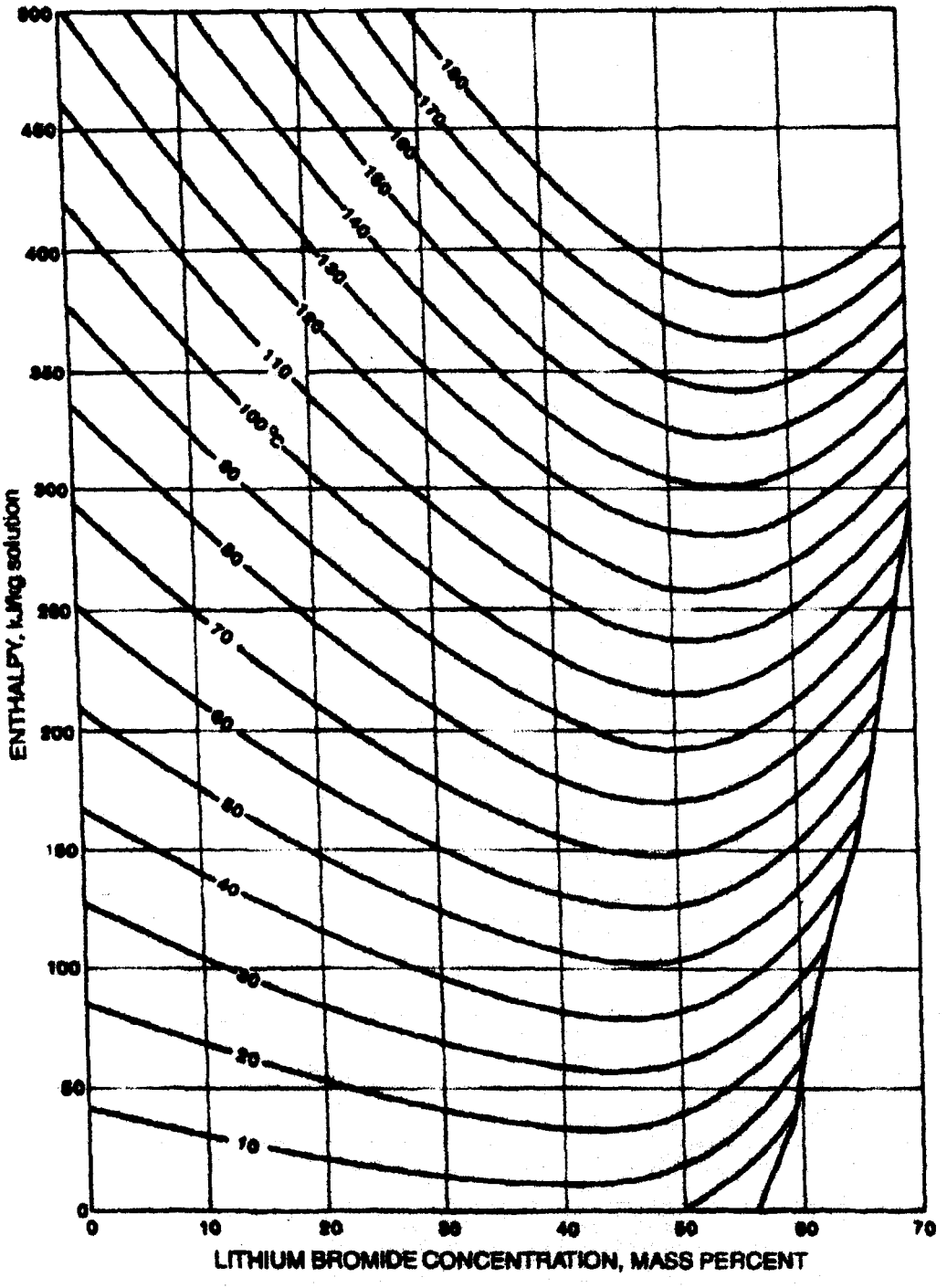

EQUATIONS CONCENTRATION RANGE 40 < X < 70% LiBr TEMPERATURE RANGE 15 < t < 165°C

$h = \sum_0^4 A_n X^n + t \sum_0^4 B_n X^n + t^2 \sum_0^4 C_n X^n$ in kJ/kg, where t = °C and X = %LiBr

$A_0 = -2024.33$	$B_0 = 18.2829$	$C_0 = -3.7008214$ E-2
$A_1 = 163.309$	$B_1 = -1.1691757$	$C_1 = 2.8877666$ E-3
$A_2 = -4.88161$	$B_2 = 3.248041$ E-2	$C_2 = -8.1313015$ E-5
$A_3 = 6.302948$ E-2	$B_3 = -4.034184$ E-4	$C_3 = 9.9116628$ E-7
$A_4 = -2.913705$ E-4	$B_4 = 1.8520569$ E-6	$C_4 = -4.4441207$ E-9

APPENDIX 4

PROGRAM 'LITH'

This Appendix gives the nomenclature and the listing of program LITH developed for modelling the LiBr-water absorption refrigeration cycle and estimating the heat exchanger sizes.

A 4.1 Nomenclature

SYMBOL	MEANING
ACOND	Condenser heat exchanger area (m^2)
ASHE	Area for solution heat exchanger (m^2)
CAP	Evaporator Capacity (kW)
COP	Coefficient of performance
COVER	Liquid Carryover from evaporator %
CPEW	Specific heat of water (J/kg-K)
CPWATER	Specific heat of water (J/kg-K)
DCIN	Condenser heat exchanger inside pipe diameter (m)
DCOUT	Condenser heat exchanger outside pipe diameter (m)
DEIN	Evaporator heat exchanger inside pipe diameter (m)
DEOUT	Evaporator heat exchanger outside pipe diameter (m)
DH	Hydraulic diameter of annulus (m)
DIN45	Solution heat exchanger inside pipe diameter (m)
DTCOND	Logarithmic mean temperature difference (LMTD), (K)
DTSHE	Logarithmic mean temperature difference (K) for solution heat exchanger
H# e.g. H4	Water vapour enthalpy at point n (kJ/kg) - refer to Figure 7.4 for point #
HFG	Latent heat of condensation (kJ/kg)
HIN45	Heat transfer coefficient for inside flow (W/m^2-K)
HINCOND	Heat transfer coefficient for inside flow (W/m^2-K)
HINE	Heat transfer coefficient for inside flow (W/m^2-K)
HOUTCOND	Heat transfer coefficient for outside flow (W/m^2-K)
KEW	Thermal conductivity of water (W/m-K)
KWATER	Thermal conductivity of water or liquid (W/m-K)
M# e.g. M4	Mass flow rate at point n (kg/s) - refer to Figure 7.4 for point #

SYMBOL	MEANING
MCONDW	Condenser water mass flow rate (kg/s)
MEW	Evaporator water mass flow rate (kg/s)
MIEW	Evaporator water absolute viscosity (N-s/m^2)
MIWATER	Water absolute viscosity (N-s/m^2)
NCPIPE	Number of condenser pipes
NEPIPE	Number of Evaporator pipes
P# e.g. P4	Pressure at point n (kPa) - refer to Figure 7.4 for point #
PG	Vapour density (kg/m^3)
PIPECOND	Number of condenser pipes - 1m length and 9.5mm diameter
POWATER	Water or liquid density kg/m^3
PRCONDW	Condenser pipe water Prandtl number
PREW	Evaporator pipe water Prandtl number
PRSOL45	LiBr solution Reynolds number
QABS	Absorber heat load (kW)
QCON	Condenser heat load (kW)
QGEN	Generator input load (kW)
RECPIPE	Condenser pipe water Reynolds number
REDH	Reynolds number based on the hydraulic diameter
REEPIPE	Evaporator pipe water Reynolds number
RESOL45	LiBr solution Prandtl number
SPECH	Specific heat of LiBr solution (J/kg-K)
T# e.g. T4	Temperature at point n (°C) - refer to Figure 7.4 for point #
TCWIN	Condenser inlet water temperature (°C)
TCWOUT	Condenser outlet water temperature (°C)
UCOND	Overall heat transfer coefficient (W/m^2-K)
VISC	Absolute viscosity (N-s/m^2)
W	Pump-work (kW)
X# e.g. X4	Solution Mass Fraction (%LiBr) at point n e.g. 55 - refer to Figure 7.4 for point #
Notation for Absorber Equations	Same as notation used in literature Chapter 7.

A 4.2 Listing of the program 'LITH'

```
50 CLS
60 CAP = 1: REM INPUT "Evaporator Capacity (kW)="; CAP
70 T10 = 6: REM INPUT "Evaporator temperature (T10°C)="; T10
80 T4 = 75: REM INPUT "Generator Solution Exit temperature (T4°C)="; T4
90 X1 = 55: REM INPUT "Week Solution Mass Fraction (%LiBr)="; X1
100 X4 = 60: REM INPUT "Strong Solution Mass Fraction (%LiBr)="; X4
101 X6 = X4
102 X5 = X4
110 T3 = 55: REM INPUT "Solution Heat Exchanger Exit temperature (T3°C)="; T3
115 T7 = 70: REM INPUT "Generator Vapour Exit temperature (T7°C)="; T7
120 COVER = .025: REM INPUT "Liquid Carryover from evaporator %=";COVER
121 C = 7.05
122 D = -1596.49
123 E = -104095.5

129 REM FIND SATURATION PRESSURE AT POINT 10
130 P10 = .000000000002# * T10 ^ 6 - .000000003# * T10 ^ 5 + .0000002 * T10 ^ 4 + .00003 * T10 ^ 3
+ .0014 * T10 ^ 2 + .0444 * T10 + .6108
150 PRINT "Saturation pressure (kPa)="; P10

160 REM FIND SATURATED WATER VAPOUR ENTHALPY AT POINT 10
162 H10 = -.00125397# * T10 ^ 2 + 1.88060937# * T10 + 2500.559
165 PRINT "WATER VAPOUR ENTHALPY (kJ/kg) AT POINT 10="; H10

170 REM ENTHALPY AT POINT 11- SATURATED WATER LIQUID
171 X = 0
172 CT = T10: GOSUB 1600
175 H11 = CH: PRINT "H11="; H11

180 TSOL = T4
185 X = X4
190 FLAG1 = 1: GOSUB 1800
195 P4 = SATPRES
196 T8 = TREFR: PRINT "T8="; T8
200 PRINT "Saturation pressure at point 4 (kPa)="; P4

209 X = X4
210 T = T4: GOSUB 1900
220 H4 = ENTH: PRINT "H4="; H4

230 X = 0
235 CT = T8
240 GOSUB 1600
250 H8 = CH: PRINT "H8="; H8
251 H9 = H8: PRINT "H9="; H9
255 M10 = CAP / (H10 + COVER8H11 - (1 + COVER) * H9): PRINT "M10="; M10
257 M11 = COVER * M10: PRINT "M11="; M11
260 M9 = M10 + COVER * M10: PRINT "M9="; M9
265 M6 = (M10 + M11) / (X6 / X1 - 1): PRINT "M6="; M6
267 M1 = X6 * M6 / X1: PRINT "M1="; M1
270 T1REF = ((-2 * E) / (D + (D ^ 2 - 4 * E * (C - LOG(P10)/2.302)) ^ .5)) - 273


275 X = X1
276 FLAG1 = 0
277 TREFR = T1REF: GOSUB 1800
278 T1 = TSOL: PRINT "T1="; T1
280 T = T1: GOSUB 1900
282 H1 = ENTH: PRINT "H1="; H1
```

```
285 M3 = M1: M2 = M1
287 M4 = M6: M5 = M6
290 X = X1: T = T3
292 GOSUB 1900
293 H3 = ENTH: PRINT "H3="; H3


295 X = X1: T = T1
300 GOSUB 2000
302 DH = VOL * (P4 - P10):
305 W = DH * M1: PRINT "PUMP-WORK="; W
307 H2 = H1 + DH: PRINT "H2="; H2
310 H5 = (M2 * H2 + M4 * H4 - M3 * H3) / M5: PRINT "H5="; H5
312 H6 = H5: PRINT "H6="; H6
320 REM  FIND T5 FROM H5 AND X5
321 X = X5: H = H5
322 FLAG3 = 1: GOSUB 1900
325 PRINT "T5="; T5

326 X = X5: FLAG4 = 1
327 FLAG1 = 0: GOSUB 1800
328 PRINT "T6="; T6

330 QABS = M10 * H10 + M11 * H11 + M6 * H6 - M1 * H1: PRINT "QABS="; QABS

334  REM  FIND ENTHALPY AT POINT 7
336 GOSUB 2020
338 H7 = HSH: PRINT "H7="; H7
339 M7 = M9
340 QGEN = M4 * H4 + M7 * H7 - M3 * H3: PRINT "QGEN="; QGEN
341 QCON = M7 * (H7 - H8): PRINT "QCON="; QCON
342 COP = CAP / QGEN: PRINT "COP="; COP
344 M8 = M7: T2 = T1
345 T9 = T10: T11 = T10
347 PRINT "PRESS ANY KEY FOR COLLECTIVE RESULTS": INPUT W$
348 CLS
349 PRINT "*************************************************************************"
350 PRINT "POINT        h(kJ/kg)      m (kg/s)              T(°C)"
351 PRINT "*************************************************************************"
352 PRINT "   1", H1, M1, T1
353 PRINT "   2", H2, M2, T2
354 PRINT "   3", H3, M3, T3
355 PRINT "   4", H4, M4, T4
356 PRINT "   5", H5, M5, T5
357 PRINT "   6", H6, M6, T6
358 PRINT "   7", H7, M7, T7
359 PRINT "   8", H8, M8, T8
360 PRINT "   9", H9, M9, T9
361 PRINT "   10", H10, M10, T10
362 PRINT "   11", H11, M11, T11
365 PRINT "Evaporator Capacity (kW)="; CAP
366 PRINT "Absorber heat(kW)="; QABS
367 PRINT "Generator input heat (kW)="; QGEN
368 PRINT "Condenser heat (kW)="; QCON
369 PRINT "Coefficient of performance="; COP
370 PRINT "LOW PRESSURE="; P10, "HIGH PRESSURE="; P4
371 PRINT "PRESS ANY KEY TO CONTINUE": INPUT W$
372 CLS
```

```
380 REM ********** CALCULATIONS FOR HEAT EXCHANGERS**********

381 REM******CONDENSER-HORIZONTAL PIPES**********

383 REM** WATER FLOW INSIDE PIPES **
385 TCWIN = 27: REM INPUT "CONDENSER INLET WATER TEMP. °C="; TCWIN
386 TCWOUT = 28.5: REM INPUT "CONDENSER OUTLET WATER TEMP. °C="; TCWOUT
388 TCWMEAN = (TCWIN + TCWOUT) / 2
390 TMX = TCWMEAN
392 GOSUB 2050
394 CPCONDW = CPWATER
395 MICW# = MIWATER#
396 KCONDW = KWATER
402 MCONDW = QCON * 1000 / (CPCONDW * (TCWOUT - TCWIN)): PRINT "CONDENSER
WATER MASS FLOW RATE (kg/s)="; MCONDW
404 NCPIPE = 1: REM INPUT"No. CONDENSER PIPES=";NCPIPE
405 MCPIPE = MCONDW / NCPIPE
406 DCIN = .0081: REM  INPUT "CONDENSER HEAT EXCHANGER INSIDE DIA. (m)="; DCIN
407 DCOUT = .0095: REM  INPUT "CONDENSER HEAT EXCHANGER OUTSIDE DIA. (m)=";
DCOUT
408 RECPIPE = (4 * MCPIPE) / (3.141593 * DCIN * MICW#): PRINT "CONDENSER PIPE WATER
RE="; RECPIPE

409 PRCONDW = CPCONDW * MICW# / KCONDW: PRINT "PRCONDW="; PRCONDW
410 IF RECPIPE < 2100 THEN HINCOND = 3.66 * KCONDW / DCIN: GOTO 418
411 LRE = LOG(RECPIPE) / LOG(10): PRINT "RECPIPE,LRE"; RECPIPE, LRE
412 FFACTOR = (1.82 * LRE - 1.64) ^ -2
413 K1 = 1 + 3.4 * FFACTOR
414 K2 = 11.7 + 1.8 / (RECPIPE ^ .3333)
417 HINCOND = (((FFACTOR / 8) * PRCONDW * RECPIPE) / (K1 + K2 * ((FFACTOR / 8) ^ .5) *
((PRCONDW ^ .66666) - 1))) * KCONDW / DCIN
418 PRINT "HINCOND="; HINCOND
419 INPUT "PRESS ANY KEY TO CONTINUE"; A$

420 REM ******* CONDENSATE FILM PROPERTIES*******

422 TMFILM = (T8 + TCWMEAN) / 2
424 TH = TMFILM: GOSUB 2160
426 PVCOND = PG: HFGCOND = HFG
428 TMX = TMFILM: GOSUB 2050
430 PLCOND = POWATER: MLCOND# = MIWATER#
432 KLCOND = KWATER
435 HOUTCOND = .725 * ((9.81 * PLCOND * (PLCOND - PVCOND) * HFGCOND * 1000 *
KLCOND ^ 3) / (MLCOND# * (T8 - TCWMEAN) * DCOUT)) ^ .25
437 PRINT "HOUTCOND="; HOUTCOND
438 TCOP = TMFILM: GOSUB 2076
440 HI = HINCOND: HO = HOUTCOND
442 GOSUB 2150
444 UCOND = U: PRINT "UCOND="; UCOND
446 CDT0 = T8 - TCWIN: CDTL = T8 - TCWOUT
448 DTCOND = (CDT0 - CDTL) / LOG(CDT0 / CDTL)
449 PRINT "T8="; T8, "TCWIN="; TCWIN, "TCWOUT="; TCWOUT, "DTCOND="; DTCOND
450 ACOND = QCON * 1000 / (UCOND * DTCOND): PRINT "AREACOND="; ACOND
455 PIPECOND = ACOND / (3.141593 * DCOUT)
457 PRINT "NO. OF CONDENSER PIPES - 1m LENGTH AND 9.5mm DIAM="; PIPECOND
460 INPUT "PRESS ANY KEY TO CONTINUE"; A$
462 CLS

600 PRINT "**** SOLUTION HEAT EXCHANGER***"

601 REM COOLED SOLUTION INLET TEMP. = T4
602 REM COOLED SOLUTION OUTLET TEMP. = T5
603 REM COOLED SOLUTION MASS FLOW RATE = M4
```

```
604 REM HEATED SOLUTION INLET TEMP. = T2 &  HEATED SOLUTION MASS FLOW RATE =
M2
605 REM HEATED SOLUTION OUTLET TEMP. = T3
606 X2 = X1: REM COOLED SOLUTION %LiBr = X4**&** HEATED SOLUTION %LiBr = X2=X1

607 PRINT "***INNER PIPE FLOW-STRONG SOLUTION BEING COOLED***"

608 DIN45 = .0081
609 REM INPUT "T4,T5,M4,X4"; T4, T5, M4, X4
610 MEANT4T5 = (T4 + T5) / 2: PRINT "MEANT4T5="; MEANT4T5
611 PERX = X4: TK = MEANT4T5 + 273
612 GOSUB 2085
613 CP45 = SPECH
614 GOSUB 2170
615 K45 = K23: PRINT "K45="; K45
616 PRSOL45 = SPECH * VISC / K45: PRINT "PRSOL4,5="; PRSOL45
617 RESOL45 = (4 * M4) / (3.141593 * DIN45 * VISC): PRINT "RESOL4,5="; RESOL45
618 IF RESOL45 < 2100 THEN HIN45 = 3.66 * K45 / DIN45: GOTO 626
620 LRESOL45 = LOG(RESOL45) / LOG(10): PRINT "RESOL45, LRESOL45"; RESOL45,
LRESOL45
622 FFACTOR2 = (1.82 * LRESOL45 - 1.64) ^ -2
623 K1 = 1 + 3.4 * FFACTOR2
624 K2 = 11.7 + 1.8 / (RESOL45 ^ .3333)
625 HIN45 = (((FFACTOR2 / 8) * PRSOL45 * RESOL45) / (K1 + K2 * ((FFACTOR2 / 8) ^ .5) *
((PRSOL45 ^ .66666) - 1))) * K45 / DIN45
626 PRINT "HIN45="; HIN45
627 INPUT "PRESS ANY KEY TO CONTINUE"; A$: CLS

628 PRINT "***OUTER PIPE FLOW-WEAK SOLUTION BEING HEATED***"

629 DIN23 = .013: DOUT45 = .0095
630 REM INPUT "T2,T3,M2,X2"; T2, T3, M2, X2
632 MEANT2T3 = (T2 + T3) / 2: PRINT "MEANT2T3="; MEANT2T3
633 PERX = X2: TK = MEANT2T3 + 273
634 PRINT "PERX="; PERX, "TK="; TK: GOSUB 2085
635 GOSUB 2170: PRINT "K23 ="; K23
636 PRSOL23 = SPECH * VISC / K23: PRINT "PRSOL2,3="; PRSOL23
637 DH = DIN23 - DOUT45
638 REDH = (M2 * DH) / (.0000618# * VISC): PRINT "REDH="; REDH
639 IF REDH < 2100 THEN HOUT23 = 3.66 * K23 / DH ELSE STOP
640 PRINT "HOUT23="; HOUT23
641 TCOP = (MEANT2T3 + MEANT4T5) / 2: GOSUB 2076
642 HI = HIN45: HO = HOUT23
643 GOSUB 2150
644 USHE = U: PRINT "USHE="; USHE
645 DT43 = T4 - T3: DT52 = T5 - T2
646 DTSHE = (DT43 - DT52) / LOG(DT43 / DT52): PRINT "DT43="; DT43, "DT52="; DT52,
"DTSHE="; DTSHE
647 ASHE = M4 * CP45 * (T4 - T5) / (USHE * DTSHE): PRINT "AREASHE="; ASHE
648 PIPESSHE = ASHE / (3.141593 * DOUT45)
649 PRINT "LENGTH  OF PIPES 9.5mm DIAM="; PIPESSHE
650 INPUT "PRESS ANY KEY TO CONTINUE"; A$

700 PRINT "*****ABSORBER*****"

701 INPUT "PRESS ANY KEY TO CONTINUE"; A$
702 CLS
704 REM INPUT "P,M,TIN,CIN,COUT,TW"; P,M,TIN,CIN,COUT,TW
706 P = P10 * 1000: M = .01
708 TIN = T6: CIN = X6 / 100
709 TW = 30.5: REM INPUT "ABSORBER TW="; TW
710 COUT = X1 / 100
715 X = CIN * 100
```

```
716 A = -2.00755 + .16976 * X - 3.133362 * .001 * X ^ 2 + 1.97668 * .00001 * X ^ 3
718 B = 321.128 - 19.322 * X + .374382 * X ^ 2 - 2.0637 * .001 * X ^ 3
720 C = 6.21147
721 D = -2886.373
722 E = -337269.46#
725 PA1 = P / 6894.8
726 LOGA = LOG(PA1) / LOG(10)
728 TA1 = ((-2 * E) / (D + (D ^ 2 - 4 * E * (C - LOGA)) ^ .5)) - 459.72
730 TWX = (5 / 9) * (A * TA1 + B - 32)
731 REM PRINT "TWX="; TWX
732 IF TWX > TW THEN X = X - .05 ELSE GOTO 740
735 GOTO 716
740 PRINT "CEQ="; X
741 AP = ((CIN - COUT) / (CIN - X / 100)) * 100: PRINT "AP="; AP
742 ALPHA = -132 * LOG((100 - AP) / 86!)
745 LAP = ALPHA * M ^ 1.33
747 IF 1 - LAP < .005 THEN GOTO 750
748 IF 1 - LAP > .005 THEN M = M + .00005: GOTO 745
750 PRINT "M5,M ="; M5, M
751 NTUBES = M5 / (M * .02983)
752 PRINT "LAP="; LAP
753 PRINT "NO. OF PIPES - 1m LENGTH AND 9.5mm DIAM="; NTUBES
755 INPUT "PRESS ANY KEY TO CONDINUE"; A$

783 REM** WATER FLOW INSIDE PIPES **

785 TAWIN = 30: REM INPUT "ABROSBER INLET WATER TEMP. °C="; TAWIN
786 TAWOUT = 31: REM INPUT "ABSORBER OUTLET WATER TEMP. °C="; TAWOUT
788 TAWMEAN = (TAWIN + TAWOUT) / 2
790 TMX = TAWMEAN
792 GOSUB 2050
894 CPABSW = CPWATER
895 MIAW# = MIWATER#
896 KABSW = KWATER
802 MABSW = QABS * 1000 / (CPABSW * (TAWOUT - TAWIN)): PRINT "ABSORBER WATER
MASS FLOW RATE (kg/s)="; MABSW
804 INPUT "No. ABSORBER PIPES="; NAPIPE
805 MAPIPE = MABSW / NAPIPE
806 DAIN = .0081: REM  INPUT "ABSORBER HEAT EXCHANGER INSIDE DIA. (m)="; DAIN
807 DAOUT = .0095: REM  INPUT "ABSORBER HEAT EXCHANGER OUTSIDE DIA. (m)=";
DAOUT
808 REAPIPE = (4 * MAPIPE) / (3.141593 * DAIN * MIAW#): PRINT "ABSORBER WATER RE=";
REAPIPE

809 PRABSW = CPABSW * MIAW# / KABSW: PRINT "PRABSW="; PRABSW
810 IF REAPIPE < 2100 THEN HINABS = 3.66 * KABSW / DAIN: GOTO 818
811 IF REAPIPE < 10000 THEN PRINT "**********RE="; REAPIPE
813 LRE2 = LOG(REAPIPE) / LOG(10): PRINT "REAPIPE,LRE2"; REAPIPE, LRE2
814 FFACTOR2 = (1.82 * LRE2 - 1.64) ^ -2
815 K12 = 1 + 3.4 * FFACTOR2
816 K22 = 11.7 + 1.8 / (REAPIPE ^ .3333)
817 HINABS = (((FFACTOR2 / 8) * PRABSW * REAPIPE) / (K12 + K22 * ((FFACTOR2 / 8) ^ .5) *
((PRABSW ^ .66666) - 1))) * KABSW / DAIN
818 PRINT "HINABS="; HINABS
819 INPUT "PRESS ANY KEY TO CONTINUE"; A$
820 PRINT "*****ABSORBER SOLUTION MEAN PROPERTIES*****"
821 PRINT "T6,T1"; T6, T1
822 TMEANABS = (T6 + T1) / 2: PRINT "TMEANABS="; TMEANABS
823 XAM = (X6 + X1) / 2: PRINT "XABSORBER MEAN="; XAM
824 PERX = XAM: TK = TMEANABS + 273
825 GOSUB 2085
826 VISCA = VISC: PRINT "VISCABS="; VISCA
827 CPABS = SPECH: PRINT "SPEC HEAT ABS="; CPABS
```

```
830 GOSUB 2170
831 KABS = K23: PRINT "KABS="; KABS
833 X = XAM: T = TMEANABS
835 GOSUB 2000
836 DENSABS = DENTX: PRINT "DENSABS="; DENSABS
837 MASS = ((M1 + M6) / 2) / NAPIPE
845 GAMMA = MASS / (3.1415 * DAOUT): PRINT "GAMMA="; GAMMA
846 DELTA = ((3 * VISCA * GAMMA) / ((DENSABS ^ 2) * 9.81)) ^ .33333: PRINT "DELTA(mm)=";
DELTA * 1000
850 RES = (4 * MASS) / (VISCA * 3.1415 * DAOUT): PRINT "RES="; RES
852 PRS = CPABS * VISCA / KABS: PRINT "PRS="; PRS
855 HS = (KABS / DELTA) * .029 * ((RES) ^ .53) * (PRS ^ .344): PRINT "HS="; HS
856 TCOP = (TMEANABS + TAWMEAN) / 2: GOSUB 2076
857 HI = HINABS
860 HO = HS: GOSUB 2150
861 PRINT "U="; U
864 DTZERO = T6 - TAWIN: DTEL = T1 - TAWOUT
866 DTLN = (DTZERO - DTEL) / LOG(DTZERO / DTEL): PRINT "DTLN="; DTLN,
867 AREA = (QABS * 1000 / NAPIPE) / (DTLN * U): PRINT "AREA="; AREA
868 LPIPE = AREA / (3.141593 * DAOUT)
869 PRINT "LENGTH. OF PIPES - 9.5mm DIAM="; LPIPE
890 INPUT "PRESS ANY KEY TO CONTINUE"; A$
899 CLS

900 PRINT "**********EVAPORATOR*********"

985 TEWIN = 27: REM INPUT "EVAPORATOR INLET WATER TEMP. °C="; TEWIN
986 TEWOUT = 17: REM INPUT "EVAPORATOR OUTLET WATER TEMP. °C="; TEWOUT
988 TEWMEAN = (TEWIN + TEWOUT) / 2
990 TMX = TEWMEAN
992 GOSUB 2050
994 CPEW = CPWATER
995 MIEW# = MIWATER#
996 KEW = KWATER
1002 MEW = CAP * 1000 / (CPEW * (TEWIN - TEWOUT)): PRINT "EVAPORATOR WATER MASS
FLOW RATE (kg/s)="; MEW
1004 INPUT "No. EVAPORATOR PIPES="; NEPIPE
1005 MEPIPE = MEW / NEPIPE
1006 DEIN = .0081: REM  INPUT "CONDENSER HEAT EXCHANGER INSIDE DIA. (m)="; DCIN
1007 DEOUT = .0095: REM  INPUT "CONDENSER HEAT EXCHANGER OUTSIDE DIA. (m)=";
DCOUT
1008 REEPIPE = (4 * MEPIPE) / (3.141593 * DEIN * MIEW#): PRINT "EVAPORATOR WATER
RE="; REEPIPE

1009 PREW = CPEW * MIEW# / KEW: PRINT "PREVAPW="; PREW
1010 IF REEPIPE < 2100 THEN HINE = 3.66 * KEW / DEIN: GOTO 1018
1011 LREV = LOG(REEPIPE) / LOG(10): PRINT "REEPIPE,LREV"; REEPIPE, LREV
1012 FFACTORE = (1.82 * LREV - 1.64) ^ -2
1013 K1 = 1 + 3.4 * FFACTORE
1014 K2 = 11.7 + 1.8 / (REEPIPE ^ .3333)
1017 HINE = (((FFACTORE / 8) * PREW * REEPIPE) / (K1 + K2 * ((FFACTORE / 8) ^ .5) * ((PREW
^ .66666) - 1))) * KEW / DEIN
1018 PRINT "HINE="; HINE
1019 INPUT "PRESS ANY KEY TO CONTINUE"; A$



END
```

```
1600 REM
*****************************************************************************************
***************
1601 REM SUBROUTINE FOR CALCULATING SOLUTION ENTHALPY IN KJ/KG OF SOLUTION
1602
REM*****************************************************************************************
*********************
1603 REM Range 0<X<40% LiBr  SPECIFY CT IN °C  ENTHALPY CH IS IN kJ/kg
1604 REM     McNeely (1979) in Keith et al., (1996)

1610 T = (CT * 9 / 5) + 32
1620 CA0 = -33.1054264#
1621 CA1 = .13000636#
1622 CA2 = .00097096#
1623 CB0 = 1.0090734#
1624 CB1 = -.01377507#
1625 CB2 = .000085131#
1630 CH = CA0 + CA1 * X + CA2 * X ^ 2 + T * (CB0 + CB1 * X + CB2 * X ^ 2)
1640 CH = CH * 2.326
1645 RETURN

1799 REM
*****************************************************************************************
************************
1800 REM  SUBROUTINE FOR CALCULATING SOLUTION AND REFRIGERANT TEMPS &
PRESSURE
1801 REM
*****************************************************************************************
************************
1802 REM Range 45<X<70% LiBr
1803 REM ASHRAE (1997)

1810 A0 = -2.00755
1811 A1 = .16976
1812 A2 = -.003133362#
1813 A3 = .0000197668#
1814 B0 = 124.937
1815 B1 = -7.71649
1816 B2 = .152286
1817 B3 = -.0007959#
1850 SUMA = A0 * X ^ 0 + A1 * X ^ 1 + A2 * X ^ 2 + A3 * X ^ 3
1860 SUMB = B0 * X ^ 0 + B1 * X ^ 1 + B2 * X ^ 2 + B3 * X ^ 3
1862 IF FLAG4 = 1 THEN FLAG4 = 0: GOTO 1894
1865 IF FLAG1 = 1 THEN GOTO 1871
1870 TSOL = SUMB + TREFR * SUMA
1871 PRINT "TSOL="; TSOL
1880 FLAG1 = 0: TREFR = (TSOL - SUMB) / SUMA
1881 PRINT "TREFR="; TREFR
1890 LGP = C + D / (TREFR + 273) + E / (TREFR + 273) ^ 2
1892 SATPRES = 10 ^ LGP
1893 RETURN
1894 T2REF = ((-2 * E) / (D + (D ^ 2 - 4 * E * (C - LOG(P10)/2.302)) ^ .5)) - 273
1895 T6 = SUMB + T2REF * SUMA: GOTO 328
```

```
1899 REM
*****************************************************************************************
*****************
1900 REM  SUBROUTINE FOR CALCULATING SOLUTION ENTHALPY IN KJ/KG OF
SOLUTION
1901 REM
*****************************************************************************************
*****************
1902 REM Range 40<X<70% libr
1903 REM ASHRAE (1997)

1910 HA0 = -2024.33
1911 HA1 = 163.309
1912 HA2 = -4.88161
1913 HA3 = .06302948#
1914 HA4 = -.0002913704#
1915 HB0 = 18.2829
1916 HB1 = -1.1691757#
1917 HB2 = .03248041#
1918 HB3 = -.0004034184#
1919 HB4 = .00000018520569#
1920 HC0 = -.037008214#
1921 HC1 = .0028877666#
1922 HC2 = -8.131301500000001D-05
1923 HC3 = .000000991166 28#
1924 HC4 = -.00000000444 1207#
1925 SUMHA = HA0 * X ^ 0 + HA1 * X ^ 1 + HA2 * X ^ 2 + HA3 * X ^ 3 + HA4 * X ^ 4
1935 SUMHB = HB0 * X ^ 0 + HB1 * X ^ 1 + HB2 * X ^ 2 + HB3 * X ^ 3 + HB4 * X ^ 4
1945 SUMHC = HC0 * X ^ 0 + HC1 * X ^ 1 + HC2 * X ^ 2 + HC3 * X ^ 3 + HC4 * X ^ 4
1950 IF FLAG3 = 1 THEN GOTO 1953
1952 ENTH = SUMHA + T * SUMHB + SUMHC * T ^ 2: GOTO 1960
1953 ALP = SUMHC: BET = SUMHB
1954 GAM = SUMHA - H5
1955 TH51 = (-BET + (BET ^ 2 - 4 * ALP * GAM) ^ .5) / (2 * ALP)
1956 TH52 = (-BET - (BET ^ 2 - 4 * ALP * GAM) ^ .5) / (2 * ALP)
1957 IF TH51 > TH52 THEN T5 = TH51 ELSE T5 = TH52
1960 RETURN

1999 REM************************************************************
2000 REM CALCULATION OF LiBr SOLUTION DENSITY
2001 REM************************************************************
2009 REM 0<T<200°C, 20<X<65% (LEE ET AL.,1990.)

2010 X = X / 100: DENTX = 1145.36 + 470.84 * X + 1374.79 * X ^ 2 - (.333393 + .571749 * X) * (273
+ T)
2111 PRINT "DENTX ="; DENTX
2012 VOL = 1 / DENTX
2015 RETURN

2017 REM************************************************
2018 REM ENTHALPY OF SUPERHEATED STEAM
2019 REM************************************************
2020 REM (CURVE FITS FROM DATA PRESENTED BY ROGERS G. F. C. AND MAYHEW Y. R.,
1992)

2021 T2REF = ((-2 * E) / (D + (D ^ 2 - 4 * E * (C - LOG(P4)/2.302)) ^ .5)) - 273
2023 T = T7 - T2REF
2027 HSH1 = 32.508 * LOG(P4) + 2513.2
2028 HSH2 = .00001 * P4 ^ 2 - .1193 * P4 + 2689
2030 HSH = ((HSH2 - HSH1) / 100) * T + HSH1
2032 RETURN
```

```
2047 REM************************************************
2048 REM WATER PROPERTIES
2049 REM ************************************************
2050 REM (CURVE FITS FROM DATA PRESENTED BY ROGERS G. F. C. AND MAYHEW Y. R.,
1992)

2052 KWATER = -6.5104167D-10 * TMX ^ 4 + .00000018923611# * TMX ^ 3 - 2.671875E-05 * TMX
^ 2 + .0027103175# * TMX + .5520119
2053 PRINT "KWATER="; KWATER
2054 MIWATER# = .000001 * (.000031538716146# * TMX ^ 4 - 8.913055428199999D-03 * TMX ^ 3
+ .9795876934# * TMX ^ 2 - 55.4567974# * TMX + 1791.74424#)
2055 PRINT "MIWATER="; MIWATER#
2058 NIWATER# = .0001 * (3.1770833333D-08 * TMX ^ 4 - .0000089652777778# * TMX ^ 3 +
.00098270833333# * TMX ^ 2 - .055322222222# * TMX + 1.7876666667#)
2059 PRINT "NIWATER="; NIWATER#
2060 POWATER = .000015451# * TMX ^ 3 - .0059003 * TMX ^ 2 - .019075 * TMX + 1002.3052#
2063 PRINT "POWATER="; POWATER
2064 CPWATER = .000003216145833# * TMX ^ 4 - .000798668982# * TMX ^ 3 + .0780295139# *
TMX ^ 2 - 3.0481614# * TMX + 4217.7377#
2065 PRINT "CPWATER="; CPWATER
2067 PRWATER = MIWATER# * CPWATER / KWATER
2069 PRINT "PRWATER="; PRWATER
2075 RETURN

2076 REM THERMAL CONDUCTIVITY OF COPPER, (CURVE FIT, OZISIK M.,1985)

2077 KCOPPER = 4.583333E-09 * TCOP ^ 4 - 2.916667E-06 * TCOP ^ 3 + 6.541667E-04 * TCOP ^ 2 -
.1108333 * TCOP + 386
2078 PRINT "KCOPPER="; KCOPPER
2079 RETURN

2081
REM*************************************************************************************
**
2085 REM VISCOSITY OF LiBr SOLUTION, 45%<X<65%  (LEE ET AL.,1990.) &
2086
REM*************************************************************************************
**
2087 REM & SPECIFIC HEAT CP J/KG K (CURVE FIT- ASHRAE, 1997)

2088  A1 = -494.122 + 16.3967 * PERX - .14511 * PERX ^ 2
2090  A2 = 28606.4 - 934.568 * PERX + 8.52755 * PERX ^ 2
2091  A3 = 70.3848 - 2.35014 * PERX + .0207809# * PERX ^ 2
2092 LNVISC = A1 + A2 / TK + A3 * LOG(TK)
2094 VISC = EXP(LNVISC) / 1000
2095 PRINT "visc="; VISC
2100 SPECH = .0976 * PERX ^ 2 - 37.512 * PERX + 3825.4
2101 PRINT "SPECIFIC HEAT="; SPECH
2102 RETURN

2150 REM**** OVERALL HEAT TRANSFER COEFFICIENT (U)***
2152 U = 1 / (1.173 / HI + 2.173 * .00009 + (.0095 / (2 * KCOPPER)) * LOG(1.173) + 1 / HO)
2153 RETURN

2058 REM*************************************************************************
2159 REM Hfg(kJ/kg) AND pg(kg/m3) FOR SATURATED WATER
2160 REM ************************ ************************************************
2161 REM (CURVE FIT- ASHRAE, 1997)

2162 HFG = -.00132635# * TH ^ 2 - 2.29983657# * TH + 2500.43063#
2164 PG = 1 / (.00001147965# * TH ^ 4 - .00297197798# * TH ^ 3 + .28077931731# * TH ^ 2 -
11.83083758# * TH + 202.9035477661#)
2165 PRINT "HFG="; HFG
```

```
2166 PRINT "PG="; PG
2167 RETURN


2168 REM************************************************************
2169 REM THERMAL CONDUCTIVITY OF LIBR SOLUTION
2170 REM************************************************************
2171 REM (DATA EXTRACTED FROM ABDULAGATOV AND MAGOMEDOV, 1997)

2172 IF TK < 313 THEN GOTO 2176
2173 IF TK >= 313 THEN KSOL1 = -.3081 * (PERX / 100) + .62979: KSOL2 = -.3191795# * (PERX /
100) + .65388
2174 DIFF12 = ((KSOL2 - KSOL1) / 20) * (TK - 313): K23 = KSOL1 + DIFF12
2175 GOTO 2180
2176 KSOL1 = -.3081 * (PERX / 100) + .62979: KSOL3 = -.291897 * (PERX / 100) + .59821
2177 DIFF13 = ((KSOL3 - KSOL1) / 20) * (313 - TK)
2178 K23 = KSOL1 + DIFF13
2180 PRINT "TK="; TK, " PERX="; PERX
2185 RETURN
```

APPENDIX 5

Modifications of computer program 'LITH' for calculating the temperature at the output of the solution heat exchanger of the fluid returning to the generator (T3, Table 9.1)

```
50 CLS
57 T3 = 55: REM INPUT "Solution Heat Exchanger Exit temperature (T3°C)="; T3
60 CAP = 2: REM INPUT "Evaporator Capacity (kW)="; CAP
.....
600 PRINT "**** SOLUTION HEAT EXCHANGER***"
.....
645 ASHE = .36873
646 Qhex = M4 * CP45 * (T4 - T5)
650 DTSHE = Qhex / (ASHE * U)
652 T333 = T3

654 DT43 = T4 - T333: DT52 = T5 - T2

655 DTSHE2 = (DT43 - DT52) / LOG(DT43 / DT52)
660 IF DTSHE2 > DTSHE THEN T333 = T333 + .1: GOTO 654

665 PRINT "T333, DTSHE2="; T333, DTSHE2
668 PRINT "T3, DTSHE="; T3, DTSHE
669 IF T333 < T3 THEN GOTO 698
670 T3 = (T3 + T333) / 2
671 T3 = T3 - .1
672 PRINT "T3="; T3
673 INPUT "PRESS ANY KEY TO CONTINUE"; A$
675 FLAG1 = 0: FLAG3 = 0
676 FLAG4 = 0: FLAG5 = 0

677 GOTO 60
```

APPENDIX 6

The TRNSYS deck file used for the simulation of the system shown in Figure 9.3

```
ASSIGN \TRNWIN\PhDAbRef\FLAT.LST  6
ASSIGN \TRNWIN\ASHRAE.COF         8
ASSIGN \TRNWIN\PhDAbRef\FLAT.OUT  21
ASSIGN \TRNWIN\WEATHER\METEONIC.DAT  20
ASSIGN \TRNWIN\PhDAbRef\FLAT.PLT  22

SIMULATION 1 8760 1
TOLERANCES 0.005 0.005
LIMITS 700 700
WIDTH 72

UNIT 9 TYPE 9 DATA READER
PARAMETERS 2
-1 20

UNIT 16 TYPE 16 SOLAR RADIATION PROCESSOR
PARAMETERS 9
7 1 3 1 35 4871 0 2 -1
INPUTS 13
9,4 9,3 9,19 9,20 0,0 0,0 0,0 0,0 0,0 0,0 0,0 0,0 0,0
0. 0.  0. 0. .2  90. 0. 90. -90. 90. 180. 90. 90.

EQUATIONS 1
*Collector slope angle = BCOLL
BCOLL=27

UNIT 17 TYPE 16 SOLAR RADIATION PROCESSOR
PARAMETERS 9
7 1 3 1 35 4871 0 2 -1
INPUTS 7
9,4 9,3 9,19 9,20 0,0 BCOLL 0,0
0. 0.  0. 0. .2  0. 0.

EQUATIONS 11
QSENS = [19,7]+[20,7]+[21,7]+[22,7]
QLAT = [19,8]+[20,8]+[21,8]+[22,8]
QSENS1=QSENS/1000.
QLAT1=QLAT/1000.
Qt=(QSENS1+QLAT1)/3.6

*Number of air changes per hour = 3
*VEN1= Ventilation volume rate (m3/h)
VEN1=(174*3)
MTCH=GT([9,5],17)
V2= VEN1*MTCH
HU1=LT([9,6],0.008)
V1=(HU1*V2)
YS4=GT([19,1],[9,5])
EQUATIONS 6
AZLOAD=[19,7]+[19,8]
AWTR1=GT(AZLOAD,0)
AWTR2=LT(AZLOAD,0)
AWTR3=EQL(AZLOAD,0)
AWTR=AWTR1*0.4+AWTR2*0.8+AWTR3*0.8
VENA=YS4*V1*(AWTR1+AWTR3)
```

```
UNIT 19 TYPE 19 DETAILED ZONE
*Refer to Figure 3.2 and Tables 3.1 & 3.2 for details

* ZONE 1
PAR 13
1 147 .1  0.017  0.049  500  7  25
.0075 21 25 0.005 0.008
INP 11
9,5 9,6 9,5 VENA  9,6 0,0 0,0 0,0 0,0 0,0 9,7
0.  0.  0.  0.  0.  0.  1 2  750.  0.  0.

*  ZONE 1 EXTERNAL SOUTH WALL (double)
PAR 30
1  1  15.8  .7  .65  4  9.58
7  7  6

*Transfer function coefficients for current and previous values of the sol-air
 *temperature, equivalent zone temperature and heat flux.
.0000000 .0001393  .0028434  .0071247  .0036940  .0004312  .0000101
 8.3299600  -20.0540100  16.7335000  -5.6940510  .7219610  -.0233240 .0002120
 -2.2696810  1.7796570  -.5648261  .0668862  -.0018851 .0000147

INP 1
16,6
0.

*ZONE 1 EXTERNAL EAST-SOUTH WALL(double)
PAR 30

2  1  21  .7  .65  4  9.58
7 7 6
.0000000 .0001393  .0028434  .0071247  .0036940  .0004312  .0000101
 8.3299600  -20.0540100  16.7335000  -5.6940510  .7219610  -.0233240 .0002120
 -2.2696810  1.7796570  -.5648261  .0668862  -.0018851 .0000147

INP 1
16,11
0.


*ZONE 1  WALL 3 SEPARATING ZONES
PAR 24
3  3  21  .7  .65  4  9.58
5  5  4
.0025797 .0715822  .1101363 .0192146  .0002567
8.3299600 -12.7745800  4.9665380  -.3190865  .0009357
-1.3958910 .4863625 -.0267993 .0000342

INP 3
21,18 21,1 0,0
0.  0.  0.

*ZONE 1 WALL 4 SEPARATING ZONES
PAR 24

4  3  21  .7  .65  4  9.58
5  5  4
.0025797 .0715822  .1101363 .0192146  .0002567
8.3299600 -12.7745800  4.9665380  -.3190865  .0009357
-1.3958910 .4863625 -.0267993 .0000342
```

```
INP 3
20,18 20,1  0,0
0.   0.  0.

EQUATIONS 1
*QFL# = Number # floor losses
QFL1=3.6*14*1.5*([9,5]-[19,1])

* FLOOR ZONE 1
PAR 5
5 4 49 .7 9.58

INP 1
QFL1
0.

*  CEILING ZONE 1 (roof)
PAR 27
6 1 49 .7 .55 4 9.58 6 6 5
.0000063 .0011465  .0055576  .0034890  .0003120  .0000028
8.9761100  -18.3087500  11.1610600  -1.8350940  .0172379  -.0000435
-1.9881840 1.1739910  -.1809929  .0012656  -.0000023

INP 1
9,4
0.

* SOUTH WINDOW ZONE 1
PAR 8
7 5 5.2 1 .8 30 1 5

INP 5
16,6 16,7 AWTR 0,0 0,0
0. 0. .8 12.3 1
* VIEW FACTORS
PAR 11
1 3 7 7 1 4 3 2 5 6 1
*WINDOW GEOMETRY
PAR 25
7 1 1 .8 1.3 4
9 4 1 4 2 4 3 4 4 4 5 4 6 4 7 2 4 2 3

EQUATIONS 1
YS5=GT([20,1],[9,5])

EQUATIONS 6
BZLOAD=[20,7]+[20,8]
BWTR1=GT(BZLOAD,0)
BWTR2=LT(BZLOAD,0)
BWTR3=EQL(BZLOAD,0)
BWTR=BWTR1*0.4+BWTR2*0.8+BWTR3*0.8
VENB=YS5*V1*(BWTR1+BWTR3)

UNIT 20 TYPE 19 DETAILED ZONE
* S-WEST ROOM
* ZONE 2
PAR 13
1 147 .1  0.017  0.049  500  7  25
.0075  21 25 0.005 0.008
INP 11
9,5 9,6 9,5 VENB 9,6 0,0 0,0 0,0 0,0 0,0 9,7
0.  0.  0.  0.  0.  0.  1.  2.  750.  0.  0.
```

```
* ZONE 2 EXTERNAL SOUTH WALL (double)
PAR 30
1 1 21 .7 .65 4 9.58
7 7 6
.0000000 .0001393 .0028434 .0071247 .0036940 .0004312 .0000101
8.3299600 -20.0540100 16.7335000 -5.6940510 .7219610 -.0233240 .0002120
-2.2696810 1.7796570 -.5648261 .0668862 -.0018851 .0000147

INP 1
16,6
0.

*ZONE 2 EXTERNAL WEST WALL (double)
PAR 30
4 1 15.8 .7 .65 4 9.58
7 7 6
.0000000 .0001393 .0028434 .0071247 .0036940 .0004312 .0000101
8.3299600 -20.0540100 16.7335000 -5.6940510 .7219610 -.0233240 .0002120
-2.2696810 1.7796570 -.5648261 .0668862 -.0018851 .0000147

INP 1
16,17
0.
*ZONE 2 WALL 3 SEPARATING ZONES-INTERNAL NORTH WALL
PAR 24
3 3 21 .7 .65 4 9.58
5 5 4
.0025797 .0715822 .1101363 .0192146 .0002567
8.3299600 -12.7745800 4.9665380 -.3190865 .0009357
-1.3958910 .4863625 -.0267993 .0000342

INP 3
22,18 22,1 0,0
0. 0. 0.

*ZONE 2 WALL 2 SEPARATING ZONES-INTERNAL EAST WALL
PAR 24
2 3 21 .7 .65 4 9.58
5 5 4
.0025797 .0715822 .1101363 .0192146 .0002567
8.3299600 -12.7745800 4.9665380 -.3190865 .0009357
-1.3958910 .4863625 -.0267993 .0000342

INP 3
19,18 19,1 0,0
0. 0. 0.

EQUATIONS 1
QFL2=3.6*14*1.5*([9,5]-[20,1])

* FLOOR ZONE 2
PAR 5
5 4 49 .7 9.58

INP 1
QFL2
0.
```

```
* CEILING ZONE 1 (roof)
PAR 27
6 1 49 .7 .55 4 9.58 6 6 5
.0000063 .0011465 .0055576 .0034890 .0003120 .0000028
8.9761100 -18.3087500 11.1610600 -1.8350940 .0172379 -.0000435
-1.9881840 1.1739910 -.1809929 .0012656 -.0000023

INP 1
9,4
0.

* ZONE 2 WEST WINDOW 2
PAR 8
7 5 5.2 1 .8 30 1 5

INP 5
16,17 16,18 BWTR 0,0 0,0
0. 0. .8 12.3 1


* VIEW FACTORS
PAR 11
1 3 7 7 1 4 3 2 5 6 1
*WINDOW GEOMETRY

PAR 25
7 4 1 .8 1.3 4
9 4 1 4 2 4 3 4 4 4 5 4 6 4 7 2 2 2 3

EQUATIONS 1
YS6=GT([21,1],[9,5])

EQUATIONS 6
CZLOAD=[21,7]+[21,8]
CWTR1=GT(CZLOAD,0)
CWTR2=LT(CZLOAD,0)
CWTR3=EQL(CZLOAD,0)
CWTR=CWTR1*0.4+CWTR2*0.8+CWTR3*0.8
VENC=YS6*V1*(CWTR1+CWTR3)

UNIT 21 TYPE 19 DETAILED ZONE
* E-N ROOM
* ZONE 3
PAR 13
1 147 .1 0.017 0.049 500 7 25
.0075 21 25 0.005 0.008
INP 11
9,5 9,6 9,5 VENC 9,6 0,0 0,0 0,0 0,0 0,0 9,7
0. 0. 0. 0. 0. 0. 1. 2. 750. 0. 0.

* zone 3 WALL 1 SEPARATING ZONE-INTERNAL SOUTH WALL
PAR 24
1 3 21 .7 .65 4 9.58
5 5 4
.0025797 .0715822 .1101363 .0192146 .0002567
8.3299600 -12.7745800 4.9665380 -.3190865 .0009357
-1.3958910 .4863625 -.0267993 .0000342

INP 3
19,19 19,1 0,0
0. 0. 0.
```

```
* ZONE 3 WALL 4 SEPARATING ZONE-INTERNAL WEST WALL
PAR 24
4 3 21 .7 .65 4 9.58
5 5 4
.0025797 .0715822 .1101363 .0192146 .0002567
8.3299600 -12.7745800 4.9665380 -.3190865 .0009357
-1.3958910 .4863625 -.0267993 .0000342

INP 3
22,19 22,1 0,0
0. 0. 0.
*ZONE 3 EXTERNAL NORTH WALL (double)
PAR 30
3 1 21 .7 .65 4 9.58
7 7 6
.0000000 .0001393 .0028434 .0071247 .0036940 .0004312 .0000101
8.3299600 -20.0540100 16.7335000 -5.6940510 .7219610 -.0233240 .0002120
-2.2696810 1.7796570 -.5648261 .0668862 -.0018851 .0000147

INP 1
16,14
0.

*ZONE 3 EXTERNAL EAST WALL (double)
PAR 30
2 1 15.8 .7 .65 4 9.58
7 7 6
.0000000 .0001393 .0028434 .0071247 .0036940 .0004312 .0000101
8.3299600 -20.0540100 16.7335000 -5.6940510 .7219610 -.0233240 .0002120
-2.2696810 1.7796570 -.5648261 .0668862 -.0018851 .0000147

INP 1
16,11
0.

EQUATIONS 1
QFL3=3.6*14*1.5*([9,5]-[21,1])

* FLOOR ZONE 3
PAR 5
5 4 49 .7 9.58

INP 1
QFL3
0.

* CEILING ZONE 1 (roof)
PAR 27
6 1 49 .7 .55 4 9.58 6 6 5
.0000063 .0011465 .0055576 .0034890 .0003120 .0000028
8.9761100 -18.3087500 11.1610600 -1.8350940 .0172379 -.0000435
-1.9881840 1.1739910 -.1809929 .0012656 -.0000023

INP 1
9,4
0.

*ZONE 3 EAST WINDOW
PAR 8
7 5 5.2 1 .8 30 1 5
```

```
INP 5
16,11 16,12 CWTR 0,0 0,0
0. 0. .8 12.3 1

* VIEW FACTORS
PAR 11
1 3 7 7 1 4 3 2 5 6 1

*WINDOW GEOMETRY
PAR 25
7 2 1 .8 1.3 4
9 4 1 4 2 4 3 4 4 4 5 4 6 4 7 2 1 2 4

EQUATIONS 7
YS7=GT([22,1],[9,5])
DZLOAD=[22,7]+[22,8]
DWTR1=GT(DZLOAD,0)
DWTR2=LT(DZLOAD,0)
DWTR3=EQL(DZLOAD,0)
DWTR=DWTR1*0.4+DWTR2*0.8+DWTR3*0.8
VEND=YS7*V1*(DWTR1+DWTR3)

UNIT 22 TYPE 19 DETAILED ZONE
* NORTH-WEST ROOM
* ZONE 4
PAR 13
1 147 .1 0.017 0.049 500 7 25
.0075 21 25 0.005 0.008
INP 11
9,5 9,6 9,5 VEND 9,6 0,0 0,0 0,0 0,0 0,0 9,7
0. 0. 0. 0. 0. 0. 1. 2. 750. 0. 0.

* ZONE 4 WALL 1 SEPARATING ZONE-INTERNAL SOUTH WALL
PAR 24
1 3 21 .7 .65 4 9.58
5 5 4
.0025797 .0715822 .1101363 .0192146 .0002567
8.3299600 -12.7745800 4.9665380 -.3190865 .0009357
-1.3958910 .4863625 -.0267993 .0000342

INP 3
20,19 20,1 0,0
0. 0. 0.

*ZONE 4 EXTERNAL WEST WALL (double)
PAR 30
4 1 21 .7 .65 4 9.58
7 7 6
.0000000 .0001393 .0028434 .0071247 .0036940 .0004312 .0000101
8.3299600 -20.0540100 16.7335000 -5.6940510 .7219610 -.0233240 .0002120
-2.2696810 1.7796570 -.5648261 .0668862 -.0018851 .0000147

INP 1
16,17
0.

*ZONE 4 EXTERNAL NORTH WALL (double)
PAR 30
3 1 15.8 .7 .65 4 9.58
7 7 6
.0000000 .0001393 .0028434 .0071247 .0036940 .0004312 .0000101
8.3299600 -20.0540100 16.7335000 -5.6940510 .7219610 -.0233240 .0002120
-2.2696810 1.7796570 -.5648261 .0668862 -.0018851 .0000147
```

```
INP 1
16,14
0.

*ZONE 4 WALL 2 SEPARATING ZONE-INTERNAL EAST WALL
PAR 24
2  3  21  .7  .65  4  9.58
5  5  4
.0025797 .0715822  .1101363 .0192146  .0002567
8.3299600 -12.7745800 4.9665380 -.3190865  .0009357
-1.3958910 .4863625 -.0267993 .0000342

INP 3
21,19 21,1 0,0
0. 0. 0.

EQUATIONS 1
QFL4=3.6*14*1.5*([9,5]-[22,1])

*ZONE 4 FLOOR
PAR 5
5 4 49 .7 9.58

INP 1
QFL4
0.
* CEILING ZONE 1 (roof)
PAR 27
6 1 49 .7 .55 4 9.58 6 6 5
.0000063 .0011465 .0055576 .0034890 .0003120 .0000028
8.9761100 -18.3087500 11.1610600 -1.8350940 .0172379 -.0000435
-1.9881840 1.1739910 -.1809929 .0012656 -.0000023
INP 1
9,4
0.

*ZONE 4 NORTH WINDOW
PAR 8
7 5 5.2 1 .8 30 1 5

INP 5
16,14 16,15 DWTR 0,0 0,0
0. 0. .8 12.3 1

* VIEW FACTORS
PAR 11
1 3 7 7 1 4 3 2 5 6 1

*WINDOW GEOMETRY
PAR 25
7 3 1 .8 1.3 4
9 4 1 4 2 4 3 4 4 4 5 4 6 4 7 2 1 2 2

EQUATIONS 17
QTOT= QSENS1+QLAT1
QTO=QSENS+QLAT
QC1=([19,11]+[20,11])/3600
QC2=([20,14]+[22,14])/3600
QC3=([22,13]+[21,13])/3600
QC4=([21,12]+[19,12])/3600
QC5=([19,15]+[20,15]+[21,15]+[22,15])/3600
QC6=([19,16]+[20,16]+[21,16]+[22,16])/3600
QC7S=[19,17]/3600
```

```
QC7W=[20,17]/3600
QC7N=[22,17]/3600
QC7E=[21,17]/3600
MT=([19,1]+[20,1]+[21,1]+[22,1])/4
QTZ1=([19,7]+[19,8])/3600
QTZ2=([20,7]+[20,8])/3600
QTZ3=([21,7]+[21,8])/3600
QTZ4=([22,7]+[22,8])/3600

UNIT 35 TYPE 33  PSYCHROMETRICS
PARA 4
4 1.013 1 1
INPUTS 2
9,5 9,6
0.0  0.0

EQUATIONS 2
*TV = Tank volume (m3)
TV=0.8
*Tank height (m)
HT=1

EQUATIONS 5
DT=((4*TV)/(3.14*HT))^0.5
TANKUA=(HT*3.14*DT+3.14*DT*DT/2)*1.5
CONHT=0.8*HT

* WINTER LOAD
TWINT=[6,1]-6
MWINT=-1*(QTO*1.05/(4.19*6))

UNIT 36 TYPE 15 ALGEBRAIC OPERATIONS
PAR 1
9
INPUT 2
QTO 0,0
0.  0.0
* Y=1, SUMMER    Y=0,WINTER

EQUATIONS 3
FLG1=GT(QTO,0)
QNEED=QTO*1.05*FLG1
QNEEDW=QNEED/3600

* ABSORPTION REFRIGERATOR
EQUATIONS 5
* QGEN = Generator load
QGENW=(QNEEDW*QNEEDW*(-0.0216)+1.6522*QNEEDW-0.7002)*FLG1
QGEN=QGENW*3600
* MASSW = Generator heating water mass flow (kg/h)
MASSW=1.26*3600
* DTGEN = Temperature difference of generator heating water (°C)
DTGEN=QGEN/(MASSW*4.2)
* TGOUT = Generator heating water outlet temperature (°C)
 TGOUT=[6,1]-DTGEN

UNIT 40 TYPE 11 FLOW CONTROLLER
PARAMETERS 1
3
INPUTS 5
TWINT MWINT TGOUT  MASSW  36,1
90  0   90   0    0
UNIT 38 TYPE 38 ALGEBRAIC TANK
```

```
PARAMETERS 11
1 TV HT CONHT 4.19 1000 0 1 TANKUA 1 70
INPUTS 5
1,1 3,2 40,1 40,2 9,5
90 0 90 0 20

UNIT 4 TYPE 2 THERMOSTAT SOLAR
* FOR PUMP 3
PARAMETERS 4
7 3 1 150
INPUTS 4
1,1 38,3 0,0 4,1
90 90 0 1

UNIT 5 TYPE 15 ALGEBRAIC OPERATIONS
PAR 1
9
INPUT 2
1,1 0,0
0.  95.0

EQUATIONS 1
MASSP=[38,2]

UNIT 3 TYPE 3 PUMP
* FOR SOLAR COLLECTOR
PARA 4
1000 4.19 360 0
INPUTS 3
38,1 MASSP 4,1
90 100 1

UNIT 1 TYPE 1 COLLECTOR
*FLAT PLATE
PARAMETERS 14
1 4 5 4.19 1 54 0.792 23.994 0 -1 4.19 1 0.1 0
INPUTS 10
3,1   3,2  0,0 9,5 17,6 9,4 16,5 0,0  17,9 BCOLL
90    100  0.0  20.  20.   0.  0. 0.2   0.  0.

UNIT 2 TYPE 2 THERMOSTAT AUX HEATER
* BOILER THERMOSTAT
PARAMETERS 4
7 1 2 150
INPUTS 4
0,0 38,3   0,0 2,1
88 90 0 1

UNIT 6 TYPE 6 AUXILARY HEATER
* BOILER
PARA 5
65000 90 4.19 10 0.85
INPUTS 4
38,3 38,4 2,1 9,5
90 100 1 20
UNIT 37 TYPE 11 FLOW CONTROLLER
* SUMMER TO AB REFR, WINTER TO LOAD
PARAMETERS 1
2
INPUTS 3
6,1 6,2 36,1
90   0   0
```

```
EQUATIONS 4
*QBOIL = Boiler heat (kW-h)
*QCOLLE = Collected heat from collectors (kW-h)
*QCOOL = Cooling load (kW-h)

QBOIL=[6,5]/3600
QCOLLE=[1,3]/3600
QCOOL=QNEED/3600
WINT=LT(QT,0)

UNIT 24 TYPE 24 QUANTITY INTEGRATOR

INPUTS 3
QCOOL  QBOIL QCOLLE
QCOOL  QBOIL QCOLLE

EQUATIONS 1
MTANKIN=[40,2]/1000

UNIT 25 TYPE 25 PRINT DESIGN LOADS
PAR 4
1 1 8760 21

INPUTS 13
TV HT 1,3  QT  QCOOL QBOIL QCOLLE 24,1 24,2 24,3 24,4  6,2  37,3
TV HT Qg  QT  Qcool QBOL QCOLL TQCOOL TQBOL TQCLLE TEXT  MBOL TINAB

EQUATIONS 1
MSP=[3,2]/1000

UNIT 65 TYPE 65 ONLINE PLOTTER
PARAMETERS 14
5 4  0  130  -10 25    1      1     3
52     7   0   2   0

*INPUTS 4
*6,1 40,1  MTANKIN  Qt
*BOUT TTANKIN  MTANKIN   Qtot(kW)

INPUTS 9
MSP 9,5 38,3 6,1 40,1 QCOOL QCOLLE  QBOIL Qt
MSP Tamp BTIN BOUT outload QCOOL QCOLLE QBOIL  Qtot(kW)

LABELS 4
DEG KW
Room temperature (Degrees C)
Total cooling load (kW)

END
```

APPENDIX 7

PUBLISHED PAPERS RELATED TO THE STUDY

A. Papers in International Scientific Journals

1. Florides G., Kalogirou S., Tassou S. and Wrobel L. (2000). Modelling of the Modern Houses of Cyprus and Energy Consumption Analysis, *Energy-The International Journal*, Vol. 25, No. 10, pp. 915-937, (Appendix 8).

2. Florides G., Tassou S., Kalogirou S. and Wrobel L. (2001). Evolution of Domestic Dwellings in Cyprus and Energy Analysis, *Renewable Energy*, Vol. 23, No. 2, pp. 219-234, (Appendix 9).

3. Florides G., Kalogirou S., Tassou S. and Wrobel L. (2001). Modelling and Simulation of an Absorption Solar Cooling System for Cyprus. Paper accepted for publication in the *Solar Energy Journal*, 33 Pages.

Papers under review:

1. Florides G., Tassou S., Kalogirou S. and Wrobel L. (2001). Measures to Lower Building Thermal Load and their Cost Effectiveness. Paper submitted to the *Energy Journal*, 40 Pages.

B. Papers in Conference Proceedings

1. Florides G., Kalogirou S. and Tassou S. (2000). Energy Consumption Analysis of a Typical House in Cyprus, *Proceedings of the 10th Mediterranean Electro-technical Conference MELeCon'2000*, Limassol, Cyprus, Vol. 3, pp. 1165-1168.

2. Kalogirou S., Florides G., Hadjioannou L. and Pashiardis S. (2000). Comparison of the Simulated Performance of a Solar System Using Typical Meteorological Year and Mean Monthly Weather Data, *Proceedings of World Renewable Energy Congress* VI, Brighton, UK, Part II, pp. 1011-1014.

3. Kalogirou S., Florides G., Neocleous C. and Schizas C. (2001). Estimation of the Daily Heating and Cooling Loads Using Artificial Neural Networks. *Proceedings of CLIMA 2000 Conference on CD-ROM*, 7th Rehva World Congress, Naples, Italy, 2001.

4. Kalogirou S., Florides G., and Tassou S. (2001). Design of a Lithium Bromide Water Absorption Refrigerator. *Proceedings of CLIMA 2000 Conference on CD-ROM*, 7th Rehva World Congress, Naples, Italy, 2001.

APPENDIX 8

Paper published in 'Energy-The International Journal'

Pergamon

Energy 25 (2000) 915–937

ENERGY

www.elsevier.com/locate/energy

Modeling of the modern houses of Cyprus and energy consumption analysis

G.A. Florides [a], S.A. Kalogirou [a,*], S.A. Tassou [b], L.C. Wrobel [b]

[a] *Mechanical Engineering Department, Higher Technical Institute, PO Box 20423, Nicosia 2152, Cyprus*
[b] *Mechanical Engineering Department, Brunel University, Uxbridge, Middlesex, UB8 3PH, UK*

Received 22 February 2000

Abstract

This study uses the TRNSYS computer program for the modeling and simulation of the energy flows of the modern houses of Cyprus followed by an energy consumption analysis. For the calculations, a Typical Meteorological Year for the Nicosia area and a typical model house are used. Initially, the Cyprus energy scene and an analysis of the number of houses employing heating and cooling equipment is presented from which it is observed that the number of systems installed has increased tremendously during the last decade. The results of the simulation show that the inside house temperature, when no air-conditioning is used, varies between 10–20°C for winter and between 30–50°C for summer. The effect on the temperature and the heating and cooling loads that various wall and roof constructions present is determined. This investigation indicates the importance of the roof insulation, which results in a reduction up to 45.5% of the cooling load and up to 75% of the heating load. The effect of mechanical ventilation, window shading, as well as that of the inclined concrete roof used for aesthetic reasons, is also examined. The life cycle analysis is used for the economic analysis of the various constructions. The results indicate that the wall insulation pays back in a twenty year period with marginal savings, whereas the roof insulation has considerable economic benefit, with life cycle savings up to EUR 22374 depending on the type of construction.

1. Introduction

The notion that the supply of fuels is cheap and limitless ended with the "energy crisis" of the mid-1970s. This crisis has led to an unreasonable rise in the cost of energy. The recent stabilization

* Corresponding author. Tel.: +357-2-306266; fax: +357-2-494953.
E-mail address: skalogir@spidernet.com.cy (S.A. Kalogirou).

0360-5442/00/$ - see front matter
PII: S0360-5442(00)00030-X

of the fuel prices, determined basically by the price of oil in the international market, is no more than a temporary pause in the inevitable increase of energy costs.

Therefore, energy conservation in the sense of fuel saving is of great importance. Considering that the overall energy consumption in commercial and residential buildings represents approximately 40% of Europe's energy budget [1], sensible economy measures, without affecting the environmental standards and the quality of life, must be introduced. These measures will result in savings of energy used in building services, like heating and air-conditioning. The reconsideration of the building structure, the readjustment of capital cost allocations and the improvement of equipment and maintenance can minimize the energy expenditure and will lead to consequent reduction in atmospheric pollution.

The reduction of the building energy requirements to a minimum is therefore an important step. This can be achieved by utilizing natural passive heating and cooling techniques, which can be used to modulate heat losses or gains. Heat-gain modulation can be achieved by properly using the thermal mass of the building itself (thermal inertia) in order to absorb and store heat during the daytime hours and return it to the space at a later time.

Combining different natural and passive cooling techniques, it is possible to prevent overheating problems, decrease cooling load and improve indoor thermal comfort conditions. In particular, it is possible to achieve about 20% overall energy conservation in new and existing buildings [2].

To ensure that some economy in fuel expenditure will result, some countries have already introduced standards (e.g. UK Building Regulations) which impose criteria to limit the energy requirements. Such measures include the maximum permissible areas of single glazed windows per exposed wall area, the maximum permissible U values with single glazing, etc.

In Cyprus there are laws covering the static design of the house which ensure that the house will be anti-seismic. Also, there are a number of regulations concerning the aesthetic appearance of the building that apply in certain preserved areas in towns and villages. Finally, there are regulations preventing the construction of wooden houses in built-up areas to avoid fire risks because of the very hot climate. However, there are absolutely no regulations concerning the thermal aspect of buildings. The thermal aspect, although it is of great importance in Cyprus because of the very diverse climate (hot in summer and cold in winter), is just now surfacing. In the past, the thermal aspect was not considered as the traditional house was constructed from massive walls, made from mud and straw blocks of about 0.5 m in thickness. The roof was also well insulated and the height of the building was large allowing thermal stratification. In this way the traditional house was well adapted to the climatic conditions and offered an acceptable living environment.

During the last few years the public showed interest in the air-conditioning of buildings and, particularly, in the heating during winter. Therefore, in the near future, the Government must guide the public towards a more economic approach and impose regulations.

The objective of this paper is to model a typical modern house in Cyprus by considering the various construction methods applied and draw conclusions on the suitable structure that should be used in the Cyprus environment. Initially, the Cyprus energy scene and an analysis of the number of houses employing heating and cooling equipment are presented.

Table 1
Energy consumption for 1994

Energy type	Consumption (TOE)[a]	% of total consumption
Crude	2101	0.17
LPG	48,594	3.67
Gasoline	179,997	13.59
Kerosene	252,366	19.05
Diesel	388,371	29.32
LFO	52,684	3.97
HFO	49,567	3.74
Coal	89,930	6.79
Electricity	174,718	13.19
Solar	86,480	6.53
Total	1,324,808	100.00

[a] TOE (tons of oil equivalent)=41.8 GJ.

2. The Cyprus energy scene

Cyprus has no natural oil resources and relies entirely on imported fuel for its energy demands. The only natural energy resource available in Cyprus is solar energy, which is used extensively for water heating with the utilisation of flat-plate collectors. The annual consumption needs for 1994, according to energy type, are presented in Table 1 [3]. The value for electricity refers to the output from the power stations and not the primary fuel energy input, which was 729,400 tons of oil equivalent (TOE) of heavy fuel oil (HFO).

Because of the rapid economic development during the last few years, mainly due to the expansion in the tourist industry and the rise in the standard of living, there is an increase in the total annual energy consumption. This is indicated in Fig. 1 which lists the total energy consumption during the years 1986–1994.

The energy consumption of various sectors of the economy in TOE, in terms of type of energy

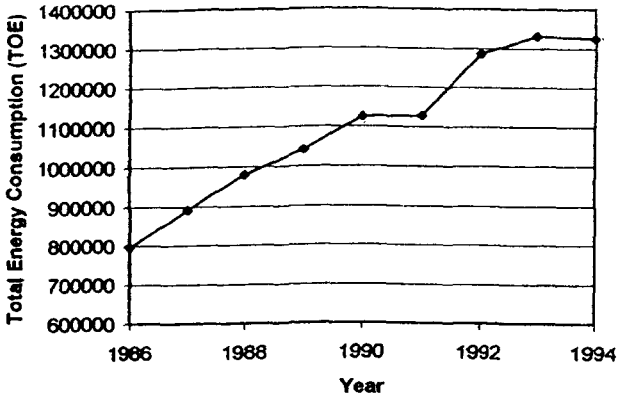

Fig. 1. Total energy consumption for the years 1986–1994.

Table 2
Energy consumption by different sectors of the economy for 1994

Sector	Fuel oil (TOE)	Electricity (TOE)	Solar (TOE)
Agricultural	64,104	5289	–
Commercial	107,432	63,859	5660
Domestic	63,612	58,055	80,820
Industrial	124,476	38,788	–
Transport	611,955	8727	–
Total	971,579	174,718	86,480

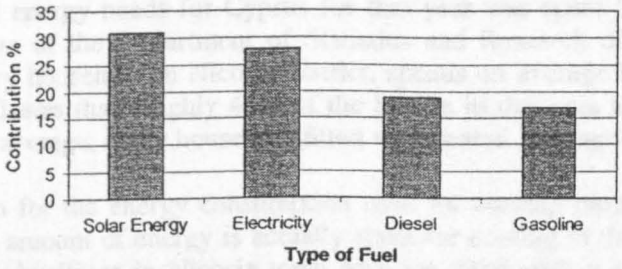

Fig. 2. The contribution of various types of fuel, used for domestic purposes, for 1993.

consumed in 1994, is shown in Table 2. This table shows that, in the domestic sector, there is a fair balance of requirements from the three types of fuels presented. Also, Table 2 shows that solar energy is used almost exclusively (93%) by the domestic sector for hot water production.

An analysis of the available data, for the year 1993, shows that 34% of the total energy consumption was spent for domestic purposes. The contribution of the various types of fuel is shown in Fig. 2.

Table 3 was constructed from unpublished data of the Department of Statistics and Research of the Government of Cyprus and shows the percentage of houses in Nicosia district, with central heating, for the years 1992 and 1997.

Similarly, the corresponding percentage of houses for Nicosia district, with air conditioning,

Table 3
Percentage of houses with central heating, in Nicosia district, for the years 1992 and 1997

Location	1992 (%)	1997 (%)
Town	31.6	46.5
Rural	11.6	29.3

for the years 1992 and 1997 are shown in Table 4. It must be noted that about 10% of these houses are equipped with central air conditioning systems. The rest 90% are equipped with room air conditioning units (split and wall types) with limited use.

The above available data, although not collected on purpose for the determination of the heating and cooling needs, can lead to the following conclusions:

1. From Fig. 2, it is shown that the energy used for heating purposes is approximately equal to the consumption of diesel and gasoline, which is mainly used as fuel for heating. To these figures an 11% of the consumption of electricity for domestic needs must be added, since this amount is spent for off-peak heating [4]. Therefore the total amount used for heating purposes represents 27% of the domestic needs for energy. Since, as mentioned above, the domestic needs for energy for 1993 represents the 34% of the total energy consumption, it is concluded that 9.2% of the total energy needs for Cyprus for that year was spent for heating purposes. From unpublished data of the Department of Statistics and Research of the Government of Cyprus for 1997, every household in Nicosia district, spends on average EUR 117 for heating purposes. Table 3 indicates that roughly 45% of the houses in that area are fitted with central heating. Therefore on average, every household fitted with central heating spends approximately EUR 260 for fuel.
2. There is no indication for the energy consumption used for cooling purposes. It can only be said that a very small amount of energy is actually spent for cooling in the form of electricity, since only 3% of the dwellings in Nicosia town area are fitted with central air conditioning devices. Another 27.2% of the dwellings in Nicosia town area are fitted with a very small number of room air conditioners, which are used for only a few hours every day in summer with a high running expense.
3. During recent years, due to the increase in the standard of living, there is an increasing trend of providing central heating to the houses. This increase for the town of Nicosia from 1992 to 1997, for which period data were collected, is 47%. For the same years there is also an increasing trend of installing room air conditioners for limited use. This increase is 65.9%.

All the above figures show the importance of proper design of houses and the need for accurate prediction of the heating and cooling loads. In this way the proper equipment can be selected to avoid oversizing which will increase further the energy savings of such dwellings.

3. TRNSYS program overview

TRNSYS is a transient systems simulation program with a modular structure and is used in the present study for deriving the results. Each module contains a mathematical model for a

Table 4
Percentage of houses with air conditioning devices, in Nicosia district, for the years 1992 and 1997

Location	1992 (%)	1997 (%)
Town	18.2	30.2
Rural	3.2	8.6

system component. The TRNSYS engine calls the system components based on the input file and iterates at each time-step until the system of equations is solved. The flow diagram of the deck file, written as part of this study is shown in Fig. 3.

For the present study TRNSYS Type 19 model is used to estimate the heating and cooling loads for a typical house. All heating and cooling loads arising from walls, windows, flat roofs and floors are calculated with the Type 19 model, by utilizing the transfer function method [5].

The Type 19 model has two basic modes of operation, i.e., the energy rate and the temperature level control modes. In the study the temperature level control mode is selected, since with this mode the temperature of the building can be maintained between specified limits and the energy required to maintain the zone in the specified temperature is given as output along with the limit temperature. The zone humidity ratio is also allowed to float between a maximum and a minimum limit specified by the user and the humidification or dehumidification energy is considered. Additionally, heat may be added or removed either by the use of a ventilation flow stream or by

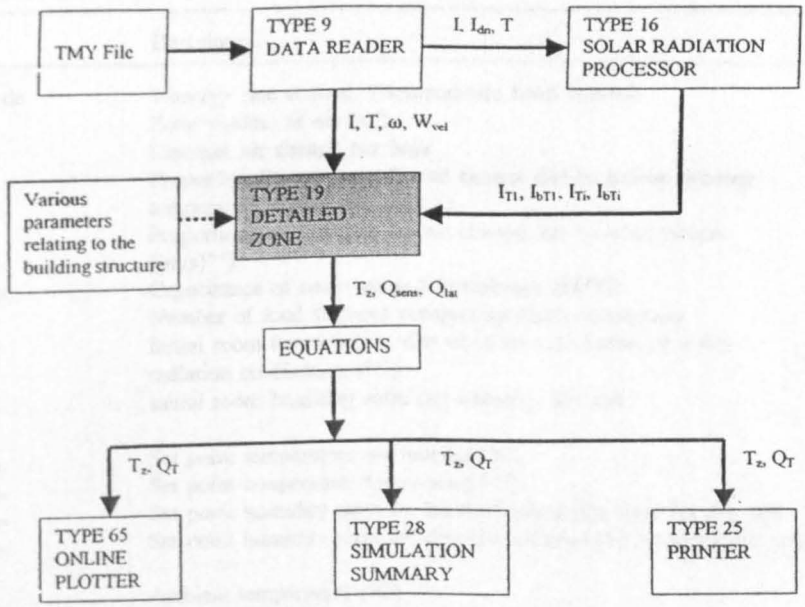

Note: the symbols represent:

I – global solar radiation on a horizontal surface at the next hour (kJ/h)
I_{dn} – direct normal solar radiation at the next hour (kJ/h)
T – dry-bulb temperature at the next time step (°C)
ω – humidity ratio at the next time step
W_{vel} – wind velocity at the next time step (m/s)
I_{T1}, I_{Ti} – total radiation on surface number 1or i (kJ/m^{2}h)
I_{bT1}, I_{bTi} – beam radiation on surface number 1or i (kJ/m^{2}h)
T_z – zone temperature (°C)
Q_{sens} – sensible load (kJ/h)
Q_{lat} – latent load (kJ/h)
Q_T – total load (kJ/h)

Fig. 3. Flow diagram of the TRNSYS deck file.

an instantaneous heat gain input. A controller is used in conjunction with this mode to control the heating or cooling equipment.

The Type 19 model uses the transfer function coefficients for the estimation of the heating and cooling loads. It should be noted that these coefficients should not include radiative resistance at the inside surface. Therefore the standard ASHRAE inside surface resistance E_0 which includes both convective and radiative resistance should not be used.

Because radiation is handled separately by TRNSYS Type 19, only an inside convective resistance of 0.1044 m^2-K-hr/kJ should be included when deriving the transfer function coefficients. This value should also be specified in the parameter list of Type 19 for calculating the sol-air temperatures. The standard ASHRAE external surface resistance A_0 can be used since the wind speed is used only to calculate the sol-air temperature. These coefficients are estimated for each construction using the routine PREP provided with the TRNSYS program. Tables 5–7 indicate

Table 5
Important zone parameters used in the calculations with TRNSYS Type 19

Parameter		Description	Set value[a]
1	Mode	1-energy rate control, 2-temperature level control	1
2	V_a	Zone volume of air (m^3)	147
3	$K1$	Constant air change per hour	0.1
4	$K2$	Proportionality constant for air change due to indoor–outdoor temperature difference $((°C)^{-1})$	0.017
5	$K3$	Proportionality constant for air change due to wind effects $((m/s)^{-1})$	0.049
6	Cap	Capacitance of room air and furnishings (kJ/°C)	500
7	N	Number of total surfaces comprising room description	7
8	T_o	Initial room temperature; also used for calculation of inside radiation coefficients (°C)	15
9	w_o	Initial room humidity ratio (kg water/kg dry air)	0.0075
Mode 1 only			
10	T_{min}	Set point temperature for heating (°C)	21
11	T_{max}	Set point temperature for cooling (°C)	25
12	w_{min}	Set point humidity ratio for humidification (kg water/kg dry air)	0.005
13	w_{max}	Set point humidity ratio for dehumidification (kg water/kg dry air)	0.008
Input number			
1	T_a	Ambient temperature (°C)	*
2	w_a	Ambient humidity ratio (kg water/kg dry air)	*
3	T_v	Temperature of ventilation flow stream (C)	*
4	v	Mass flow rate of ventilation flow stream (kg/hr)	0
5	w_v	Humidity ratio of ventilation flow stream (kg water/kg dry air)	*
6	I	Rate of moisture gain (other than people) (kg/hr)	0
7	N_{people}	Number of people in every zone	1
8	I_{act}	Activity level of people	2
9	Q_{IR}	Radiative energy input due to lights, equipment, etc. (kJ/hr)	750
10	Q_{int}	Sum of all other instantaneous heat gain to space (kJ/hr)	0
11	W	Wind-speed (m/s)	*

[a] *Parameter read from TMY file.

Table 6
Important wall parameters used in the calculations with TRNSYS Type 19

Parameter		Description	Set value
4	r	Reflectance of inner surface to solar radiation	0.7
5	α	Absorptance of exterior surface to solar radiation	0.65
7	h_c	Inside convection coefficient (kJ/hr−m²−C)	9.58

Table 7
Important window parameters used in the calculations with TRNSYS Type 19

Parameter		Description	Set value[a]
5	t_d	Transmittance for diffuse solar radiation	0.833
6	$h_{c,i}$	Inside convection coefficient (kJ/hr−m²−°C)	31.5
7	N_1	Number of surfaces on which transmitted beam radiation strikes	1
8	k	First surface number of which beam of radiation strikes	5
Input number — Window Mode 1			
1	I_T	Total incident radiation (kJ/m²−hr)	*
2	I_{bT}	Incident beam radiation (kJ/m²−hr)	*
3	t	Overall transmittance for solar radiation	0.833
4	U_g	Loss coefficient of window (+ night insulation) not including convection at the inside or outside surface (kJ/hr−m²−°C)	12.3
5	f_k	Fraction of incoming beam radiation that strikes surface k	1

[a] *Parameter calculated by the solar radiation processor.

the important parameters used in the calculations with TRNSYS Type 19. The parameter number shown in these Tables refer to the TRNSYS numbering system.

For calculating the losses of the floor area the following equation is used [6]:

$$q=F_2P(t_i-t_o) \tag{1}$$

where: q=heat loss through perimeter (W); F_2=heat loss coefficient per meter of perimeter (W/m−K); P=perimeter of exposed edge of floor (m); t_i=indoor temperature (°C); t_o=outdoor temperature (°C).

TRNSYS runs through hourly values of various weather parameters included in a typical meteorological year (TMY) file. The general climatic conditions of Cyprus are mostly very sunny with an average solar radiation of 5.4 kWh/m² per day on a horizontal surface. This radiation is among the highest in the world and the solar energy input is particularly high during the dry summer that lasts from April to October. During the rest of the year sunshine duration remains considerable even in the coldest months. Weather data are needed to perform the simulations with TRNSYS. The Typical Meteorological Year (TMY) for Nicosia–Cyprus, developed by Petrakis et al. [7], is used. These have been generated from hourly measurements of solar irradiance (global and diffuse on horizontal surface), for a seven-year period from 1986 to 1992.

4. Model house construction

TRNSYS model 19 is used in order to simulate the temperature variation observed within a typical house in Nicosia–Cyprus. The model house illustrated in Fig. 4 has a floor area of 196 m^2 and consists of four identical external walls, 14 m in length by 3 m in height, with a total window opening of 5.2 m^2 on each wall.

The window area is approximately equal to the area that a typical house would have, but instead of considering a number of windows on each wall, only one window is considered. Since the same model will be used in evaluating the load for various constructions this simplification is not important but will assist in drawing conclusions since similar constructions are present on every wall. The model house is further divided into four identical zones and the partition walls are considered as walls separating the four zones. For every zone a separate TRNSYS Type 19 unit is necessary.

The houses in Cyprus are usually built with hollow bricks made of fired clay. The usual density of these bricks is 940 kg/m^3 with a thermal conductivity of 0.310 W/mK, for a temperature difference of 15°C (20–35°C).

5. Results/discussion

This section presents the simulated inside temperatures and loads of the model house obtained by TRNSYS and the TMY weather file.

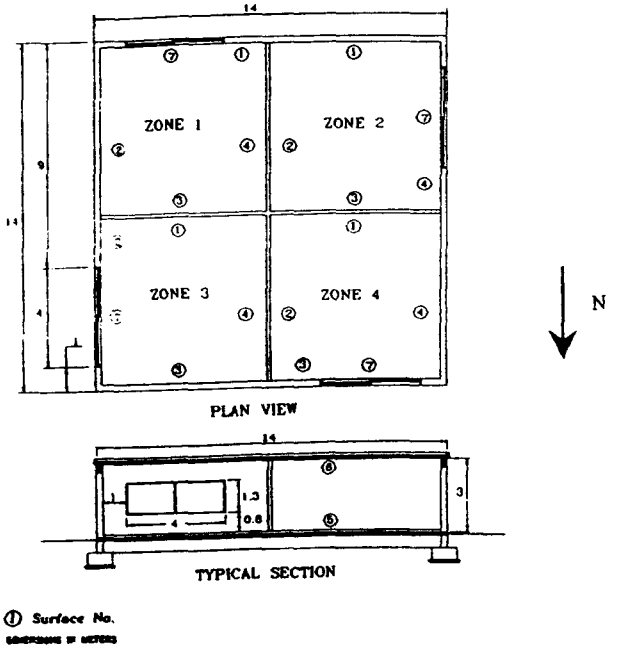

Fig. 4. Model house.

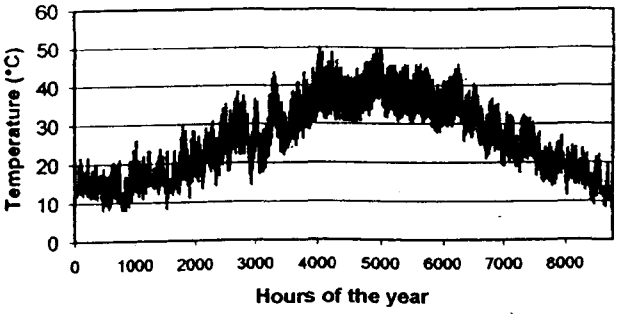

Fig. 5. Temperature variation of a typical house for each hour of a typical year.

The hourly response of the model house during a typical year is shown in Fig. 5. The temperature varies approximately between 10–20°C during winter and raises to 30–50°C during summer.

Since the model house is divided in four similar zones, the load resulting from each zone can be observed. In mid-January (Fig. 6) the S–E zone (1) gives the highest temperature and thus the lowest load. The N–W zone (4) gives the highest load. It is also of interest to observe the effect of the direct sun radiation falling on the N–E zone (3) during the morning hours which causes the zone temperature during this time to increase abruptly.

During mid July (Fig. 7), the N–E zone (3) maintains a higher temperature during the day and this causes the highest load. This is due to the fact that the sun faces the North and East walls from the early morning hours.

The annual cooling and heating loads per unit area arising from every zone, is indicated in Table 8. These loads are estimated by considering that the room temperature is maintained at 25°C during summer and 21°C during winter. As it is observed the cooling load is bigger for the N–E and S–E zones and the heating load is bigger for the N–W and S–W zones where the gains from the environment are smaller.

An analysis of the heat gains and losses arising from every element of the model house is shown in Table 9. As it is observed the main load is due to the roof construction, which must

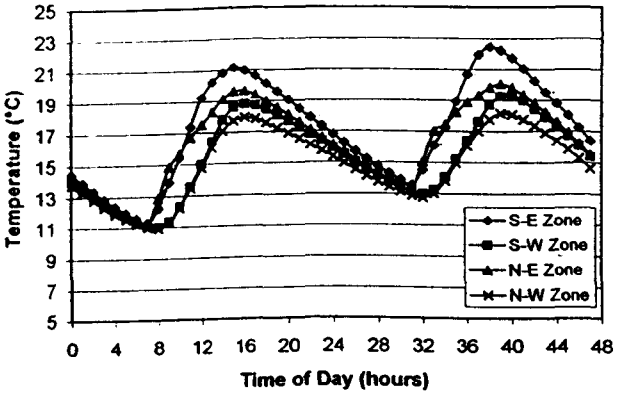

Fig. 6. Zone temperatures during the 13th and 14th of January.

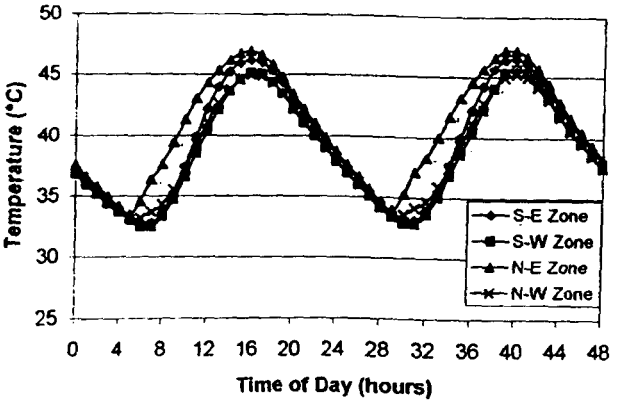

Fig. 7. Zone temperatures during the 16th and 17th of July.

Table 8
Annual zone cooling and heating load per unit floor area

Zone	Cooling load (kWh/m²) for 25°C	Heating load (kWh/m²) for 21°C
S–E (Z1)	227.9	73.8
S–W (Z2)	201.7	86.3
N–E (Z3)	239.6	75.5
N–W (Z4)	196.4	91.5

Table 9
Heat gains and losses arising from every constructional element of the model house

House Element	Heat Gains (kWh/m²) for 25°C	Heat losses (kWh/m²) for 21°C
External South wall	46.6	14.8
External East wall	61.3	12.7
External North wall	43.2	18.5
External West wall	38.1	20.6
Floor	48.7	14.8
Roof	80.2	32.6
South window	68.8	81.9
East window	63.1	84.6
North window	61.5	86.0
West window	71.0	82.1
Walls between zones	44.3	9.2
Other	6.9	5.0

be well insulated. Concerning the wall orientation, the heat gains are higher for the East and South external walls which receive and transfer inside the house more solar heat during the early hours of the summer days. The large difference observed between the load of the external East and West walls is due to the fact that the East wall warms earlier during the morning hours and maintains its temperature throughout the day. The West wall is cool in the morning hours and is exposed to the afternoon westward winds, which usually blow during the summer, thus keeping the wall temperature low.

The heating load is higher for the North and West external walls since they receive and transfer less solar heat during the winter days.

The load from the windows, shown in Table 9, is about the same irrespective of the window orientation. The reason for this is that the transmitted solar and thermal energy is calculated internally, considering that this energy is striking the floor. Also the walls between zones give loads approximately equal to the external wall loads. The reason for this phenomenon is that these walls are modelled in the same manner as the external walls, with the exception that the sol-air temperature is replaced by an equivalent zone temperature. The equivalent zone temperature is the temperature of the adjacent zone which in the absence of all radiation exchanges gives the same heat transfer at the inside of adjacent zone surface as actually occurs.

5.1. *Load analysis of various construction methods*

In this section the effect on the house temperature that various wall construction methods present is investigated. The analysis is performed for the following three cases:

1. 0.2 m single hollow brick wall with 0.02 m plaster on each side,
2. double-wall with 0.1 m hollow brick and 0.02 m plaster on each side and a layer of 0.025 m insulation in between, and
3. double-wall with 0.1 m hollow brick and 0.02 m plaster on each side and a layer of 0.05 m insulation in between.

It must be noted that in all the above cases a non-insulated roof, constructed from fair–face 0.15 m heavy concrete was assumed. This roof type is a common construction method. The results shown in Fig. 8 for winter and Fig. 9 for summer indicate that the wall type is not of any

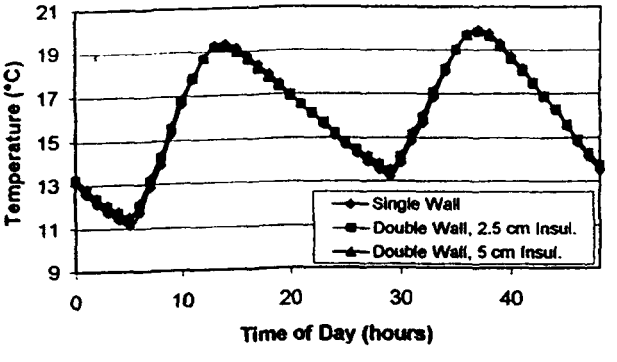

Fig. 8. Temperature variation for various wall constructions during the 13th and 14th of January.

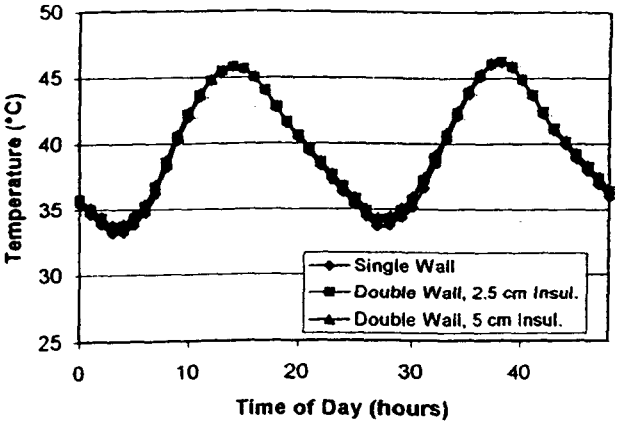

Fig. 9. Temperature variation for various wall constructions during the 16th and 17th of July.

importance as during the whole year the temperature variation in the model house is extremely small.

This of course does not mean that the wall insulation is completely useless. The variation of the heating load can be seen in Fig. 10, where the hourly heating load for two January days is plotted, for two types of wall construction. As it is seen, a reduction of the heating load of a maximum of 0.5 kWh results in every case.

The value of the wall insulation is better understood if the heating and cooling load is calculated throughout the year and summed in order to evaluate any savings. The results for keeping the temperature in the range of 18–25°C and the humidity ratio between 0.005–0.008 (kg water/kg dry air) are indicated in Table 10. Thus for keeping the temperature at 25°C, a cooling load of 42,300 kWh is needed for the single wall construction. A load reduction of 1.8% results for a double wall with 2.5 cm insulation and a reduction of 2.4% results for a double wall with 5 cm insulation. The heating load presents a reduction of 7.9–9.4% for a double wall with 2.5 cm insulation and a reduction of 10.6–12.5% for a double wall with 5 cm insulation for maintaining

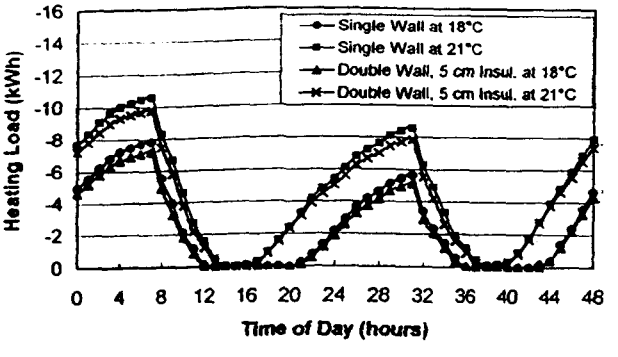

Fig. 10. Heating load (kWh) against time of day (hours), during the 13th and 14th of January, for keeping the inside temperature at 18°C and 21°C.

Table 10
Annual cooling and heating loads for keeping the model house at various room temperatures

Load	Single wall (kWh)	Double wall with 2.5 cm insulation		Double wall with 5 cm insulation	
		(kWh)	% load reduction	(kWh)	% load reduction
Cooling at 25°C	42,300	41,550	1.8	41,300	2.4
Heating at 18°C	8260	7485	9.4	7226	12.5
Heating at 19.5°C	11,792	10,786	8.5	10,445	11.4
Heating at 21°C	16,012	14,746	7.9	14,312	10.6

the house temperature at 18–21°C. It is also important to note that by increasing the house temperature from 18°C to 21°C, the heating load is approximately doubled.

The importance of the roof construction is subsequently evaluated. For this test, runs are performed for a 0.2 m single hollow brick wall with 0.02 m plaster on each side and the following three variations in roof construction:

1. a non-insulated roof constructed from fair–face 0.15 m heavy concrete,
2. insulated roof constructed from fair–face 15 cm heavy concrete, 2.5 cm polystyrene insulation, 7 cm screed and 0.4 cm asphalt covered with aluminum paint of 0.55 solar absorptivity, and
3. insulated roof constructed from fair–face 15 cm heavy concrete, 5 cm polystyrene insulation, 7 cm screed and 0.4 cm asphalt covered with aluminum paint of 0.55 solar absorptivity.

The temperature variation inside the model house can be observed in Figs. 11 and 12 for typical winter and summer days respectively. It is obvious, a major saving can result for insulating the roof. In winter (Fig. 11), there is a temperature increase in the room of a maximum of 4°C for an insulated roof and the temperature variation is closer to the required room temperature. In summer (Fig. 12), the insulated roof does not allow the room temperature to exceed 40°C while with a non-insulated roof the temperature rises up to 46°C, i.e., a significant reduction in the resulting room temperature is obtained. An analysis of the annual cooling and heating loads for

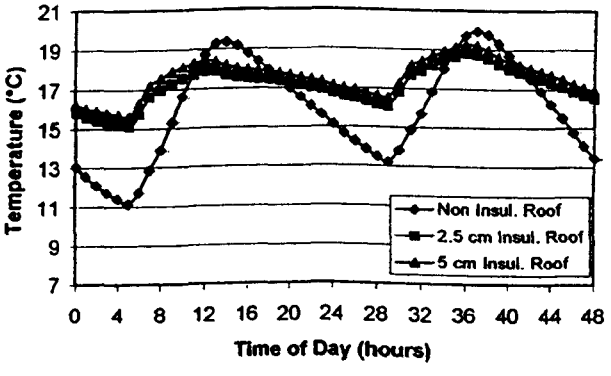

Fig. 11. Temperature variation for various roof constructions during the 13th and 14th of January.

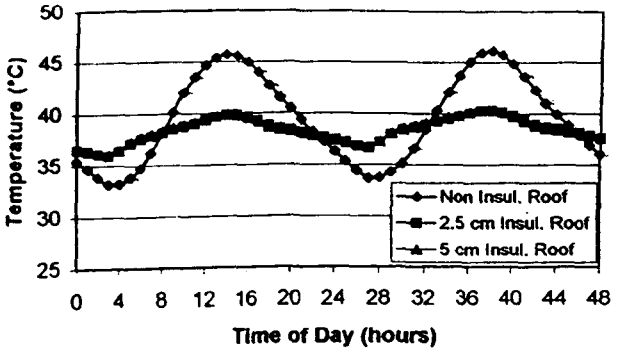

Fig. 12. Temperature variation for various roof constructions during the 16th and 17th of July.

various roof constructions for keeping the model house at various room temperatures is indicated in Table 11.

Thus for keeping the house temperature at 25°C, a cooling load of 42,300 kWh is needed for the single wall construction. A load reduction of 41.7% results for a roof insulation of 2.5 cm and a reduction of 45.5% results for a roof with 5 cm insulation. The heating load presents a reduction of 68.1% for a roof with 2.5 cm insulation and a reduction of 75.1% for a roof with 5 cm insulation for maintaining the house temperature at 18°C. Maintaining the model house at 19.5°C, a saving of 63.1% results for 2.5 cm insulation and 70.3% for 5 cm insulation. At 21°C the respective saving is 59.4% for 2.5 cm insulation and 66.6% for 5 cm insulation.

5.2. *Effect of ventilation*

ASHRAE Standard 62.2 P, ventilation and acceptable indoor air quality in low-rise residential buildings, specifies the minimum requirements for mechanical and natural ventilation in spaces intended for human occupancy within single-family houses and low-rise multifamily structures. For a model house of 196 m^2, assuming three bedrooms as in practice, the required mechanical and or natural ventilation is about 0.31 air changes per hour (ACH). This requirement, according to a study in the current stock of buildings in USA, can be met through infiltration alone, since

Table 11
Annual cooling and heating loads for various roof constructions, keeping the model house at various room temperatures

Load	Single wall no-roof insulation (kWh)	Single wall with 2.5 cm roof		Single wall with 5 cm roof	
		insulation (kWh)	% load reduction	insulation (kWh)	% load reduction
Cooling at 25°C	42,300	24,660	41.7	23,050	45.5
Heating at 18°C	8260	2636	68.1	2055	75.1
Heating at 19.5°C	11,792	4355	63.1	3500	70.3
Heating at 21°C	16,012	6506	59.4	5348	66.6

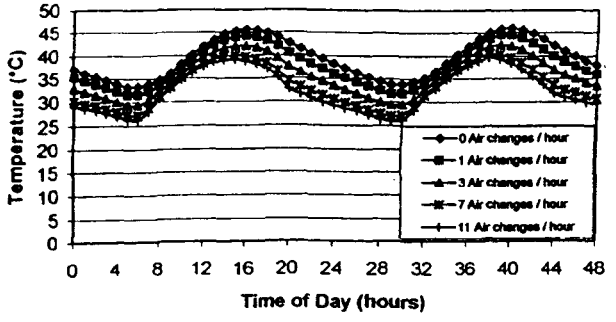

Fig. 13. Temperature variation of a typical house indicating the effect of ventilation during the 16th and 17th of July.

the buildings are quite leaky [8]. Also, according to Balaras [2], new buildings allow for 0.2–0.5 air changes per hour by infiltration, while with the windows wide open during summer it is possible to achieve 15–20 ACH. The formula used in the calculations for TRNSYS Type 19 exceeds the requirements in the majority of the hours of the day, with the rest of the cases being near the required ACH. For this reason no extra rate of ventilation flow stream (v, in Table 5) was introduced in the calculations.

In this section the effect of introducing naturally or mechanically ambient air into the space when the outdoor air is of a lower temperature than the indoor air during summer and visa-versa during winter is investigated.

The simulations show that the effect on the house temperature that this amount of ventilation air will have, when the outside temperature is greater than the house temperature in winter, is negligible. In summer when ventilation air enters into the house whenever the outside temperature is less than the house temperature and the room is not conditioned is indicated in Fig. 13.

Obviously the ventilation has an effect depending on the number of air changes per hour. This effect is further illustrated in Fig. 14, where in July the maximum temperature of a 0.2 m brick house without roof insulation, can reach 46°C. With ventilation, this temperature will be less by about 2°C for one air change per hour, 3°C for two air changes per hour and so on, reaching 7°C for eleven air changes per hour. Also as illustrated in Fig. 14, the effect of ventilation on the house temperature is about the same for a house with roof insulation.

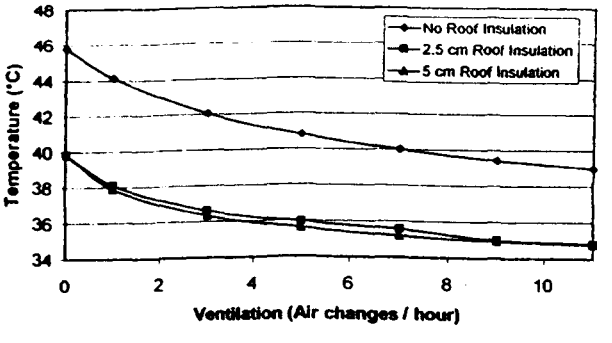

Fig. 14. Ventilation effect on different types of construction.

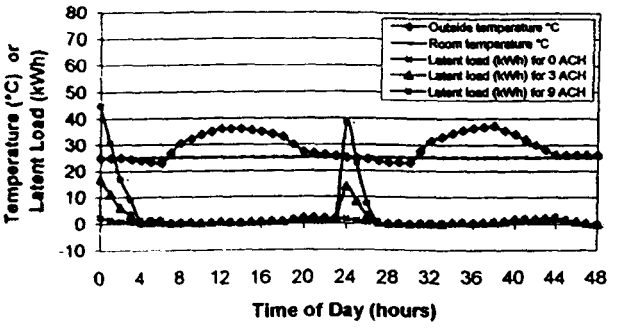

Fig. 15. Latent heat load introduced in the house, for various ventilation rates as it occurs during the 16th and 17th of July.

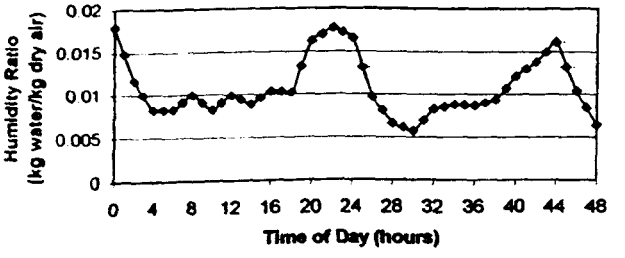

Fig. 16. Humidity ratio as occurs in two consecutive days during the 16th and 17th of July.

When the model house is maintained at 25°C, increasing the ventilation (air changes per hour) does not mean that the cooling effect will be increased, as happens in the above case. Fig. 15 shows the latent heat load introduced in the house, for various ventilation rates and for the humidity ratio illustrated in Fig. 16. By increasing the ventilation rate at certain hours, when the outside temperature is lower than the house temperature, a greater latent load may be introduced when the humidity ratio is greater than 0.008 kg of water per kg of dry air. This load obviously increases when the mass of air is greater.

By utilising an intelligent control unit that would allow air to enter the house only when it would produce a useful cooling effect, the graph indicated in Fig. 17 is obtained. As it is seen

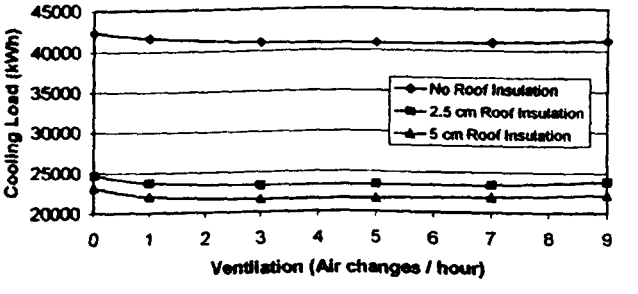

Fig. 17. The effect of ventilation on the annual cooling load for maintaining the model house at 25°C.

the maximum reduction on the cooling load, for maintaining the model house at 25°C, is obtained at three to five air changes per hour, which is the optimum rate for houses employing the three roof types examined.

Table 12 presents the annual cooling and heating loads for various roof constructions. As it is seen, in winter there is no appreciable load reduction arising from ventilation. In summer, ventilation leads to a reduction of about 1.6% to 6.3%, provided that the control unit will shut off ventilation when the sensible cooling effect produced is smaller than the latent load introduced.

5.3. *Effect of internal shading*

In this section an analysis of the impact of window shading on the cooling load is presented. For the following results, approximately half the transmittance (0.4 instead of 0.833) for solar radiation was used in the calculations, corresponding to a Venetian blind shading device. Table 13 presents the results of the simulations. As it is observed, a saving in the cooling load of 3300–4600 kWh can result, depending on the construction type. The saving increases with the amount of insulation of the construction resulting in savings of 8–20% of the cooling loads.

5.4. *Inclined roofs*

Finally the effect of constructing an inclined roof instead of the traditional flat roof is examined. This is a construction mostly applied nowadays in Cyprus mainly due to aesthetic reasons. As it is seen in Table 14, the inclined roof results in an increase of load between 5.3% and 13.2% depending on its orientation and time of year, when constructed in the same way as the flat roof.

Table 12
Annual cooling and heating loads for various roof constructions indicating the effect of ventilation

Ventilation (air changes per hour)	Process	Single wall no-roof insulation		Single wall with 2.5 cm roof insulation		Single wall with 5 cm roof insulation	
		Load (kWh)	Load reduction (%)	Load (kWh)	Load reduction (%)	Load (kWh)	Load reduction (%)
0	Cooling at 25°C	42,300	–	24,660	–	23,050	–
	Heating at 21°C	16,012	–	6506	–	5348	–
1	Cooling at 25°C	41,606	1.6	23,688	3.9	22,007	4.5
	Heating at 21°C	16,012	0.0	6504	0.0	5347	0.0
3	Cooling at 25°C	40,997	3.1	23,301	5.5	21,595	6.3
	Heating at 21°C	15,999	0.1	6500	0.1	5345	0.1
5	Cooling at 25°C	40,870	3.4	23,405	5.1	21,673	6.0
	Heating at 21°C	15,979	0.2	6496	0.2	5342	0.1
7	Cooling at 25°C	40,969	3.1	23,433	5.0	21,890	5.0
	Heating at 21°C	15,967	0.3	6489	0.3	5338	0.2
9	Cooling at 25°C	41,196	2.6	23,921	3.0	22,182	3.8
	Heating at 21°C	15,948	0.4	6490	0.2	5339	0.2

Table 13
Effect of window shading on annual cooling loads

Wall and roof construction	Cooling load (kWh)	Cooling load with window shading (kWh)	Cooling load difference (kWh)	Cooling load difference %
Single wall, no roof insulation	42,300	39,012	3288	7.8
Double wall with 5 cm insulation, no roof insulation	41,300	37,862	3538	8.6
Single wall, 5 cm roof insulation	23,050	18,464	4586	19.9

It must be noted though, that for the inclined roof the typical construction is 15 cm heavyweight concrete, 0.4 cm asphalt for waterproofing, 5 cm plaster and clay tile on top. This construction, used as a decorative element, is an imitation of the traditional roof (made from a wood frame and tiles) and results in a reduction of the air-conditioning load of about 41–55%.

6. Economic analysis

The method employed for the economic study is the life savings analysis. This method takes into account the time value of money and allows detailed consideration of the complete range of costs. Insulated buildings are generally characterized by high initial cost and low operating costs due to improved thermal resistance of the building envelope. Thus, the basic economic problem is that of comparing an initial known investment with the estimated future operating costs.

Life cycle cost (LCC) is the sum of all the costs associated with an energy delivery system over its lifetime in today's money, and takes into account the time value of money. The life cycle savings (LCS), for an insulated building, is defined as the difference between the LCC of a non-insulated building and the LCC of an insulated one. This is equivalent to the total present worth (PW) of the gains from the reduced fuel and electricity costs for an insulated building compared to the fuel and electricity costs for a non-insulated one.

6.1. Method description

The parameters required for the various calculations are shown in Fig. 18.

With reference to Fig. 18, by multiplying the area dependent cost with the wall or roof area the total cost of the insulation related to the size of the building is obtained. The total system cost can be obtained by adding to the above the area independent cost, which refers to labour.

The analysis is performed annually and the following amounts are evaluated [9]:

— Fuel savings
— Extra mortgage payment
— Electricity savings

Table 14
Annual cooling and heating loads for flat and inclined roofs

Load	Flat concrete roof, no insulation (kWh)	N–S, 15° Inclined roof				E–W, 15° Inclined roof			
		Concrete roof, no insulation	% Load Increase	Tile, plaster and insulation on concrete roof	% Load decrease	Concrete roof, no insulation	% Load Increase	Tile, plaster and insulation on concrete roof	% Load decrease
Cooling at 25°C	42,300	44,545	5.3	24,960	41.0	45,098	6.6	24,750	41.5
Heating at 21°C	16,012	18,122	13.2	7280	54.5	17,981	12.3	7257	54.7

INPUT PARAMETERS	VALUE	UNITS
Fuel inflation rate	6	%
Area	168 m^2 (wall) or 196 m^2 (roof)	m^2
Area dependent extra cost:		
Double wall, 2.5 cm polystyrene insulation:	5.69	EUR/m^2
Double wall, 5 cm polystyrene insulation:	7.87	EUR/m^2
Insulated roof, 2.5 cm polystyrene insulation:	17.5	EUR/m^2
Insulated roof, 5 cm polystyrene insulation:	22.75	EUR/m^2
Inclined roof, tile covered:	26.25	EUR/m^2
Area independent cost	0	EUR
Annual market discount rate	8	%
Price of electricity	0.092	EUR/kWh
Annual increase in electricity cost	2.6	%

Fig. 18. Economic analysis input parameters.

— Extra tax savings
— Building energy savings

The word "extra" appearing in some of the above items assumes that the associated cost is also present for a non-insulated building and therefore only the extra part of the cost incurred by the installation of the insulation should be included. The inflation, over the period of economic analysis, of the fuel savings is estimated by using the equation:

$$F=c(1+i)^{N-1} \tag{2}$$

Where i is the fuel annual inflation rate, c the purchase cost at the end of year N, and F the future fuel cost.

The income tax law varies from country to country. In Cyprus, the law determines that interests paid for loans made for building a house are tax relieved up to EUR 875. Actually the interest paid each year is subtracted from the income, or 40% of what is paid for interests is reclaimed. The equation used for the tax savings estimation is:

$$\text{Tax savings}=0.4\ [\text{Interest paid}] \tag{3}$$

The building energy savings can be represented in the following equation form:

$$\text{Building energy savings}=\text{Extra mortgage payment}+\text{Electricity savings}+\text{Fuel savings}+\text{Extra tax savings} \tag{4}$$

Actually the savings are positive and the costs are negative. In this case appropriate signs have been used. Finally the present worth of each year's savings is determined by using equation:

$$P=F/(1+d)^N \tag{5}$$

where F is the cash flow, occurring N years from now, reduced to its present value P, and d is

the market discount rate (%). The values of P's are added for all years considered to give the total PW of the building energy consumption over its life.

Applying the method described above for the various construction methods studied, the results indicated in Table 15 were obtained.

As it is observed the double wall construction method pays back the initial capital expenditure. Looking at it from the environmental point of view and the saving in fuel, which is imported, it is advisable to do. The main load in the building comes from the roof, therefore its insulation results in large savings of up to EUR 22,374 for a 20-year period, depending on the construction. It should be noted that these numbers refer to savings in fuel and electricity when the building is conditioned at all hours of the year.

7. Conclusions

The objective of this work was to investigate a typical house heating and cooling load variation for various building constructions encountered in Cyprus. This was achieved by using the TRNSYS program, which performs the above analysis by employing the transfer function method. For the calculations, a typical meteorological year for the Nicosia area and a typical model house are used.

The Cyprus energy scene and an analysis of the number of houses employing heating and cooling equipment is presented from which it is observed that the number of systems installed has increased tremendously during the last decade.

The results of the simulation indicate that the inside house temperature, when no air-conditioning is used, varies between 10–20°C for winter and between 30–50°C for summer. The evaluation of the heating and cooling loads for various wall and roof constructions indicates the importance of the roof insulation, which results in a reduction up to 45.5% of the cooling load and up to 75% of the heating load.

Also the effects of ventilation, and window shading, as well as that of the inclined concrete roof used for aesthetic reasons, are examined. Air is allowed to enter the house, when in winter the outside temperature is higher than the house temperature and vice versa in summer. This analysis indicates that in winter there is no appreciable effect whereas in summer it leads to a maximum saving of 6.3% with an optimum of 3–5 air changes per hour. Window shading in summer, results in savings of 8–20% of the cooling loads with the savings increasing with the

Table 15
Saving in EUR for cooling at 25°C and heating at 21°C for a 20 year period

Type of construction	Saving in EUR
Double wall with 2.5 cm insulation	473
Double wall with 5 cm insulation	593
Single wall with 2.5 cm roof insulation	20,185
Single wall with 5 cm roof insulation	22,374
N–S, Inclined roof tile covered	18,055
E–W, Inclined roof tile covered	18,300

amount of insulation of the construction. The inclined roof results in an increase of load between 5.3% and 13.2% depending on its orientation and time of year, when constructed in the same way as the flat roof. The inclined roof, used as a decorative element, is an imitation of the traditional roof and results in a reduction of the air-conditioning load of about 41–55%.

It should be noted that the results presented in this paper have not been experimentally verified. A verification of the results can be performed using an energy model house tested under actual weather conditions. By recording the actual weather data and running TRNSYS with them the simulations can be validated.

Finally a feasibility study is presented. The life cycle cost analysis is used for the economic analysis of the various building constructions considered. The results indicate that the wall insulation pays back in a twenty year period whereas the roof insulation has considerable economic benefit with life cycle savings up to EUR 22,374 depending on the room temperature and the insulation thickness.

References

[1] Santamouris M, Argiriou A, Dascalaki E, Balaras CA, Gaglia A. Energy characteristics and savings potentials in office buildings. Solar Energy 1994;52:59–66.
[2] Balaras C. Cooling in buildings. In: Santamouris M, Asimakopoulos D, editors. Passive cooling of buildings. 1997:1–34.
[3] Kalogirou S. Solar water heating in Cyprus. Current status of technology and problems. Renew Energy J 1997;10(1):107–12.
[4] Centre of Applied Research of Cyprus College. Research for the collection of data in relation to the fuel expenditure for various groups of consumers (in Greek). A research for the Ministry of Commerce, Industry and Tourism, 1994.
[5] Klein et al. TRNSYS manual, University of Wisconsin, 1998.
[6] ASHRAE Handbook of Fundamentals, 1997.
[7] Petrakis M, Kambezides HD, Lykoudis S, Adamopoullos AD, Kassomenos P, Michaelides IM, Kalogirou SA, Roditis G, Chrysis I, Hadjigianni A. Generation of a typical meteorological year for Nicosia Cyprus. Renew Energy 1998;13(3):381–8.
[8] Sherman M. Indoor air quality for residential buildings. ASHRAE J., 1999:26–30.
[9] Kalogirou S. Economic analysis of solar energy systems using spreadsheets. Proc 4th World Renew Energy Cong Denver, Colorado, USA 1996;2:1303–7.

APPENDIX 9

Paper published in 'Renewable Energy'

PERGAMON

Renewable Energy 23 (2001) 219–234

RENEWABLE ENERGY

www.elsevier.nl/locate/renene

Evolution of domestic dwellings in Cyprus and energy analysis

G.A. Florides [a], S.A. Tassou [b], S.A. Kalogirou [a,*], L.C. Wrobel [b]

[a] *Mechanical Engineering Department, Higher Technical Institute, P.O. Box 20423, Nicosia, Cyprus*
[b] *Mechanical Engineering Department, Brunel University, Uxbridge, Middlesex UB8 3PH, UK*

Received 2 May 2000; accepted 19 July 2000

Abstract

This study describes the evolution of domestic dwellings in Cyprus during the twentieth century with respect to their heating and cooling requirements. The methods of construction employed and materials used are also presented. TRNSYS is used for modelling and simulation of the energy flows of various types of houses. For the calculations, a typical meteorological year for the Nicosia area and a typical model plan of a house are used. The inside house temperature, for the various construction methods, when no air-conditioning is used, is estimated. The temperature inside the traditional house varies in a similar manner with a well-insulated modern house. This variation is 16–20°C for winter and between 25–35°C for summer compared to 11–20°C for winter and 33–46°C for summer for a non-insulated house with a flat roof. The summer temperatures drop considerably, by about 5°C, when ventilation air is used for cooling, depending on the number of air changes.

1. Introduction

The objective of this study is to describe the evolution of domestic dwellings in Cyprus during the twentieth century with respect to their heating and cooling requirements. The houses in Cyprus changed radically in three phases during the last century. At the early years of the century, houses were constructed from easily obtainable local materials. Between 1960–1985 the construction changed to more readily available industrial materials like brick and concrete, resulting in a very cheap

* Corresponding author. Tel.: +357-2-306266; fax: +357-2-494953.
E-mail address: skalogir@spidernet.com.cy (S.A. Kalogirou).

0960-1481/01/$ - see front matter
PII: S0960-1481(00)00160-9

construction and gradually from 1985 onwards to a more insulated and expensive construction.

Cyprus is called the "Sun Island" because sun shines for about 300 days per year, which implies that solar energy is in abundance in the island. During summer time (in July), mean monthly temperatures for Nicosia, at 14.00 hours are about 35°C with the temperature sometimes reaching 42°C, which results in a consequent increase of the indoor temperature. Therefore in order to simulate the behaviour of a dwelling, there is a need to use a program that will give in addition to the heating and cooling loads, the daily variation of the indoor temperature of a house.

For this purpose the TRNSYS program is used for modelling and simulating the energy flows of the traditional and modern houses of Cyprus. TRNSYS is an acronym for a "transient simulation program" and is a quasi-steady simulation model. This program was developed by the University of Wisconsin by the members of the Solar Energy Laboratory [1] and is written in ANSII standard Fortran-77. The program consists of many subroutines that model subsystem components. The mathematical models for the sub-system components are given in terms of their ordinary differential or algebraic equations.

With a program such as TRNSYS which has the capability of interconnecting system components in any desired manner, solving differential equations and facilitating information output, the entire problem of system simulation reduces to a problem of identifying all the components that comprise the particular system and formulating a general mathematical description for each.

For the present study, TRNSYS Type 19 model is used to estimate the heating and cooling loads. All heating and cooling loads arising from walls, windows, flat roofs and floors are calculated by utilising the transfer function method. The Type 19 model has two basic modes of operation, i.e., the energy rate and the temperature level control modes. In the study the temperature level control mode is selected, since with this mode the temperature of the building can be maintained between specified limits and the energy required to maintain the zone in the specified temperature is given as output along with the limit temperature. The zone humidity ratio is also allowed to float between a maximum and a minimum limit specified by the user and the humidification or dehumidification energy is considered. The indoor design temperatures are crucial for estimating the heating and cooling loads. In this case, 21°C for winter and 25°C for summer were considered, which are widely accepted levels of temperature for comfort conditions.

The Type 19 model uses the transfer function coefficients for the estimation of the heating and cooling loads. These coefficients are estimated for the wall and roof type of each construction using the routine PREP provided with the TRNSYS program.

TRNSYS runs through hourly values of various weather parameters included in a typical meteorological year (TMY) file. The general climatic conditions of Cyprus are mostly very sunny with an average solar radiation of 5.4 kWh/m^2 per day on a horizontal surface. This radiation is among the highest in the world and the solar energy input is particularly high during the dry summer that lasts from April to October. During the rest of the year, the duration of sunshine remains considerable

even in the coldest months. Weather data are needed to perform the simulations with TRNSYS. For this purpose the Typical Meteorological Year (TMY) data for Nicosia, Cyprus, developed by Petrakis et al. [2], are used. These have been generated from hourly measurements, of solar irradiance (global and diffuse on a horizontal surface), for a seven-year period, from 1986 to 1992. The measurements were performed by the Meteorological Service of the Ministry of Agriculture and Natural Resources of Cyprus, at the Athalassa region, an area located in the suburbs of Nicosia.

Section 2 of the paper presents the evolution of the buildings in Cyprus during the last century. This is followed by the analysis of the heating and cooling requirements of the buildings and the maximum and minimum resulting temperatures. The comfort conditions created from the various constructions applied over the years are presented. The last section gives the conclusions gleaned from this study.

2. Evolution of domestic dwellings in Cyprus

Traditional houses of Cyprus were developed through experience to meet the everyday needs of the occupants and provide comfort. Availability of materials, functionality, climate, topography and style were the major factors that were considered in the construction of the houses. The building materials were chosen according to their local availability and consequently the buildings were in harmony with the environment. In places like the mountain areas, stones that were the prevailing material, were used for building the walls. Wood, bush branches, soil and clay tiles were used for the construction of the roof. In the valleys like Mesaoria, which is the area around the capital Nicosia, the stones were replaced with mud mixed with straw for the construction of the walls. The walls were also covered with gypsum plastering on both sides. Additionally, marble plates were placed on the top end of the walls, projecting to the outer sides, for protecting the wall surface from the rain (Fig. 1).

The foundation of these buildings was very simple. A shallow trench, 0.5 m wide by 0.5 m deep was usually excavated along the length of the walls. The trench was filled with large blocks of stone and was raised about 0.5 m above the ground level. In this way a stable base for the wall was constructed and the wall was also protected from the rain-water and moisture (Fig. 2).

The most important constructional element is that the walls were built from blocks of mud mixed with straw, as mentioned above. These blocks had standard dimensions of 30 cm (length) by 45 cm (width) by 5 cm (thickness). The finished wall had also a layer of gypsum plaster covering each side and the total width of the walls was 50 cm. This wall thickness was necessary since no supporting columns were used for the roof and the walls took all the weight. The height of the house was also important. In the middle the roof reached 5–6 m and at the corners about 4 m. In this way the ratio of volume to the external area exposed to solar radiation is increased. This increase is preferable for a building that it is desired to heat up slowly. During summer, in low latitudes, the surface most exposed to solar radiation is the roof. High ceilings, which are traditionally met in hot climates, have little

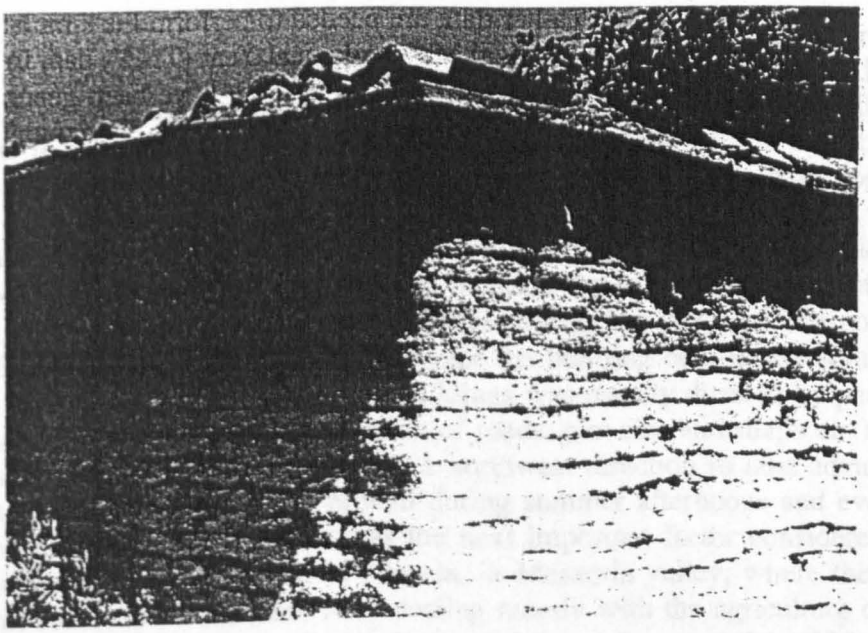

Fig. 1. Roof and wall of a Mesaoria house.

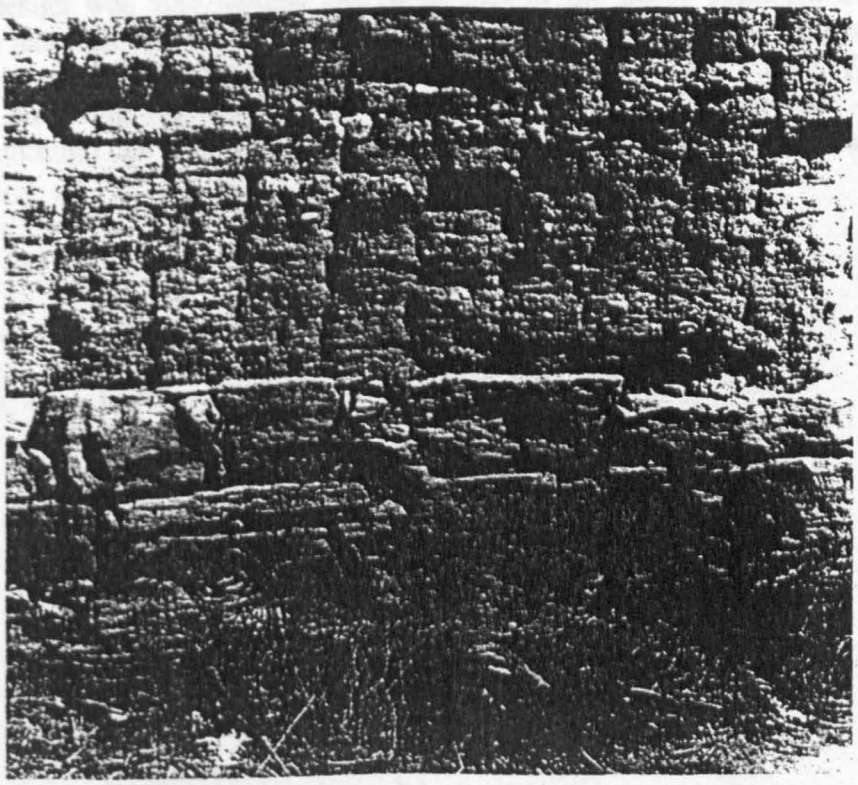

Fig. 2. Stone blocks were used for the wall foundation.

effect on the airflow pattern but they allow thermal stratification and decrease the transfer of heat gains through the ceiling. The cooling effect of the room height is greater in spaces with very high ceilings where stratification of the air allows the occupants to inhabit the lower space [3]. It should be noted that it is not easy to simulate such effects in order to quantify the benefits against the extra cost of the walls.

The doors were rather high and the window openings tall with small width. The large openings were necessary in order to increase the night ventilation rate of the building and keep the house as cool as possible during the summer. The good insulation of the house and its large volume kept the building cool in the summer and warm in winter. The orientation of the buildings was usually dictated by parameters not related to energy factors (e.g. location of roads, plot size and shape etc.). Whenever possible bedrooms were located in a northwest direction to take advantage of the western winds which usually prevail during summer afternoons and evenings.

The occupation of the dwellers was the next important factor considered in the design of the house. In the area of Nicosia, in Mesaoria valley, where the present study will focus, the inhabitants were dealing mainly with the agriculture of wheat and barley and were raising goats and sheep until the early years of the 20th century. For this reason their house was constructed in such a way so as to provide shelter to humans and animals at the same time. Fig. 3, shows the basic design of this house and Fig. 4 shows photographs of the front and rear view of an actual building.

The design was very simple. The front part of the house consisted of a main entrance hall, through which two main rooms were accessed, one at each side. One room was usually used for sleeping and the other for sitting and dining. There was no wall enclosing the main entrance hall at the backside and the yard could be reached through that area. In the yard and adjacent to one wall, one or two additional

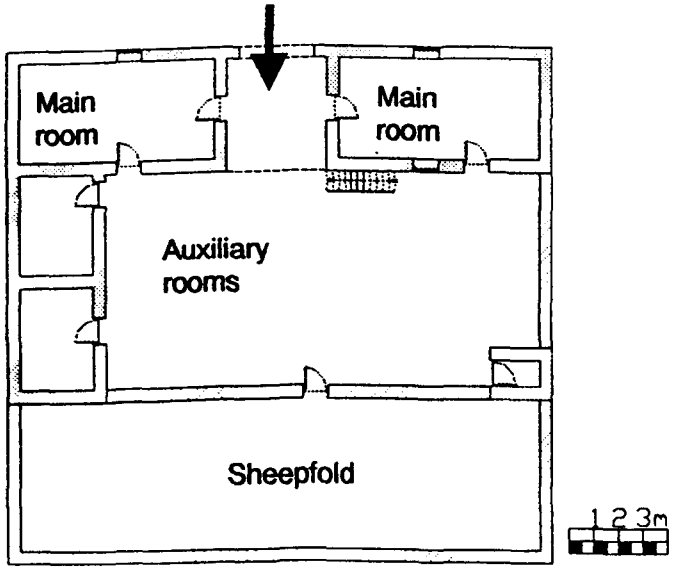

Fig. 3. Basic design of Mesaoria house.

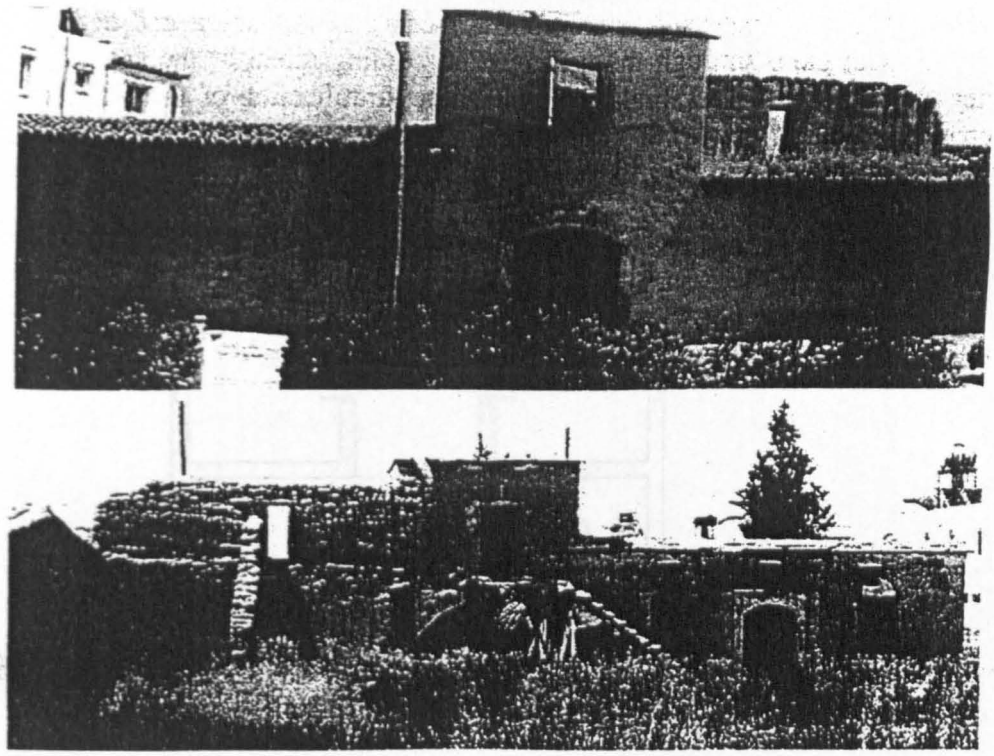

Fig. 4. Front and rear view of a typical Mesaoria house before 1920.

rooms were built, in which all the every day jobs, like cooking and washing were carried out.

The flocks were passed through the main entrance and kept in the sheepfold at the back of the house. The whole construction was enclosed in tall walls isolating the house area, for safety and protection.

From about 1920 till 1960 the occupation of the inhabitants of Mesaoria changed. Instead of growing crops and raising animals, they worked as builders and quarried soft stones from the nearby area for the construction work, and dealt with the labours needed for every day life in a village. Since the needs changed, the form of the house changed as well. The design of the house of this time is shown in Fig. 5. As can be seen the basic shape of the house of the older generation was kept unchanged, with two extra rooms added at the back of the house for a more comfortable life. No sheepfolds were needed any more and therefore they were not constructed.

The constructional materials remained basically the same since they were cheap and, from experience, they provided a comfortable house environment.

After the independence of Cyprus in 1960, the life of the inhabitants and their needs changed again. The sudden tourist development and the flow of foreign ideas led to alteration of the inhabitants' needs and character. New styles and morphological standards were used destroying the indigenous traditional values. Designers introduced plans from the west, which were used in industrialised societies. These designs have been applied to the Cypriot environment with no changes to fit the social or

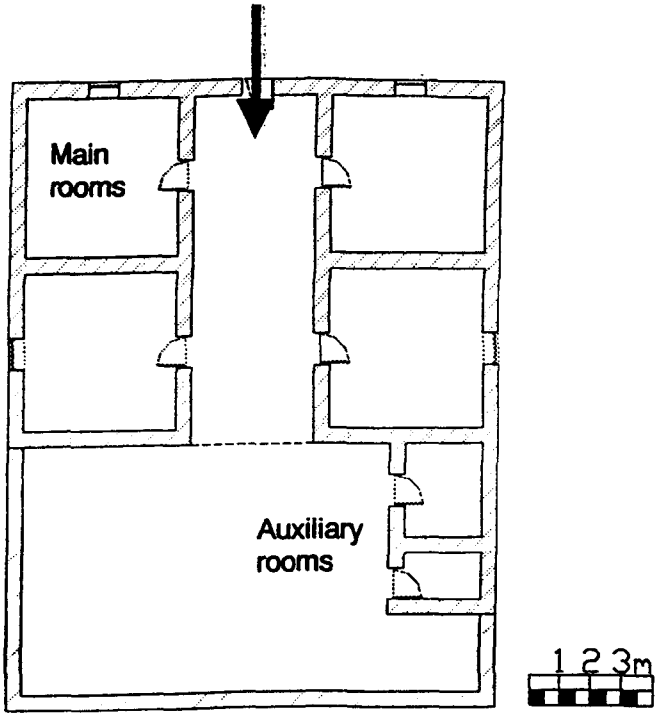

Fig. 5. Basic design of the house of 1920 to 1960.

climatic conditions, losing the comfort offered by the traditional house environment. Others, in an effort to keep the Cypriot character to the houses, imposed traditional patterns like arcades and facades on new buildings destroying the essence of Cypriot architecture.

The residential buildings during this period were constructed from hollow bricks, resulting in a finished wall thickness of 25 cm, and had a flat concrete roof of 15 cm in thickness with no insulation. These constructions were very cheap and offered no comfort.

The sudden increase of the population of the towns and the desolation of the villages of Cyprus, especially after the military events of 1974, was the next step that changed completely the character of the dwellings. Multi-storey buildings were built and the absence of town planning and regulations had a bad influence on the environment.

During the last two decades building codes and town planning have been imposed but the values for ecologically sound buildings are still not followed. The present trend in residences is to construct very large houses, well in excess of the needs of the occupants with a lot of impressive elements for decoration but environmentally incorrect (Fig. 6).

The present construction method is basically the same all over Cyprus. The bearing structure of a building, which may be either a large multi-storey building or a single-storey one, consists of the foundations, the columns, the beams and slabs. The bearing structure is made of reinforced concrete (Fig. 7). For the concrete mixture Portland cement, fine aggregate (sand) and coarse aggregate is used.

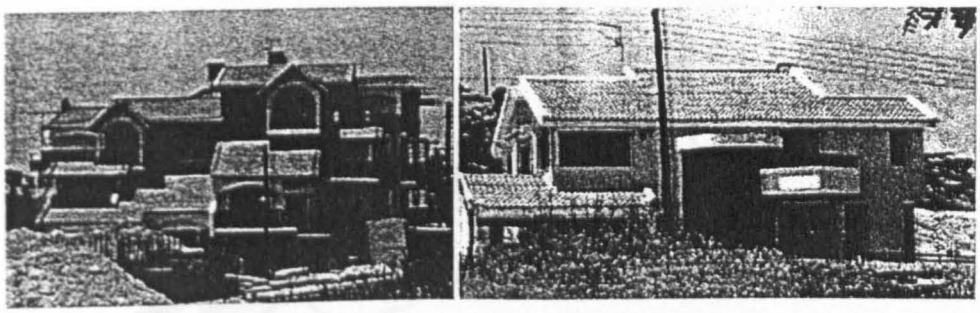

Fig. 6. Common contemporary Cypriot houses.

Fig. 7. Private dwellings in the construction stage.

The walls are constructed from hollow bricks, covered with plaster on both sides. The dimensions of the bricks are 30 cm by 20 cm by 10 cm. External walls have a thickness of about 25 cm and internal walls a thickness of about 15 cm. During recent years there is a trend to use cavity external walls, constructed of two brick walls with a layer of insulation of about 5 cm in between, as illustrated in Fig. 8. The total thickness of the insulated external wall is about 30 cm.

The floors are made of concrete slabs, covered with a layer of sand or screed of about 10 cm in which all plumbing and other services are placed. The floor finishing consists of a layer of mortar usually covered with tiles, marble, or granite blocks.

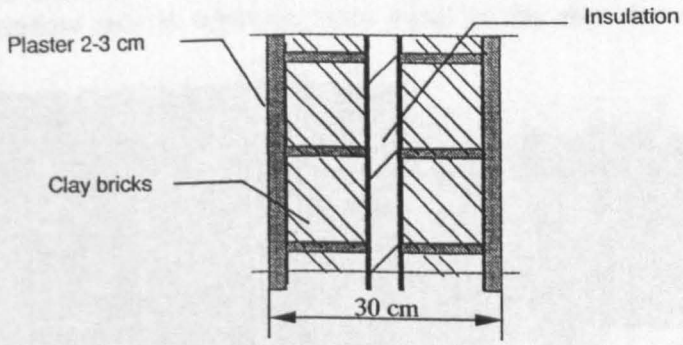

Fig. 8. External wall detail.

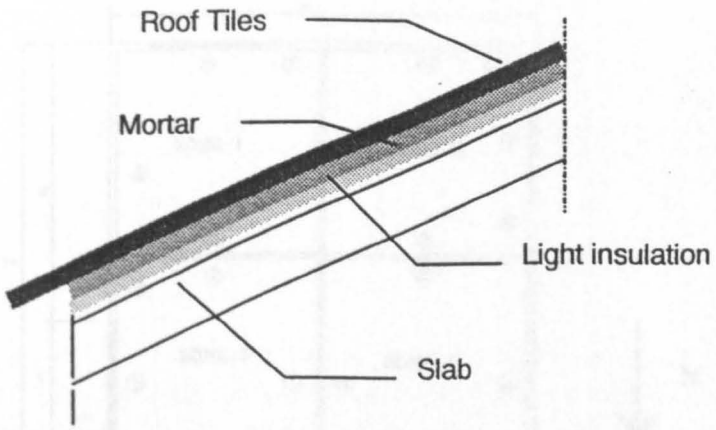

Fig. 9. Roof construction detail.

Flat roofs consist of the slab, usually 150 mm in thickness, with an additional layer of plaster of 3 cm on the underside, applied if the slab is not fair-faced, i.e. smooth without irregularities on the underside. The roof is usually water-proofed with a thin layer of bitumen and painted a white or aluminium colour on top.

During recent years, the trend that prevails is to use an inclined, fair-face slab, insulated very lightly and covered with a layer of mortar and roof tiles on top (Figs. 9 and 10). This method is used because there is no need for any special skills and therefore results in a simpler and cheaper construction compared to the traditional roof. The construction of the buildings results in a total weight of about 800 kg/m^2 of floor area.

3. Analysis of the energy requirements of buildings

The simulations consider a typical Cypriot house of 196 m^2 floor area. A typical and symmetric house plan was considered, as shown in Fig. 11, in order to enable comparisons between the various constructions. This plan is very similar to the basic plan of houses built between 1920–1960, shown in Fig. 5. The typical house consists of four identical external walls. Every wall is 14 m in length and has a window of 5.2 m^2. The window area is approximately equal to the area that a typical house

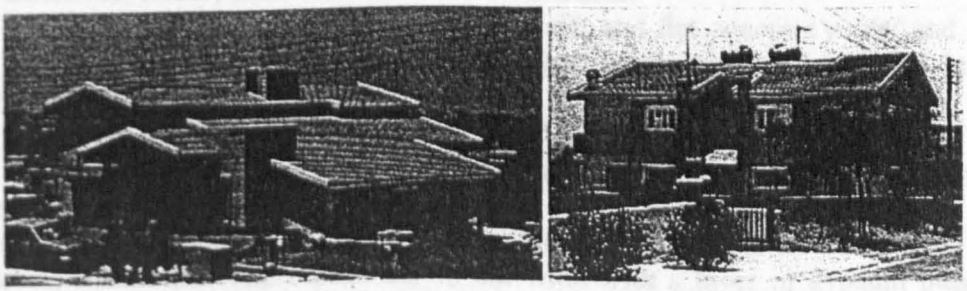

Fig. 10. Inclined concrete slabs covered with roof tiles.

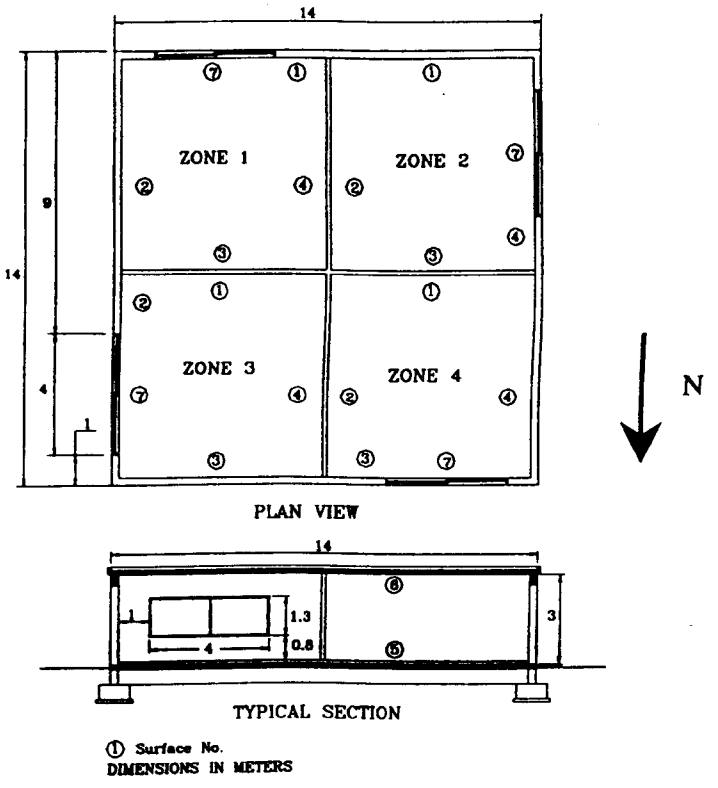

Fig. 11. Model house.

would have, but instead of considering a number of windows on each wall, only one window is considered. Since the same model will be used in evaluating the load for various constructions this simplification is not important but will assist in drawing conclusions since similar constructions are present on every wall.

The model house is further divided into four identical zones and the partition walls are considered as walls separating the four zones. For every zone a separate TRNSYS Type 19 unit is used. For calculating the cooling and heating load of the house the loads from the four individual zones are added. The house temperature is considered as the mean value of the four zones.

The objective is to check the conditions resulting in a:

a. traditional house, built from traditional materials,
b. flat roof house, built from hollow brick walls and flat concrete roofs; and
c. insulated house, built from insulated hollow brick walls and inclined insulated roofs.

Each one of these houses corresponds to the three construction periods as outlined above.

The traditional house is constructed from blocks of mud mixed with straw, as previously mentioned. The blocks are 45 cm wide with a layer of gypsum plaster covering each side. The height of the house is taken to be 4 m at the corners, with

Table 1
Corresponding volumes and external wall and roof areas for the three construction models

Parameter	Insulated house	Traditional house	Flat roof house
External wall area (m^2)	173.5	229.5	147.2
Volume (m^3)	193	242	147
Roof area (m^2)	203	203	196

a 15° inclined roof in the east–west direction with a ridge height of 5.9 m. The roof is constructed from clay tiles of a semi-circular shape, 1 cm thick, an air gap of about 5 cm just below the tiles, mud-blocks material 10 cm thick and 1 cm wood further below.

For the flat roof house a 20 cm single hollow brick wall with 2 cm plaster on each side is considered. The wall height is 3 m and has a non-insulated flat roof, constructed from fair-face 15 cm heavy concrete.

Finally for the insulated house, double-walls with 10 cm hollow brick and 2 cm plaster on each side and a layer of 5 cm polystyrene insulation in between is assumed. The wall height is 3 m and the roof is constructed from fair-face 15 cm heavyweight concrete, 0.4 cm asphalt for waterproofing, 5 cm plaster and clay tile on top. Also the roof is inclined by 15° in the east–west direction.

Table 1 shows the corresponding volumes and wall areas of the three construction models.

Due to the very large thickness of the traditional walls, TRNSYS cannot perform the calculations directly. This happens because TRNSYS can handle up to ten b, c, and d transfer function coefficients but the 50 cm block wall results in twelve. To overcome this problem the annual expected load can be extrapolated from the load of walls of smaller thickness. Thus, as can be seen in Fig. 12 where the extrapolation is shown graphically, a resulting annual load of the traditional house would be 6200

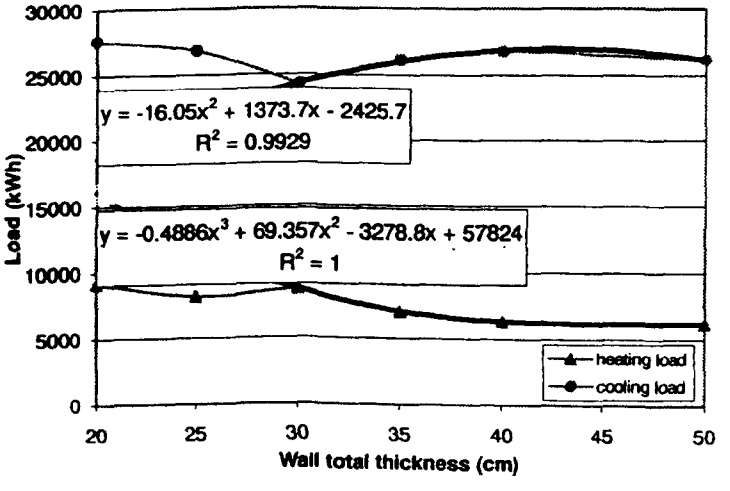

Fig. 12. Annual cooling and heating loads (kWh) plotted against mud-block wall total thickness (cm).

kWh for heating and 26100 kWh for cooling when keeping the house between 21°C and 25°C, respectively.

Also in Fig. 12, it is observed that for a mud-block wall of 30 cm total thickness a minimum annual cooling load occurs. This is due to the stored heat for a greater wall thickness, which is absorbed during the hot hours of the day and enters into the room at a later time.

Table 2 indicates the corresponding cooling and heating loads for the three construction types. As is shown, the construction method followed nowadays (insulated house) gives the smallest loads.

The traditional house which is greater in volume (by 12.5%) and in external wall area (by 13.2%) than the insulated house, has a cooling load increase of 9.7% and a heating load increase of 33.0% compared to the insulated one.

By examining the effect that the height of the traditional house would have on the loads, it is found that a three-meter high traditional house having exactly the same dimensions as the insulated house, would require a cooling load of 25500 kWh and a heating load of 3300 kWh. This would mean that the heating load would have a decrease of 29.2% as the building has a smaller exposed area and the cooling load an increase of 7.2% as the heat from the roof affects to a greater extent the inside temperature.

The flat roof house, although it has a smaller volume (by 7.6%) and a smaller external wall area (by 8.5%) than the insulated house, presents a cooling load increase of 77.8% and a heating load increase of 243.6% due to the poor thermal insulation of the construction.

Allowing the temperature to flow freely inside every model house, the temperature variation can be observed. During two typical winter days (Fig. 13) there is a great variation in a flat roof house, which was the type of construction used approximately from 1960 to 1980. This variation is between 11 to 20°C. The traditional house acts in a very similar way as a highly insulated and high cost house (insulated house), with the temperature varying between 16 and 20°C.

It should be noted that for the case of the traditional house the temperature was obtained from the temperature variations of buildings with smaller wall thicknesses, the maximum that TRNSYS can handle (35 and 40 cm), by assuming a linear extrapolation for the required thickness. This is considered adequate, as the difference between the readings for the smaller wall thicknesses is very small.

During summer similar effects are observed. As can be seen in Fig. 14, there is

Table 2
Cooling and heating loads of the model houses considered

Load	Insulated house (kWh)	Traditional house (kWh)	% load increase	Flat roof house (kWh)	% load increase
Cooling at 25°C	23790	26130	9.7	42300	77.8
Heating at 21°C	4660	6200	33.0	16012	243.6

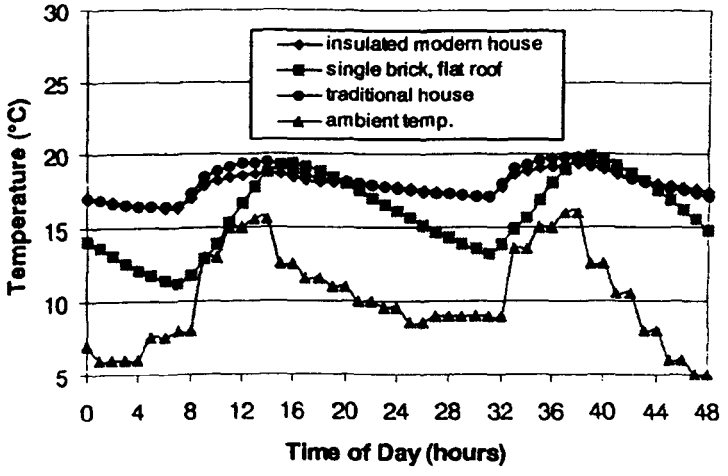

Fig. 13. Temperature variation in the model houses during the 13th and 14th of January.

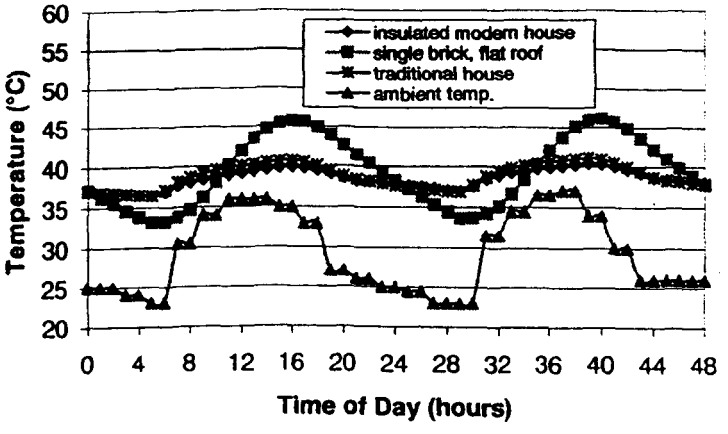

Fig. 14. Temperature variation in the model houses, during the 16th and 17th of July.

a greater variation in a flat roof house, between 33 to 46°C. The traditional and insulated houses act in approximately the same way, with the temperature varying between 36 and 40°C.

It is also of interest to note that there is a 3–4 hours time lag that occurs between the maximum ambient temperature and the maximum inside temperature of the building.

In the following section the effect of introducing ambient air into the model houses for cooling is investigated. This method was used extensively for the traditional house in order to keep the temperature between acceptable limits during summer. The main parameters influencing the air flow levels are:

a. The inlet and outlet surface areas of the openings and their relative position,
b. The wind velocity and direction,
c. The temperature difference between the indoor and outdoor environments; and

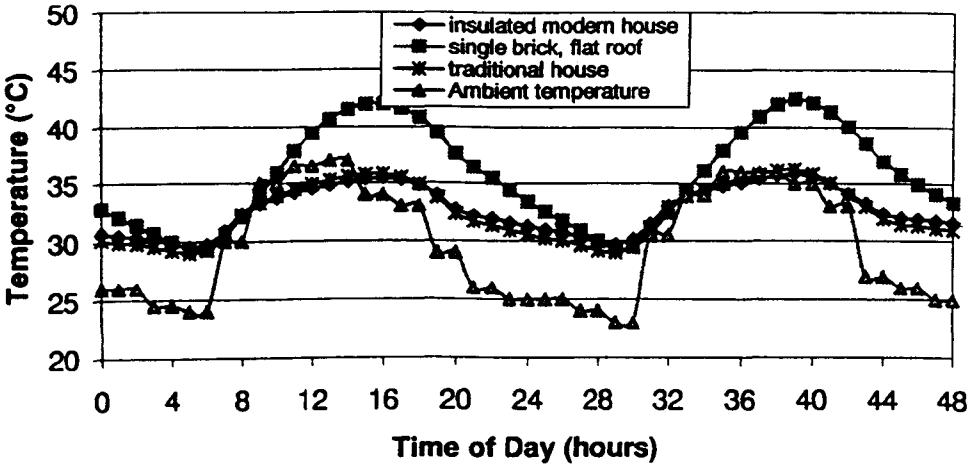

Fig. 15. Temperature variation in the model houses indicating the ventilation effect for 3 air changes per hour, during the 16th and 17th of July.

d. The relative wind shadowing of the building [4].

As the air changes per hour (ACH) of the ventilation flow can vary, a number of simulations were performed.

In winter the simulations show that the effect on the house temperature that the amount of ventilation air will have is negligible.

In summer, ventilation air enters into the house when the ambient temperature is less than the house temperature. This effect is indicated in Figs. 15–18. The ambient temperature is also plotted in the figures to indicate when ventilation air is added to the house.

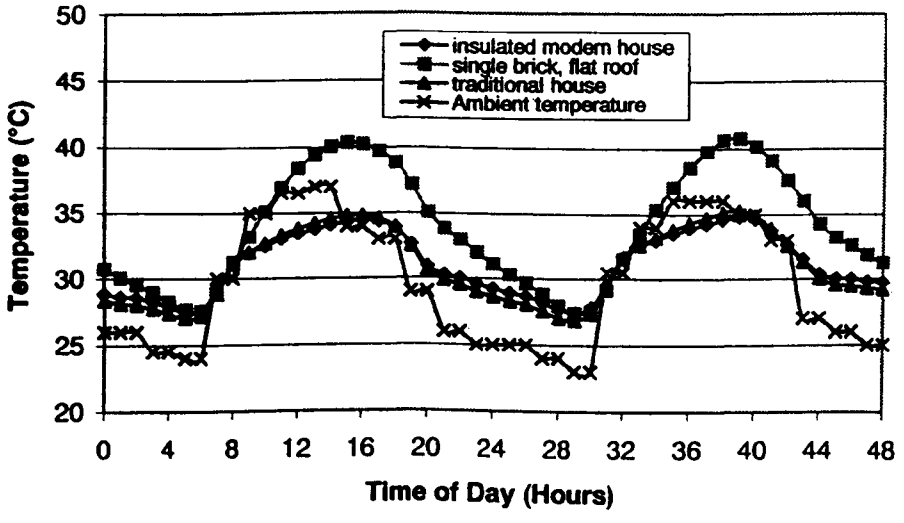

Fig. 16. Temperature variation in the model houses indicating the ventilation effect for 6 air changes per hour, during the 16th and 17th of July.

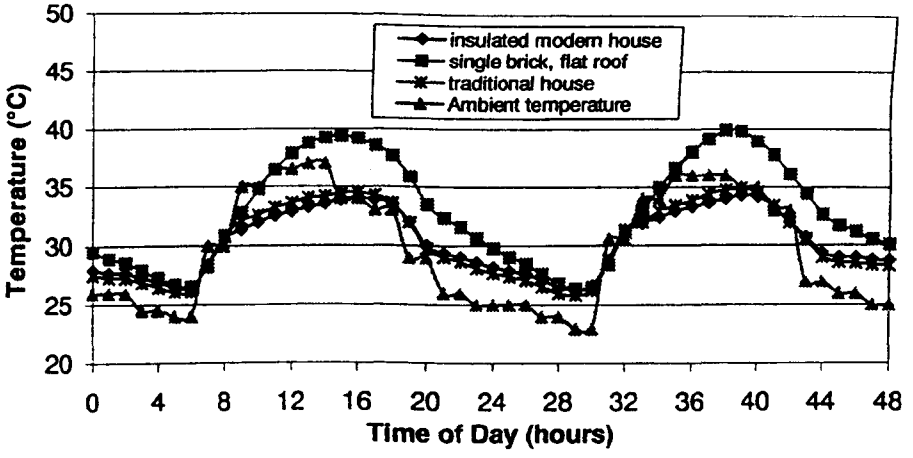

Fig. 17. Temperature variation in the model houses indicating the ventilation effect for 9 air changes per hour, during the 16th and 17th of July.

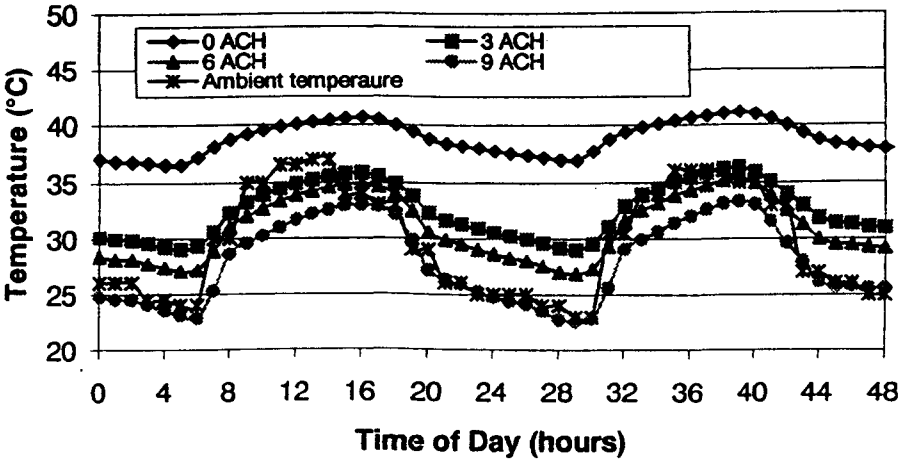

Fig. 18. Temperature variation in the traditional house indicating the effect of ventilation for 0–9 air changes per hour, during the 16th and 17th of July.

Obviously the ventilation effect depends on the number of ACH and this effect minimises the house inside temperature for all types of construction. In July the maximum temperature in the flat roof house can reach 46°C. With ventilation this temperature will be less by about 4°C for three ACH, 6°C for six ACH and reaches about 7°C for nine ACH. For the insulated house, which reacts in a similar way to the traditional house, in July the maximum temperature is about 40°C. With ventilation this temperature drops by about 4°C for three ACH, 5°C for six ACH, and about 6°C for nine ACH.

Finally the response of the traditional house to ventilation during the cooler hours of the day for various ACHs is indicated comparatively in Fig. 18. As observed, the greater the number of ACH the greater the temperature variation during the day, with the maximum temperature progressively diminishing. This shows the reason

for allowing large openings (like doors, reaching a height of 2.5 to 3 m) in the walls directed preferably on the side of the prevailing wind during the night.

4. Conclusion

The objective of this work is to present the various house construction methods encountered during the last century in Cyprus and investigate their temperature response during the year and the load variations. This was achieved using the TRNSYS program, which performs the necessary calculations by employing the transfer function method. For the simulations, a typical meteorological year for the Nicosia area and a typical model house plan are used.

The cooling load for keeping the house at 25°C is 23,790 kWh for the insulated house, 26,130 kWh for the traditional house and 42,300 kWh for the flat roof house. The corresponding heating loads for 21°C are 4460 kWh, 6200 kWh and 16,012 kWh for the three cases, respectively.

The temperature inside the traditional house and the insulated house varied between 16–20°C for winter and between 25–35°C for summer compared to 11–20°C for winter and between 33–46°C for summer for a flat roof house. These temperatures drop considerably, by about 5°C, when ventilation air is used for cooling, depending on the number of air changes.

The results of the simulations indicate that the materials and construction habits, like allowing high ceilings and doors and positioning doors and windows towards the prevailing night winds, resulted in a low cost house offering the same temperature conditions as a highly insulated and expensive modern house.

References

[1] Klein et al. TRNSYS manual. University of Wisconsin, 1998.
[2] Petrakis M, Kambezides HD, Lykoudis S, Adamopoullos AD, Kassomenos P, Michaelides IM, Kalogirou SA, Roditis G, Chrysis I, Hadjigianni A. Generation of a typical meteorological year for Nicosia, Cyprus. Renewable Energy 1998;13(3):381–8.
[3] Dimoudi A. Urban design. In: Santamouris M, Asimakopoulos D, editors. Passive cooling of buildings. 1997:95–128.
[4] Dascalaki E, Santamouris M. Natural ventilation. In: Santamouris M, Asimakopoulos D, editors. Passive cooling of buildings. 1997:220–306.